Chromosomal integration *in vitro* and *in vivo* of high capacity adenoviral vectors

INAUGURAL-DISSERTATION

Zur Erlangung des Doktorgrades der

Mathematisch- Naturwissenschaftlichen Fakultät

der Universität zu Köln

vorgelegt von

Sam Laurel Stephen,

aus Trivandrum, Indien.

2007

Referees/Berichterstatter Prof. Dr. Stefan Kochanek
Prof. Dr. Jonathan Howard

Date of oral examination/ Tag der mündlichen Prüfung: 12.1.2007

The present work was carried out under the supervision and the direction of PD Dr. Stefan Kochanek at the Center for Molecular Medicine, University of Cologne, Germany from October 1998 to December 2004.

Diese Arbeit wurde von Oktober 1998 bis Dezember 2004 am Zentrum für Molekulare Medizin, Universität zu Köln unter der Leitung und der Betreuung von PD Dr. Stefan Kochanek durchgeführt.

Acknowledgements

It is with great pleasure and a profound sense of gratitude that I thank Prof. Stefan Kochanek for the guidance, support and encouragement that I received at his hands. Stefan had spared neither time nor energy to aid me whenever I was in need of his help and had believed in me when I started in his lab as an absolute novice in Molecular Biology and Genetics, straight from a M.Sc. in Biology.

I sincerely thank Prof. G. Pfitzer, Institut für Physiologie, Universität zu Köln, and all of the members of her lab, who had very generously allowed me to use the lab facilities to finish my experiments there and for their hospitality during the four months of my residence in the guest house of that Institute.

I express my gratitude to Prof. M. Grompe, Oregon Health Sciences University, Portland, Oregon, to the members of his lab and to Dr. M. Finegold, Baylor College of Medicine, Houston, Texas, for the help that they rendered during the collaborative work and for the plasmids. The invaluable help of Dr. M. Al-Dhalimy, lab manager, Grompe Lab, OHSU, Oregon, is very gratefully acknowledged.

I thank Prof. Scharffetter-Kochanek, Universität zu Ulm, for the FF-95 cells and Dr. I. Semkova, Universität zu Köln, for the HRPE cells.

I thank the Böhringer Ingelheim Fonds for their generous travel bursary that enabled me to carry out the work in Oregon.

Special thanks are due to my colleague and dear friend Dr. S.G. Vijayshankar, whose support went far beyond the call of duty, and to his family.

I thank the following employees of the Universität zu Köln for their help: Dr. M. Krüger, Dr. V. Hasse, Dr. L. Lubomirov, Ms. F. Elhamine, Mrs. L.Glahé, Mr. F. Stassen, all from the Institut für Physiologie, Mrs. U. Cullmann from the ZMMK servicing lab, Dr. D. Grosskopf-Kroiher, Dr. H-J. Schäffer, Prof. B. Kawhol, and Mrs. C. Zander.

I also thank the following staff of my current employer, the University College, London. Specially, I thank Prof. M. Collins for her patience, encouragement and support. I also thank Ms. A. Gutierrez Granda, Dr. D. Escors-Murugarren, Dr. F. Gennari, Dr. M. Devannieuax, Mr.A. Khan, Dr. K. Dheda and Mr. J. Walton for their valuable support.

I thank all the friends in Köln and Bonn, who were very hospitable and made my stay in Germany a very happy and memorable one. In particular, I wish to thank Mr. D. A. John, Dr. D.A. Verse, Mr. S. Helbrig, Mrs. M. Ishida, Sensai A. Wallraff and Rev. Fr. I. Wright.

I sincerely thank Dr. Dr. M. Mannoussaka, Mr. J.M.Tsang and Dr. J. Röes, from the University College, London, Mrs. H. Cox, Universität zu Ulm, and Dr. A. Stachora, Stachora Consulting Pvt. Ltd., for helping me with the corrections and the printing of this thesis.

I thank four of my former teachers who had encouraged and guided me since my school days: Mr. T. Jayaraj, Christ Nagar School, Trivandrum, Dr. V.S. Sugunan, Rajiv Gandhi Centre for Biotechnology, Trivandrum, Dr. D.M. Shotton, University of Oxford, UK, and specially, my teacher and mentor for the past 13 years, Dr. G.R. Jayasree Nair, University College, Trivandrum.

I thank my father, Prof. J. Stephen, my mother, Mrs. Pamela Stephen, and my sisters Dr. Ruth Stephen, and Ms. Sarah Stephen, for their patience, love, support, and encouragement. I thank my extended family and friends from India for their support and prayers.

Above all, I thank Almighty God, whose boundless grace alone is responsible for all of the blessings that I have enjoyed.

Abbreviations

Abbreviation	Full Form
Ist Gen. AdV	First generation adenoviral vector
IInd Gen. AdV	Second generation adenoviral vectors
Ad2	Human Adenovirus Serotype 2
Ad5	Human Adenovirus Serotype 5
Ad12	Human Adenovirus Serotype 12
AdV	Adenoviral vector
AAV	Adeno Associated Virus
bp	Base pairs
CIP	Calf intestinal phosphatase
Chr	Chromosome
DNA	Deoxyribonucleic acid
ds	Double stranded
DSB	Double stranded breaks
DBP	DNA binding protein
EDTA	Ethylenediaminotetraacetic acid
FAH	Fumarylacetoacetate hydrolase
Fah+ve	Fah positive
Fah-ve	Fah negative
FAA	Fumarylacetoacetate
FCS	Fetal calf serum
HC-Ad vector	High capacity adenoviral vector
HR	Homologous recombination
ITR	Inverted terminal repeat of the adenoviral genome
i.u.	Infectious Units
Kbp	Kilo base pairs
LITR	Left ITR of the adenoviral genome
moi	Multiplicity of infection
NHEJ	Non Homologous end joining
dNTPs	Deoxribonucleotides
OD	Optical density
p.f.u.	Plaque forming units
PCR	Polymerase chain reaction
pTP	Pre terminal protein
RITR	Right ITR of the adenoviral genome
RV	Retro virus
SDS	Sodium dodedcyl sulphate

ssDNA	Single stranded DNA
TBS	Tris buffered saline
TP	Terminal Protein
Tris	Tris-(hydroxylmethyl)aminomethane
wt	Wild type

Table of contents

I Introduction

I.1 Scope of the work

"Nothing in life is to be feared; it is only to be understood." So wrote Prof. Maria Sklodowska-Curie in her Diary (Caporale, 2002). Viruses are greatly feared as harbingers of death, with fears that influenza pandemic may cause hundred thousand deaths in an outbreak in the USA alone (Lee & Krilov, 2005), and had claimed 20- 40 million human lives in the past (Perez et al., 2005). Like the impartial death that ensnares both kings and the common people, referred to in the famous poem "Death the Leveller" by James Shirley (Quiller-Couch, 1919), viruses have often been the bane of humans, time and again in the course of our history, have been accused of taking millions of paupers and princes, like King Rameses V in 1157 BC, to the grave (Mahalingam et al., 2004). The recent threats of terrorists who may use biological warfare as means to achieve their ends, have only added more fuel to these fears (Agarwal et al., 2004). However, the idea that these agents can be used for beneficial purposes to help humanity has not escaped the notice of science and that has been put into action. The fact remains that viruses can also be used for therapeutic purposes for humankind and so far offers the best gene delivery system to treat acquired and inherited genetic disorders (Verma & Weitzman, 2005).

Gene therapy, which has been labelled as the "twenty first century medicine", seems to be ideal for the treatment of inherited and acquired diseases. The fundamental idea of gene therapy is to introduce to the target diseased cells a fragment of genetic material that will at least slow down the progression of the disease or better still cure it outright (Verma & Weitzman, 2005). To deliver the genetic material to the target cells, gene transfer systems have been developed that can be classified as non-viral or viral gene delivery systems (Kootstra & Verma, 2003). Non-viral methods used in gene therapy include liposomes (Stern et al., 2003), nano particles (Yamada et al., 2003), plasmid DNA (Liu et al., 1999), chimeric RNA:DNA oligonucleotides (Kren et al., 2002) and transposable elements (Montini et al., 2002) [reviewed in (Glover et al., 2005, Griesenbach et al., 2004, Li & Huang, 2000)].

Viral gene delivery systems (except in the case of suicide gene delivery (Campbell & Gromeier, 2005) use replication deficient viral vectors, where part or the complete coding region of the viral genome is replaced by the genetic material of the therapeutic gene. The *cis*-acting regulatory sequences essential for the packaging of

the vector genomes and, in certain viruses, responsible for the integration into the host, are left intact. Non-replicating viral vectors are produced when the viral vector is introduced into a producer cell, which by itself, or by the aid of another system, is able to provide the viral structural proteins essential for the growth. Currently, the viral vectors used for gene therapy are based on retrovirus, adeno-associated virus, herpes simplex virus type-1 and adenovirus [reviewed in (Kootstra & Verma, 2003)].

Gene therapy was first used in humans subjects in 1989 (Rosenberg et al., 1990) and had its first taste of success in the pioneering experiments in 1992 in which two girls suffering from a from a type of SCID caused by a deficiency in the enzyme adenosine deaminase (ADA) were treated successfully (Anderson, 1992). The first subject used in the trial has maintained a circulating level of 20 to 25% gene-corrected T cells and a normal life-style with amelioration of her disease symptoms (Anderson, 2000). Further successes have been observed in the treatment of a small number of individuals with other diseases and clinical trials are going on [reviewed in (Edelstein et al., 2004, Selkirk, 2004)]. However, leukaemia induction was observed in an animal model of retroviral gene marking following the retroviral vector integration into the murine gene ecotropic viral integration site-1 (Evi 1) (Li et al., 2002). Gene therapy received a setback at the death of an ornithine transcarbamylase (OTC) deficient human subject during the clinical trials (Raper et al., 2003). The risks of insertional mutagenesis were put into the spotlight during the SCID trials conducted in France (Hacein-Bey-Abina et al., 2003a), (Fischer et al., 2004) (Hacein-Bey-Abina et al., 2003b), (Woods et al., 2003). The recent work on viral vectors seems to suggest that an integration pattern exists even in the integration of viruses that were previously thought to integrate very randomly into the genome (Bushman, 2003) (Mitchell et al., 2004).

The work done on Adenoviruses and adenoviral vectors suggested that the Adenoviruses remain as episomal DNA, albeit with rare integration events which were observed since the late 1960s (Doerfler, 1968), (Doerfler, 1970), (Doerfler et al., 1975), (Doerfler et al., 1989), (Knoblauch et al., 1996), (Muller et al., 2001), (McDongall et al., 1975), (Sambrook et al., 1975), (Harui et al., 1999). In background of the recent developments during gene therapy trials, it is imperative that a thorough study of the integration patterns of high capacity adenoviral vectors (HC-AdV) be carried out before they could be safely used for gene therapy. In particular, the integration of HC-AdV into the genome *in vitro* and *in vivo* has to be characterised to

allow a prediction of potential insertional mutagenesis of HC-AdV when applied in clinical gene therapy trials. This evaluation of the biosafety of the HC-AdV was the aim of the work presented in this thesis.

I.2 Adenovirus

I.2.1 Adenovirus classification

Adenoviruses were first isolated from surgically removed adenoidal tissue while establishing tissue culture lines and during the investigations into the causative agent of respiratory illnesses among military recruits (Rowe et al., 1953), (Hilleman & Werner, 1954), (Huebner et al., 1954). Adenoviruses are also responsible for epidemic keratoconjunctivitis, acute haemorrhagic cystitis and gastroenteritis (Garnoff A, 1999). The *Adenoviridae* family of viruses are comprised of the genus *Aviadenovirus*, *Mastadenovirus*, *Atadenovirus,* S*iadenovirus* and possibly a yet unnamed genus isolated from fish (Davison et al., 2003, Kovacs et al., 2003). Based on the resistance to neutralisation by antisera to other known adenovirus serotypes and recently on the DNA sequence data, 51 human adenoviral serotypes have been identified (Verma & Weitzman, 2005). Based on their ability to agglutinate red blood cells and the resistance to neutralisation to antisera, these serotypes are categorized into 6 subgroups (Davison et al., 2003, Kootstra & Verma, 2003) (See Table 1). Serotypes 5 and 2 of subgroup C Adenoviruses have been used mainly as the basis for the generation of gene transfer vectors.

Species	**Serotype**	**Haemagglutination groups**
A	12, 18, 31	IV (no or little agglutination)
B	3, 7, 11, 14, 16, 21, 34, 35	I (complete agglutination of monkey erythrocytes)
C	1, 2, 5, 6	III (Partial agglutination of rat erythrocytes)
D	8, 9, 10, 13, 15, 17, 19, 20, 22-30, 32, 33, 36-39, 42-49	II (Complete agglutination of rat erythrocytes)
E	4	III
F	40, 41	III

Table 1. The classification of Adenoviruses [based on (Davison et al., 2003, Shenk, 2000)]

I.2.2 Adenovirus structure

Adenovirus is a double stranded DNA virus. The nonenveloped icosahedrally shaped virion has 20 triangular facets and 12 vertices and is 60-90 nm in diameter comprising of an inner DNA-protein core complex surrounded by an outer protein shell, the capsid, which is made up of 240 hexons, 12 pentameric penton bases and 12 trimeric fiber proteins.

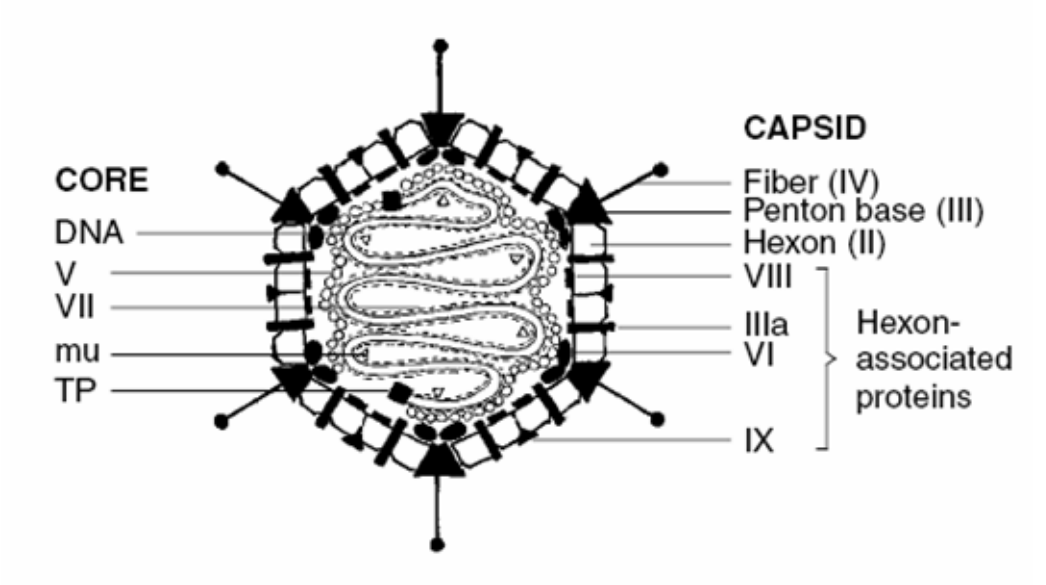

Fig. 1. Structure of Adenovirus obtained from (Volpers & Kochanek, 2004)

Each of the triangular facets is composed of 12 copies of the hexon trimer. The trimeric hexon (polypeptide II) is the most abundant of the structural proteins and makes up 63% of the total protein mass (Burnett, 1985, van Oostrum & Burnett, 1985). The facets are rounded to bring hexons from adjoining facets into close contact at the edges. The capsid is sealed at each of the 12 virion vertices by the Penton complex, composed of the pentameric Penton base (polypeptide III) and the trimeric fiber proteins. The Penton base has a 30- Å diameter filled by the fiber protein. The monomeric polypeptide IIIa acts as a rivet to stabilize the interface between two adjacent capsid facets. The hexameric Polypeptide VI acts as a cementing protein that anchors the five peripentonal hexons and connects the capsid to the core (Stewart & Burnett, 1995). It is also a cofactor for the adenovirus protease. Polypeptide VIII is present inside the capsid along the edges where it might act as a "measuring rod" to determine the size of the virion. The trimeric Polypeptide IX acts as a cement to hold the central nine hexons in each facet together as a unit. The viral genome, composed of a linear double stranded DNA, 30-40 kb long, and 4

virus-coded proteins all together comprise the core. The function of the Polypeptide X (μ protein) is yet to be elucidated. The major core protein, Polypeptide VII acts as a histone-like center around which the viral DNA is wrapped. Polypeptide V binds to the penton base and acts as a bridge between the core and the capsid. The terminal protein, which is covalently attached to the ends of the viral DNA, is involved in the attachment of the viral genome to the nuclear matrix and acts as the primer for DNA replication (See Fig. 1). Ad protease, a cysteine endopeptidase that is involved in the maturation of the viral particle, is also present in the virions [reviewed by (McConnell & Imperiale, 2004, Nicklin et al., 2005, Rux & Burnett, 2004, San Martin, 2003, Shenk, 1995, Volpers & Kochanek, 2004)].

I.2.3 Adenovirus life cycle

The Ad penton and fiber capsid proteins play an important role in Ad infection. The carboxy terminal part of the fiber folds into a knob that contains a reception-binding region and a trimerization domain (Henry et al., 1994). The coxsackievirus-adenovirus receptor (CAR) cell surface protein binds with high affinity to the fiber protein (Bergelson et al., 1997). CAR might act as a pathfinder protein during embryogenesis directing the organ formation, and also in the formation of cell aggregates and in cell adhesion (Fechner et al., 2003), (Noutsias et al., 2001). The permissivity of various cell lines to adenovirus may differ and many factors such as the expression of CAR may be responsible for this (Carson et al., 1999, Hidaka et al., 1999, Kibbe et al., 2000, Leon et al., 1998). CAR may not be the only receptor recognized by the Ad fiber. The expression levels of other molecules such as heparin sulphate proteoglycans (Dechecchi et al., 2000), MHC class I (Hong et al., 1997), the αv integrins (Wickham et al., 1993), the actin cytoskeleton (Patterson & Russell, 1983), phosphatidylinositol –3-OH kinase (Li et al., 1998b), CD46 (Segerman et al., 2003), the Rho family GTPases (Li et al., 1998a) might also play a part in the permissivity of the individual cell lines to Adenovirus.

Following the docking of the Adenovirus to the cell membrane, the penton proteins bind to αvβ3 and αvβ5 integrins through a Arg-Gly-Asp (RGD) consensus motif (Goldman & Wilson, 1995, Karayan et al., 1997, Mathias et al., 1994). Following this, the fiber trimer is released and the penton structure gets altered (Nakano et al., 2000, Schoehn et al., 1996). This leads to integrin clustering where up to 5 integrin

molecules bind to each homopentamer, and this integrin ligation triggers cytoskeletal changes, leading to the local formation of clathrin-coated pits (Chiu et al., 1999). Ad Penton - integrin binding results in the activation of phosphatidylinositol-3-OH kinase (PI3K). PI3K activates Rac and CDC42 GTPases, leading to the polymerization of actin and viral endocytosis into the clathrin-coated pits (Lamaze et al., 1997, Li et al., 1998a). During this process, all of the fiber proteins get detached. As the endosome matures, the vesicular pH goes down and at pH 6 the virus breaks out of the endosome into the cytosol (Greber et al., 1993). Up to recent times, the mechanism by which Ad capsid penetrates the endosomal membrane was not quite clear. The penton was believed to be involved in this process, because at low pH the conformation of the protein changes, exposing hydrophobic regions that bind nonionic detergents (Seth et al., 1985). The Ad protease too was thought to have been responsbile; for though it is inactivated after capsid release from the cell, it is reactivated after entry into acidified endosomes (Greber, 1998). Recent work has suggested another model. According to this, partial disassembly of the capsid is triggered by the endosome acidification. The capsid disassembly liberates peripentonal hexons, penton base, IIIa and VI proteins from the structure. The free protein VI associates with the endosomal membrane and ruptures it (Wiethoff et al., 2005).

Following the escape from the endosome, Ad capsids are trafficked to the cell nucleus periphery via the microtubules by a signaling pathways mediated by the cAMP-dependent PKA. The integrin binding activates PKA and the intracellular cAMP levels regulate microtubule dependent vesicle transport towards the nucleus (Reese & Haimo, 2000, Reilein et al., 1998). The Penton might still be involved in this too, since the fiber-binding site, which matches the sorting signal found in trafficking proteins, the dileucine motif, might bind to clathrin-associated adaptor protein complexes that mediate endocytic and secretory pathways (Heilker et al., 1999, Hong & Boulanger, 1995, Kirchhausen, 1999). At the nuclear pore complex, the Ad capsids are dismantled and the internal protein VI is degraded. The nuclear pore complex glycoproteins themselves might also be involved in the dismantling of the capsid (Greber et al., 1997, Greber et al., 1996). Once this happens, the viral DNA and protein VII pass through the nuclear pore into the nucleus (Greber et al., 1993), but the method by which this takes places is still unclear [reviewed by (Medina-Kauwe, 2003, Nemerow, 2002)]. On reaching the nucleus, the Adenovirus manipulates the

cell into i. entering the S phase of the cell cycle, so as to enable the optimal viral DNA replication; ii. shutting down the anti-viral host response; iii. using the cellular proteins together with the viral gene products to carry out the viral DNA replication.

The Ad genome is a linear double stranded DNA genome of 30 to 40 kb. At each end of the genome are the ≅120 bp inverted terminal repeats (ITR), the first 50 bps of which contain the replication origins. At each 5' terminus of the genome, the terminal protein is covalently attached. At the left end (the 5' end in the left to right orientation) of the genome, a cis-acting packaging element that enables the polar encapsidation of viral genome into capsids is present. The Ad genome contains one immediate- early region, the E1A region, four early transcription regions, the E1B, the E2, the E3 and the E4 regions, two delayed early regions, the IX and the IVa2 regions and one late region that encodes five families of mRNA, the L1, the L2, the L3, the L4 and the L5 families (see Table 2). The early regions have their own individual promoters, and the late transcripts are initiated from the major late promoter. The genome is transcribed from both ends. A ≅ 200-nt leader sequence (tripartite leader), that directs efficient specific translation of Ad late mRNAs independent of the host cell initiation factor eIF4F, is present in the 5' ends of all late mRNAs (see Fig. 2).

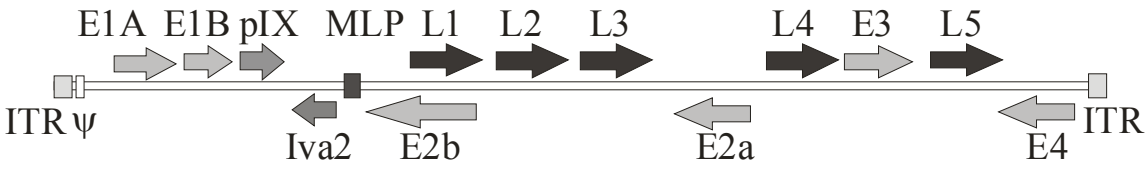

Fig. 2: Scheme of the transcription of the Ad genome [adapted from (Evans, 2002)]

Region	**Function**	**Action**
E1A	Transactivates Modulates host cell gene expression and proliferation	Activates transcription from other early promoter regions. Interacts with i. Retinoblastoma tumour suppressor pRb and related family members ii. Sequesters p300, the transcriptional coactivator for p53- dependent gene expression iii. transcription factors such as TATA binding protein (TBP), ATF family and the Srb mediator complex iv. E2F, resulting in the promotion of G1 and S phase progression
E1B	Inhibits apoptosis Increases viral protein production	Inhibits p53-induced transcription. E1B19K is a functional homolog of Bcl-2 and also blocks the oligomerization of death-inducing complexes. Complexes with E4OFR6 and selectively stabilizes and transports viral mRNA, while inhibiting host cell mRNA transport.

E2	Ad DNA replication	Encodes Ad DNA polymerase (Ad Pol), preterminal protein (pTP) and DNA binding protein (DBP).
E3	Counteracts host immune response Cell death	E3gp19K tethers MHC I to the Endoplasmic reticulum. E3 RID and 14.7K clears Fas and TNFR1 and other proteins involved in the apoptotic pathway. E3 11.6K promotes cell death later in the life cycle
E4	Viral DNA replication, viral mRNA transport and splicing, regulation of apoptosis.	E4 ORF 6 inhibits p53 and targets it for degradation and together with E4ORF3 inhibits DNA-protein kinase, blocking the formation of viral DNA concatomers. E4 ORF4 regulates mRNA splicing E4 ORF6/7 enhances production of E2 products.
IV a	Packaging	IVa2 product is responsible for the recognition of the packaging signal.
L1-5	Structural proteins. Host mRNA translation inhibition Assembly of viral particles	100K late protein binds to eIF4, and shuts off translation of any mRNA lacking the tripartite leader sequence.

Table 2: Ad viral gene products and their function [reviewed by (Evans, 2002, Shenk, 2000)].

In the Ad life cycle, the Ad DNA replication starts after the expression of the Ad early genes. Ad Pol, pTP, and DBP are essential for Ad DNA synthesis. The cellular proteins NFI/CTF, NFII and NFIII/Oct-1 increase the replication rate (de Jong & van der Vliet, 1999, Hay et al., 1995, Van der Vliet, 1995). The minimal replication origin (core origin) is located in the terminal 18 bp and contains an essential triplet repeat at the ends (5'-CATCAT in Ad5). The next 32 bps constitute the auxiliary replication origin region and contain binding sites for NFI/CTF and NFIII/Oct-1. Taken together, the first 50 bps constitute the origin of Ad DNA replication.

The DNA replication can be divided into two phases. In the first phase, DNA synthesis starts at either termini and proceeds to the corresponding end of the genome, producing a duplex consisting of a parental and daughter strand, and one single strand of DNA. In the second phase, the complementary strand to the single strand is produced.

The pre-initiation complex consisting of Ad Pol-pTP, DBP, NFI/CTF and Oct-1 form at the origin, and the DNA is bound by the DBP. NFI/CTF and Oct-1 interacts with the auxiliary region (enhanced by DBP) and stabilizes the interaction of the Ad Pol-pTP heterodimer complex with the core origin (Mul et al., 1990, Stuiver & van der

Vliet, 1990). The TP, covalently bound to the genome, enhances this complex. The first dCTP is covalently coupled to the Ser-580 residue of the pTP by the pol, forming a pTP-dCMP complex essential for the protein priming. The conserved Asp-578 and Asp-582 are essential to the maintenance of the optimally functioning active site of the pol leading to effective initiation (Mysiak et al., 2004). The origin is unwound by the DBP and the Ad Pol-pTP complex forms a pTP trinucleotide intermediate. The complementary sequence from bp 4-6 (3'GTA) is used to synthesize the pTP-CAT. The NFI/CTF then unbinds from the binding site and the pTP-CAT moves back from position 4-6 and binds to the 1-3 GTA. Ad Pol unbinds from the pTP and the elongation starts. The replication is carried out by the Ad Pol, and the DBP not only unwinds the DNA but also binds to ssDNA to protect it from nucleases. The single stranded DNA is used as the template at the next stage. The left and right ITRs anneal to form a loop structure (pan handle) that appears as the terminus of the actual genome and contains the covalently linked TP and the cycle continues [reviewed in (Evans, 2002)].

A *cis*-acting packaging domain located between ≅ 200 and 400 bp, containing 7 redundant elements (the A repeats), most of which share a bipartite consensus motif 5'TTTGN$_8$CG-'3, packs the Ad DNA in a polar manner from left to right into the virus particles (Grable & Hearing, 1990, Grable & Hearing, 1992, Schmid & Hearing, 1995, Schmid & Hearing, 1997). Trans acting packaging components too have been reported (Schmid & Hearing, 1998). The empty capsid (light particle) is the first stage of the assembly. The viral DNA and core proteins are packaged into this as they mature into heavy intermediate particles. The protease cleaves numerous proteins within the particle and it matures into the infectious virus (Weber, 1995). The E3-11K protein, which is synthesized only in low amounts during the early stage from the E3 promoter, is expressed in large amounts from the Ad MLP. The Adenovirus Death Protein (ADP) kills and lyses the cell (Doronin et al., 2003, Tollefson et al., 1996). The Ad virions are liberated and the life cycle is completed [reviewed in (Evans, 2002, Shenk, 2000)].

I.2.4 Gene transfer vectors based on adenovirus

E1A gene products are not only essential for the expression of the early and late viral genes, but also encode the oncogenic transforming functions of the virus and so the

first successful adenovirus based vectors for gene therapy had deletions in the E1 gene. The E1 gene region was replaced by the transgene and the vector could not replicate in its absence (Fig. 3). The E1 functions necessary for the replication were provided in *trans* by cell lines like the 293 cells which contain the left end (bp 1 to 4344) of the Ad5 genome including the left ITR, packaging signal sequences (Ψ), E1A, E1B, IX and a part of the IVa2 regions (Graham et al., 1977, Morsy & Caskey, 1999, Rosenfeld et al., 1991, Stratford-Perricaudet et al., 1990, Zabner et al., 1993). The sheared Ad5 DNA had, after the transfection, integrated into Chr 19q13.2 into the pregnancy specific β-1 glycoprotein 4 (PSG 4 gene) (Louis et al., 1997). In this method, up to 5 kb of transgene could be accommodated in the first generation adenoviral vectors (I^{st} gen AdV) (Bett et al., 1993). Many of the I^{st} gen AdV had additional deletions in the E3 region and up to 8 kb of foreign DNA can be accommodated in these vectors [reviewed by (Shenk, 1995)]. The vector plasmid with the deletions in the genome is linearised and transfected into the cell line and an agarose overlay is plated over the monolayer. The successfully generated AdV appear as plaques in the plate, which are picked and further seeded and isolated by another round of plaque purification. The AdV is then grown on a larger number of cells. When the cells display a cytopathic effect (CPE), they are collected and disrupted by repeated freezing and thawing and the vectors purified by ultracentrifugation on a Cesium Chloride (CsCl) density gradient (for the detailed protocol, see the Materials and Methods section). These vectors could be produced in titers up to 10^{13} vector particles/ml and can transduce proliferating and quiescent cells [reviewed by (Volpers & Kochanek, 2004)]. Nevertheless, I^{st} gen AdV are not the ideal vector for long term gene therapy for inherited diseases. Recombinant replication competent Adenovirus (RCA) can arise as a result of the recombination between the adenoviral sequences in the cell line and homologous sequences in the vector (Lochmuller et al., 1994). Furthermore, it was observed that *in vitro*, the early and late AdV genes were expressed, albeit in a low level, from the I^{st} gen AdV (Christ et al., 1997). Some of the late viral proteins themselves are toxic, and in addition, the expression of the viral proteins results in the stimulation of a cellular immune response *in vivo*, leading to the transduced cells being cleared from the body (Yang et al., 1995, Yang et al., 1994). Inflammation reaction to the Ad was observed in *in vivo* experiments involving mice and baboons (Schiedner et al., 1998, Simon et al., 1993,

Yang et al., 1994). Therefore, only a transient transgene expression was observed in immuno-competent test animals following gene transfer with Ist gen AdV. The second generation Adenoviral vectors (IInd gen AdV) were developed to circumnavigate the immune response generated by the Ist gen AdV. Deletions in the E2 and/or E4 regions were introduced and the functions were provided in *trans* by cell lines stably expressing DBP, pTP, Ad Pol or all the three (Armentano et al., 1995, Engelhardt et al., 1994, Gao et al., 1996, Wang et al., 1997).

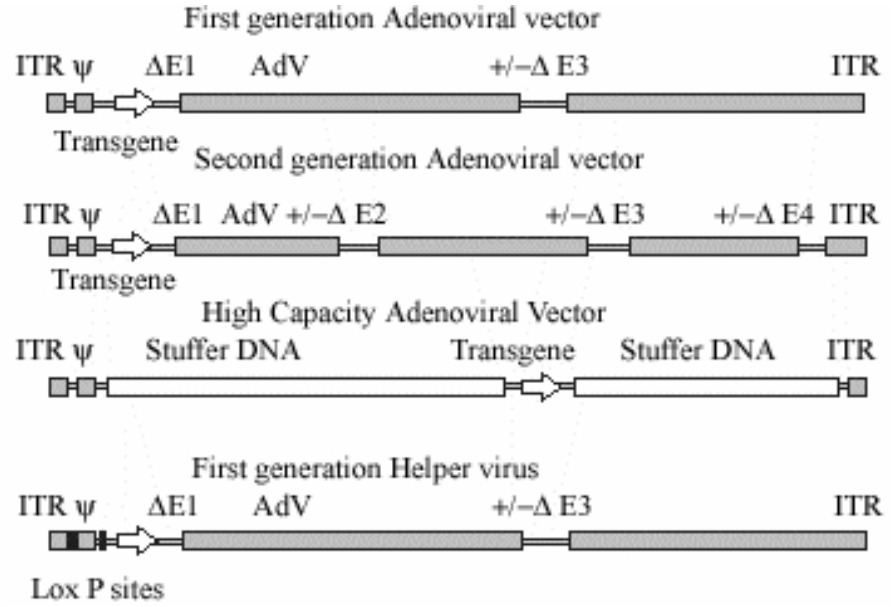

Fig. 3: Schematic representation of the different types of adenoviral vectors used for gene transfer.

Owing to the ambiguous nature of the efficiency of the IInd gen AdV (McConnell & Imperiale, 2004, Volpers & Kochanek, 2004), adenoviral vectors with larger deletions in the genome were developed (Clemens et al., 1996, Fisher et al., 1996, Kochanek et al., 1996, Mitani et al., 1995a) (see Fig. 3). The term high capacity adenoviral vectors (HC-AdV) is used in this study to describe these vectors. HC-AdVs contain only the *cis* viral elements essential for propagation and packaging, the Ad ITRS and the Ψ signal, with a transgene carrying capacity between 26 to 36 kb. The necessary viral proteins, apart from E1, are provided in *trans* by a replication deficient Ist gen AdV helper Virus (HV). The Ψ of the helper virus is flanked by two lox P sites (Floxed) [reviewed by (Branda & Dymecki, 2004)] and when it is

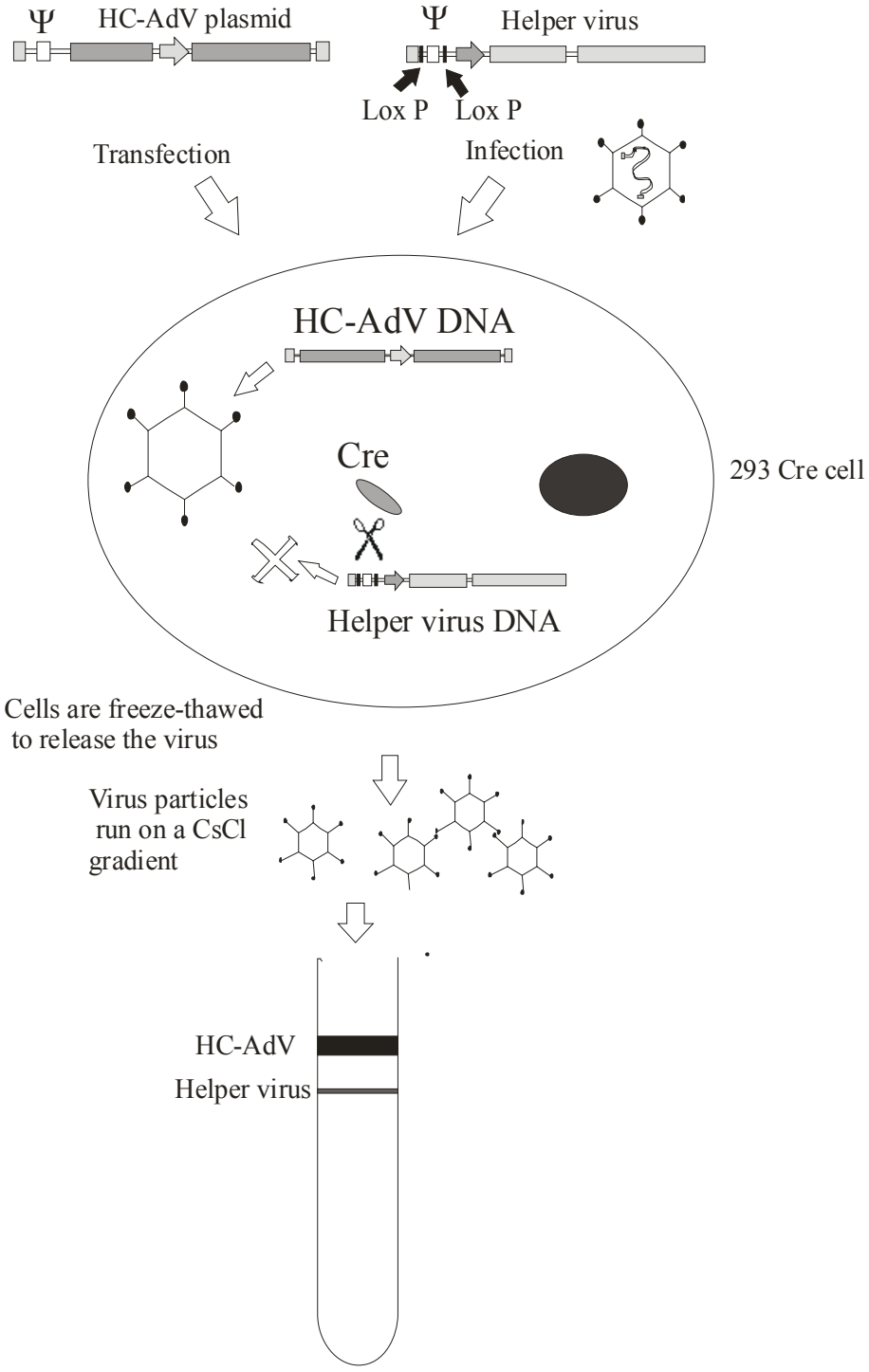

Fig. 4 Schematic diagram of the production of HC-AdV

transduced into a cell line that expresses both E1 and Cre like 293 Cre, then, although all of the viral proteins are expressed, the Cre mediated excision of the Ψ prevents the helper virus itself from getting packaged into the virions. For production, the HC-AdV vector plasmid is linearised and transfected into the cell line, which is then infected with the HV. The cells are collected when they start exhibiting the CPE and

the virus is harvested and used to transduce a larger amount of cells, which are co-infected with the helper virus. Thus, through successive rounds of transduction, the vector is serially amplified and can be finally isolated from any helper virus contamination in the preparation by ultracentrifugation in a CsCl density gradient (for the detailed protocol, see Materials and Methods) (see Fig. 4).

Adenoviral vectors have been used in gene therapy trials involving the liver, muscle, brain, lungs and eye [reviewed by (Alba et al., 2005, Kochanek, 1999, Morsy & Caskey, 1999, Palmer & Ng, 2005, Volpers & Kochanek, 2004)]. As of date (Sept 2006), of all the viral vector systems, the largest number of clinical trials are carried out using vectors based on Adenovirus (n = 305), 26 % of the total number of clinical trials worldwide (visit http://www.wiley.co.uk/genmed/clinical/ for more details).

The advantages that HC-AdV offers to gene therapy of inherited diseases are evident. Transgenes up to 37 kb in size can be accommodated in the vector in comparison to the 8 kb limit in the size of the transgene that can be delivered using the I^{st} gen AdV. In *in vivo* experiments, in contrast to the effects observed when I^{st} gen AdV were used, the HC-AdV did not elicit the immune response directed against the production of the viral proteins in the cell. Furthermore, the acute and chronic hepatotoxicity, which was the hallmark of the *in vivo* experiments conducted with I^{st} Gen AdV, was absent following injection with HC-AdV (Kim et al., 2001, Morral et al., 1998, O'Neal et al., 2000, Schiedner et al., 1998).

However, the toxicity conferred by the incoming Ad capsid itself, cannot be overlooked in a gene therapy trial. The innate immunity is initiated shortly after vector injection, before the viral genes themselves might be expressed, and also even when transcriptionally inactive vector had been injected (Muruve et al., 1999, Muruve et al., 2004, Zhang et al., 2001). This was confirmed when baboons were injected with HC-AdV. On the injection of $5.6x10^{12}$ VP/kg, the immune response subsided after 24 hrs, but on the injection of $1.1\ x10^{13}$ VP/kg, the animal had to be euthanized, as a result of the severe toxicity (Brunetti-Pierri et al., 2004). The amount used in the ornithine transcarbamylase (OTC) gene therapy trial using II^{nd} Gen AdV, that resulted in the death of one of the participants was $6\ x10^{11}$ VP/kg (Raper et al., 2003).

As opposed to the short term expression of the transgene following gene therapy with I^{st} gen AdV, experimental animals injected with HC-AdV displayed long term expression of the transgene. Human α-1 antitrypsin (hAAT) was expressed for more

than 1 year in baboons (Morral et al., 1999), transgene expression was maintained for about 2 years in baboons (Brunetti-Pierri et al., 2006), and Apolipoprotein E (Apo E) was expressed for practically the whole life (2.5 years) in ApoE deficient mice (Kim et al., 2001) following injections with HC-AdV. Phenotypical correction was demonstrated in the hemophilia B dog model for about 2 years (Brunetti-Pierri et al., 2005), and for about a year in a mouse model of glycogen storage disease type II (Kiang et al., 2006). A life term correction of hyperbilirubinemia in a rat model, with negligible levels of toxicity was also reported (Toietta et al., 2005) and long term correction coupled with similar levels of toxicity was observed in the mouse model of the disorder (Mian et al., 2004). These results suffice to demonstrate the promise that HC-AdV offer in the field of gene therapy.

I.3 Vector DNA –chromosomal DNA recombination during gene transfer with viral vectors

I.3.1 Recombination and DNA repair mechanism

The ancient Greek myths spoke of terrible monsters like the Chimera whose body was composed of parts of 3 different animals, or the Hydra that had many heads grafted on to a single body. Myths apart, the various methods of recombination and DNA repair are present to protect the cellular DNA that gets continuously damaged by external sources such as mutagens, ultraviolet rays and internal reactions such as methylation, oxidation and hydrolysis. According to the current model, DNA recombination and DNA repair are no longer considered as two separate systems but as components of a single system that maintains the DNA integrity (Volodin et al., 2005).

Repair via Homologous Recombination (HR) occurs more frequently in the lower forms of life, whereas the repair of DNA by non homologous end joining (NHEJ) repair is preferred by the cells of the higher forms of life. It has been proposed that two protein family complexes, the Rad52 and Ku compete for the broken ends of the DNA and based on the protein that binds first, the repair would take place via HR or NEHJ (Van Dyck et al., 1999). The latest model suggests that in mammals, repair by HR involves an array of gene products from the RAD family. ATM kinase acts as a sensor of the broken ends leading to the binding of the MRE11-RAD50-NBS1 (MRN) complex to the DNA ends. Single stranded overhangs are obtained by the resection of the DNA, either by the MRN complex or replication protein A (RPA). If the double

strand breaks (DSB) had occurred in between repeats, and the cell is in G1 phase of the cell cycle, then the Single Strand Annealing (SSA) of DNA takes place. RAD52 binds the complementary single strands together, and the ssDNA overhangs are removed by ERCC1/XPF, resulting in the deletion of the region between the complementary ssDNA. In the case of the classical HR, which occurs when the cell is in S or G2 phase of the cell cycle, the RPA are replaced by BRCA2, which in turn, recruits RAD51 to the site as the XRCC3/RAD51C complex. RAD51 binds to ssDNA, and crosses over and pairs with the homologous sequences with the aid of RAD54. The break is repaired either by using the intact DNA as a donor or with a classical crossing over of the strands.

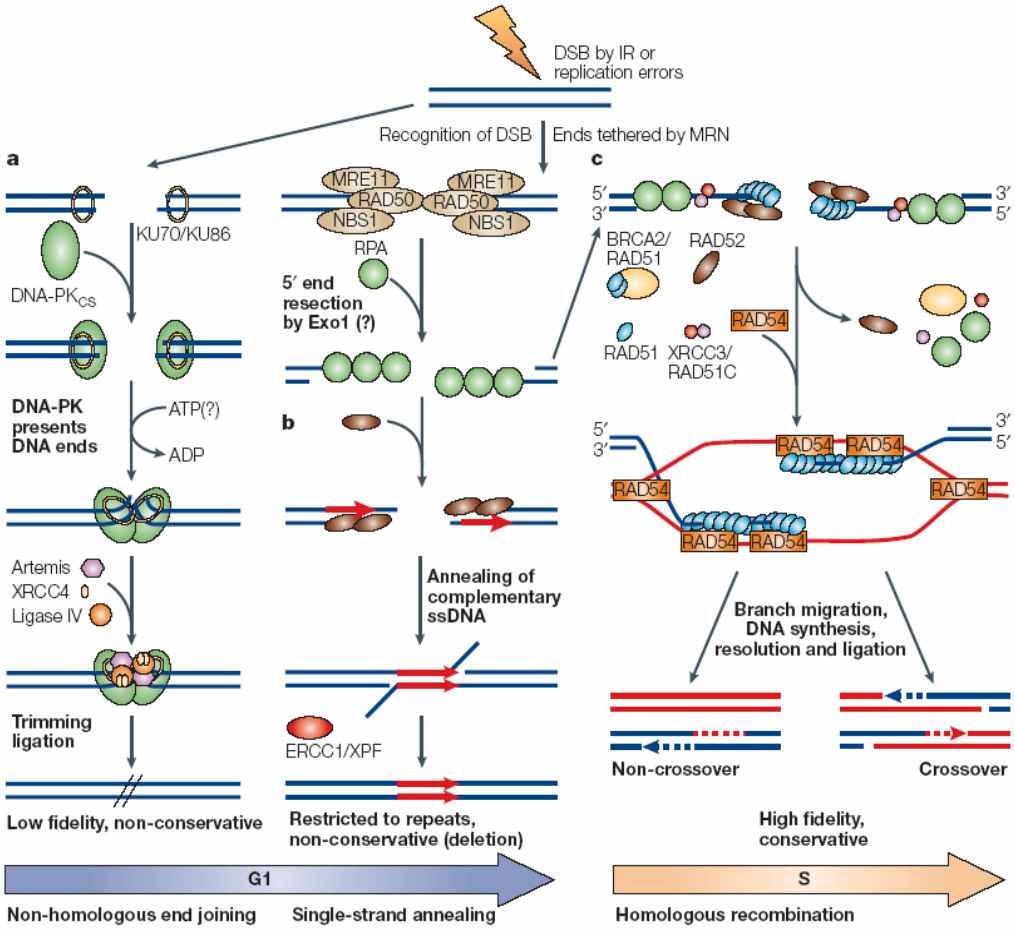

Fig. 5: The various DNA repair pathways present in mammalian cells [from (Vasileva & Jessberger, 2005)}

However, in mammalian cells, the non mutagenic effects of rate of repair via HR is masked by the rate of repair by NHEJ, which occurs predominantly in the G1 phase, by a 1000 to 10000 fold (Wurtele et al., 2003). Inositol 6 Phosphate (IP6) binds to the KU70/KU86 complex, which in turn envelopes the end of the DNA, and recruits

protein kinase, DNA-activated, catalytic polypeptide PRKDC (DNA-PKcs) which bridge the DNA ends. There is evidence to believe that short homologous sequences of 1-4 bps at or near the site of break influence the alignment of the broken ends. DNA-PKcs recruits the nuclease Arthemis that processes the DNA ends. Pol X family members Pol μ and Pol λ fills in the small gaps in the DNA generated during the alignment and nucleolytic processing of the DNA ends. DNA-PKcs also forms a complex with DNA ligase IV/ XRCC4 complex that ligates the broken ends.

When ds DNA breaks are repaired via HR, no mutations take place in the DNA. During SSA, the region between the repeats involved in the repair will be deleted and during NHEJ, massive mutations can take place [reviewed by (Haber, 1999, Hefferin & Tomkinson, 2005, Helleday, 2003, Jeggo, 1998, O'Driscoll & Jeggo, 2006, Taylor & Lehmann, 1998, Valerie & Povirk, 2003, Vasileva & Jessberger, 2005, West, 2003)] (see Fig. 5).

I.3.2 Recombination between chromosomal and viral/viral vector DNA derived from wt Ad and AdVs

Within just 9 years of the first publication about adenoviruses, it was demonstrated that adenoviruses could induce tumour formation in hamsters (Yabe et al., 1962). Six years later, it was proved that adenovirus DNA could integrate into the host genome in semi and non permissive cells where the lytic part of the Ad life cycle could not take place. Infact it, along with a paper on SV40 DNA integration published in the same year, were the first instances of viral DNA integration into the genome (Doerfler, 1968, Sambrook et al., 1968). Ad2 was observed to integrate as simple copies or in a rearranged form, where the viral sequences of the junction site could be amplified. The integrations into the genome appeared to have taken place in a random manner (Sambrook et al., 1980a, Sambrook et al., 1980b). It was observed that the integrated Ad2 DNA could undergo rearrangements and deletions after integration in 8617 rat embryo fibroblasts (Sharp et al., 1974). In hamster cells, Ad7 was observed to integrate as multiple (≅25) copies, which had undergone rearrangements and fragmentation (Fujinaga et al., 1975). Deletions were also observed in the viral genome in Ad5 and Ad2 infected hamster cells (Vardimon & Doerfler, 1981, Visser et al., 1980). In contrast, Ad12 genome had integrated into mouse and hamster genome without the internal deletions (Fanning & Doerfler, 1976,

Stabel et al., 1980, Starzinski-Powitz et al., 1982). Three types of patterns of integration of AdV into the genome were proposed. i. Multiple integrations in different locations. ii. Multiple integrations present in a single site as a tandem, which could arise from repeated replication of a single monomer, or integrated directly as a multimer. iii. A single integrated copy that had undergone multiple rounds of initiation of DNA replication to form a railroad structure (Sambrook et al., 1975). Ad2 and Ad12 were observed to cause chromosomal aberrations in rat and mouse/human hybrid cells (McDongall et al., 1975).

Data on the detailed analysis of Ad integration junction sites in the genome were available from the early 1980s. In the Ad2 transformed rat embryo brain line F4, the virus had integrated with deletion of the last 2 (5'-CA) bps of the viral right terminus. In the Ad12 induced hamster tumour line CLAC3, where 4-5 viral genomic molecules had integrated into the cellular genome, a 45 bp deletion of the viral left terminus was observed. In the Ad2 transformed hamster cell line HE5, two copies of the viral genome were present. No mutations were introduced in the cellular sequence, but 10 and 8 bps deletions were observed in the left and right termini respectively. The site of linkage between the two Ad2 DNA fragments was analysed, a novel dinucleotide was observed to be present between the two recombining molecules. The Ad12 induced tumour cell line CLAC1 had 10-13 copies of integrated viral genomes and on analysis of a left terminus, the first 174 bps of the terminus were absent. A much larger deletion of 572 bps was observed in the Ad5-DNA transformed hamster cell line BHK268-C31. A direct linkage of the 108^{th} bp of the right terminus and the 63^{rd} bp of the left terminus was seen in site of linkage between the left and right termini of the Ad5 DNA transformed rat line 5RK20. In the hamster based Ad12- induced tumour T1111(2), which had 10-11 copies of the Ad genome, a deletion of the terminal 64 bps of the LITR was observed. The 135 bps of cellular DNA was sandwiched by another left terminus, with a deletion of 1296 bps, suggesting that complicated rearrangements of sequences can also take place during the integration of Ad DNA into the cellular genome. A deletion of the first 9 bps was observed in the left terminus sequence obtained from the mouse based Ad12 tumour CBA-12-1-T, which had 20-30 adenovirus genomes. Limited homology (patchy homology/microhomology) extending up to 18 bps between the virus and cellular DNA was observed in almost all cases. The analysis of all of these cell lines and tumours demonstrated that the Ad integrates through the termini, and that deletions in

the termini do occur during the process, which seems to be influenced by the limited homology between the cellular and viral DNAs [reviewed by (Doerfler et al., 1984)]. The data presented in that paper agreed with those already published about the integrations sites of the cell-Ad2 DNA junction where rearrangements of the viral DNA was observed (Sambrook et al., 1980a). The integrations could occur without modifying the cellular DNA (Gahlmann & Doerfler, 1983) or with deletions in the cellular genome of up to 1.6 kb (Schulz & Doerfler, 1984). Sequence data from the "os2" RITR of the Ad in the cell line T637 showed that the terminus was present with a deletion of the first 2 bps and the first 6 bps of the junction were the same in both the cellular DNA and the Ad terminus. In the "os3" junction of the same clone, the LITR with a deletion of 7 bps was joined to a RITR with a 14bp deletion via cellular DNA bridge suggesting that Ad12 genome can integrate in a non true tandem manner, but interspersed with cellular DNA. In the Ad12 induced tumor T191, the left terminus of one Ad genome recombined with the left terminus of another with cellular and internal Ad12 DNA in between (Knoblauch et al., 1996). In a cell free system, using a fragment of Ad12, it was demonstrated that the recombination took place between two short stretches of homology, with the first partner being at or near the site of recombination and the second partner could be remote from the site of the first cross over in a recombination that may not be conservative (Wronka et al., 2002).

The rates of transformation of rat CREF cells by wt Ad5 and of the temperature sensitive mutant H5ts125 were calculated to be around $2x10^{-4}$ for wt Ad and $2\ x10^{-3}$ for the mutant. Almost all the isolated clones of the cell line had the complete Ad5 genome integrated in the cellular genome (Fisher et al., 1982). Fowl Adenovirus type 1 also did not have any specificity towards any particular chromosome in a rat cell line during integration into the genome, but nevertheless, integrations were observed in regions where genomic rearrangement had taken place. These mutations might have been responsible for the transformation (Ishibashi et al., 1987).

Some of the cellular sites at or around the junction of integration between the viral and the cellular genome were observed to be transcriptionally active (Doerfler et al., 1984, Schulz et al., 1987), with significant alterations in the patterns of cellular methylation. In certain cases, not only some neighboring genes, but also ones located remote from the integration site had alterations in the methylation pattern, which were caused by factors other than transgene transcripts from the integrated virus (Lichtenberg et al., 1988, Remus et al., 1999), [reviewed by (Hohlweg et al., 2004)].

Ad DNA was found to be associated with chromosomal DNA within 2 hrs post infection. When Ad12 DNA covalently linked to the TP was added to the medium, it was 20 fold more efficient in reaching the nucleus as apposed to the naked Ad12 DNA (Schroer et al., 1997).

To summarize, the wt Ad genome does integrate at a low rate, in a random manner (Wronka et al., 2004), through the termini, with deletions occurring in the termini. Multiple copies of the virus may be present in the cellular genome, but not necessarily in a truly tandem manner. Rearrangements and deletions of the viral and cellular DNA too can occur. Short sequences of homology between the viral and cellular DNA are present in and around the site of recombination. Many of the integrations had taken place into transcriptionally active regions of the cellular genome [reviewed by (Fechteler et al., 1995)].

The first study of the rates of integration of a adenoviral vector involved the transduction of simian CV1 and Rat2 cells with a Ist Gen AdV carrying a neo-R gene. The vector DNA was shown to integrate at rates of $2x10^{-6}$ to $8.5x10^{-5}$ in Rat2 cells and $5x10^{-5}$ to $2x10^{-4}$ in CV1 cells at mois between 1 to 20 per pfu of virus. At a higher moi of 200, the vector DNA integrated at $4x10^{-3}$ and $7.5x10^{-3}$ in Rat2 and CV1 cells, respectively. The CV1 cells contained single copies of full length viral genomes and the Rat2 cells contained also tandemly repeated viral DNA where the left and the right termini were joined together (Van Doren et al., 1984). A Ist Gen AdV encoding a β-gal marker gene was found to integrate at rates of $1.5x10^{-1}$, when ionizing radiation was used, in mouse NIH3, human A549 and primary human cells (Zeng et al., 1997).

Stable integration into the genome into zona free eggs by a Ist Gen, Ad5 based AdV, was demonstrated in mice. Expression of a *LacZ* gene tagged with a nuclear localization signal under the control of a CAG (chicken β-actin and CMV-IE) promoter was demonstrated even in the F1 progeny. Almost the entire vector DNA had integrated as single copies, randomly throughout the genome, though the terminal fragments at both ends were missing in the integrants (Tsukui et al., 1996). Integration by a Ist Gen AdV expressing β-gal, into the genome *in vivo*, was also demonstrated using immunocompromised B6D2F1 mice transplanted with congenic splenocytes and bone marrow cells. When $2x10^{9}$ to $1x10^{10}$ viral particles were injected, transgene expression was observed for over 6 months in colonic epithelial

cells, but not in the liver, lung, kidney or spleen (Brown et al., 1997). When Ist Gen AdV was injected with doses of 1x10^{8} to 2x10^{10} viral particles into 14-15 day's gestation Balb/c mice fetuses, integration was observed at the site of injection and in the liver. Integration was also observed in the lung, bone marrow, and spinal nerves (Yang et al., 1999). The fumarylacetoacetate hydrolase (*FAH*) knockout mice were injected a Ist gen AdV encoding the FAH cDNA at mois of 5x10^{9} pfu, and integration of the vector was observed in the liver (Overturf et al., 1997). In an *in vivo* study using Ist Gen AdV on a transgenic mouse system, the rate of gene targeting via homologous recombination was observed to be less than 1/20,000, and not significantly different from the controls (Ino et al., 2005).

When a Chinese hamster ovary (CHO) cell line deficient for the adenine phosphoribosyl transferase (*aprt*) was transduced with a moi of 10 by a Ist Gen AdV, gene correction via homologous recombination of the vector into the genome, resulting in the regeneration of the APRT phenotype, was observed in the range of 10^{-6} to 10^{-7}. The correction was of a classical replacement type homologous recombination with no sequences derived from the viral vector or the Moloney Murine Sarcoma Virus (MoMSV) promoter present in the region of correction (Wang & Taylor, 1993). An inserted mutant neo gene in a self replicating extrachromosomal plasmid DNA in the mouse cell line C127 was targeted with a Ist gen AdV carrying the correct copy. At a moi of 400, the rate of homologous recombination was as high as 8.3x10^{-4} with respect to the number of cells used. At a moi of 4, the rate of G418 resistant colony formation was 7.3x10^{-5}. The gene was corrected in all of the clones; however in 25 % of the cases, non homologous recombination was observed outside the region of homology. The rate of homologous recombination with AdV was 3 logs higher than that with calcium phosphate transfection and electroporation. It was suggested that a part of the nonhomologous recombination observed might have been mediated by homologous recombination between the DNA partners (Fujita et al., 1995). The rate of homologous recombination of Ist gen AdV on mouse embryonic stem cells at the *fgr* locus ranged from 1.4x10^{-6} to 1.2x10^{-5} at mois of 100 and 1000 respectively. The rates of integration ranged from 5.2x10^{-6} to 2.1x10^{-4} under the same mois. Each of the recombination event analysed by Southern Blot had only one copy of integrated vector. In 7/12 clones analysed, Ad sequences too were present. In certain experiments, the targeting efficiency (homologous recombination rate/integration rate) percentage was up to 40 % (Mitani et al., 1995b).

The rates of integration of HC-AdV and Ist Gen AdV into the host genome, analysed on the human cell lines HeLa, HT1080, and KB, the simian cell lines CV-1 and Vero and the rodent cell lines BHK, CHO and NIH 3T3 with a fusion β-geo marker (fusion of β-galactosidase and the *neo* genes) infected at a moi of 10, were in the range of 10^{-3} to 10^{-5} per cell, depending on the cell line, with slightly higher rates for the HC-AdV. In HT1080 cells, the Ist Gen AdV integrated at rates between 3.3 x10^{-4} to 2.4 x10^{-3} and the HC-AdV integrated at rates between 2.9x10^{-4} to 1.8x10^{-3}. The rates of integration in HeLa cell for the Ist gen AdV ranged from 3x10^{-5} to 3.1x10^{-4} and those for the HC-AdV ranged from 5.5x10^{-5} to 9.3x10^{-4}. In the clones analysed by Southern Blot, multiple integrations of the right terminus, and possibly one case of a rearranged right terminus, were observed. These were observed in clones where only one copy of transgene was detected. Interestingly, in a clone (clone 4) where 2 copies of the transgene were observed, only one terminus was seen. No internal deletion was observed in the majority of the clones generated via HC-AdV integration, but in one (clone 5), rearrangement of the vector was detected (Harui et al., 1999).

HC-AdV and Ist Gen AdV carrying a *neo* transgene showed rates of integration of 1.7x10^{-4}/ cell and 2.6x10^{-5}/cell respectively, in the human glioblastoma cell line U87-MG when infected at a moi of 0.1. Integration had taken place randomly with the vector integrating as a monomer through the termini. In 50 % (n=16) of the clones, both the termini were present, and in 81 %, the integration had taken place with little or no loss of termini sequences. The HC-AdV contained a 27 kb stuffer DNA from the X chromosome and no event of homologous recombination was observed in the 200 clones analysed (Hillgenberg et al., 2001).

During the preparation of this thesis, two new papers on the rates of recombination of HC-AdV into the genome, have been published. In the first paper, Ist gen AdV and HC-AdVs, carrying varying lengths of *hprt* stuffer DNA (from 1.7 kb to 18.6 kb) were used to transduce male mouse ES cells with a known mutation in the *hprt* exon 3. In the HC-AdV carrying the 18.6 kb *hprt* stuffer, the rate of homologous recombination was 2 x10^{-4}/cell at a moi of 1000. The rate of random integration was in the range of 10^{-3} to 10^{-4}/cell at mois of 10, 100 and 1000. Of the 20 clones analysed, 3 junction sites from both termini were obtained, the other gave sequences from only one of the terminus. 72 % of the integrations took place in non coding regions. Deletions ranging from 1-99 bps in the termini and a case of inversion of the

chromosomal DNA were reported. Limited homologies between the termini and the chromosomal DNA and insertions of novel sequences up to 30 bp were also observed in the junction sites (Ohbayashi et al., 2005).

In the second paper, HC-AdV-AAV hybrids were used in human MO7e cells and in cord derived human CD34+ cells. Two of the hybrid vectors contained the β-globin locus control region, derived from Chr 11. Most of the clones had multiple integrants. 33 % (11/33) of the integrations had taken place in the chr 11, out of which 4 were in the LCR. 30 % (10/33) of the integrations had occurred in active genes. Deletions from 2 to 205 bps were observed in the integration events that had integrated through the Ad terminus. In 3 clones, both the 5' and 3' junctions of the clones were sequenced and deletions of 14, 24 and 567 bps were observed in the chromosomal DNA of the junction sites. Transposition of the chromosomal DNA was observed in many of the integrants with the AAV terminus. A HC-AdV-AAV hybrid vector with a 18.1 kb X chr stuffer DNA was also used. 41.6 % (10/24) of the integrations were in active genes, including one in the *vav2* oncogene. One integration had taken place in the X chr. Deletions were observed in the terminal sequences (Wang et al., 2005).

The gist of all of these publications is that it can be concluded that adenoviral vectors can recombine into the host genome via homologous or random recombination at low frequencies, and the structure of the junction sites between the vector and the cellular DNA are very similar to those observed during wt Ad integration. The integrations seem to occur through the termini, though deletions in the termini are also observed. The vectors use limited homology between the termini and the chromosomal target to guide the process and deletions and rearrangements also may occur in the host genome during the process.

I.3.3 Recombination between chromosomal and vector DNA during gene transfer with vectors derived from the family *Retroviridae*

The family *Retroviridae* consists of enveloped RNA viruses in whose life cycles an obligatory integration of the provirus into the genome takes place. Integration takes place through the termini and they are left intact, apart from the last 2 bps of each terminus, which gets deleted. The only modification to the cellular DNA involves the first 5 bps of the junction site. The first 5 bps of the cellular DNA from the 5' LTR

junction site is duplicated at the 3' LTR junction site, and thus serves as a marker to identify the validity of the junction site (Vincent et al., 1990).

Though it was earlier believed that viral vectors based on the *Retroviridae* family integrate randomly into the genome, it was demonstrated that the integration pattern of retroviral gene transfer vectors (RVV) into human stem cell genome was not as random as expected (Laufs et al., 2003). The partiality of a hybrid RVV to integrate into transcription start regions was observed in the 186 integration sites analysed (Laufs et al., 2004). When 903 murine leukemia virus (MLV) and 379 human immunodeficiency virus (HIV) integration sites were studied, it was observed that the region near the transcriptional start was preferentially targeted by the MLV, whereas the HIV integrated throughout active genes, but not upstream of the transcriptional start (Wu et al., 2003). After analyzing 3127 integration sites from vectors based on HIV, MLV and avian sarcoma-leukosis virus (ASLV), it was reported that the pattern of integration of HIV based gene transfer vectors displayed a bias towards active genes. MLV based gene transfer vectors (MLVV) displayed a preference for integrating into the transcription start sites, while ASLV based gene transfer vectors showed a weak preference for active genes and no preference for the transcriptional start site (Mitchell et al., 2004). This was reconfirmed in a study where 491 MLVV and 501 Simian immunodeficiency virus (SIV) vector integration sites were analysed. MLVV integrations were observed more around the transcription start sites and SIV based gene transfer vector integration sites were observed in active genes and gene rich areas of the genome (Hematti et al., 2004). The correlation between the retroviral based gene transfer vector integration sites and the active genes was published (Wagner et al., 2005). Analysis of foamy viral (FV) vector integration sites showed that the virus preferred not to integrate in active genes. Nevertheless, integrations in active genes too were observed near transcription start sites and in CpG islands (Trobridge et al., 2006).

To summarize, retrovirus based gene transfer vectors display a strong tendency to integrate into active genes, with no rearrangement of the vector and cellular sequences apart from the deletion of the first 2 bps of each terminus and the duplication of the 5 bps of the cellular DNA.

I.3.4 Recombination between chromosomal and vector DNA during gene transfer with vectors derived from the family *Parvoviridae*

Parvoviruses consist of non enveloped small viruses with linear single stranded DNA packaged into a 18-25 nm icosahedral capsid. Wt Adeno Associated virus (AAV) integrates preferentially into a specific locus in Chr 19q13.3 (AAVS1) into the slow skeletal troponin T gene. Studies with gene transfer vectors derived from AAV (AAVV) demonstrated intregration frequencies of $0.2\text{-}1x10^{-3}$ per vector genome. The integrations seem to take place through the termini, with small deletions in the termini (Rutledge & Russell, 1997). Limited homology of 2-5 bps between the cellular and viral DNA were observed at the junction. During the analysis of 977 AAVV integration sites, it was noticed that a larger number of integrations took place in active genes. A significantly higher proportion of integrations took place in CpG islands, within the first 1 kb of genes and in ribosomal DNA repeats. Deletions of up to 2 kb of the cellular DNA, and insertions of novel sequences of up to 13 bps were observed at the junction sites (Miller et al., 2005). Chromosomal translocations at the junction sites too have been reported [reviewed in (McCarty et al., 2004)]. *In vivo* data suggested a much more higher percentage (72.5 %) of AAVV integration into genes, which were active in the liver (Nakai et al., 2003). Concatomerisation of the vector and deletions and amplifications of viral and cellular DNA were also observed (Miller et al., 2002, Nakai et al., 1999). The preference of AAVV for integration into CpG islands in the genome was observed in 347 AAV1 junction sites analysed. 3.5 % of the integrations took place in cancer related genes (Nakai et al., 2005). AAV integrations had occured around chromosome breakage sites (Miller et al., 2004).

The rate of gene targeting via homologous recombination of AAVV into the cellular genome was reported as $8x10^{-3}$ at an moi of 40,000 and $2.7x10^{-2}$ at mois of 400,000 (Russell & Hirata, 1998). Ten individual mutations (up to around 20 bps) were corrected by gene targeting using AAVV in a different experiment. However, rearrangements at the 5' end of the homology was reported in one of the events (Inoue et al., 1999). Transgenes of up to 1 kb was introduced via homologous recombination of AAVV with rates of gene targeting going up to $7x10^{-3}$ at mois of 20,000 (Hirata et al., 2002). The effects of random integration of the vector into the genome at these mois were not discussed in these papers.

Vectors based on Parvo Minute Virus of Mice recombine via homologous recombination and random integration at the same rates as AAVV (Hendrie et al.,

2003). It has also been reported that the invertebrate parvovirus *Junonia coenia* Desnovirus (JcDNV) based vectors integrate in a similar manner as AAVV into the genome, with concatomerization and rearrangements of the vector (Bossin et al., 2003).

When the recombination potential of parvovirus based vectors is studied, it can be concluded that they integrate at frequencies of up to $1x10^{-3}$ into the genome. A higher proportion of the integrations takes place in active genes and rearrangements and modifications of the genomic DNA may accompany such events. Under certain conditions, AAVV genome can undergo homologous recombination with the cellular genome at rates of $2.7x10^{-2}$.

I.3.5 Recombination between chromosomal and vector DNA during gene transfer with vectors derived from the family *Papillomaviridae*

Papilloma viruses are non enveloped DNA viruses with a dsDNA genome of 8 kb and an icosahedral capsid. Vectors based on bovine papilloma virus (BPV), which can be grown *in vitro*, were tested as early as 1987 (Elbrecht et al., 1987). It has been reported that wt BPV and BPV vector remain as episomes (Amtmann et al., 1980, Tammur et al., 2002), nevertheless, integrations of BPV into the genome with small deletions in the termini of the viral DNA has been reported (Agrawal et al., 1992). In fact, an equine skin tumor has been associated with BPV (Chambers et al., 2003). Though there is not a lot of published data regarding the integration of Papilloma vectors, wt human papilloma virus (HPV) was associated with cervical cancer and was observed to integrate frequently into the genome (Gilles et al., 1996). During integration into the genome, the E1 and the E2 regions, which span 4 kb of the genome from the 5' side, were found to be frequently deleted (reviewd in (Yoshinouchi et al., 1999). Random integration of the HPV genome into the cellular DNA with minor deletions in the viral DNA was observed (Kalantari et al., 2001, Luft et al., 2001). It was observed that HPV integrates into active genes, especially genes involved in cellular growth and differentiation (Klimov et al., 2002). HPV16 integrations were observed near fragile sites in the genome (Thorland et al., 2003), whereas HPV18 not only displayed a similar preference for the fragile sites, but 30% of the integrations took place in a specific location at Chr 8q24 (Ferber et al., 2003b).

To summarize, papilloma viruses display a tendency to integrate non randomly into active genes, near protooncogenes or at fragile sites in the genome. Parts of the terminal sequences of the virus might get deleted during the process.

I.3.6 Recombination between chromosomal and vector DNA during gene transfer with vectors derived from the family *Herpesviridae*

Herpesviridae are large enveloped viruses with an icosahedral capsid that is located in the tegument inside the envelope and a ds DNA genome of about 150 to 230 kbps. Vectors based on Herpes Simplex Virus (HSV) and Epstein Barr Virus (EBV) are currently in use in *in vitro* and *in vivo* studies (Basu & Banerjee, 2004, Glorioso & Fink, 2004, Hellebrand et al., 2006, Ren et al., 2006, Tomiyasu et al., 1998). During the latent infection in the life cycle of the virus, the genome remains as a circular episome through the joining of the termini. Nevertheless, integration of the virus into the host genome through intact termini has been observed [reviewed in (Chang et al., 2002)]. Translocation of a chromosome at the integration site of the viral DNA into human genome (Debiec-Rychter et al., 2003) and integration via intact termini at a fragile site near a protooncogene and the subsequent expression of that gene (Luo et al., 2004) has been reported during integration of EBV into the genome. The virus was present as tandem repeats (Takakuwa et al., 2005). Site specific integration into chr 19 was achieved using hybrid HSV-AAV vectors (Bakowska et al., 2003, Liu et al., 2006, Wang et al., 2002).

Though in the latent infection most of the *Herpesviridae* viral genomes remain as episomes, there is a possibility that integration of the virus in a random manner into the host genome, possibly as concatamers, can occur through the termini sequences.

I.3.7 Recombination between chromosomal and vector DNA during gene transfer with vectors derived from the family *Hepadnaviridae*

Hepadnaviridae are small enveloped viruses with an icosahedral capsid and a circular dsDNA genome of 3.5 kb. 15-20% of one of the strands of the Hepatitis B virus (HBV) DNA is single stranded. Vectors based on HBV have been developed (Untergasser & Protzer, 2004). During the life cycle, the viral DNA remains as a covalently closed circular duplex DNA. However, integration of the viral genome with rearrangements such as deletions, chromosomal translocations and duplication in the cellular DNA, and activation of cellular genes has been observed [reviewed in

(Wang et al., 2001)]. The integration was observed throughout the genome, with a number of integrations near protooncogenes [reviewed in (Ferber et al., 2003a)]. It was suggested that HBV DNA integration takes place in regions of chromosomal DNA breaks via non homologous end joining (Bill & Summers, 2004). Deletion of viral DNA during integration was reported (Kimbi et al., 2005). Analysis of junction sites of viral integration showed that 90 % of integrations took place into cellular genes that could confer growth advantage. Mutations in the viral DNA (Koike et al., 1983, Mizusawa et al., 1985) and chromosomal DNA (Tokino et al., 1987) have been reported. Integration was also mapped into tumour supressors and apoptosis genes (Murakami et al., 2005).

It can be concluded that HBV viral DNA can integrate into the genome and the events are marked with mutations in the cellular DNA. The data published so far suggests that the viral DNA can integrate in genes that may have oncogenic potential.

I.3.8 Recombination between chromosomal and vector DNA during gene transfer with vectors derived from the family *Polyomaviridae*

Polyomaviridae are small non-enveloped viruses with an icosahedral capsid and a circular ds DNA genome of around 5 kb, that lacks terminal repeats. During the life cycle of wt Simian Virus 40 (SV40), the virus may exist either as a minichromosome or in an integrated form. Wt SV40 DNA integrates randomly into the genome, with no apparent hotspot within the viral DNA for integration. Vectors based on SV40 have been developed (Zern et al., 1999), used in *in vitro* and *in vivo* experiments [reviewed by (Vera & Fortes, 2004)] and were found to integrate randomly into the genome with loss of viral DNA (Strayer et al., 2002, Strayer, 1999). During the integration of a vector based on polyoma virus integrated into the rat genome deletions of the cellular DNA was reported (Wallenburg et al., 1987). The upregulation of gene expression due to polyomaviral integration in mouse tumors was also reported (Hollanderova et al., 2003). Integration of wt SV40 has also been recorded in human tumors (Shivapurkar et al., 2002, Vilchez et al., 2003). Polyoma JC virus was linked to colorectal cancer and was shown to induce chromosomal mutations in colonic cells (Ricciardiello et al., 2003).

From the available data, it may be concluded that polyoma viruses integrates randomly into the host genome, with deletions observed in the viral DNA, and mutations in the host genome.

Some viruses used as gene thransfer vectors integrate into the genome as a part of their life cycle. Though it was once thought to occur in a random manner into the chromosomal DNA, the data compiled here display a strong bias displayed towards integration into active genes. In the case of viral vectors that may not necessarily integrate into the genome as a part of the viral life cycle, integrations have been observed, and they display all the hallmarks of the canonical NHEJ pathway.

II Objectives

Gene transfer with adenoviral vectors has now been well established and currently clinical trials using this vector type are ongoing. Adenoviral vectors are currently perceived as non-integrating vectors, although earlier work demonstrated that adenovirus DNA can integrate into chromosomal DNA under certain circumstances. HC-AdVs represent a more recent adenovirus-based vector version with several advantages over earlier generation adenoviral vectors and have, therefore, considerable potential for clinical application. However, very little information on the fate of adenoviral vector genomes following gene transfer is available. Very limited work with Ist Gen AdV pointed to rare chromosomal integration events. However, when this thesis work was started, there were no data available on the recombination potential of HC-AdVs.

The development of leukaemia in several subjects during a clinical trial using a retroviral vector reiterated the importance of studies on the insertional mutagenesis potential of gene transfer vectors used in the clinic. Therefore, the overall aim of this thesis project was to gain scientific information on the recombination potential of HC-AdV DNA with the chromosomal DNA. The first specific aim was to determine the rates of heterologous and homologous recombination of the HC-AdV DNA with the chromosomal DNA *in vitro* in primary cells and in established cell lines. To address this question, two well established models were chosen. The hprt model, which has been extensively used in DNA recombination studies, was used to study homologous recombination of HC-AdV DNA with the chromosomal DNA. The second model involved the use of a selection marker expressed from the vector, which allowed for the investigation of random integration events into the chromosomal DNA.

The second specific aim of this project was to investigate heterologous and homologous recombination events of HC-AdV DNA with chromosomal DNA *in vivo*. Here, the Fah$^{\Delta \text{ exon } 5}$ knockout mouse was chosen as an excellent model that allows to monitor recombination events in hepatocytes *in vivo*. The final aim of this project was to analyse integration events of HC-AdV DNA at the molecular level, so that precise information on the integrity of the vector genomes and the junctions between vector DNA and the chromosomal DNA was obtained. This would then also allow the analysis of potential integration preferences of HC-Ad vector genomes.

Taken together, these studies were designed to provide detailed safety-related information on rates of recombination of HC-AdV DNA with chromosomal DNA, the insertional mutagenesis potential of HC-AdVs, and the integration patterns of the vector DNA.

III Materials and Methods

III.1 Materials and Instruments

III.1.1 Materials

All chemicals, unless specially mentioned, were purchased from the company Applichem GmbH (Germany). The solutions were prepared using water obtained from EASY pure instrument (Werner Water Purification System, (Germany). The bacterial media and agar was purchased from Invitrogen (Germany). The Enzymes were purchased from NEB (Germany). Oligonucleotides were purchased from Invitrogen, Qiagen or MWG Biotech (Germany). Cell culture media when not specially mentioned were purchased from Invitrogen (Germany). All cell culture materials (cell culture dishes, pipettes etc.) were purchased from Renner (Germany).

III.1.2 Instruments and equipment

Autoclave	Systec (Wettenberg)
Cell culture hood	Clean Air Technique. (Netherlands)
Cell culture Incubator	Forma Scientific, (U.S.A)
Centrifuges	Biofuge fresco (Germany) Eppendorf 5417C (Germany) Sigma 6K15 (Germany)
Heating block	VWR (Germany)
Incubator (Bacterial culture, enzyme reactions, pipette sterilization)	VWR (Germany)
Mini hybridization oven	Biometra Biomedizinische Analytik GmbH (Germany)
PCR thermocycler Uno II	Biometra Biomedizinische Analytik GmbH (Germany)
pH-meter pH526	WTW GmbH (Germany)
Spectrophotometer	Pharmacia Biotech (Germany)
Ultracentrifuge	Beckman, L7-65 with SW41- Rotor (USA)

III.1.3 Buffer and Solutions

DNA-loading buffer (6x)

30%	Glycerin
60 mM	EDTA
0.1%	Bromophenol Blue
0.1%	Xylene cyanol Blue

HBS-Buffer (2x)

50 mM	HEPES
280 mM	NaCl
1.5 mM	Na_2HPO_4
pH	7.13

Hybridization buffer for slot blot and Southern blot

2x	SSC
10 %	Milk powder solution
0.5 mg/ml	Herring sperm
10 %	Dextran sulfate

Tra**nsfer buffer for Southern blot analysis**

0.4 N	NaOH

Wash Buffer I for Southern blot

2x	SSC
0.1 %	SDS

Wash Buffer II for Southen blot

0.1x	SSC
0.1 %	SDS

Milk powder solution for the above work

5.0 %	Milk powder
10 %	SDS

PCR-Mix

DNA	Plasmid DNA at 1-10 ng concentration
	Genomic DNA at 1-2 µg concentration
Taq polymerase buffer	1x
Taq polymerase	1.25 units [Stratagene (Netherland)]
dNTP-Mix	40 nmol [(La Roche (Germany)]
dH_20	up to a volume of 50 µl

Sodium phosphate-buffer pH 8.0 (100 mM)

46.6 ml	1M Na_2HPO_4
3.4 ml	1M NaH_2PO_4
8.8 gm	NaCl
500 ml	dH_2O

SSC Solution (20x)

3 M	NaCl (sodium chloride)
0.3 M	$C_6H_50_7\ Na_3\ 2H_2O$ (tri-sodium citrate)
pH	7.0 (adjusted with NaOH)

TAE-Buffer (50x)

2.0 M	Tris-Base
0.05 M	Acetic acid
0.05 M	EDTA
0.225 M	Tris base
0.225 M	Boric acid
0.02 M	EDTA

TBS-Buffer (1x) for resuspension of virus

137 mM	NaCl
2.7 mM	KCl
25 mM	Tris-Base
pH	7.4 (adjusted with HCl)

(The solution was sterilized by autoclaving)

TE Buffer (1x)

10 mM	Tris-HCl, pH 7.5
1 mM	EDTA

TELT Buffer

50 mM	Tris-HCl, pH 8.0
62.5 mM	EDTA
2.5 M	LiCl
0.6 %	Triton X-100

One spatula of Lysozyme

Lysis Buffer for DNA isolation

10mM	Tris.Cl (pH 7.4)
10mM	EDTA
10mM	NaCl
0.5 %	Saodium Lauryl Sarcosinate
1mg/ml	Proteinase K

Suspension medium (S.M.) for Lambda DNA isolation

1.5 mM	NaCl
2 gm	$MgSO_4.H_2O$
50 ml	1 M Tris.HCl pH. 7.5
5 ml	2% Gelatin Solution
To 1 lit	H_2O

Soln I for hepatocyte isolation

Earles basic Salt Solution (EBSS) without Ca and Mg, [Gibco 310-4150 AJ]

0.5 mM	EGTA [Sigma 4378]

Soln II for hepatocyte isolation

EBSS with Ca and Mg [Gibco 310-4010 G]

10mM	Hepes, pH 7.4

Soln III for hepatocyte isolation

High Glucose DMEM [Gibco 320-1960 AJ] complete

0.3 mg/ml	Collagenase [Boehringer, grade D] soln
0.04 mg/ml	Soybean trypsin inhibitor [Sigma T9128]
10mM	Hepes and Mg,

III.1.4 Oligodeoxyribonucleotides

The oligodeoxyribonucleotides were purchased from Invitrogen, Qiagen and MWG Biotech. The lyophilized oligonucleotides were dissolved in 1xTE buffer and were stored at –20^{o}C. Oligodeoxyribonucleotides used for ligation were dissolved in 10 mM Tris buffer. The details are given in Table 3.

Name	**Sequence 5'- '3**	**Binds to/Comments**
Fiber I	ATGAAGCGCGCAAGACCGTCTG	31042-31063, Ad 5
Fiber II	CCAGATATTGGAGCCAAACTGCC	32368-32390, Ad 5
ITR I	AACGCCAACTTTGACCCGGAACGCGG	438-413, Ad 5
ITR II	CATCATCAATAATATACCTTATTTTG	1-26, Ad 5
SamStephenI	CAGTATCACCAGGTTATGACCTTTGAT ATCTTTTGCATACCTAATCATTATGC	13480-13525, SLS 11 T nucleotide + *Eco RV* site
SamStephen II	ATTCAATACCAGGTAAGGTTT	13977-13957, SLS 11
InvPCR LITR1	CGCCCAGGTGTTTTTCTCAGGT	399-420, SLS 11
InvPCR LITR2	GCAACATCACACTTCCGCCAC	141-121, SLS 11
InvPCR RITR1	CATCACTCCGCCCTAAAACCTA	30224-30247, SLS 11
InvPCR RITR2	TTGATTTAATTAAGGCCGGCCC	30191-30170, SLS 11
AdRITR new	GCTTATCGATACCGTCGAGACCTCG	30192-30216, SLS 11
AdRITR2	CGTCACCCGCCCCGTTCCCACGC	30247-30269, SLS 11
AdLITR new	CCGTCGCTTACATGTGTTCCGC	170-149, SLS 11
AdLTR2	CTACTACGTCACCCGCCCCGT	119-99, SLS 11
Ad11LITRnew	CGTCGCTTACATGTGTTCCGCCAC	169-146, SLS 11
LITRnested	TACTACGTCACCCGCCCCGT	117 to 99, SLS 11
Inv LITR new	CGCCCAGGTGTTTTTCTCAGGT	399-420, SLS 11
InvPCRLITR2nest	CCGCGTTCCGGGTCAAAGTTGGC	426-449, SLS 11
InvLITR1new	GCAACATCACACTTCCGCCAC	141-121, SLS 11
SLS16RsvFah1	GACAGGTCTGACATGGATTGG	484-504, FAH cDNA cassette
SLS16RsvFah2	CTCCTTCCATGCAGCTTGACC	881-861, FAH cDNA cassette
RITR1	CATCACTCCGCCCTAAAACCT	30225-30245, SLS 11
RITR1nest	TAAAACCTACGTCACCCGCC	30238-30258, SLS 11

RITR2	GGTCTCGACGGTATCGATAAGC	30211-30192, SLS 11
RITR2 nest	TTGATTTAATTAAGGCCGGCCC	30190-30170, SLS 11
RITR4Tsp	CCCTCGAGGTCTCGACGGTAT	30220-30200, SLS 11
RITR4nestTsp	CGACGGTATCGATAAGCTTGA	30208-30188, SLS 11
LITRx	TCCGTCGCTTACATGTGTTCC	171-151, SLS 11
LITR1	GCAACATCACACTTCCGCCAC	140-129, SLS 11
LITR1nest	TACTACGTCACCCGCCCCGT	118-99, SLS 11
LITR2	CGCCCAGGTGTTTTTCTCAGGT	398-420, SLS 11
LITR2nest	GCGTTCCGGGTCAAAGTTGG	428-446, SLS 11
LITR4Tsp	TGACGTTTTTGGTGTGCGCCG	183-203, SLS 11
LITR4nestTsp	GCCGGTGTACACAGGAAGTGA	200-220, SLS 11
SSHPRT1	GTATCCTGTAATGCTCTCATTG	13421-13442, SLS 11
SSHPRT2	AGCATTCAATACCAGGTAAGG	13979-13960, SLS 11
Fah A	CTAGGTCAATGGCTGTTTGG	6571-6590, m FAH gene
Fah B	GGACATACCAATTTGGCAAC	6705-6686, m FAH gene
Fah C	TAAAATGAGGAAATTGCATCG	3911-3931 pcDNA3

Table 3: List of oligonucleotides used in this study

III.2 Bacterial Methods

III.2.1 Bacterial culture techniques

a) Culture of bacteria in Luria Broth Base

E.coli was cultured in Luria Broth Base in the presence of the antibiotic ampicillin at a concentration of 100 μg/ml. For small-scale preparation (1.5 ml) eppendorf tubes with a capacity of 2.0 ml were used. For large scale preparation (200 ml), Erlenmeyer flask with a capacity of 500 ml were used. The cultures were incubated for 12h with shaking at 250-300 rpm at 37^{o}C.

b) Culture of bacteria in Luria Broth Agar

E.coli was cultured in 10 cm plates containing 20 ml of Luria Broth Agar containing ampicillin at a concentration of 100 μg/ml.

c) Culture of Bacteria in NZYCM medium

E.Coli XL1 Blue MRA P2 [Stratagene] was cultured in 50 ml NCYZM + 0.1 gm Maltose

III.2.2 Transformation of *E.Coli*

Transformation with plasmid DNA

Transformation of *E.coli* with plasmid DNA was performed by incubating 20 µl of XL-2 blue ultra competent bacteria (Stratagene, Germany) with 10-100 ng of plasmid in a 1.5 ml Eppendorf reaction tube for 5 min in ice. After five minutes incubation in ice, the bacteria were placed in a water bath at a temperature of 42^{o} C for 45 seconds. The bacteria were then immediately placed in ice for 2 min and SOC medium was added. The bacteria were incubated for 1h at 37°C. After 1h the bacteria were transferred to LBA plates containing antibiotic ampicillin and were incubated for 12h.

Transformation with plasmid DNA from ligation

To transform bacteria using a ligation mix, 50 µl of XL-2 blue ultra competent bacteria (Stratagene, Heidelberg) were incubated with 0.5 µl of 2-Mercaptoethanol (1.42 M) for 10 minutes on ice. After 10 minutes, 2 µl of ligation mix was added and the bacteria were further incubated for 30 min in ice. The bacteria were placed in a water bath having a temperature of 42^{o} C for 45 seconds. The bacteria were then immediately placed in ice for 2 min and 200 µl of SOC medium was added. The bacteria were incubated for 1h at 37° C before being transferred to LBA plates containing antibiotic and were incubated for 12h

III.2.3 Isolation of plasmid DNA

Analytical plasmid isolation ("Mini prep")

Mini prep of DNA was performed to analyze the integrity of DNA by restriction digestion. Isolated bacterial clones picked from Luria Broth Agar plates were grown over night (12-14h) in 1.5 ml of LB shaker culture containing ampicillin at 100 µg /ml. The bacteria were pelleted by centrifuging at 5000 RPM for 3 minutes at RT. The bacterial pellet was re-suspended in a volume of 200 µl of TELT buffer. The re-suspended bacterial pellet was incubated at 96ºC for 3 min followed by incubation in ice for 5 minutes. The supernatant containing DNA was collected by centrifugation at 14,000 RPM for 10 minutes. The DNA present in the collected supernatant was precipitated by mixing the supernatant with equal volume of isopropanol and centrifuging at 20000 g for 10 minutes. The precipitated DNA was washed once with 300 µl of 70 % ethanol. The DNA was finally suspended in a volume of 30 µl of TE and was stored at 4ºC until further use. 3 µl of the re-suspended DNA was used for restriction digestion.

Preparative plasmid Isolation. ("Maxi prep")

Maxi prep of DNA was performed to obtain large quantities of DNA for transfection, cloning etc. The DNA was prepared using the Qiagen Maxi Plasmid Kit (Qiagen). The protocol prescribed by the manufacturer was followed.

III.3 Molecular Biology Methods

III.3.1 Purification of the DNA cloned into Lambda Phage Vectors

a. Preparation of the plating bacteria.

The bacterial host XL1 Blue MRA P2 [Stratagene] was streaked on to a LB plate and incubated at 37^0C overnight. A colony was inoculated on to 50 ml of sterile LB medium, supplemented by 0.2 % maltose and incubated overnight. The bacteria was centrifuged down and resuspended in 20 ml 0.01 M $MgSO_4$ and store at 4^0C.

b. Plating the bacteria onto the LB plates with the phage.

0.7% LB agar was made in suspension medium and incubated at 47^0C water bath.

Ten fold serial dilutions of the λ stock in SM was made. 100 ml of plating bacteria was added to each of the dilutions and incubated at 37^0C for 20 mins. 3 ml of the agar was poured into each tube, and the plate was incubated at 37^0C overnight.

c. Picking of the λ plaques:

A drop of chloroform was added in 1 ml of SM. The plaques were jabbed with a micopipette tip, the agar in the region was pipetted into an eppendorf tube. 1 ml of SM was added to it and the tube was stored at 4^0C.

d. Preparation of plate lysate stock.

Dilutions of the picked plaque were made and mixed with 100 ml of plating bacteria each and incubated 37^0C for 20 mins. 3 ml of molten top agar was added and the plate incubated at RT for 5 mins before incubating it at 37^0C for 10 hrs. 5 ml of SM was added on to the plate and was store at 4^0C overnight with intermittent shaking. The SM was harvested and 0.1 ml of $CHCL_3$ added and the centrifuged. The supernatant was collected and stored at 4^0C with a 1 drop of $CHCL_3$.

e. Large scale preparation of the λ vector.

A starter culture of the bacterial host in 50 ml of NCYZM + 0.1 gm maltose was produced till the $O.D._{600}$ nm reached 5 (approx. 2.5 hrs). Different diluations of the starter culture was added to 50 ml of NCYZM + 0.1 gm maltose and incubated at

37^0C till the medium cleared and fine splintery precipitate or stringy clumps was observed. A drop of $CHCL_3$ was added and the supernatent were harvested and stored at 4^0C.

f. Preparation of the Lambda DNA using Qiagen Lambda Kit.

100µl of Buffer L1 was added to the pellet and mixed 10 ml of Buffer L2 was added and the reaction and the pellet resupended in 3 ml of Buffer L3. 3 ml of Buffer L4 was added and the reaction incubated at 70^0C water bath for 10 mins. 3 ml of L5 was added, the reaction centrigufed and the supernatnat poured into a Qiagen tip 100 equilibrated with buffer QBT. The tip was washed with Buffer QC and the DNA eluted with Buffer QF. DNA precipitation was carried out as in a standard Mediprep.

III.3.2 Isolation of DNA from mammalian cell lines

$1x10^7$ cells were spun down and resuspended in 500 µl of Lysis Buffer and incubated overnight at 60^0C. 1250 µl of precipitation buffer (3 µl 2.5 M NaCl / 100 µl Ethanol) was added and centrifuged to obtain the DNA pellet that was washed three times with 70% ethanol before being resuspended in TE.

III.3.3 Determination of the concentration of DNA

The concentration of DNA was determined using spectrophotometry. The concentration of the DNA present in the solution was calculated using Lambert Beers Law which states concentration of double stranded DNA in mg/ml= A_{260} x 50 x dilution factor, whereby A is the adsorption coefficient of DNA at 260 nm. The solution was also measured to determine the absorption at 280 nm for proteins. DNA samples containing A_{260}/A_{280} values of 1.7-2.0 were used for experiments.

III.3.4 Storage of DNA

For routine use, plasmid DNA was stored in TE buffer, pH 8 at 4^oC. For long-term storage, plasmid DNA was dissolved in 70% ethanol and was stored at -20^oC. Oligodeoxynucleotides and vector inserts used for ligation were stored in 10 mM Tris buffer.

III.3.5 Precipitation of DNA

Ethanol precipitation

Ethanol precipitation of solution containing DNA was performed by mixing 0.1 volume of sodium acetate solution (3 M, pH 5.2) and 2 volumes of 100 % ethanol. After mixing, DNA was collected by centrifuging at 20,000 g for 30 min at 4^{o}C. The supernatant was discarded and the pellet was washed with 70 % ethanol by centrifuging at 20,000g for 30 min at 4^{o}C. The supernatant was discarded and the pellet was air dried at RT for 5-10 min. The pellet was dissolved in TE buffer. Vector inserts and oligodeoxynucleotides were dissolved in 10 mM Tris buffer.

Isopropanol precipitation

Isopropanol precipitation of solution containing DNA was performed by mixing the DNA solution with 0.5 volume of isopropanol. After mixing, the DNA was pelleted by centrifuging at 20.000 g for 20 min at RT. After discarding the supernatant, the pellet was washed with 70 % ethanol for 30 min at 4 ^{o}C. The supernatant was discarded and the DNA was air dried at RT for 5 min before being resuspended in TE buffer.

III.3.6 Phenol chloroform extraction of DNA

Phenol-chloroform extraction of DNA was performed when DNA was used for ligation or for transfection of cells. 200 µl of DNA containing solution was mixed with an equal volume of TE equilibrated phenol (Invitrogen, Germany). After mixing the aqueous and organic phase were separated by centrifugation at 20,000 g for 4 min at RT and the organic phase was discarded. The aqueous phase was once again mixed with equal volume of chloroform/isoamyl alcohol (24:1) and the aqueous phase was separated by centrifuging at 20.000 g for 4 min at RT. The DNA present in the aqueous phase was finally precipitated by using ethanol.

III.3.7 Restriction digestion of DNA and agarose gel electrophoresis

The restriction analysis was performed with 10 µg or 200 ng of DNA for preparative or analytical digest respectively. DNA was digested with restriction enzyme (5 IU/µg of DNA) in the prescribed buffer for 2h. DNA was digested in a total volume of 20 µl or 200 µl. In the case of double digestion of DNA with enzymes having different prescribed buffers, the digested DNA was precipitated with ethanol and was re-suspended in Tris-HCl (pH 8.5), before being re-digested. The digested DNA

fragments were dissolved in DNA loading buffer, and were separated in a 0.8 % agarose gel. The agarose gel used for the separation of DNA bands contains ethidium bromide for visualizing the DNA. TBE running buffer was used for analytical preparation of DNA. TAE running buffer was used for preparative digests of DNA.

III.3.8 Isolation of DNA fragments from agarose gels

Digested DNA for preparative analysis was separated by agarose gel electrophoresis. The separated DNA was visualized under U.V. light. The desired DNA band was cut out using a sharp scalpel. DNA bands having a size of less than 5 kb were isolated using QIAEX II Gel extraction kit. DNA bands having a size of more than 5 kb were isolated by electroelution using the Elu trap electrophoretic system (Schleicher & Schuell, Germany). The isolated DNA was precipitated using ethanol and was re-suspended in 20 of µl 1x TE buffer.

III.3.9 Filling up of 5´ends (Klenowing)

Filling up of 5´ends of DNA fragments was performed to ligate non-cohesive ends. Klenowing of DNA was done by incubating DNA (50 ng/ µl) with 2 units of Klenow enzyme for 15 minutes in Klenow buffer. After 15 min, the Klenow enzyme was inactivated by the addition of 5 mM EDTA and incubation at 75ºC for 10 min. The dephosphorylated DNA was extracted with an equal volume of phenol followed by chloroform: isoamylalcohol mix (24:1). The DNA was finally extracted with chloroform and was precipitated with twice the volume of 100 % ethanol and 1/10 amount of 3 M sodium acetate (pH 5.2). The precipitated DNA was re-suspended with 20 µl of 10 mM Tris-HCl (pH 8.5).

III.3.10 Dephosphorylation of DNA fragments

Dephosphorylation of the digested vector DNA was performed to prevent self-ligation. Dephosphorylation was done by incubating 1-2 µg of DNA with 1U of calf intestinal phosphatase (CIP) at 37ºC for 1h at 50 ng/µl concentration. CIP was inactivated by the addition of 5 mM EDTA and incubation at 75 ºC for 10 min. The dephosphorylated DNA was extracted with an equal volume of phenol followed by chloroform: isoamylalcohol (24:1). The DNA was finally extracted with chloroform and was precipitated with twice the volume of 100 % ethanol and 1/10 amount of 3 M

sodium acetate. The precipitated DNA was re-suspended with 20 µl of 10 mM Tris-HCl (pH 8.5).

III.3.11 Ligation of DNA fragments

Ligation of DNA fragments and dephosphorylated vector DNA was performed in 1x T4 ligase buffer overnight at room temperature in the presence of T4 DNA ligase (6 Weiss units). The amount of vector DNA and DNA fragments were in a molar ratio of 1:1 and 1: 3. The entire reaction was assembled on ice untill the ligase was mixed into the solution. The total volume of the ligation mix was 10 µl. The specific ligation conditions for inverse PCR is given separately.

III.3.12 Polymerase chain reaction

Construction of primers for PCR

The primers used for PCR had generally 18-21 nucleotides. The melting temperature for the oligonucleotide primer used in PCR was determined using the formula used by MWG biotech, Germany Tm[C] = 69.3 + 41 [(nG + nC)/n]– (650/5n)

T represents thymine base, G represents guanine base, C represent cytosine base and A represent adenine base.

a. Standard PCR

Polymerase chain reaction was performed in a total volume of 100 µl. The equipment used for PCR was a PCR – Automat Uno II (Biometra, Götingen). The dNTPs were used in a concentration of 200 µM, primers at a concentration of 300 nM and $MgCl_2$ at an end concentration of 1.5 mM. When not specially mentioned Hot Star Taq polymerase (Quiagen, Germany) was used for preparation of probes and pfu polymerase (Stratagene, Germany) was used for sequencing and for cloning purposes. Genomic DNA was used at a concentration of 1-2 µg and plasmid DNA was used at a concentration of 1-10 ng. The denaturing temperature was set at 95°C for 15 min. The annealing temperature was set at 5°C below the melting temperature of the primers. In general 25 –31 cycles were used for amplification of desired fragments.

b. Inverse PCR

1µg of DNA was digested with the enzyme and purified using Qiagen PCR purification kit as per manufactarer's protocol. 200 µg of the digested DNA was used for ligation in 500µl volume on the thermocycler with 800 rounds of 30 seconds each at 12 and 19 degree celsius. The product was purified using YM-30 Microcon

columns, and ½ of the product was used for the PCR, which was run uder standard conditions. 1/100 of the product was used for the nested PCR and 1/20 of the product was used for analysis. 30 µl of the nested PCR product was run on a 2% gel TAE agorose gel and the band of interest was excised and purified on a Qiagen Gel purification kit column as per manufacterer's protocol and cloned into TOPO Cloning kit (Invitrogen) and transformed on TOP-10 *E.coli* (Invitrogen) as per their protocol. The miniprep of the clones was carried out using Qiagen Mini prep kit as per their protocol and 1/10 of the product was sent for sequencing.

III.3.13 Purification of PCR product

PCR products were purified using a PCR purification kit (Qiagen). The PCR product was checked using agarose gel electrophoresis.

III.3.14 Southern blot analysis of DNA

15µg of the cellular DNA and the controls, (+ve has spiked plasmid at 1, 2 and 4 copies/cell), were digested in 50 µl and loaded on to a TAE agarose gel of appropriate concentration and run on a low voltage. The gel was stained with ethidium bromide and photographed with a fluorescent ruler for noting the position of the marker bands. The gel was shaken in 0.25 N HCl to depurinate the DNA. Then the gel was washed with water followed by shaking in 0.4 N NaOH to denature the DNA. The blotting apparatus was preapared using a tray filled with 0.4 N NaOH and plastic plates placed horizontally across it. The bridge of wartman paper was placed on the plate and the gel and the membrane (Hybond N+ from Amersham) were sandwiched between two strips of wartman paper soaked in 0.4 N NaOH. The bale of absorbent paper towels was placed on the top and the sides were insulated with Saran wrap. Another plastic plate along with a small weight was placed on the top. Transfer of the DNA to the membrane was carried out overnight and the membrane was neutralised in 2X SSC prior to baking at 80^0C for 45 minutes to complete the cross linking. The prehybridisation mix was made with 3 ml 20X SSC, 3 ml 10X milk powder mix, 1 ml salmon sperm DNA, 6 ml of 50 % dextran sulphate solution and filled up with water to 30 ml, and boiled for 15 minutes and snap cooled on ice-water mix. The membrane was pre-hybridised at 68^0C overnight. The probe was radioactively labeled with 50 µCi ^{32}[P] dCTP (Amersham Pharmacia, Germany) using the Ready to go DNA

Labeling Kit (Amersham Pharmacia, Germany). The membrane was hybridized using the radioactive probe overnight at 68 ºC and washed at 68^0C with buffer I for 15 minutes followed by a second wash with wash buffer II for 20 minutes. The membrane was dried on Whartmann paper and exposed to a Kodak film at -80^0C and the film was exposed as per standard conditions.

III.3.15 Generation of DNA probes for slot blot and Southern blot analysis

The probes for slot blot analysis namely the ITR and the fiber probes were prepared using PCR. The 438 bp long ITR probe binds to the Ad-ITR (nucleotide 1 to 438). The primers used for the generation of ITR probe were the ITR and ITR II. The 1348 bp long fiber probe binds to the Ad–fiber DNA (nucleotide 31042 to 32390). The primers used for the generation of the fiber probe were fiber I and fiber II. PCR amplification was carried out for 2 min at 94ºC followed by 20 cycles of 1 minute at 94^0C, 1 minute at 55^0C, 1 minute at 72ºC and a final extension of 10 minutes at 72^0C. The probes for the different Southern blot experiments were generated by digesting the target DNA with the appropriate enzyme. The probes generated by PCR were purified using the QIA quick PCR purification Kit (Qiagen). The probes were stored at –20 ºC. The concentration of the probes was determined spectroscopically and by agarose gel electrophoresis.

III.4 Cell culture techniques

III.4.1 Cell lines and media

The cell culture media and foetal calf serum (FCS), when not otherwise mentioned, were purchased from Invitrogen (Germany). Hygromycin B (10687-010) and HAT (21060-017) supplement were purchased from Invitrogen and 6TG (A4882) was purchased from Sigma Aldrich. Minimum essential medium (MEM) and α-MEM powder were dissolved at room temperature in 4.5 L of water. 11 g of $NaHCO_3$ was added to the prepared media and the medium was adjusted to pH 7.1 with 1 N HCl. The media was made up to a volume of 5L and was filtered through a 0.2 µm filter.

All cell culture and viral techniques were performed in the S2 laboratory facility. The cells were harvested by centrifugation at 250g. The cell lines were passaged once or twice per week. For passaging of cells plated in 15 cm cell culture dishes, the medium was aspirated, and the cells were washed once with 10 ml of PBS. After washing, the

PBS was aspirated and the cells were detached using 3.0 ml of Trypsin-EDTA solution. After detachment, the trypsin was neutralized with 10 ml of medium containing 10% FCS. The cells were centrifuged and were resuspended in new medium for passaging.

293 : This cell line is a hypotriploid embryonic kidney cell line with a integrated 4.34 kb of adenoviral DNA (Graham et al., 1977) located in chromosome 19q-30. The cell line was cultured in αMEM/10 % FCS/ 1x penicillin-streptomycin and was passaged 1:3, twice every week.

293 Cre 66: The cell line was based on HEK 293. 293 Cre 66 expresses the Cre recombinase constitutively. The cell line was used for the amplification of high capacity adenoviral vectors. It was a kind gift of Dr. G. Schiedner. The cell line was cultured in MEM/10 % FCS/ 1x penicillin-streptomycin and was passaged 1:3, twice every week.

HeLa: The cell line is a cervical carcinoma cell line derived from a female patient (Gey et. al., 1952). The cell line was purchased from Cell line services, Heidelberg. The cell line was used for transduction with HC-Ad vector to estimate the levels of transgene expression *in vitro*. The cell line was cultured in αMEM/10 % FCS/ 1x penicillin-streptomycin and was passaged 1:3 once every week.

HT1080: The cell line is a fibrosarcoma cell line derived from a male, containing a single X chromosome (Rasheed et al., 1974). The cell line was cultured in αMEM/10 % FCS/ 1x penicillin-streptomycin and was passaged 1:6 twice every week.

C-32: The cell line is a melanoma cell line, derived from a male, containing a single X chromosome (Chen & Shaw, 1973), (Chen, 1983). The cell line was cultured in αMEM/10 % FCS/ 1x penicillin-streptomycin and was passaged 1:3 twice every week.

FF-95: These cells are primary human fibroblasts derived from a male patient in the Department of Dermatology, Universität zu Köln and is a generous gift of Prof. K.

Scharffetter-Kochanek. These cells were cultured in αMEM/10 % FCS/ 1x penicillin-streptomycin and were passaged 1:3 twice every week.

Human Retinal Pigmented Epithelium (HRPE): These cells are primary human cells derived from the eye and are a generous gift of Dr. I. Semkova, Augenklinik, Universität zu Köln. These cells were cultured in αMEM/10 % FCS/ 1x penicillin-streptomycin and were passaged 1:3 twice every week.

III.4.2 Freezing of eukaryotic cells for long term storage

For freezing, early passages of cells were used. The cells were washed twice with PBS and were detached using trypsin-EDTA solution. The cells were pelleted and resuspended using freezing mix. The freezing mix was aliquoted in 2 ml cryotubes (Nunc, Wiesbaden). The cryotubes were placed at RT for 15 min and were placed in a isopropanol bath, which was frozen at –80^{o}C for overnight. The cryotubes were placed in a liquid nitrogen container until further use. The freezing mix used was 90 % FCS, 10 % DMSO (Sigma-Aldrich, Germany).

III.4.3 Transfection of eukaryotic cells

The transfection of eucaryotic cells was performed using Fugene transfection reagent (Roche, Germany) as described by manufacturer. The cell lines were plated at a density of 50 – 80% confluency for 24h before transfection. The DNA used for transfection was purified using phenol-chloroform extraction method (Chapter III.3.6). For transfecting cells in 6 well plates, 1.5 µg of DNA was added to transfection solution containing 6 µl of Fugene transfection reagent diluted in 100 µl of serum free medium. The transfection solution was incubated at RT for 15 min for complex formation. The transfection solution was added drop wise on the cells and the cells were swirled to equally distribute the DNA complex. The volume of the culture supernatant was made to 1 ml. The medium containing the expressed transgene was collected at 48 h post transfection.

III.5 Adenovirus methods

III.5.1 Storage of virus

Adenoviral vectors were purified using PD10 Sepahdex 25 columns (Amersham) after double cesium chloride centrifugation. The viral vectors were eluted in TBS and mixed with 10 % glycerol. The vectors were stored at –80^{o}C deep freezer until further use.

III.5.2 Agarose overlay and isolation of plaques

Agarose overlay medium

0.5 %	autoclaved agarose (FMC products, USA)
1x	MEM
0.5 %	penicillin/streptomycin
0.05 %	yeast extract
5.0 %	FCS

Isolation of the plaques

293 cells were plated at 60-70 % confluency in a 6 well plate. 24 h after seeding, the cells were either transfected with a plasmid used for the generation of first generation virus or infected with the first generation vector. After 16 h, the transfected or infected cells were overlaid with agarose and were incubated at 37 ºC in a cell incubator containing 5 % CO_2 for a maximum period of two weeks. The cells were observed for two weeks under a light microscope for focal areas of lysed cells called plaques. Individual plaques representing single rescue events of vector are caused by a single clone of virus and were picked using sterile Pasteur pipettes The plaques were re-suspended in 1 ml of TBS and were frozen at –80^{o}C.

III.5.3 Generation of high capacity adenoviral (HC-Ad) vectors

Cre 66 cells were used for the generation of HC-Ad vectors. The plasmid used for the generation of the HC-Ad vector was digested with *Pme* I to release the ITRs. For the first amplification, the Cre66 cells ($2x10^6$ cells in a 6 cm plate) were transfected with the plasmid using effectene reagent (Qiagen). 16 h after transfection, the cells were infected with 5 moi of helper virus. The infected cells showing CPE at 48 h were harvested. The harvested Cre 66 cells were re-suspended in 2 ml of TBS followed by three times freeze thawing to release the vector particles. During the second and the

third amplification, Cre 66 cells ($3x10^6$ cells in 6 cm plate) were infected with half the supernatant from the cell lysate of the earlier amplification, and 5 moi of helper virus. During the fourth and fifth amplifications, Cre 66 cells were plated at a density of $3x10^7$ cells in 15 cm plates were infected with half the supernatant (from the cell lysate of the earlier amplifications) and 5 moi of helper virus. For a large-scale preparation, Cre66 (ten 15 cm plates, each with $3x10^7$ cells) were infected with the supernatant (containing the virus) from the fifth amplification or 10 MOI of HC-Ad vector (if the titre has been previously determined) and 5 moi of helper virus. The infected cells were harvested after 48 h and were re-suspended in TBS containing glycerol.

III.5.4 Purification of adenoviral vectors using CSCl density gradient ultracentrifuation

The re-suspended cells were freeze thawed for vector release. The vector containing supernatant was collected by centrifugation at 200g to remove the cell debris. The supernatant was made up to a volume of 20 ml and CsCl was added at a concentration of 0.5 gm/ml. The virus was centrifuged twice at 32,000 RPM at 4ºC for 22 h in an ultracentrifuge (Ultracentrifuge L7-65 with SW41- Rotor, Beckman, USA) The adenoviral vector floats as a ring in the CsCl gradient at a density of 1.34 gm/cm^3. The virus was aspirated using a 2 ml syringe fitted to a needle. After the second gradient, the virus was desalted in PD 100 columns using TBS buffer. Glycerol was added to the eluted vector at a concentration of 10 %. The virus was stored at -80^0C.

III.5.5 Titration of helper virus or first generation adenoviral vectors

HeLa cells were used for determining the titer of first generation vectors and helper virus vectors. The cells were plated at a density of $2x10^6$ in 6 cm plates. The plated cells were infected with different dilutions of the vector. 16h after infection the cells were overlaid with 10 ml of agarose overlay medium for 15 minutes at room temperature. The cells were incubated at 37^0C in cell incubator containing 5 % CO_2 for 5-14 days. The plates were observed under light microscope for plaques. The average number of plaques at a given dilution represents the plaque forming units (pfu) of the virus.

III.5.6 Titration of HC-Ad vector using slot blot analysis

The slot blot method was used to determine the infectious units, total particle and the helper virus contamination titers. HeLa cells were used for the determination of infectious units of the HC-Ad vectors. The cells were plated for overnight at a density of $1x10^5$ cells in a 24 well plate before infection with HC-Ad vector. HC-Ad vectors were diluted at 1:20 in TBS, and 4 to 20 µl of the diluted HC-Ad vector was used to infect HeLa cells in duplicates. 16 h after infection, the cells were washed intensively with PBS and were incubated with 200 µl of PBS/5mM EDTA for 15 minutes to detach the cells from the plate. The detached cells were incubated with 200 µl of 0.8 N NaOH for 30 minutes to lyse the cells. The plasmid p GS46, added to the uninfected cells at copy numbers ranging from $1x10^6$ to $1x10^8$, acted as the standard.

The total particle titre of HC-Ad vectors was determined using a cell free system. The HC-Ad vector was diluted 1: 400 in TBS buffer. Four to 20 µl of the diluted HC-Ad vector was made up to a volume of 200 µl of TBS and was lysed with 200 µl of 0.8 N NaOH for 30 min at room temperature. The plasmid p GS46 was used as the standard and, was diluted in TBS (to a volume of 200 µl) to represent copy numbers ranging from $1x10^6$ to and $1x10^8$. The diluted standards were mixed with 200 µl of 0.8 N NaOH and were incubated for 30 min at room temperature.

The helper viral contamination was determined using a cell free system. The HC-Ad vector was diluted 1: 200 in TBS. Four 20 µls of the diluted virus was made up to a volume of 200 µl of TBS and was lysed with 200 µl of 0.8 NaOH for 30 min at room temperature. The plasmid pGS 46 was used as the standard and, was diluted in TBS (to a volume of 200 µl) to represent the copy numbers ranging from $1x10^6$ to and $1x10^8$. The diluted standards were mixed with 200 µl of 0.8 N NaOH and were incubated for 30 min at room temperature.

300 µl of cell or particle lysate was transferred to a nylon membrane Bio Dyne membrane (PALL Corporation, USA) using the slot blot apparatus (Hoefer PR 648, Bio-Rad Laboratories, Munich). After transfer, the membrane was washed with 2 x SSC buffer followed by baking at 120^0C for 30 minutes. The baked membrane was pre-hybridized with hybridization buffer for 4h at 68^0C. The probe used for the determination of infectious units and total particle binds to the left ITR of the adenovirus (nucleotide 1- 438). The probe used for the determination of the helper virus particle binds to the fiber (nucleotide 31042 to 32390) The PCR probe was radioactively labeled with 50 µCi ^{32}[P] dCTP (Amersham Pharmacia, Germany) using

the Ready to go DNA Labeling Kit (Amersham Pharmacia,Germany). The membrane was hybridized using the radioactive probe for 16 h at 68^0C. The membrane was washed at 68^0C with buffer I followed by a second wash with wash buffer II for 20 minutes. The membrane was transferred to a phospho-imager cassette and the signal was read using a Phospho imager 445SSI (Molecular Dynamics,USA). The titer of the HC-Ad vector was estimated by comparing the signal intensity between the HC-Ad vector and the plasmid standards.

III.6 Animal handling techniques

129SvJ Fah $^{\Delta exon5}$ (5-8 week old) mice were used for all the experiments. The animals were maintained under pathogen free conditions at the animal facility of the Oregon Health Sciences University. The mice were fed with standard diet (B&K universal) and sterilized water with or without the recommended dosage of NTBC. All mice were cared for in compliance with the guidance prescribed by OSHU.

III.6.1 Harvesting of the mouse liver

The animal was anaesthetised and then killed by cervical dislocation. Four limb immobilization was carried out using tape on a moisture absorbing surface. The abdomen was opened, the liver removed and placed on a glass slide. The smaller lobes 4, 5 and 6 (behind the gall bladder) were identified, and each was cut individually and placed along with the larger lobes 1, 2 and 3 on glass slides. Each lobe was sliced lengthwise into 3 pieces. The middle piece was stored in the solution for histology. The bottom piece for was used for DNA extraction and the top piece was quick frozen and stored.

III.6.2 Isolation and serial transplantation of hepatocytes into recipient livers

The peristaltic pump tubing was rinsed with 70 % ETOH and then with PBS, and all the solutions were prewarmed to 37^0C. The i.v. infusion set was attached and Soln I was run through it. The donor mouse was anaesthetised, and four limb immobilization carried out using tape on a moisture absorbing surface inside a tissue culture hood. The abdomen was cut open and the inferior vena cava and the portal vessels located under the liver were located. The i.v. catheter was rinsed with Soln I and then the inferior vena cava was cannulated. The i.v. tubing was attached to the catheter and

the pump was started. When the liver filled up with the solution, the portal vein was cut. The chest of the mouse was opened and the superior vena cava was clamped. The peristaltic pump was run at a rate of 5 ml/minute. After 3 minutes of perfusion with Soln I, the liver was perfused with Soln II for 2 minutes and then with Soln II. When the liver was digested, the catheter was removed, and the liver was transferred to a petri dish in a second tissue culture hood. The liver capsule was disrupted with forceps in 5 ml of Soln III and the hepatocytes washed out. The cells were filtered through the nylon mesh into a 50 ml tube that contained 10 ml prewarmed DMEM with serum. Cells were pelleted and resuspended in 50 ml high glucose DMEM plus serum. The washes were repeated three times and the cells resuspended in plating medium (high glucose DMEM with serum). The recipient mouse was anaesthetised and had the abdominal fur shaved off, and the region sterilized with 70% ETOH. The abdomen was cut, the spleen located, and the syringe needle containing the hepatocytes was inserted into the spleen and the region above the point of entry of the needle was clamped and the hepatocytes injected. The peritoneum and the skin were sewn back, and the mouse was allowed to recover.

III.6. 3 Calculation of the rates of recombination HC AdV *in vivo*

The histology slides containing the liver samples were scanned on a Canon Flat bed scanner along with a size standard. The software NIH Image was used to determine the size of the liver samples and the cell numbers as described in (Wang et al., 2002), from which the correction factor was also used. The number of vector molecules reaching the hepatocytes were calculated as described in pg 137. The slides were checked for brown (Fah+ve) cells and nodules. Photos were taken using a Zeiss PVCAM Inverted Microscope and a PCIAIA camera from Hamamatsu (Open lab 3.03 software).

For example, in mouse 301, the rate of recombination was calculated as follows.
Total amount of cells (obtained by calculating the total surface area in the liver sections using NIH Image J) = 9.4×10^5
Amount of virus reaching these cells after the injection (for 1×10^{10} inf.units, see pg 138) = 10 viruses/cell
$\therefore$, total number of virus in the hepatocytes analysed from mouse 301 = 9.4×10^6

Number of nodules observed in the liver sections from mouse 301 = 30

∴, rate of recombination = 1/313333

Correction factor (Wang et al., 2002) = 5

∴, actual rate of recombination = 1/1566666.7

$= 6.4 \times 10^{-7}$

Ensembl Version

Human and mouse genome releases 38, April 2006 were used in this study.

III.7 Hprt model

Nucleotides are synthesized either totally from the beginning from amino acids, tetrahydofolates, CO_2 and NH_4^+ (*de novo* synthesis pathway) or are reused from existing nucleotides (salvage pathway). The central molecule in both pathways is 5-phosphoribosyl-1-pyrophosphate (PRPP) (see Fig. 6).

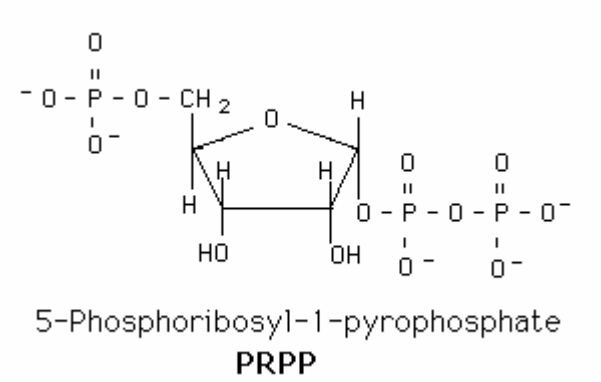

Fig. 6: Fig.ure of PRPP (from http://www-medlib.med.utah.edu/NetBiochem/pupyr/pp.htm)

In the *de novo* pathway, the first stage is the synthesis of a closed ring 5-Aminoimidazole ribonucleotide from PRPP. The gist of the pathway is as follows: The amino group from a glutamine replaces the Ppi, and a glycine is added to it. A formyl group is added to the α-amino terminal of glycine by N^{10}-formyltetrahydrofolate. A glycine donor converts the amide group of the compound into an amidine group and the ring is closed to form the 5 membered ring of the purine skeleton, 5-aminoimidazoleribonucleotide. Following carboxylation, an aspartate is added to the ring. The fumarate part of the moiety is removed leaving only the amino group. Another formyl group is donated by the N^{10}-

formyltetrahydrofolate, a water molecule is removed and the ring is closed to generate inosinate (IMP), from which adenylate (AMP) and guanylate (GMP) are synthesised (see Fig. 9).

In the purine salvage pathway, the ribose phosphate moiety of PRPP is transferred on to the free purine bases obtained during the degradation of nucleic acids and nucleotides. The formation of adenylate from adenine is catalysed by Adenine phosphoribosyl transferase (APRT), and the conversion of hypoxanthine and guanine to inosinate and guanylate are catalysed by hypoxanthine-guanine phosphoribosyl transferase (HGPRT) (See Fig. 7).

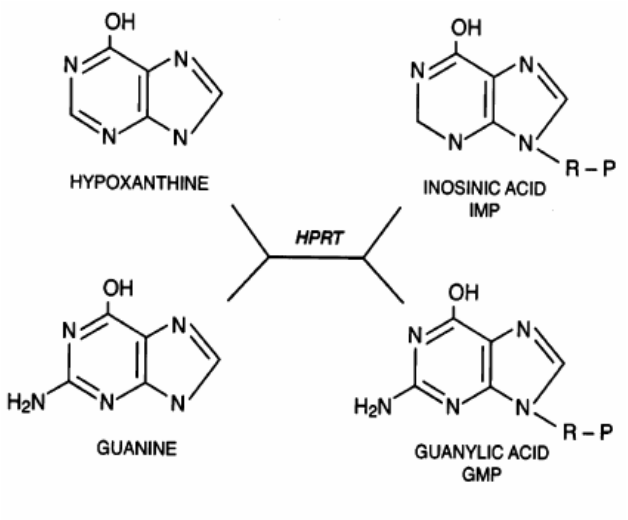

Fig. 7. Schematic diagram of purine salvage pathway based on (Nyhan, 2005)

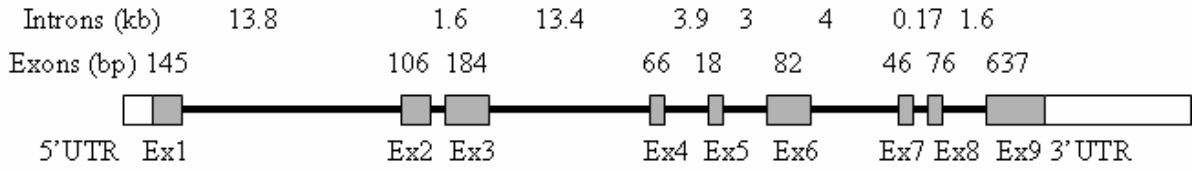

Fig. 8. Schematic diagram of the human Hprt gene based on (Stout & Caskey, 1985)

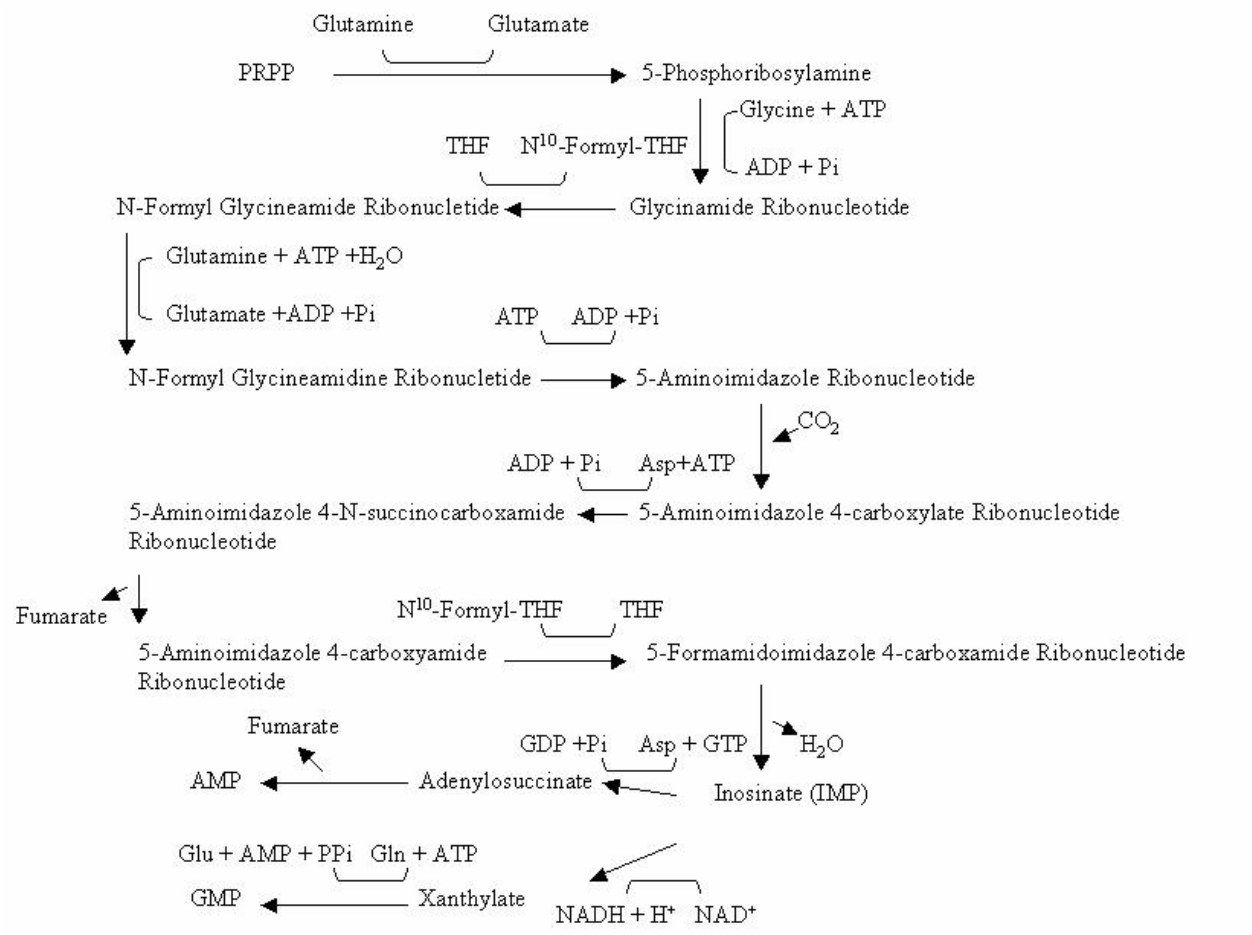

Fig. 9. Diagram of the Purine *de novo* synthesis, based on (Stryer, 1998)

The enzyme dihydrofolate reductase (DHFR) converts 7,8-Dihydrofolate to 5,6,7,8,-Tetrahydrate folate. The drug aminopterin is an analogue of Dihydrofolate and competitively inhibits DHFR. When combined with hypoxanthine and thymidine, the drug (HAT) is used to select for cells that are HPRT positive (Szybalski & Szybalska, 1962). HPRT itself can bind and ribosylate toxic purine analogues such as 6-Thioguanine (6TG) with toxic results for the cell. So HPRT-cells can be selected for by the addition of 6TG to the medium (Stutts & Brockman, 1963).

HPRT is a housekeeping gene. In humans, the gene encoding HPRT is 44 kb long, consists of 9 exons and is located on the q arm of the X chromosome between bps 133421923 to 133462354 [reviewed in (Caskey & Stout, 1989, Stout & Caskey, 1985)] (see Fig. 8). Deficiency of HPRT leads to Lesh Nyhan Syndrome in humans (Nyhan, 2005, Schepis et al., 1996). Of the various mutations in the HPRT gene that result in the syndrome, HPRT $_{CHICAGO}$, where the insertion of a single T nucleotide

resulted in the formation of a stop codon (Davidson et al., 1989) was of particular interest in this study.

The HPRT locus has been used extensively for studies on gene targeting. In pioneering studies using plasmids, the rates of homologous recombination was observed to be in the range of 10^{-6} and the rate of random integration in the range of 10^{-3} with respect to the number of cells. The rate of homologous recombination was also observed to increase in proportion to the amount of homology between the DNA fragments (Capecchi, 1989, Deng & Capecchi, 1992, Doetschman et al., 1987, Hasty et al., 1991, Manivasakam et al., 2001, Thomas & Capecchi, 1987, Wade-Martins et al., 2000, Yun et al., 2004, Zheng et al., 1991). The results published with work using viral vectors on the HPRT locus have been mentioned earlier.

III.8 Fumarylacetoacetate hydrolase (Fah) mouse model

In the pioneering work that linked metabolic disorders to genetics, Archibald Garrod postulated the relationship between genes and enzymes when he published his findings on alcaptonuria, a condition caused by the absence of homogentisate oxidase. It is a part of the phenylalanie and tyrosine degradation pathways, where an aromatic ring is broken by molecular oxygen and the products are passed on into the citric acid cycle. Phenylalanine is hydroxylated into tyrosine, which is converted into 4-hydroxyphenylpyruvic acid, which reacts with O_2 to form homogentisic acid. O_2 cleaves the aromtic ring producing maleylacetoacetic acid. It is converted into its isomer fumarylacetoacetic acid (FAA) by fumarylacetoacetate hydrolase (FAH), which is hydrolysed into fumaric acid and acetoacetic acid, which are passed on into the citric acid cycle [reviewed in (Tanguay et al., 1996)] (see Fig. 10).

Deficiency of the enzymes in the pathway results in various forms of hypertyrosinemia. The loss of FAH enzyme results in tyrosinemia type 1, characterized by progressive liver and renal damage. The compartmentalization of FAA, and its subsequent reaction to glutathione and protein thiol groups lead to mutagenic, cytostatic, and apoptogenic activites in cells (Endo & Sun, 2002, Jorquera & Tanguay, 1997, Jorquera & Tanguay, 1999, Kubo et al., 1998, Tanguay et al., 1996). FAA was proven to induce mitotic abnormality and genomic instability by activating the extracellular signal-regulated protein kinase (ERK) pathway, and this

was postulated to be responsible for the hepatic cancer developing in 37 % of the human cases (Jorquera & Tanguay, 2001).

In competing with other plants, certain members of the *Myrtaceae* family and the symbionts, the lichens, produce diketone and triketone alkaloids that specifically inhibit the 4-hydroxyphenylpyruvate dioxygenase (HPPD) of the neighbouring plants. One such competitive inhibitor of HPPD, triketone, 2-[2-nitro-4-(trifluromethyl)benzoyl]-1,3-cyclohexanedione (NTBC), that binds strongly to the HPPD and FeII complex, was used to treat the patients (Holme & Lindstedt, 1998, Kavana & Moran, 2003). Tyrosinemic livers were found to be not only FAH-ve tissue, but mosaics with FAH+ve tissues where the actual reversion of the original mutation had occurred. The nodular growth of the FAH+ve cells pointed out to the selective advantage those cells have in a FAH-ve liver (Kvittingen et al., 1993).

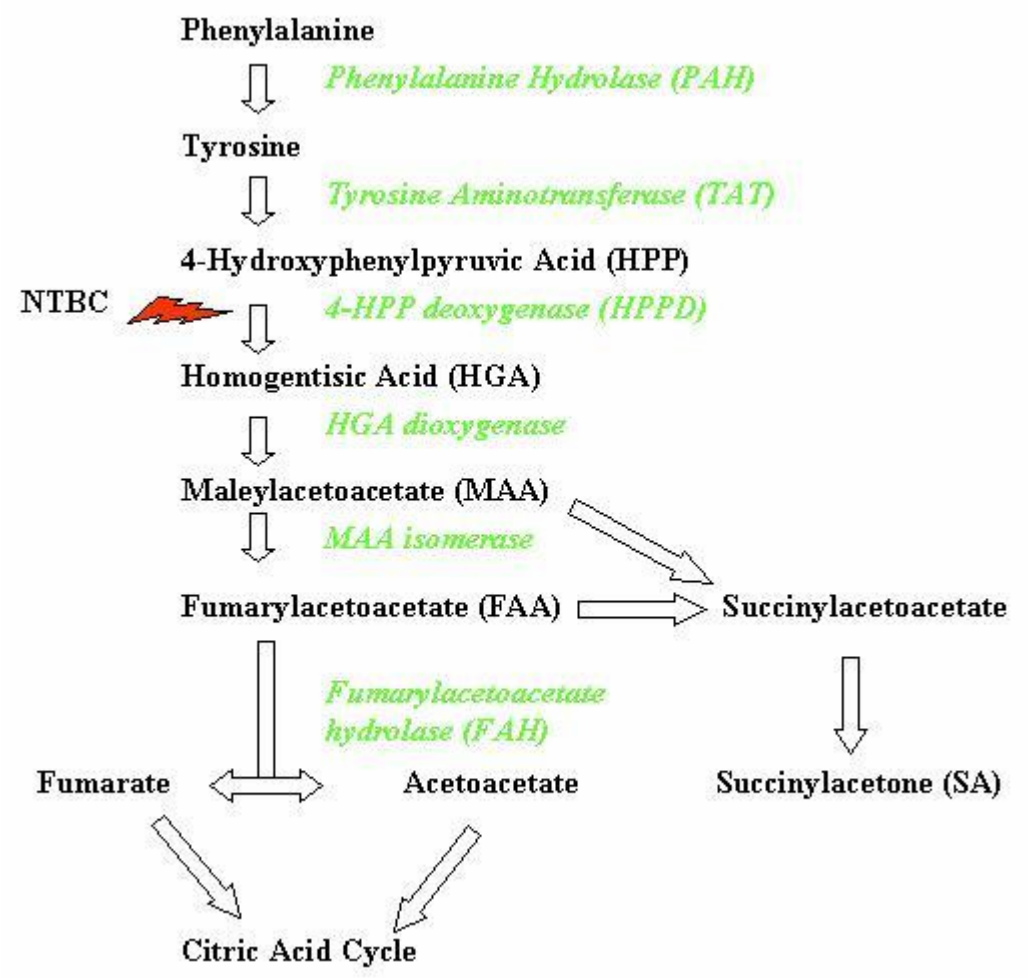

Fig. 10. Diagram of the Tyrosine metabolism pathway adapted from (Grompe et al., 1995)

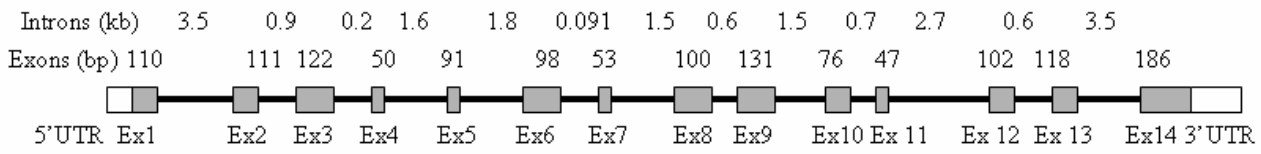

Fig. 11. Schematic diagram of the murine FAH gene

In the mouse, the FAH gene, consisting of 14 exons, is located in Chr 7 between bps 80506746- 80527407 (see Fig. 11). The C^{14CoS} albino mouse, with a large deletion in Chr 7, including the *Fah* gene (Klebig et al., 1992), displays neonatal death (Gluecksohn-Waelsch, 1979). This phenotype was shown to arise from the lack of FAH (Kelsey et al., 1993). Knockout mice ($FAH^{-/-}$ mice) with a targeted insertion of a neo cassette into the exon 5 of the FAH gene, displayed the same phenotype (Grompe et al., 1993). The use of NTBC alleviated the neonatal lethal phenotype in the mice for up to 2 years (Al-Dhalimy et al., 2002, Grompe et al., 1995). Correction of the phenotype was observed when liver cells transduced with a retroviral vector carrying the FAH cDNA were injected on recipient mice (Overturf et al., 1998). As expected, given the regeneration capacity of the liver [reviewed by (Michalopoulos & Khan, 2005)], as few as 1000 transplanted wt FAH +ve cells were able to repopulate a FAH-ve liver in knockout mice, with normal liver function (Grompe et al., 1998, Overturf et al., 1996). The work done on the model using a I^{st} gen AdV carrying the FAH cDNA under the control of a RSV promoter, and an AAV vector carrying the cDNA, have been mentioned in the introduction.

III.9 Plasmids

III.9.1 Construction of plasmid p SLS 11

The aim of generating this plasmid was to generate a high capacity adenoviral vector capable of both disrupting exon 2 of the human *hprt* gene in the event of the vector DNA undergoing homologous recombination in the genome, and also inserting a selection cassette into the genome in the event of random recombination. To disrupt the *hprt* gene, the clinical mutation hprt Chicago (Davidson et al., 1989) was utilised. A T nucleotide was incorporated at the 30th bp of exon 2 (nucleotide 13162 of hprt gene), resulting in the generation of a stop codon and an unique *Eco RV* site was engineered downstream of the mutation by substituting the T at nucleotide 4 and A at nucleotide 6 with A and C nucleotides respectively (Fig. 23).

The plasmid p SLS 1 was constructed to introduce a *Swa I* site into the multiple cloning site of plasmid pBluescript II KS (p BSIIKS). p BSIIKS (Stratagene) was cut with *Eco RV* and the oligonucleotide 24129/24130, carrying a *Swa I* site (donated by Dr. Schiedner) was cloned into the site to generate p SLS 1.

The plasmid p SLS 2 was constructed to sublone the 11.5 kb of the Hprt fragment from p STK 129. p STK 129 was digested with *Swa I* and *Not I* and the fragment (base pairs 8913 –20424 of pSTK129) was purified. p SLS 1 was digested with *Swa I* and *Not I* and the electroeluted insert was cloned in to generate p SLS 2.

The plasmid p SLS 3 was constructed to remove the exon 2 of the hprt from p SLS 2. Plasmid p SLS 2 was grown in a *dcm*- strain (GM 2163, NEB), digested with *Sex AI* to excise out the 484 base pair *Sex AI* fragment containing the exon 2 (base pairs 133,435,071- 133,434,587 of the hprt gene) and was religated to generate p SLS 3.

The plasmid p SLS 4 was constructed to generate a stop codon within the exon 2 of the hprt and to alter its reading frame. PCR was performed on p SLS 2 template using the primers Sam Stephen I and Sam Stephen II to generate a 493 base pair fragment containing an insertion of a T nucleotide and an *Eco RV* site into the exon 2 of the hprt gene. p BSIIKS was digested with *Eco RV* and this pfu PCR generated product was cloned into the site to generate p SLS 4.

The plasmid p SLS 5 was constructed to generate a stop codon within the exon 2 and to alter its reading frame of the hprt fragment contained in p SLS 3. p SLS 4 was digested with *Sex AI*, and the electroeluted fragment was cloned into the *Sex AI* site of p SLS 3 to generate p SLS5.

The plasmid p SLS 6 was constructed to introduce the stop codon and the altered reading frame of the *hprt* into the stuffer DNA of p STK129. p STK 129 was digested with *Swa I* and *Not I* and CIPed. p SLS5 was double digested with *Swa I* and *Not I* and the 11.5 kb fragment was cloned into the above mentioned p STK 129 to generate p SLS 6.

The plasmid p SLS 11 was constructed to include a Hygromycin-EGFP (Enhanced Green Fluorescent Protein) fusion cassette into the p SLS 6 so as to generate a vector plasmid capable of introducing the stop codon into the exon 2 of the hprt gene as well as inserting a Hyg-EGFP cassette into the genome. p SLS 6 was digested with *Not I* and klenowed. p HygEGFP (Clontech) was double digested with *Bgl II* and *Cla I*. The 3.1 kb fragment containing the expression cassette including the promoter and the poly A signal was cloned into the above mentioned vector.

The cloning scheme for the construction of the plasmid is shown in Fig. 12.

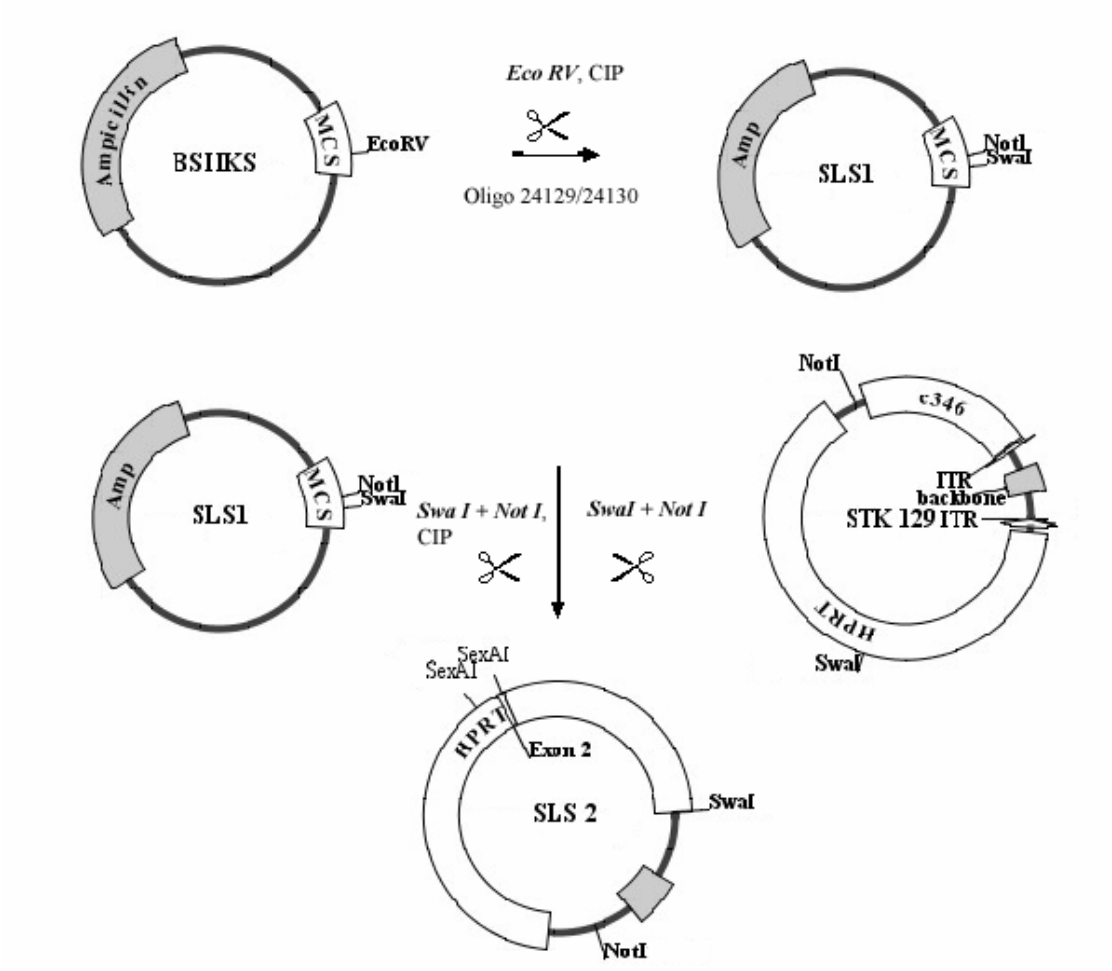

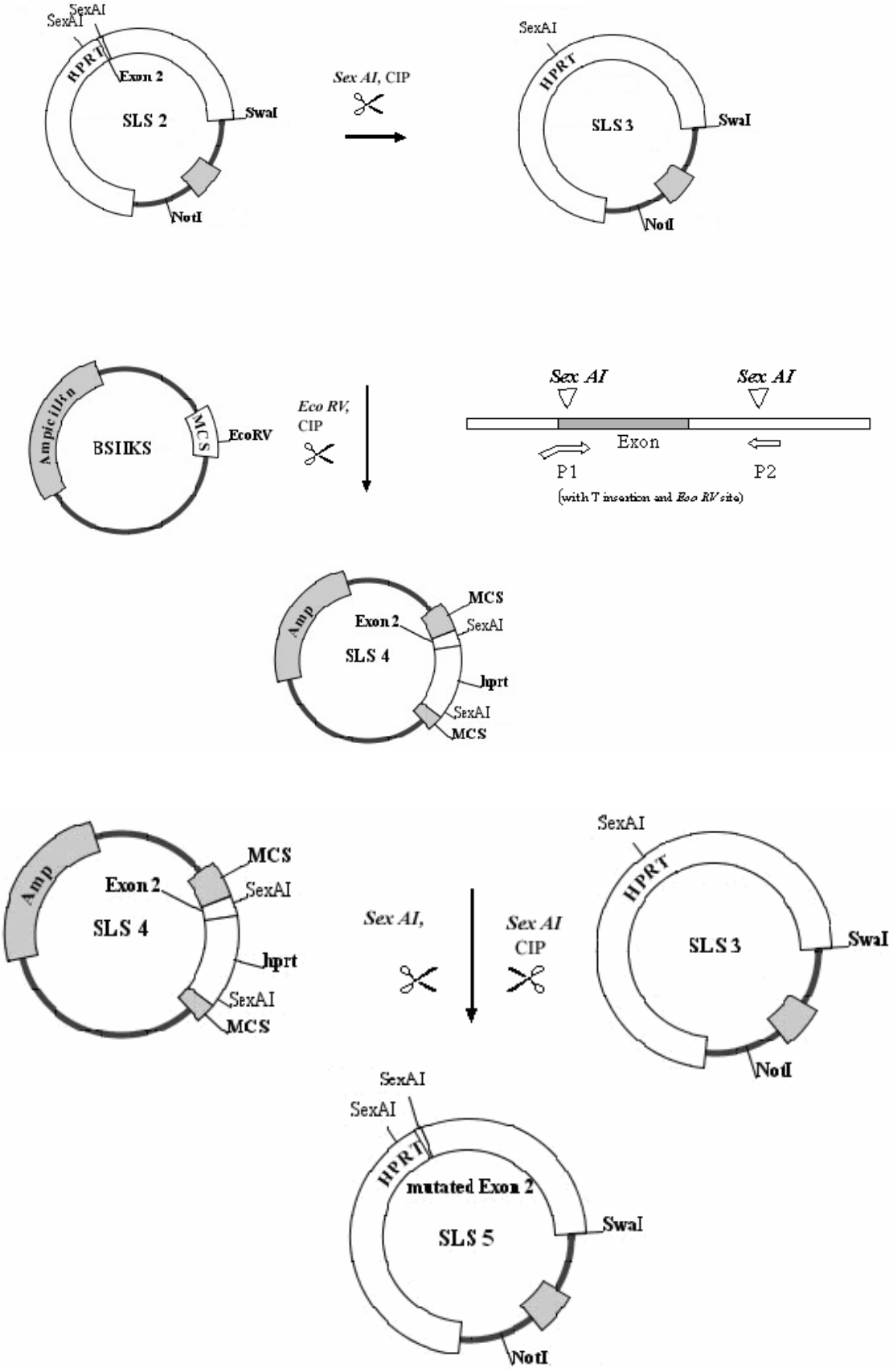
SexAI
SexAI
HPRT
Exon 2
SLS 2
SwaI
NotI
Sex AI, CIP
SexAI
HPRT
SLS 3
SwaI
NotI
Ampicillin
BSIIKS
MCS
EcoRV
Eco RV,
CIP
Sex AI
Sex AI
Exon
P1
P2
(with T insertion and Eco RV site)
Amp
Exon 2
SLS 4
MCS
SexAI
Jprt
SexAI
MCS
Amp
Exon 2
SLS 4
MCS
SexAI
Jprt
SexAI
MCS
Sex AI,
Sex AI
CIP
SexAI
HPRT
SLS 3
SwaI
NotI
SexAI
SexAI
HPRT
mutated Exon 2
SLS 5
SwaI
NotI

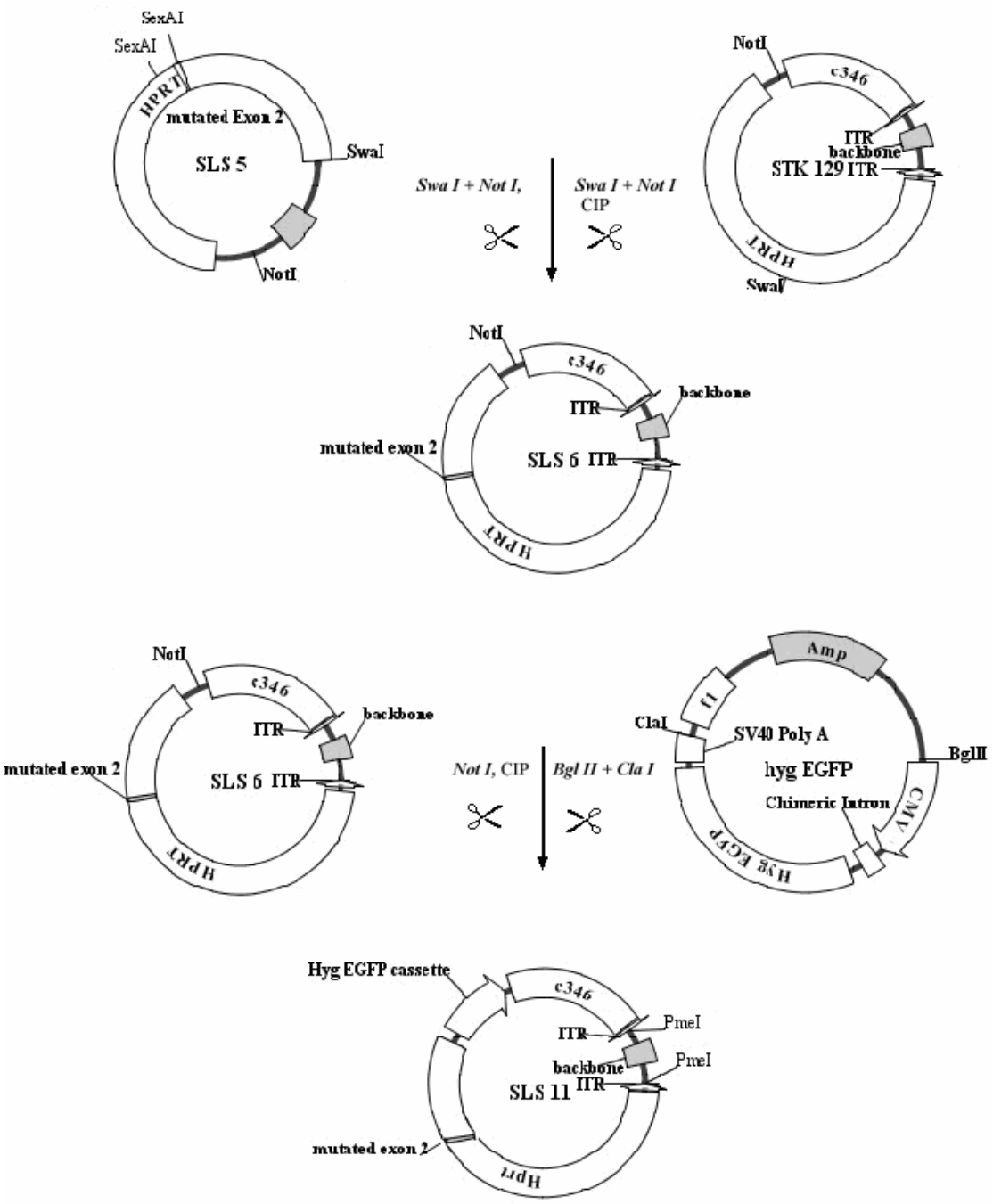

Fig. 12: Scheme showing the construction of p SLS 11

III.9.2 Construction of plasmid p SLS 14

This plasmid was generated to produce a HC-AdV capable of replacing the mutated exon 5 of the *fah* gene in the Fah$^{-/-}$ mouse with the wild type Fah exon 5, thereby restoring the gene function. The exons 2 to 9 were cloned into the plasmid.

p SLS 13 was generated to create a viral vector plasmid that can be rescued using *Sna BI* instead of the standard *Pme I*, due to the presence of a *Pme I* site in the intron 5-6

of the murine fah gene. p STK 68 and p STK 5 were digested with *Pme I* and the 16 kb fragment of p STK 68 was cloned into the digested p STK 5 to generate p SLS 13.

p SLS 9 was created to subclone the 16.4 kb fragment from the murine fah gene including the exons 1-5 from the λ Dash II phage vector. λmFAH6 was digested with *Not I* and *Cla I* and the 12.3 kb fragment of the fah gene containing exons 2, 3, 4 and 5 was ligated onto p BKRSV (Stratagene) cut with the same enzymes to generate p SLS 9.

p SLS 14 was generated to create the vector plasmid. p SLS13 was cut with *Eco RV* and p SLS 9 was cut with *Cla I* and *Not I*, and the 12.3 kb fah fragment was cloned into the vector to generate p SLS 14.

The cloning scheme for the construction of the plasmid is shown in Fig. 13.

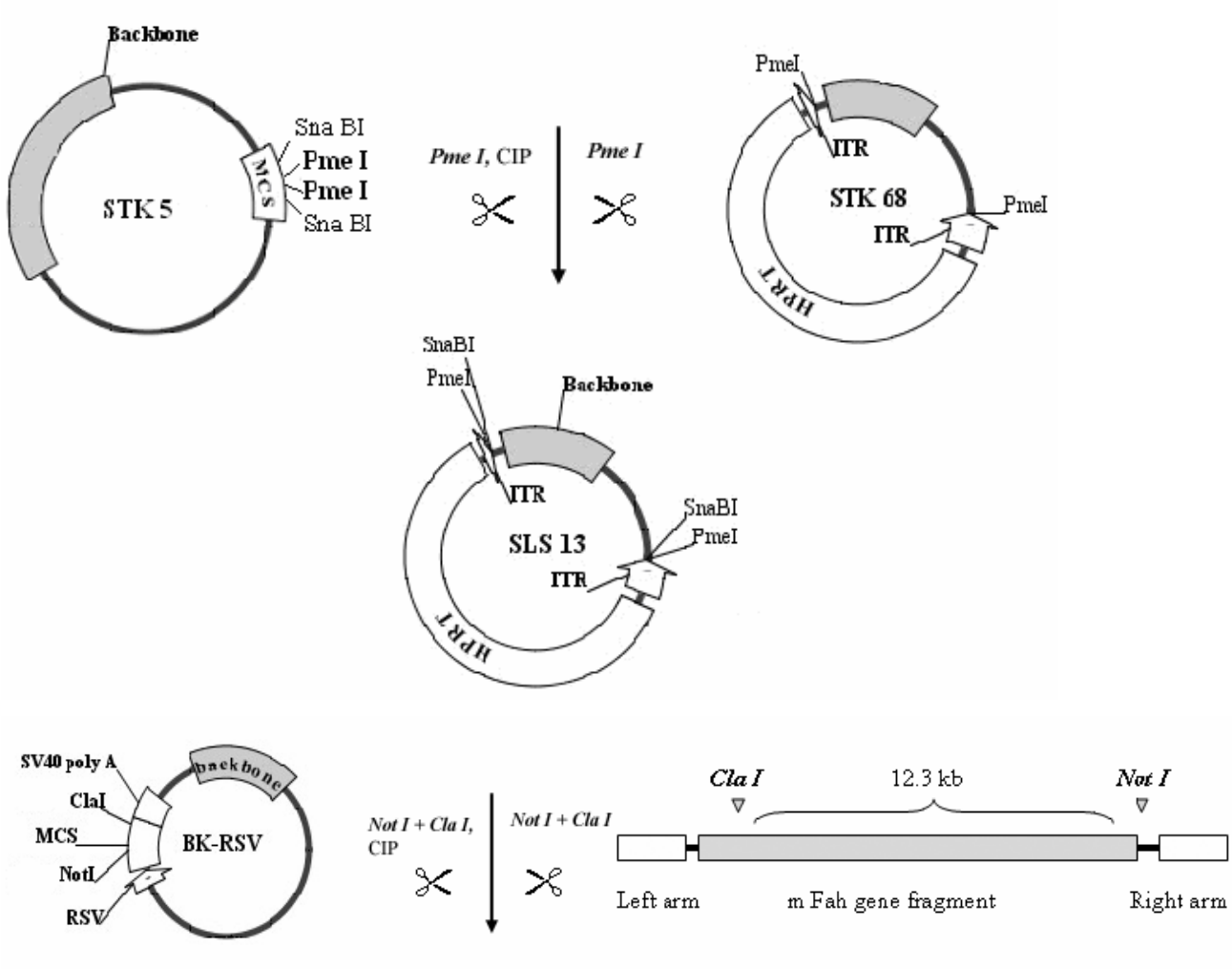

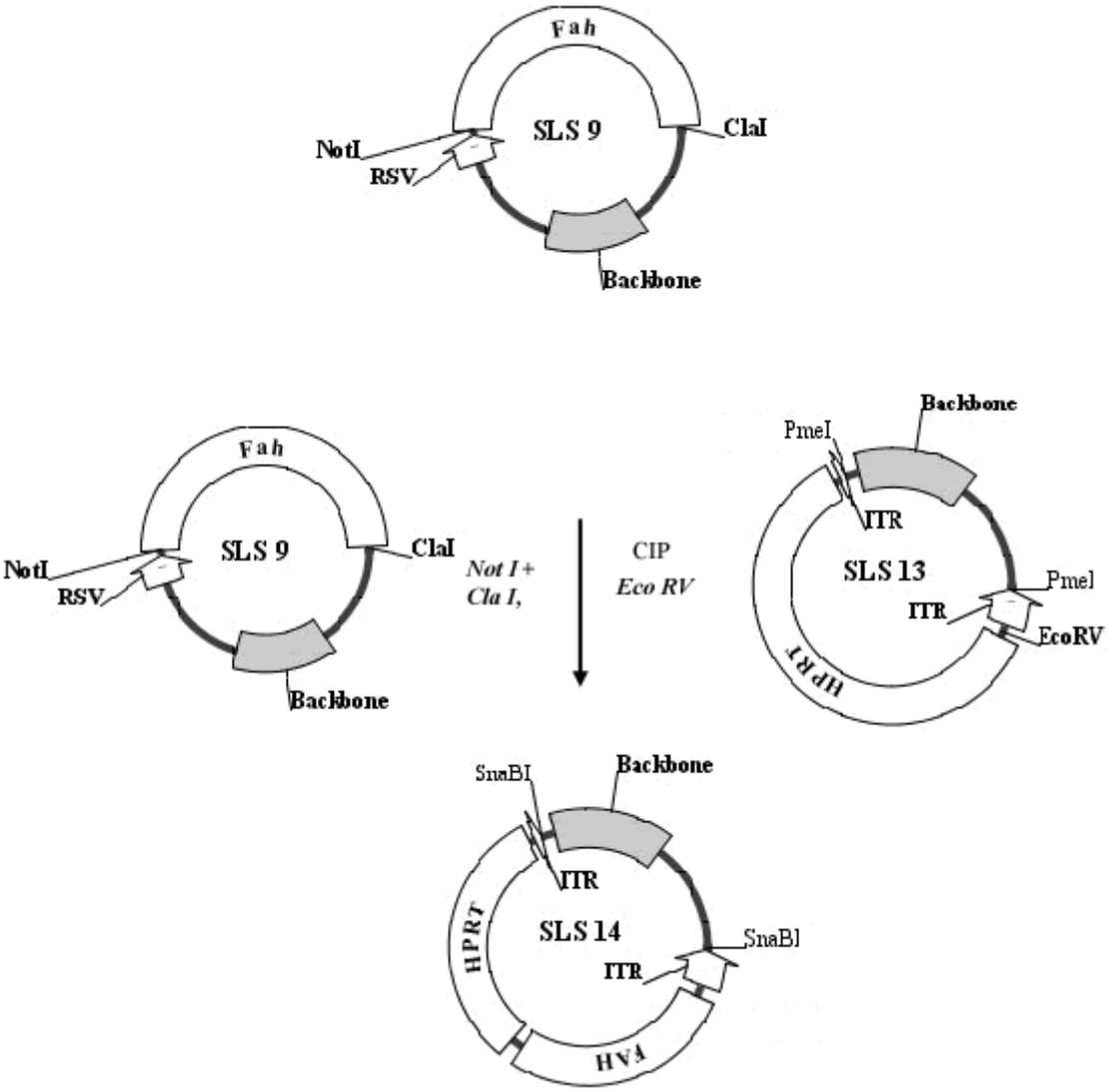

Fig. 13: Scheme showing the construction of p SLS 14

III.9.3 Construction of plasmid p SLS 16

This plasmid was generated to produce a HC-AdV carrying a murine fah cDNA under the control of a RSV promoter, to restore the fah gene function in Fah-ve cells.

p SLS 15 was generated to clone the murine FAH cDNA into the MCS of the p Rc/RSV so as to enable it to be expressed from the RSV promoter. p mFAH4AR1 (donated by Prof. Grompe) was digested with *Eco RI*, ends blunted using Klenow enzyme and purified by gel electoelution and cloned into the *Hind III* site of p Rc/RSV that had been made blunt using the Klenow enzyme to generate p SLS15.

The vector plasmid p SLS 16 was produced by cloning in the RSV-mFAH cDNA-BGH polyA cassette into p STK 120. p SLS 15 was digested with *Nru I* and *Pvu II*, and the DNA termini were made blunt using Klenow enzyme. The cassette was

purified using electroelution and cloned into p STK120 that had been digested with *Swa I* and the ends made blunt with Klenow enzyme to generate p SLS 16.

The cloning scheme for the construction of the plasmid is shown in Fig. 14.

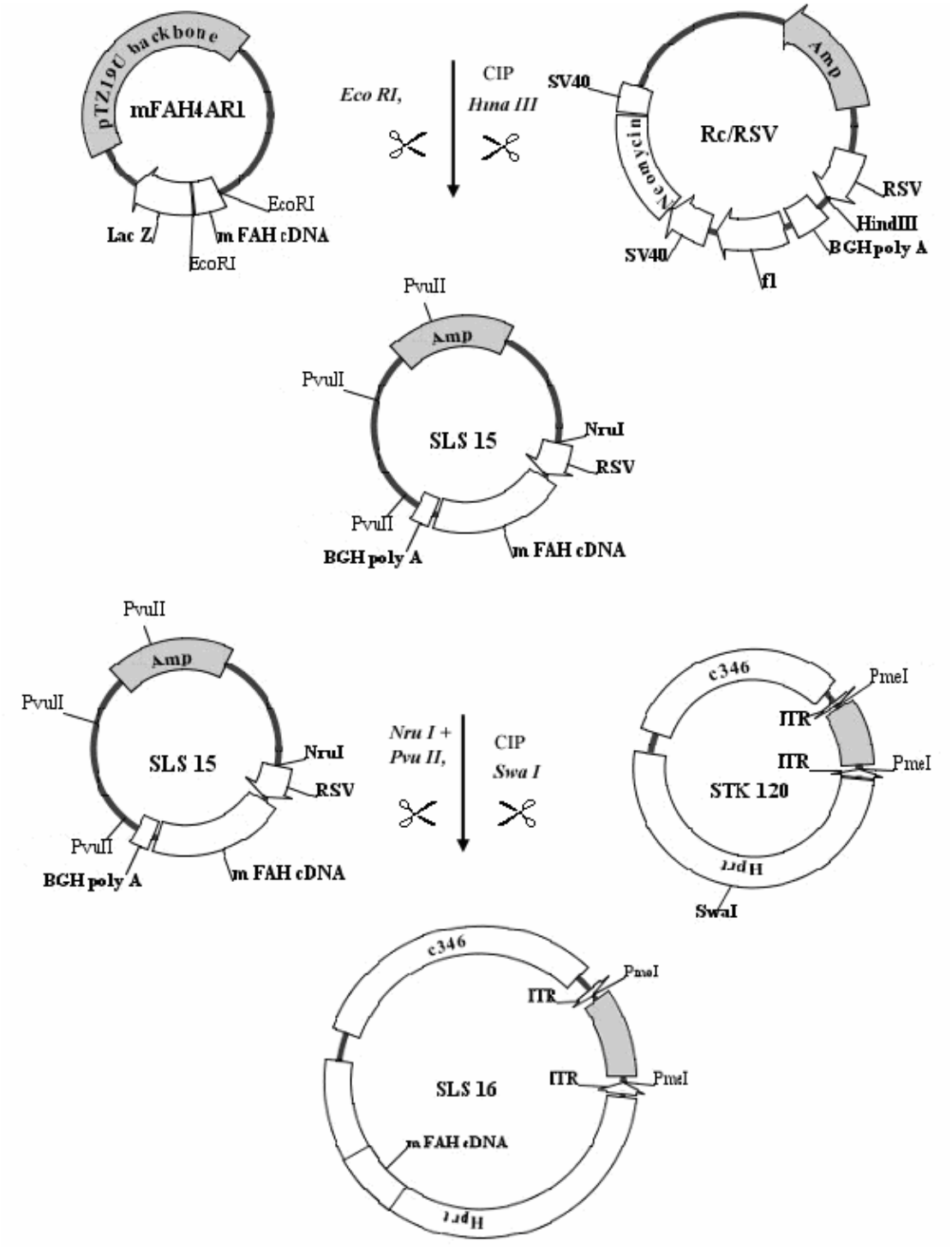

Fig. 14: Scheme showing the construction of p SLS 16

IV Results

IV.1 Calculation of the amount of Hygromycin B required to select out untransduced cells

Hygromycin B ($C_{20}H_{37}N_3O_{13}$) is an aminoglycoside antibiotic, produced by *Streptomyces hygroscopicus,* and inhibits the growth of prokaryotic and eukaryotic cells by inducing the mistranslation of the mRNA (Moazed & Noller, 1987, Spahn & Prescott, 1996), the mistranslocation of the mRNA (Cabanas et al., 1978, Hausner et al., 1988) and the inhibition of 75-80 % of the ATPase activity of the 70S ribosomes (Ganoza & Kiel, 2001). The *E.coli* hph gene encodes Hygromycin phosphotransferase (Gritz & Davies, 1983). The phosphorylation of the 4-OH group results in the alteration of the stereostructure of Hygromycin B (Hyg B), resulting in a loss of its ability to bind to the ribosome.

Experimental setup:

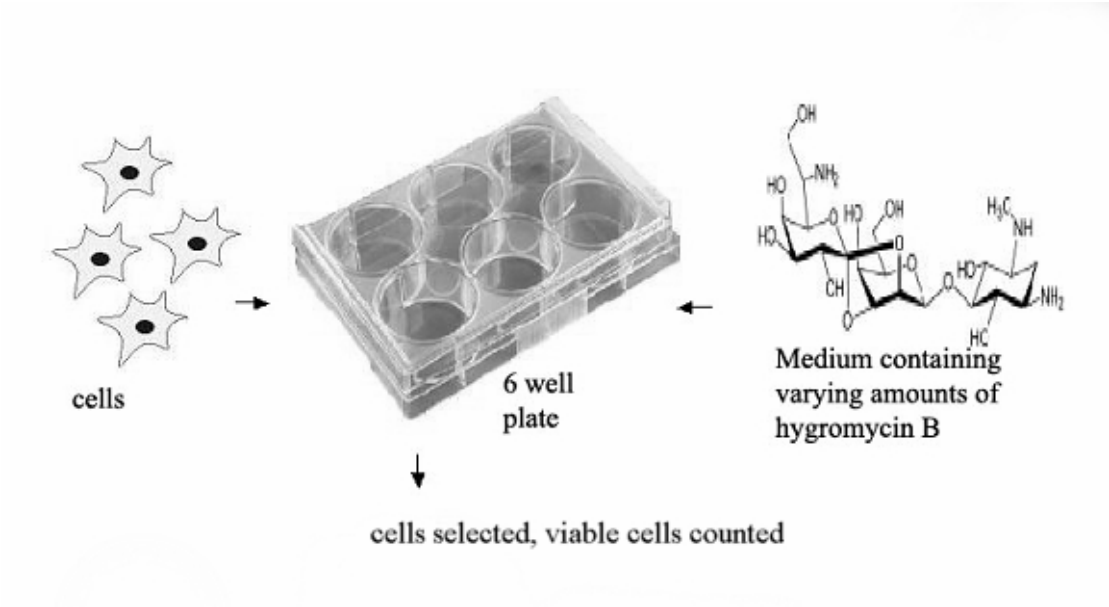

Fig. 16: Scheme of the vitality curve experiments. Cells were plated on to 6 well plates and grown on medium supplemented with varying amounts of Hyg B, and the number of living cells, based on Trypan Blue exclusion was calculated.

To determine the optimal amount of Hygromycin B to be used in the experiments for the determination of the rates of random integration *in vitro*, vitality curves of the different cell lines were plotted in different concentrations of Hygromycin B (see Fig.

16). $1x10^5$ cells of each cell line were plated in 6 well plates and were maintained in one of the following mediums with α-MEM as the base (see Table 4).

Code number	Amount of Hygromycin B (mg/ml) in α-MEM
a	0
b	0.1
c	0.15
d	0.2
e	0.25
f	0.3
g	0.5

Table 4: List of the amount of Hygromycin B (mg/ml) used in the experiment

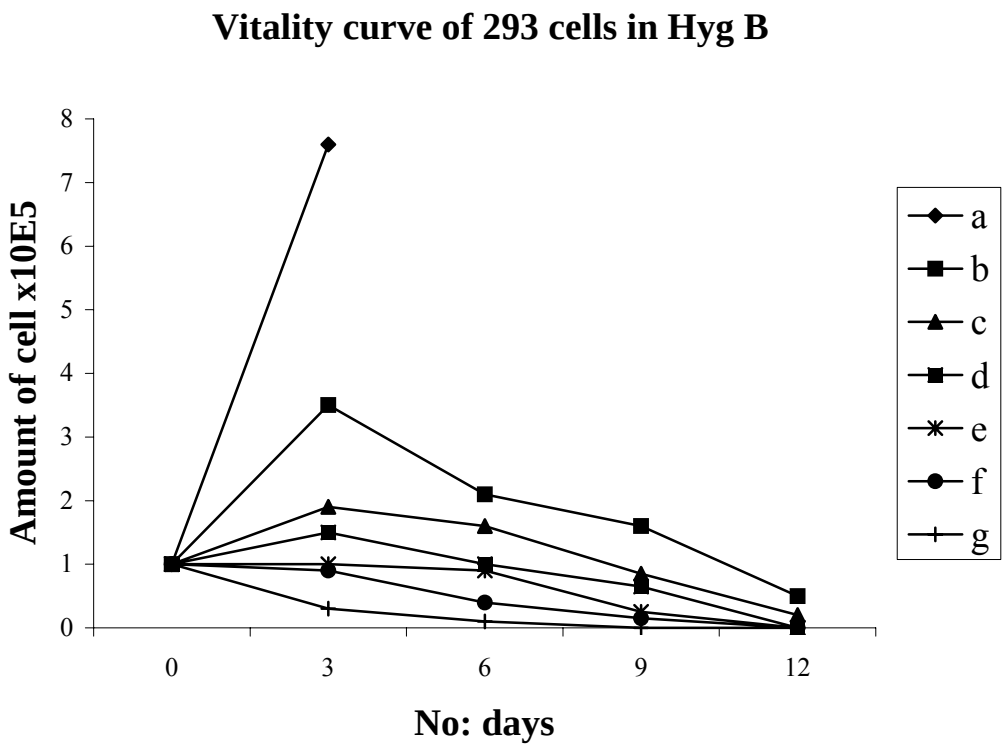

Fig. 17: Vitality Curve of 293 cells in medium supplemented with varying amounts of Hyg B. Cells were grown in 6 well plates and were selected in Hyg B containing medium. The number of cells was counted with a haemocytometer on Trypan Blue exclusion, and the data was mapped on to the graph above.

Cell count using Trypan Blue staining was taken once in three days and the number of the viable cells, counted using a Haemocytometer, was plotted in a graph which was

used to determine the optimal amount of Hygromycin B to be used. Six cell lines were used in the study. The vitality curve of 293 cells in Hyg B is shown here as an example (See Fig. 17). The following cell lines were used:

1. 293 cells
2. HT1080 cells
3. C-32 cells
4. FF-95 cells
5. HeLa cells
6. Human Retinal Pigmented Epithelium (HRPE) cells

The aim of the experiment was to optimise the amount of Hygromycin B to be added to the medium for selection. In all of the cell lines used, a concentration of 0.25 mg/ml of Hygromycin B was sufficient to kill all of the non-resistant cells by day 12 of the experiment and this concentration was used in the *in vitro* experiments.

IV.2 Determination of the permissivity of different cell lines to transduction with HC-AdV

Before the rates of integration and homologous recombination of HC-AdVs *in vitro* could be determined accurately, it was imperative that a calculation on the permissivity of the cell lines used in the study was carried out so that the number of recombination events per infection unit of the vector could be accurately calculated. The permissivity of various cell lines to adenovirus may differ and many factors such as the expression of CAR may be responsible for this (Carson et al., 1999, Hidaka et al., 1999, Kibbe et al., 2000, Leon et al., 1998). The expression levels of other molecules such as heparin sulphate proteoglycans (Dechecchi et al., 2000), MHC class I (Hong et al., 1997), the αv integrins (Wickham et al., 1993), the actin cytoskeleton (Patterson & Russell, 1983), phosphatidylinositol –3-OH kinase (Li et al., 1998b), the Rho family GTPases (Li et al., 1998a) might also play a part in the permissivity of the individual cell lines to adenovirus. To determine the permissivity of the cell lines used in the *in vitro* experiments, a modification of the slot blot experiment (Kreppel et al., 2002), the same that is used in the titration of the stocks of the HC-AdVs produced, was carried out. Cells of each of the cell lines were plated at

$1x10^5$ cells per well of a 24 well tissue culture plate. A HC-AdV of characterised titre, was used to infect the cell lines at various multiplicities of infection (moi) and the infectivity on the various cells was calculated using the above mentioned method, against that measured for HeLa cells (Fig. 18). The moi of HC-AdV in a given cell line, that gave a radioactive signal that corresponded to the moi 1 in Hela was taken as moi 1 for that particular cell line.

Experimental Setup

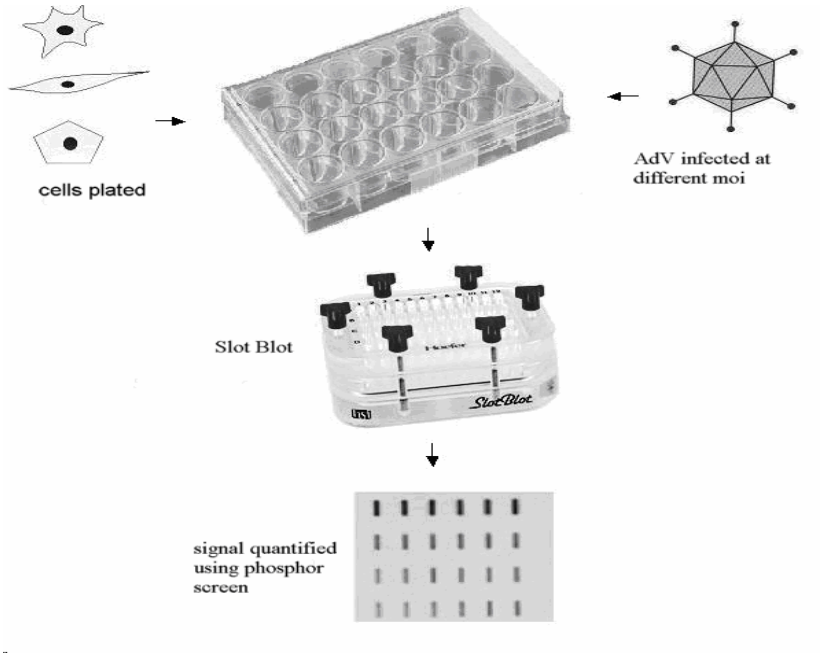

Fig. 18: Scheme of the experiment to determine the permissivity of the cell lines to AdV. Cells were plated on 24 well plates and infected with different dilutions of the vector and the viral load was calculated as per slot blot procedure. The left terminus of Ad5 was used as the probe.

The results obtained from the experiment are summarised in the following table (Fig. 19).

The aim of the experiment was to calculate the amount of viral vector needed to infect the various cell lines used the experiment at such an moi so as to obtain one vector copy per cell. During the experiment, it was found out that different cell lines needed different mois, summarised above, so as to obtain a single vector copy per cell.

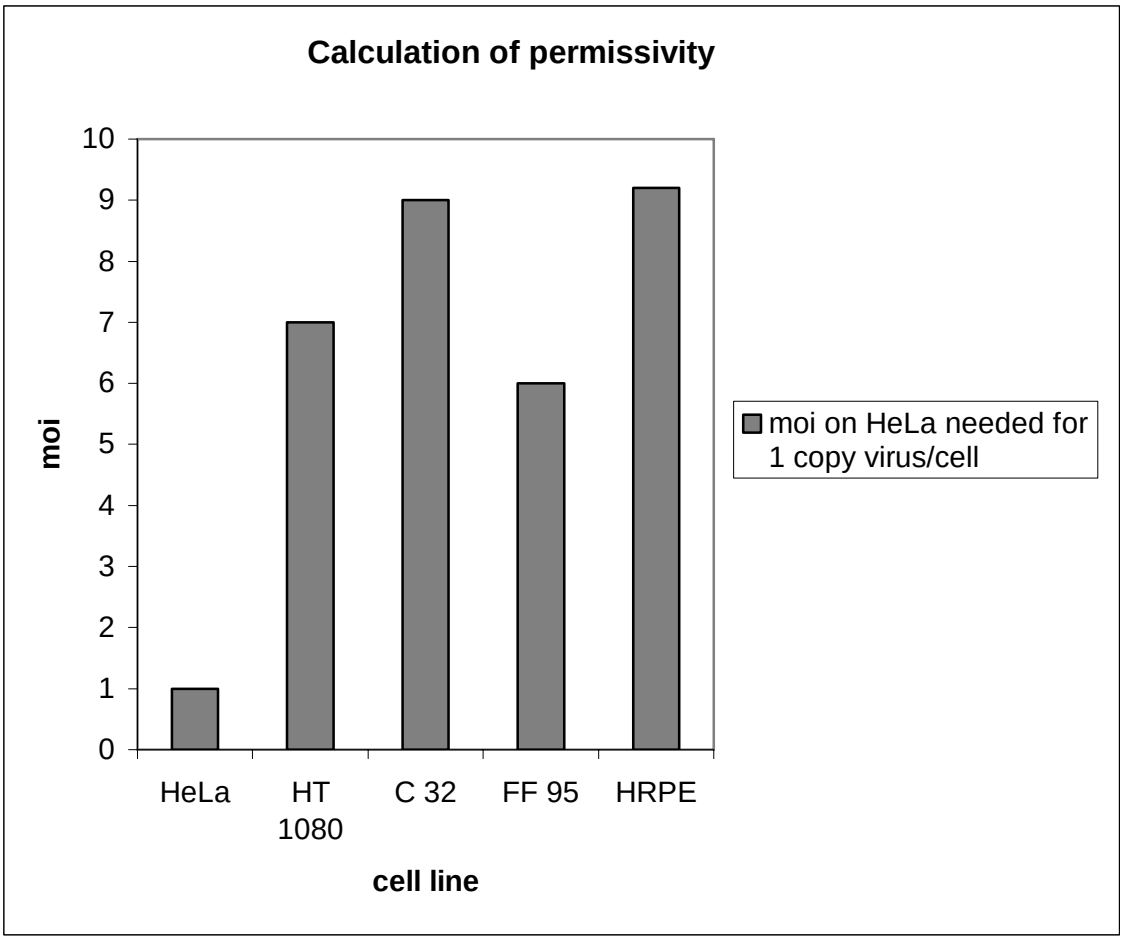

Fig. 19: Graph showing the permissivity of the different cell lines to adenovirus. Cells were transduced with varying mois with an AdV of a known titer and the copy load of vector DNA per cell was calculated using the slot blot method and plotted as the graph above.

IV.3 Determination of the rate of integration of HC-AdV *in vitro*

This series of experiments were carried out to determine the rate of integration of HC-AdVs *in vitro*. The vector used was Ad SLS 11, based on the plasmid p SLS 11. The structure of the vector is shown in Fig. 20 and the full details of the cloning procedure have been given on pg 65. In Ad SLS11, the exon 2 of the Hprt gene has been mutated to generate a stop codon. This mutation was designed to mimic the mutation that has been observed in a patient with Lesh Nyhan Syndrome (Davidson et al., 1989). A novel *Eco RV* site was designed downstream of the above mentioned mutation by substituting two nucleotides. In addition, a Hyg-EGFP expression cassette was cloned into the plasmid outside the Hprt fragment.

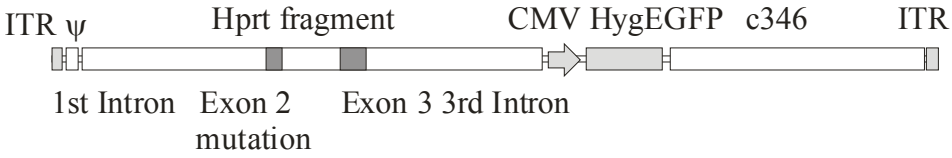

Fig. 20: Diagram of the HC-AdV vector Ad SLS 11, detailing the location of the various components.

The vector was designed to generate Hprt negative clones on the event of the vector DNA undergoing homologous recombination into the genome of normal Hprt positive cells. The vector was also designed to confer resistance to Hygromycin B in all of the transduced cells, and to form hygromycin resistant colonies in the event of the integration of the vector DNA into the cellular genome.

The plasmid was rescued with helper virus and serially amplified and purified using a CsCl gradient. The titre of the vector was determined using Slot Blot procedure**.**

Experimental setup:

HT1080, C-32, FF 95, HRPE and HeLa cells were infected at a moi of 1 with Ad SLS 11 on day 0 in 6 cm tissue culture dishes. On day 2, the cells were trypsinised, diluted and replated on to 15 cm tissue culture dishes. Cells infected with Ad SLS21 (that does not carry the EGFP-Hyg fusion cassette, and used in another project) and TBS treated cells were used as controls. On day 3, the cells were grown in medium containing 0.25 mg/ml of Hygromycin B, and were selected untill all the cells in the controls died out (Fig. 21). The number of hygromycin resistant colonies from each experiment was counted and is summarised in Table 5.

Cell line	**Number of experiments**	**Mean of the frequencies**	**SD**
HT 1080	n = 9	5.43×10^{-3}	4.6×10^{-4}
C 32	n = 12	1.47×10^{-3}	7.3×10^{-5}
FF 95	n =10	3.51×10^{-3}	3.4×10^{-4}
HRPE	n = 8	1.1×10^{-4}	2×10^{-5}
HeLa	n = 7	4.66×10^{-3}	3.01×10^{-4}

Table 5: The data obtained from the experiment for calculating the rate of random integration of the HC-AdV into the cellular genome.

The results obtained from all of the experiments were plotted as a graph in Fig. 22.

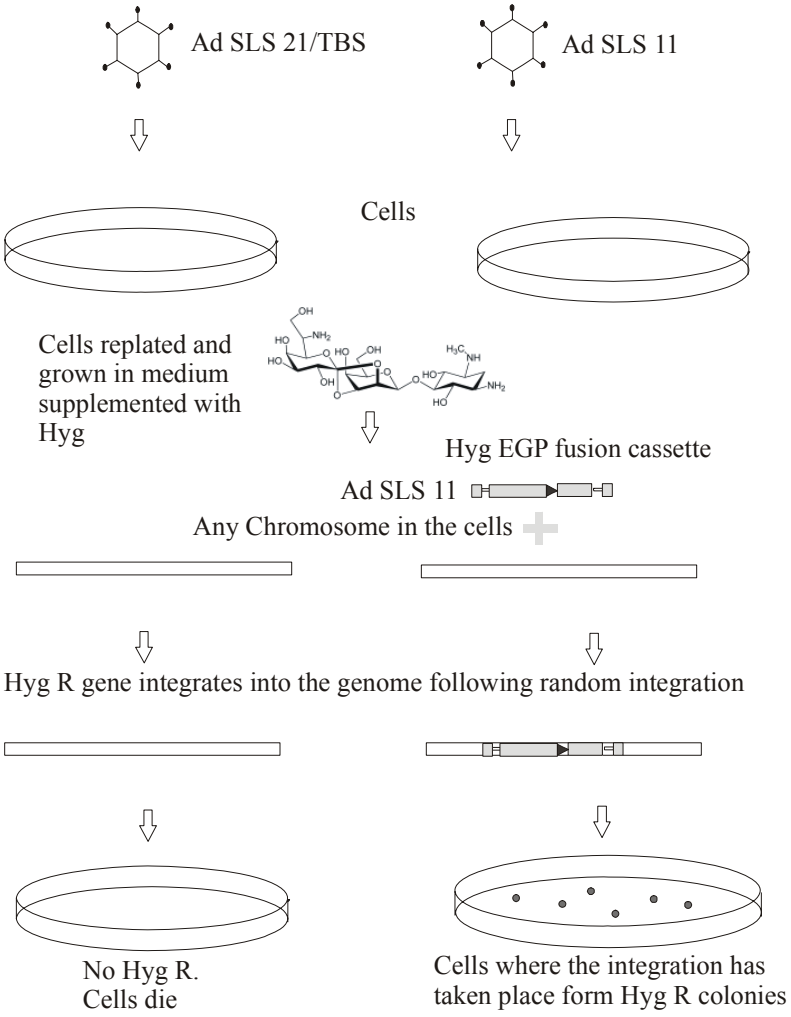

Fig. 21: Scheme of the experiment used to calculate the rate of random integration of the HC-AdV *in vitro*. Cells were infected at 1 moi either with Ad SLS 11, raised in medium supplemented with Hyg B, and the number of Hyg resistant colonies was taken when the control cells (1X TBS treated or infected with Ad SLS 21) had died out.

Significant differences in the rates of integration of the HC-AdV in between different cell lines were observed when One-way Analysis of Variance (ANOVA) was carried out on the means. The P value obtained was < 0.0001, which is considered highly significant, indicating that the variation among column means is significantly greater than expected by chance.

To summarise, the rate of integration of the HC-AdV DNA into the genome varied in different established and primary cell lines and was found to be between 5.43×10^{-3} to 1.1×10^{-4} events per vector that enters the cell.

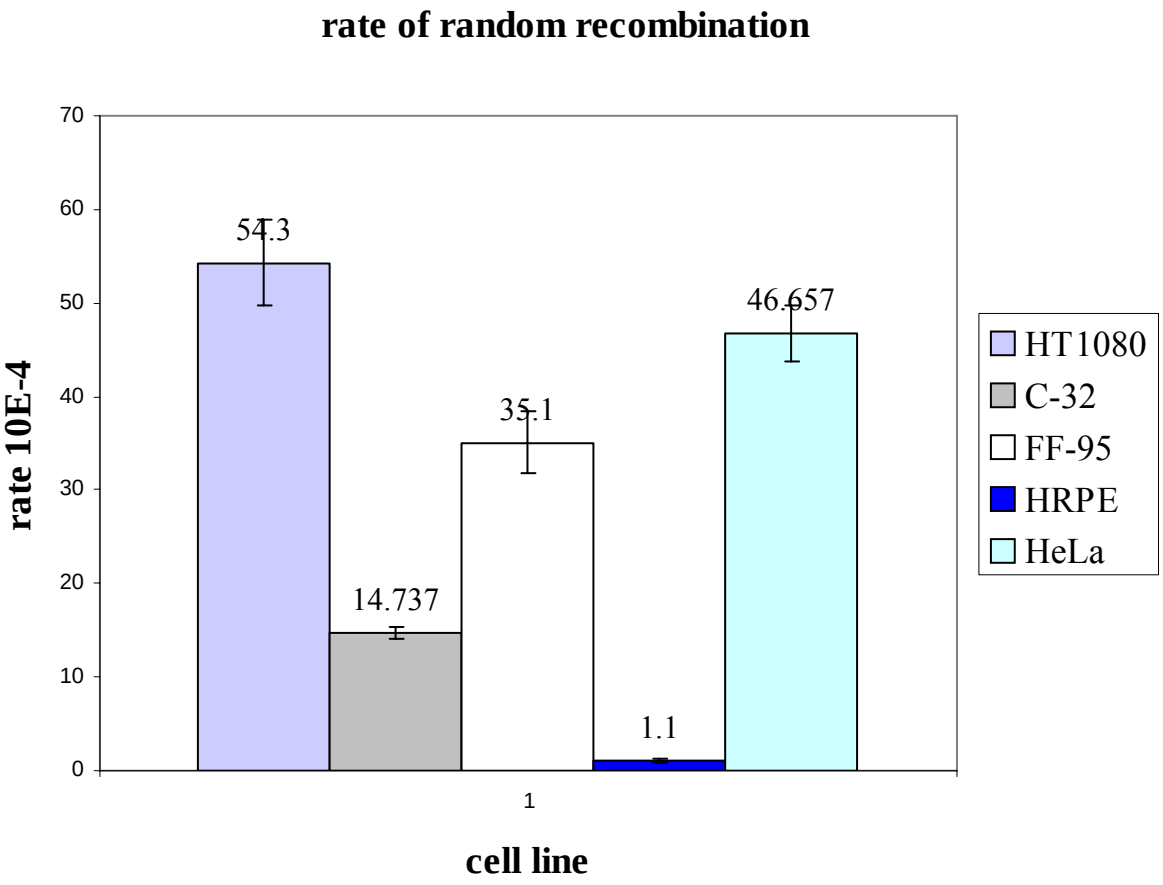

Fig. 22: Graph showing the rate of random integration of HC-AdV into the genome *in vitro*. The results from Table 5 were plotted on to the graph.

IV.4 Determination of the rate of homologous recombination of HC-AdV DNA *in vitro*

This series of experiments were carried out to determine the rate of integration of HC-AdVs *in vitro*. Ad SLS 11 was designed to carry a T insertion (nucleotide 13162 of hprt gene) in the exon 2 of the HPRT fragment resulting in the formation of a stop codon mimicking the published mutation HPRT $_{CHICAGO}$ (Davidson et al., 1989) observed in a human subject. A novel *Eco RV* restriction site was also engineered into the region by two substitutions (Fig. 23).

The rationale of the experiment was that the vector, on undergoing homologous recombination in a cell carrying a single X chromosome, would introduce a stop codon in the hprt gene, thereby shutting it off. This in turn would shut off the purine salvage pathway, thereby preventing the incorporation of the toxic purine analogue 6-

Thioguanine (6TG). Thus a successful homologous recombination event would lead to the formation of a 6TG resistant clone (Fig. 24).

A

B

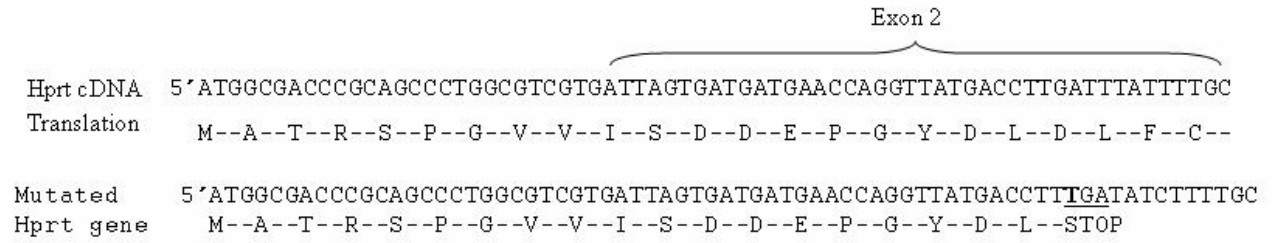

Fig. 23 A. Diagram comparing the mutations introduced into the mutant Hprt gene via Ad SLS 11 to the sequence in the wt Hprt gene

Fig. 23 B. Diagram showing the translation of the Hprt gene at the site of the introduced mutation and the introduction of the stop codon.

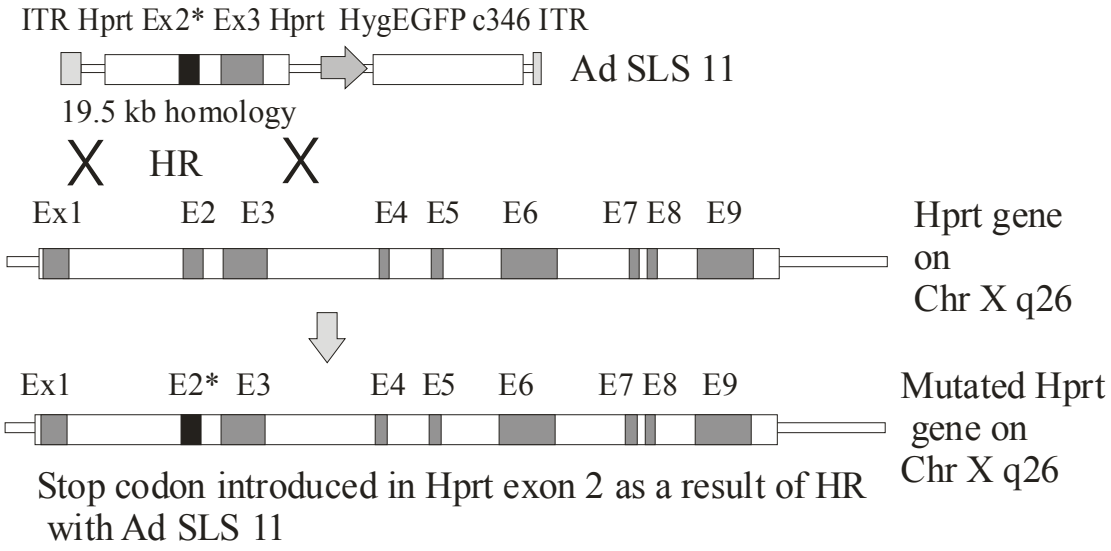

Fig. 24 : Scheme showing the formation of 6TG resistant cells following HR with Ad SLS 11 DNA.

Experimental set up:

HT1080, C-32 and FF 95 were infected at 1 moi with Ad SLS 11 on day 0 in 6 cm tissue culture dishes. On day 2, the cells were trypsinised, diluted and replated onto 15 cm tissue culture dishes. Cells infected with AdSLS 21 that does not posses the

Hprt fragment, and TBS treated cells were used as controls. From day 3 onwards, the cells were grown on medium containing 0.2 mg/ml of 6TG, and were selected till all the cells in the controls died out (Fig. 25). The number of 6TG resistant colonies from each experiment was counted, the mean was calculated and the experiment is summarised in Table 6.

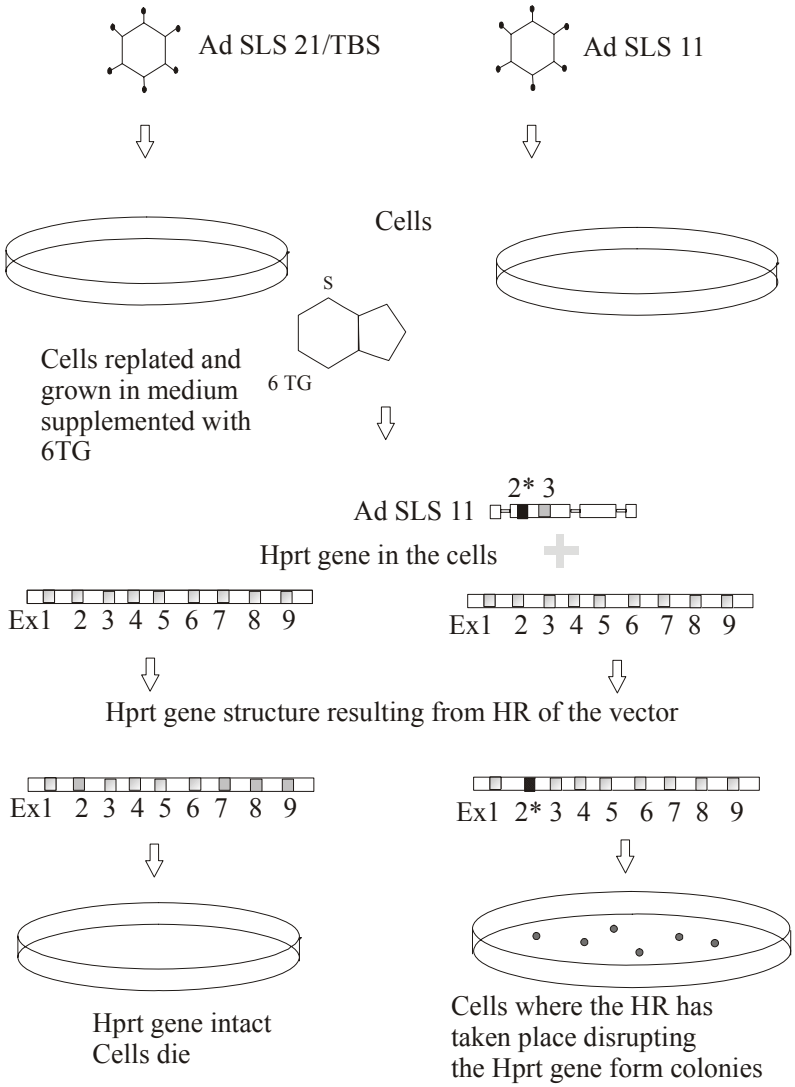

Fig. 25: Scheme of the experiment to determine the rate of HR of HC-AdV DNA with the chromosomal DNA *in vitro*.

Cell line	**Number of experiments**	**Mean of the frequencies**	**SD**
HT 1080	n =9	1.197×10^{-6}	6.7×10^{-7}
C 32	n = 9	2.02×10^{-5}	3.2×10^{-6}
FF 95	n = 10	1.05×10^{-5}	1.18×10^{-6}

Table 6: The data obtained from the experiment for calculating the rate of homologous recombination of the HC-AdV into the cellular genome *in vitro*. Cells were infected at 1 moi, raised in medium supplemented with 6TG, and the number of 6TG resistant colonies was taken when the control cells (1X TBS treated or infected with Ad SLS 21) had died out.

The means obtained from all of the experiments were plotted on to a graph below.

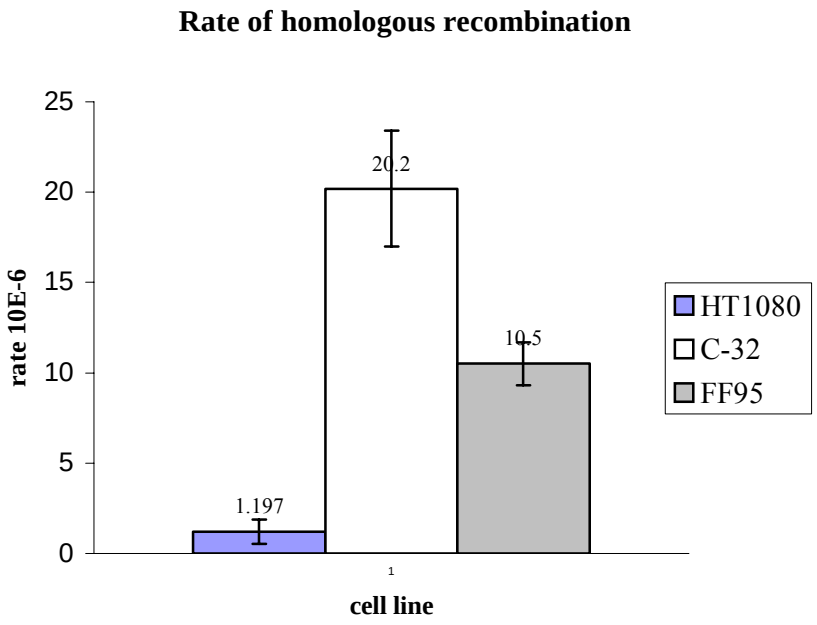

Fig. 26: Graph showing the rate of homologous recombination of HC-AdV DNA with the chromosomal DNA *in vitro.* The results from Table 6 were plotted on to the graph.

Significant differences in the rates of homologous recombination of the HC-AdV in between different cell lines were observed when One-way Analysis of Variance (ANOVA) was carried out on the means. The P value obtained was < 0.0001, which is considered highly significant, indicating that the variation among column means is significantly greater than expected by chance.

Taken together, the rate of homologous recombination of HC-AdV DNA into the chromosomal DNA varied in different cell lines and primary cells and was calculated to be between 2.02×10^{-5} to 1.197×10^{-6} events per vector that enters the cell, depending on the cell line.

IV.5 Molecular analysis of the DNA from the isolated clones

To analyse the molecular structure of the integrated HC-AdV DNA, individual clones from the experiments described above were isolated and propagated. DNA was isolated from 2 $\times 10^7$ cells. Southern blot experiments and PCR reactions were performed on the DNA, as described in the materials and methods section. In the Southern blot photos, -c refers to the negative control (cellular DNA), +c1 refers to

the positive control of the cellular DNA spiked with 1 copy of vector plasmid per 6 pg of DNA, +c2 refers to the positive control of the cellular DNA spiked with 2 copies of vector plasmid per 6 pg of DNA, +c4 refers to the positive control of the cellular DNA spiked with 4 copies of vector plasmid per 6 pg of DNA, +c5 refers to the positive control of the cellular DNA spiked with 5 copies of vector plasmid per 6 pg of DNA, cp refers to the positive control of the plasmid DNA.

IV.5.1 Randomness of integration

To ascertain whether the HC-AdV DNA integrated in a random manner during the events that conferred the individual cell lines their resistance to Hygromycin B, this series of Southern blots were performed on the DNA obtained from the clones isolated after the experiments described above. The DNA from the 6TG resistant clones was also used in the experiment to determine whether the homologous recombination that had taken place was of a replacement type or an insertion event.

IV.5.1.A Southern blot of the HT 1080 based clones, digested with *Sac I*

The DNA was extracted from the clones derived from the cell line HT 1080 followed by digestion with the restriction endonuclease *Sac I*. The vector DNA does not posses a *Sac I* site downstream of the HygEGFP cassette. The digested DNA was run in a 0.8 % TBE gel, blotted onto a nitrocellulose membrane and hybridized with a 2.3 kb probe derived from pHygEGFP and containing the whole of the Hygromycin EGFP fusion cassette, including the promoter (Fig. 27). Since the right terminus was 9 kb downstream of the Sac I site that was located upstream of the hygromycin EGFP cassette, following an event of random integration, the size of the DNA fragment which would cross hybridize with the probe, was expected to be above 9 kb of size, dependent on the location of the next *Sac I* restriction site downstream of the integration site in the genomic locus. However, the sizes of the individual bands were expected to be different from one another in the event of random integration. And no hybridization with the probe, to the DNA extracted from the 6TG resistant clones, was expected in the case of events of a classic replacement homologous recombination.

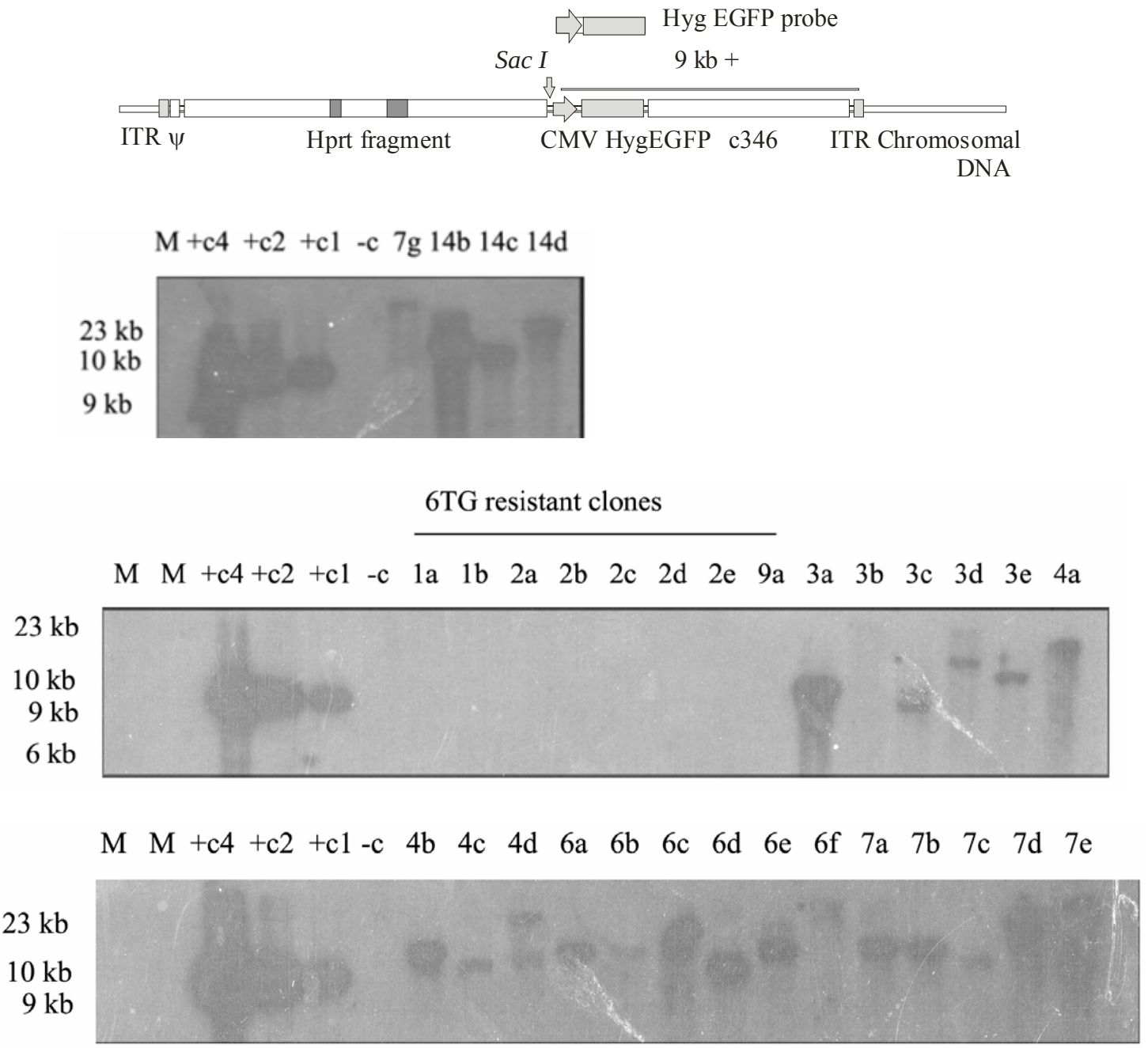

Fig. 27: Scheme and the Southern blots of the HT 1080 derived clones. DNA was digested with *Sac I*, run on a 0.8 % 1X TBE gel, blotted on to a nitrocellulose membrane and hybridized with the 2.3 Hyg EGFP probe. 1a to 9a denote the 6TG resistant clones. M stands for marker, -c denotes 20 µg of HT1080 DNA, +c1 stands for 20 µg of HT1080 DNA spiked with 1 copy/cell of p SLS 11 digested with *Pme I*, +c2 stands for 20 µg of HT1080 DNA spiked with 2 copies/cell of p SLS 11 digested with *Pme I*, +c4 stands for 20 µg of HT1080 DNA spiked with 4 copies/cell of p SLS 11 digested with *Pme I*.

From these Southern blots, it was evident that the integration of the vector in the genome had taken place in a random manner. Integrations of multiple Ad SLS 11 copies were observed in some clones and no evidence of random integration was

observed in the 6TG resistant cell lines. More details of the data have been summarised on pg 92.

IV.5.1.B Southern blot of the HT 1080 based clones, digested with *Kpn I*

To reconfirm the above result, the DNA extracted from the clones derived from the cell line HT 1080, was digested with the restriction endonuclease *Kpn I*. The digested DNA was run for a longer period in a 0.6 % TBE gel, blotted onto a nitrocellulose membrane and hybridized with a 1.8 kb probe derived from pHygEGFP and containing the just the whole of the Hygromycin EGFP fusion cassette (without the promoter). The sizes of the hybridised bands were expected to be greater than 9 kb, since the *Kpn I* upstream of the cassette was 9 kb away from the right terminus. Following an event of random integration, the size of the DNA fragment which would cross hybridize with the probe, was expected to be above 9 kb of size, dependent on the location of the next *Kpn I* restriction site downstream of the integration site in the genomic locus (Fig. 28). However, the sizes of the individual bands were expected to be different from one another in the event of random integration. And no hybridization with the probe, to the DNA extracted from the 6TG resistant clones, was expected in the case of events of actual homologous recombination.

From these two Southern blots, and those described on pg 83 it was observed integration of the vector in the genome had taken place in a random manner and no evidence of random integration was observed in the 6TG resistant cell lines. More details of the data have been summarised on pg 92.

IV.5.1.C Southern Blot of the C 32 based clones, digested with *Kpn I*

The DNA extracted from the clones derived from the cell line C 32, was digested with the restriction endonuclease *Kpn I*. The digested DNA was run for a longer period in a 0.6 % TBE gel, blotted onto a nitrocellulose membrane and hybridized with a 1.8 kb probe derived from pHygEGFP and containing the just the whole of the Hygromycin EGFP fusion cassette (without the promoter). The sizes of the hybridised bands were expected to be greater than 9 kb, since the *Kpn I* upstream of the cassette was 9 kb away from the right terminus. Following an event of random integration, the size of the DNA fragment which would cross hybridize with the probe, was expected to be above 9 kb of size, dependent on the location of the next *Kpn I* restriction site downstream of the integration site in the genomic locus (Fig. 29). However, the sizes

of the individual bands were expected to be different from one another in the event of random integration. And no hybridization with the probe, to the DNA extracted from the 6TG resistant clones, was expected in the case of events of actual homologous recombination.

The presence of the smaller second band was not expected. It can also be visualised in the controls in Fig. 28. This might be due to star activity. Though the enzyme supplier, New England Biolabs, does not report any star activity for *Kpn I,* the supplier Fermentas has reported it. http://www.fermentas.com/catalog/re/kpni.htm

From these Southern blots, it was evident that the integration of the vector in the genome had taken place in a random manner. Integrations of multiple Ad SLS 11 copies were observed in some clones and no evidence of random integration was observed in the 6TG resistant cell lines. More details of the data have been summarised in pg 92.

IV.5.2 Presence of the terminus in the clones

This series of Southern Blots were performed on the DNA obtained from the isolated from the isolated colonies, to determine whether the termini of the vector were present in the molecules that underwent integration or homologous recombination into the cellular genome.

The DNA extracted from the clones derived from the cell lines HT1080 and C 32, was digested with the restriction endonuclease *Sau 3A1*. The digested DNA was run for a longer period in a 1 % TBE gel, blotted onto a nitrocellulose membrane and labeled with a PCR fragment of the Adenoviral vector, which produces a 350 bp probe containing the whole of the terminus of the Adenovirus type 5. The sizes of the bands expected were greater than 457 bp and 190 bp on the left and right termini respectively, since a *Sau 3 AI* site was 457 bp downstream of bp1 of the left terminus, and a *Sau 3 AI* site was present 190 bps upstream of the last bp of the right terminus. Following an event of random integration, the sizes of the DNA fragment which would cross hybridize with the probe, was expected to be above 457 bp and 190 bp of size, dependent on the location of the next *Sau 3 AI* restriction site upstream or downstream of the integration site in the genomic locus (Fig. 30). As in the experiment described in earlier, the sizes of the individual bands would be different from one another in the event of random integration. The DNA extracted from the

6TG resistant clones, would not be expected to hybridize with the probes in the case of an event of a classical replacement homologous recombination.

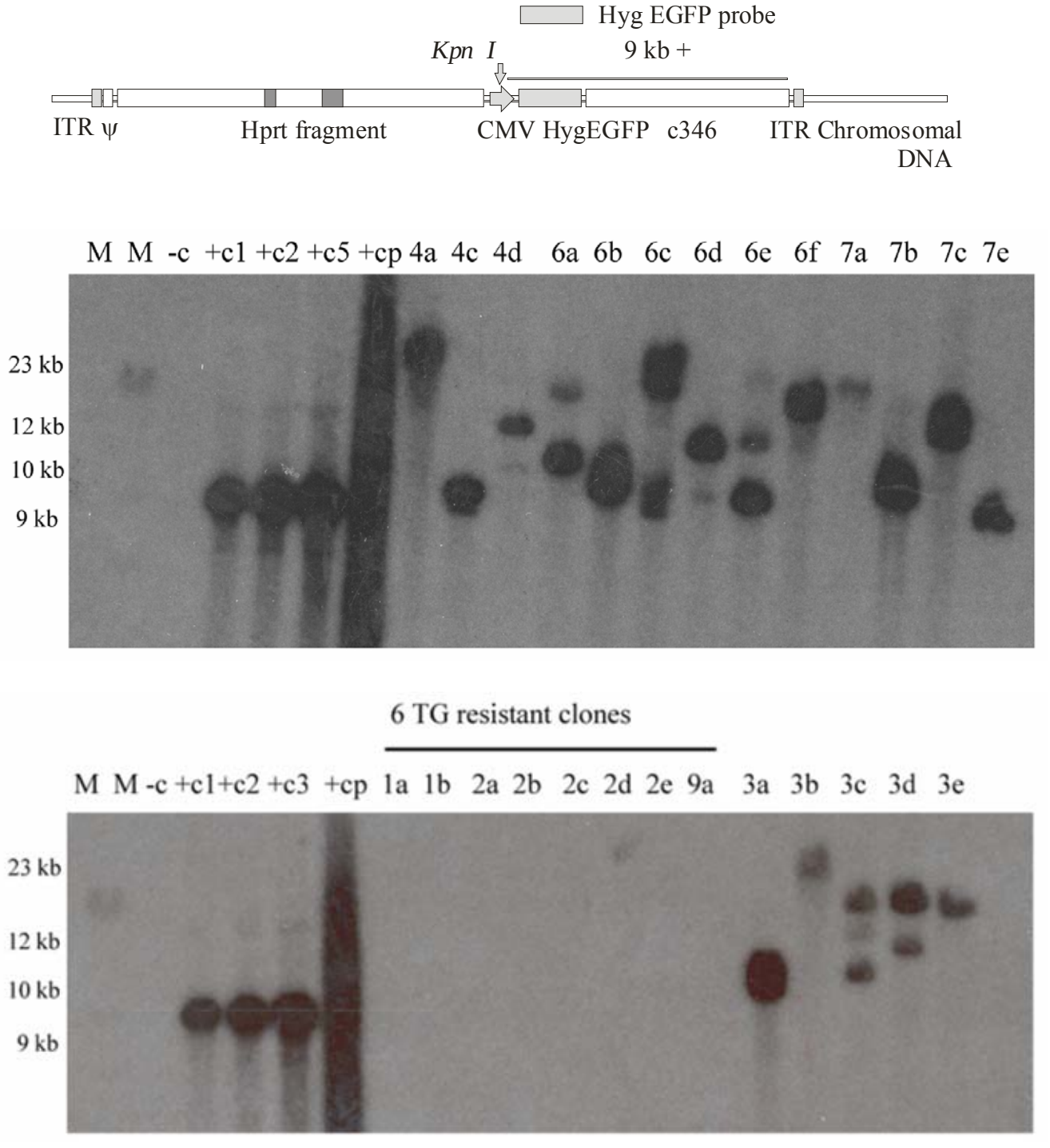

Fig. 28: Scheme and the Southern blots of the HT 1080 derived clones. DNA was digested with *Kpn I*, run on a 0.6 % 1X TBE gel, blotted on to a nitrocellulose membrane and hybridized with the 2.3 Hyg EGFP probe. 1a to 9a denote the 6TG resistant clones. M stands for marker, -c denotes 20 µg of HT1080 DNA, +c1 stands for 20 µg of HT1080 DNA spiked with 1 copy/cell of p SLS 11 digested

with *Pme I*, +c2 stands for 20 µg of HT1080 DNA spiked with 2 copies/cell of p SLS 11 digested with *Pme I*, +c3 stands for 20 µg of HT1080 DNA spiked with 3 copies/cell of p SLS 11 digested with *Pme I*. +cp stands for plasmid DNA

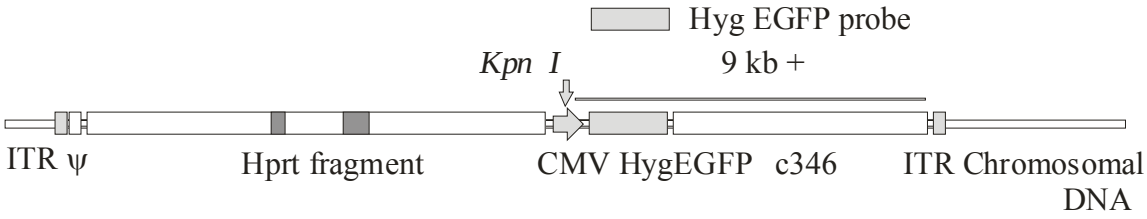

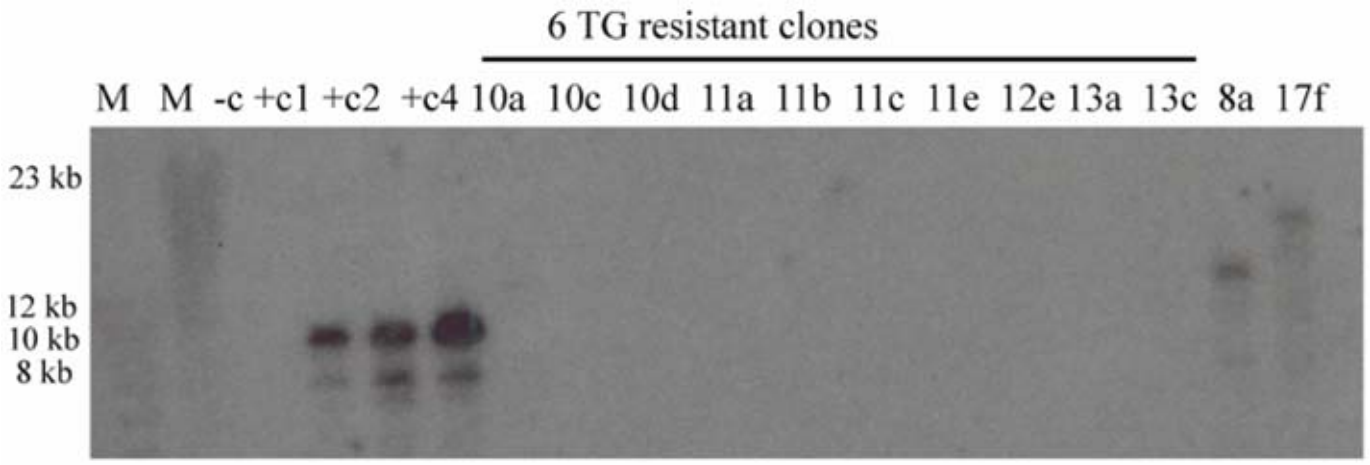

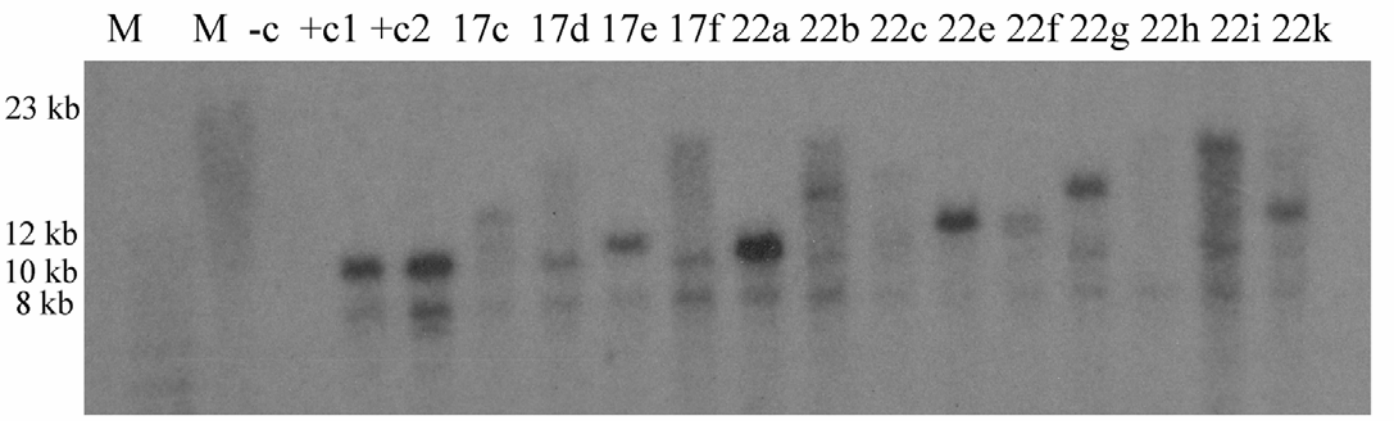

Fig. 29: Scheme and the Southern blots of the C 32 derived clones. DNA was digested with *Kpn I*, run on a 0.6 % 1X TBE gel, blotted on to a nitrocellulose membrane and hybridized with the 1.8 Hyg EGFP probe. 10a to 13c denote the 6TG resistant clones. M stands for marker, -c denotes 20 µg of C32 DNA, +c1 stands for 20 µg of C32 DNA spiked with 1 copy/cell of p SLS 11 digested with *Pme I*, +c2 stands for 20 µg of C32 DNA spiked with 2 copies/cell of p SLS 11 digested with *Pme I*, +c3 stands for 20 µg of C32 DNA spiked with 3 copies/cell of p SLS 11 digested with *Pme I*. +cp stands for plasmid DNA.

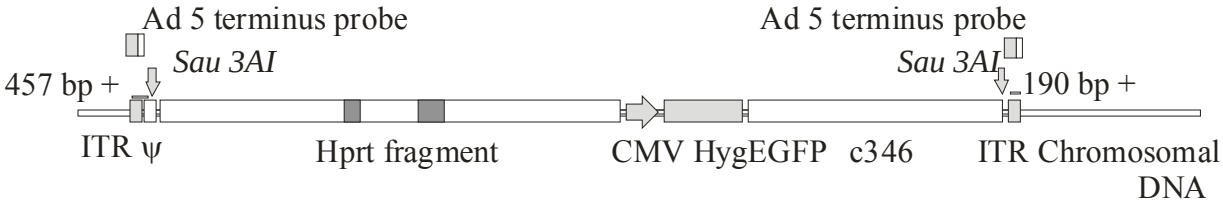
Ad 5 terminus probe
Sau 3AI
457 bp +
Ad 5 terminus probe
Sau 3AI
190 bp +
ITR ψ
Hprt fragment
CMV HygEGFP
c346
ITR Chromosomal DNA

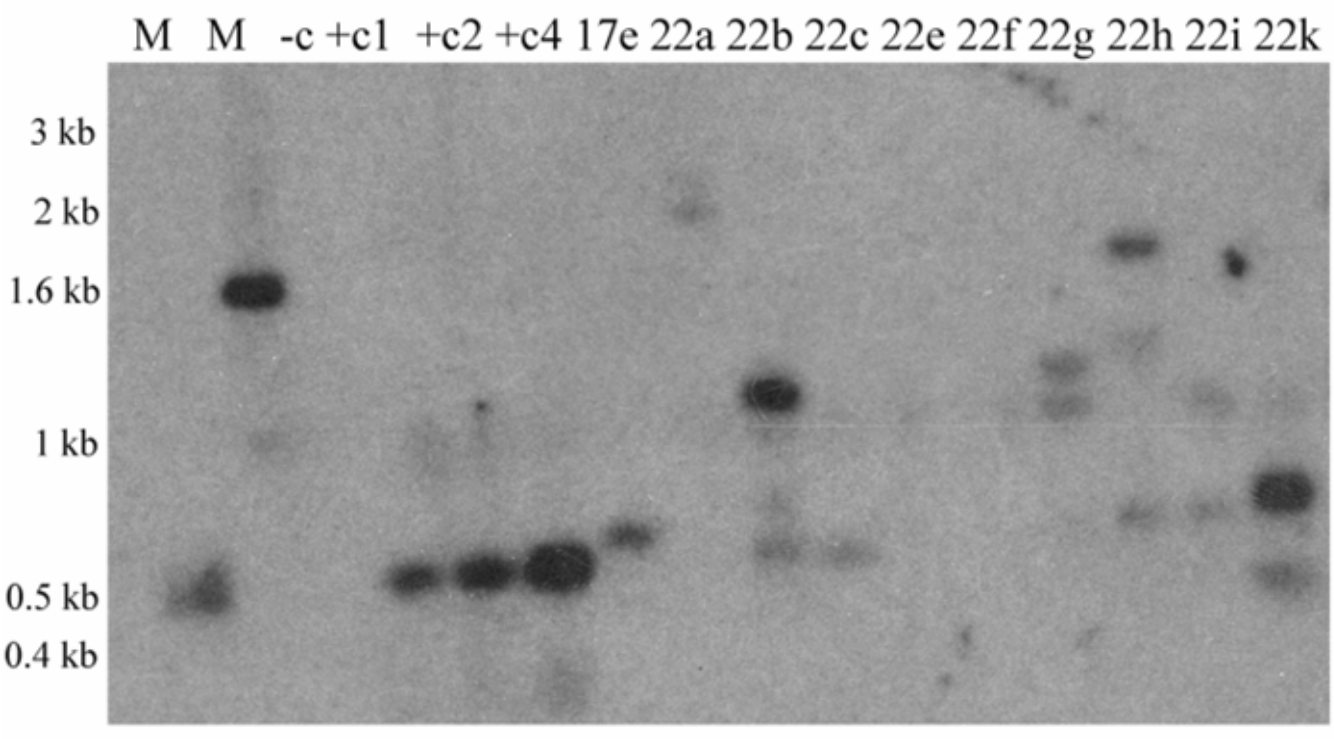
M M -c +c1 +c2 +c4 17e 22a 22b 22c 22e 22f 22g 22h 22i 22k
3 kb
2 kb
1.6 kb
1 kb
0.5 kb
0.4 kb

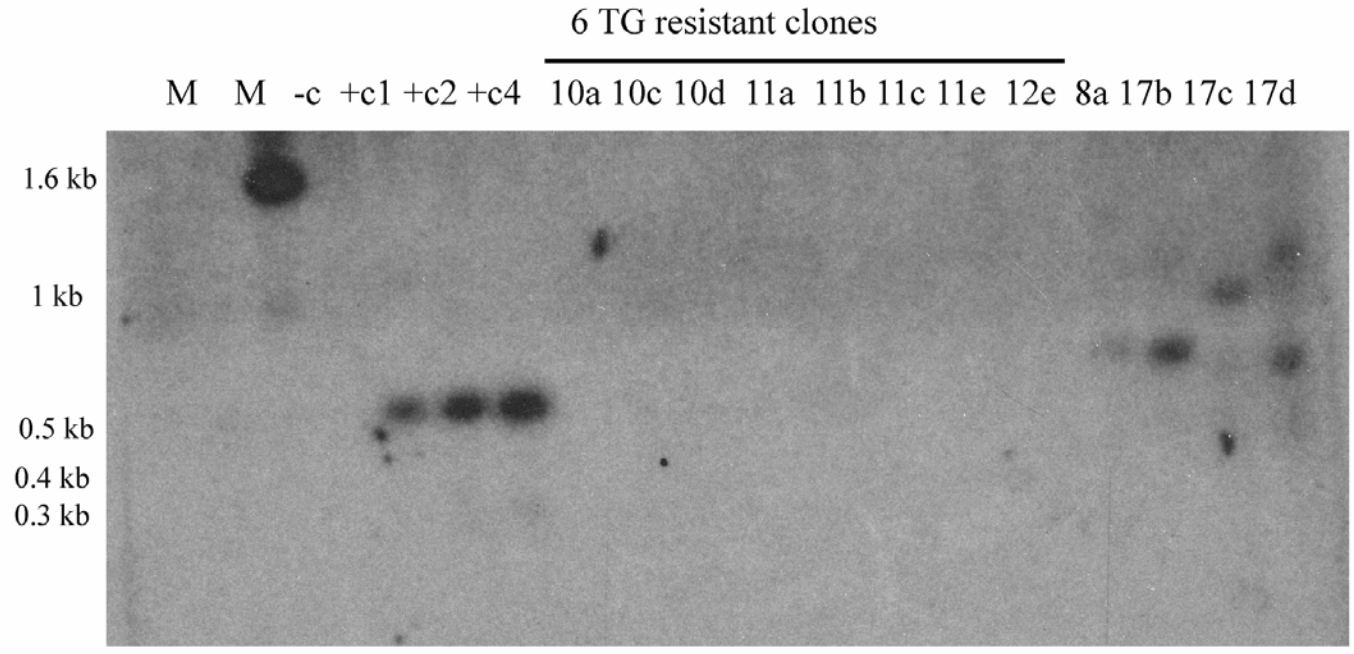
6 TG resistant clones
M M -c +c1 +c2 +c4 10a 10c 10d 11a 11b 11c 11e 12e 8a 17b 17c 17d
1.6 kb
1 kb
0.5 kb
0.4 kb
0.3 kb

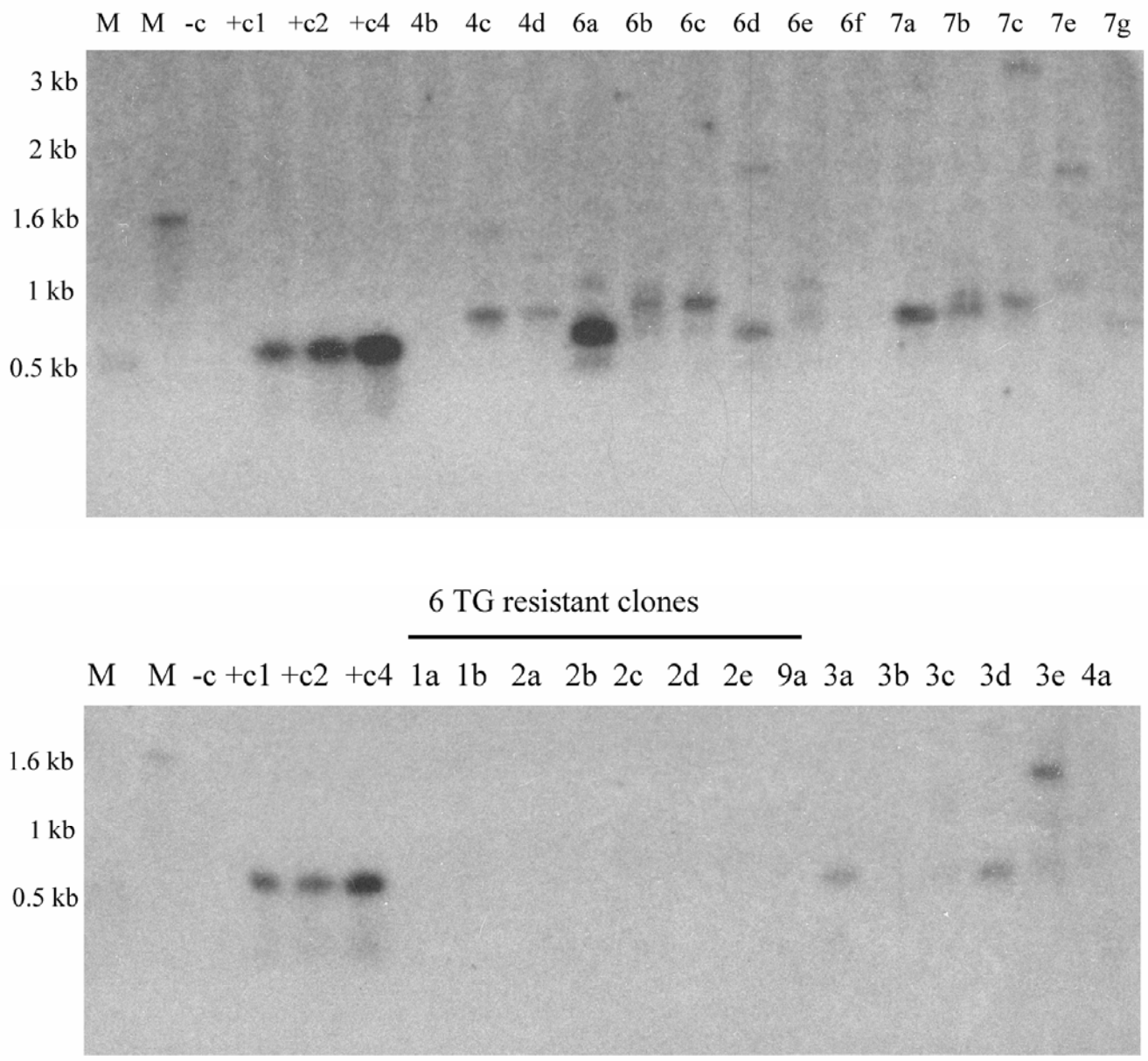

Fig. 30: Scheme and the Southern blots of the C 32 and HT 1080 derived clones. DNA was digested with *Sau 3A I*, run on a 1 % 1X TBE gel, blotted on to a nitrocellulose membrane and hybridized with the Ad5 terminus probe. 1a to 9a and 10a to 12e denote the 6TG resistant clones. M stands for marker, -c denotes 20 µg of HT1080/ C32 DNA, +c1 stands for 20 µg of HT1080/ C32 DNA spiked with 1 copy/cell of p SLS 11 digested with *Pme I*, +c2 stands for 20 µg of HT1080/ C32 DNA spiked with 2 copies/cell of p SLS 11 digested with *Pme I*, +c4 stands for 20 µg of HT1080/ C32 DNA spiked with 4 copies/cell of p SLS 11 digested with *Pme I*.

From these Southern blots, it was evident that the integration of the vector in the genome had taken place in a random manner. Integrations of multiple Ad SLS 11 copies were observed in some clones and no evidence of random integration was observed in the 6TG resistant cell lines. More details of the data have been summarised on pg 92.

IV.5.3 Structural integrity of the integrated vector

This Southern Blot was carried out to ascertain whether during the process of integration, the structural integrity of the vector had been compromised.

The DNA extracted from the clones derived from the cell line HT 1080, was digested with the restriction endonuclease *Pac I*. The digested DNA was run for a longer period in a 0.6 % 1X TBE gel, blotted onto a nitrocellulose membrane and hybridized with the 1.8 kb probe containing the whole of the Hygromycin EGFP fusion cassette. If the vector had integrated as an intact molecule, then the band size expected would be 22.5 kb, and if deletions had been present in the genome, the size would be less (Fig. 31).

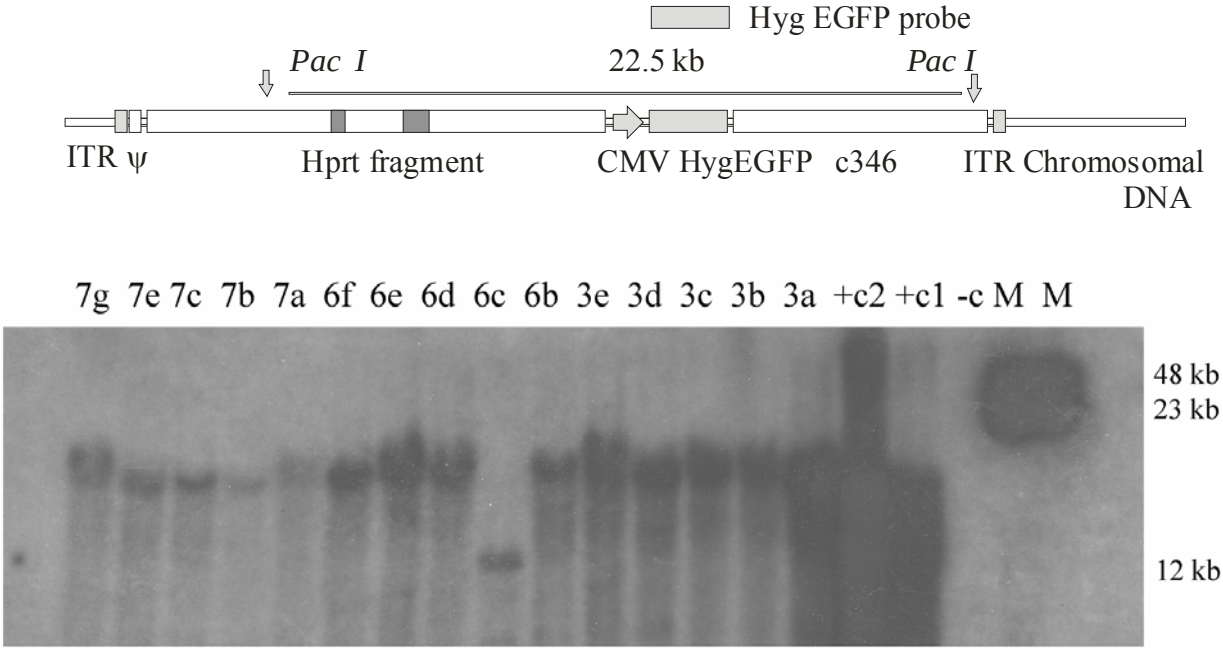

Fig. 31: Scheme and the Southern blots of HT1080 derived clones. DNA was digested with *Pac I*, run on a 0.6 % 1X TBE gel, blotted on to a nitrocellulose membrane and hybridized with the 1.8 Hyg EGFP probe. M stands for marker, -c denotes 20 µg of HT1080 DNA, +c1 stands for 20 µg of HT1080 DNA spiked with 1 copy/cell of p SLS 11 digested with *Pme I*, +c2 stands for 20 µg of HT1080 DNA spiked with 2 copies/cell of p SLS 11 digested with *Pme I*.

From this Southern blot, it was evident that in most of the clones, the internal 22.5 kb fragment was intact. More details of the data have been summarised on pg 92.

IV.5.4 Summary of the results obtained from the Southern blot experiments on the isolated clones

The results from the Southern blot have been summarized in the following tables. Details are given only from the Hyg resistant clones, since the 6TG resistant clones did not give any bands, as expected.

Name of clone	***Sac I* digest 9 kb +**	***Kpn I* digest 9 kb +**	***Sau 3AI* 0.5 kb + and 0.2 kb +**	***Pac I* digest 22.5 kb**
Probe	**Hyg**	**Hyg**	**Terminus**	**Hyg**
3a	1	1	1 strong band at 0.45 kb	1
3b	0	1	-	1
3c	2	2	1 weak band 500 bp; 1 weak band 0.7 kp; 1 weak band 0.8 kb	1
3d	1	2 (1 strong, 1 weak	1 strong band 0.45 kp; 1 weak band about 1.2 kb	1
3e	1	1	1 strong band close to 1 kb; 1 weak band about 0.65 kb; 1 weak band at 0.45 kb	2?
4a	1	1	1 weak band at 0.6 kb; 1 weak band at 0.8 kb	-
4b	1	1	1 very weak band at 0.5 kb	-
4c	1	1	1 strong band at 0.6 kbs; 1 weak band about 1 kb	-
4d	2?	1	1 weak band at 0.6 kb; 1 very weak band at 0.65 kb; 1 very weak band at 0.8 kb.	-
6a	1	2	1 strong band above 0.5 kp; 1 weak band at 0.4 kb; 1 weak band at 0.7 kb; 1 very weak band at1.2 kb	-
6b	-	1	1 weak band at 0.6 kb, 1 very weak band at 1 kb; 1 very weak band at 0.7 kb	1
6c	1	2	1 strong band at 0.6 kb; 1 very weak at 0.5 kb	1 (smaller)
6d	1	1	1 strong band at 0.5 kb; 1 very weak band at 1 kb;	1

			1 weak band at 1.5 kb	
6e	1	2	1 weak band at 0.65 kb; 1 weak band at 0.55 kb	1
6f	1?	1	-	1
7a	1	1	1 strong band at 0.55 kb	1
7b	1	1	1 strong band at 0.55 kb; 1 weaker band at 0.6 kb	1
7c	1	1	1 strong band at 0.5 kb; 1 strong band > 2 kb	1
7d	1	1	1 weak band at 0.6 kb; 1 strong band at 1.2 kb; 1 weak band at 1.5 kb	-
7e	1	1	1 weak band at 0.5 kb	1
7g	1?	1	-	2?

Name of the clone	***Kpn I* digest** **9 kb +**	***Sau 3AI*** **0.5 kb + and 0.2 kb +**
Probe	**Hyg**	**Terminus**
8a	1	1 strong band, 0.6 kb
17b	1	1 strong band, 0.6 kb
17c	2-3	1 strong band, 0.6 kb; 1 weak band 0.5 kb
17d	1	1 strong band, 0.5 kb; 1 strong band 1.2 kb
17e	1	1 strong band, 0.6 kb; I very weak band at 0.3 kb
17f	1	-
22a	1	1 weak band, 2 kb; 1 weak band 2.5 kb
22b	1-2	1 strong band 1.3 kb; 1 weak band 0.5 kb; 1 v.weak band, 0.7 kb; 1 veryweak band 1.2 kb
22c	2	1 weak band 0.5 kb, 1 very weak band ,1 kb (?)
22d	-	-
22e	1	1 very weak band, 1 kb?
22f	2	0
22g	2	1 weak band 1.1 kb; 1 weak band 1.2 kb
22h	?	1 strong band, 1.9 kb; 1 weak band 1.4 kb; 1 weak band 0.7 kb
22i	2	1 weak band, 0.6 kb; 1 weak band 1 kb
22k	1-2	1 strong band, 0.7 kb; 1 weak band 0.4 kb; 1 weak band 1.1 kb

Tables 7: Data regarding the number and size of bands, obtained from the Southern Blot experiments on C 32 and HT 1080 derived clones

From the Southern blot experiments carried out the following results can be inferred:

i. The integration of the vector took place in a random manner (difference in sizes of the bands.)

ii. In all of the 16 6TG resistant clones analysed, no presence of the adenovirus terminus was detected, as was expected in the case of homologous recombination between the vector and the genomic DNA.

iii. In all of the 18 6TG resistant clones analysed, no presence of the HygEGFP cassette was observed as was expected in the case of homologous recombination between the vector and the genomic DNA.

iv. In 9 confirmed and 14 possible (very weak bands) clones out of the 37 Hyg resistant clones (24 – 38%), more than one copy of the transgene was present, suggesting multiple integration events.

v. In only one of the 15 Hyg resistant clones analysed does the vector molecule seem to have undergone an internal deletion.

vi. At least in 8 out of the 37 (21 %) Hyg resistant clones analysed, there were more number of Ad termini than expected for the number of transgenes detected in the clone.

IV.5.5 Analysis of the junction sites of integration of HC-AdV DNA

These series of experiments were conducted to determine the sites within the human genome where the Ad SLS 11 DNA had integrated. Three methods, *viz* the LAM PCR method (Schmidt et al., 2001), Splinkerette PCR (Mikkers et al., 2002), (Devon et al., 1995), Inverse PCR (Triglia et al., 1988) was tested on the DNA that was extracted. The best results were obtained with the modified inverse PCR as described in the materials and methods section. Basically, the DNA was digested with a 4 base pair cutting enzyme and religated to form circular molecules. A modification of the ligation reaction (Lund et al., 1996) was used. wt DNA and wt DNA spiked with varying amounts of the plasmid were used as controls. 0.5 % of the product was used as a template in the nested PCR. The products were separated on a high percentage (2 %) TAE agarose gel, and the bands were cut out, cleaned and subcloned into the TOPO TA cloning vector (Invitrogen). The DNA was sequenced. The sequences were

analysed for the TOPO TA vector DNA sequences and they, the primers, the termini sequences and restriction site that were used were marked and separated. The flanking sequences were subjected to NCBI BLAST search and the locations of high percentage matches were plotted. Holding the mouse over the plot in the map viewer, over the component master map (CMM), the co-ordinates of the genomic DNA clone identified uying the BLAST search was located at the chromosomal level. The co-ordinates were used to confirm the results obtained when the DNA sequences were subjected to ENSMBL BLAST search, and the exact location of the integrated Ad SLS 11 was determined, right up to the exact nucleotide. Possible locations of the sequences involved in the actual recombination event (patchy homologies) were also identified. Chromosomal locations were denoted by the exact words used in the databases.

Inverse PCR

A modification of the inverse PCR protocol reported in (Silver & Keerikatte, 1989, Triglia et al., 1988) was re-adapted to fit in with the conditions of amplification of the adenoviral terminus junction sites. A modification of the ligation procedure reported in (Lund et al., 1996) was used for the ligation experiment. The full details of the protocol are given in the materials and methods section of the thesis (Fig. 32). Inverse PCR using a different enzyme *Tsp 509L* was carried out on 18 of the junction sites to reconfirm the sites.

Junction sites obtained:

Due to space constraints, the sequences obtained from one clones, clone 17e is exhibited as an example to demonstrate how the full calculation was carried out. Only the processed data from all the remaining clones is given.

By convention, when the same nucleotides were found in the junction that corresponded to the Ad5 and the genomic DNA, it was taken as having originated from the AdV terminus. In the sequences that are presented, the Ad5 ITR sequences are given in the first line, the junction site sequences in the second line and the genomic DNA sequence where the integration had taken place is given in the third line. The junction site sequences with homology to the Ad5 ITR sequence and their counterpart in the Ad5 terminus, is denoted by a gray box; whereas the junction site sequences with homology to the genomic DNA sequences, and their counterparts in

the genomic DNA, are marked by a yellow box. In the junction sequences, (-) refers to positions in the sequences derived from viral temius and (+) to the positions derived from chromosomal DNA.

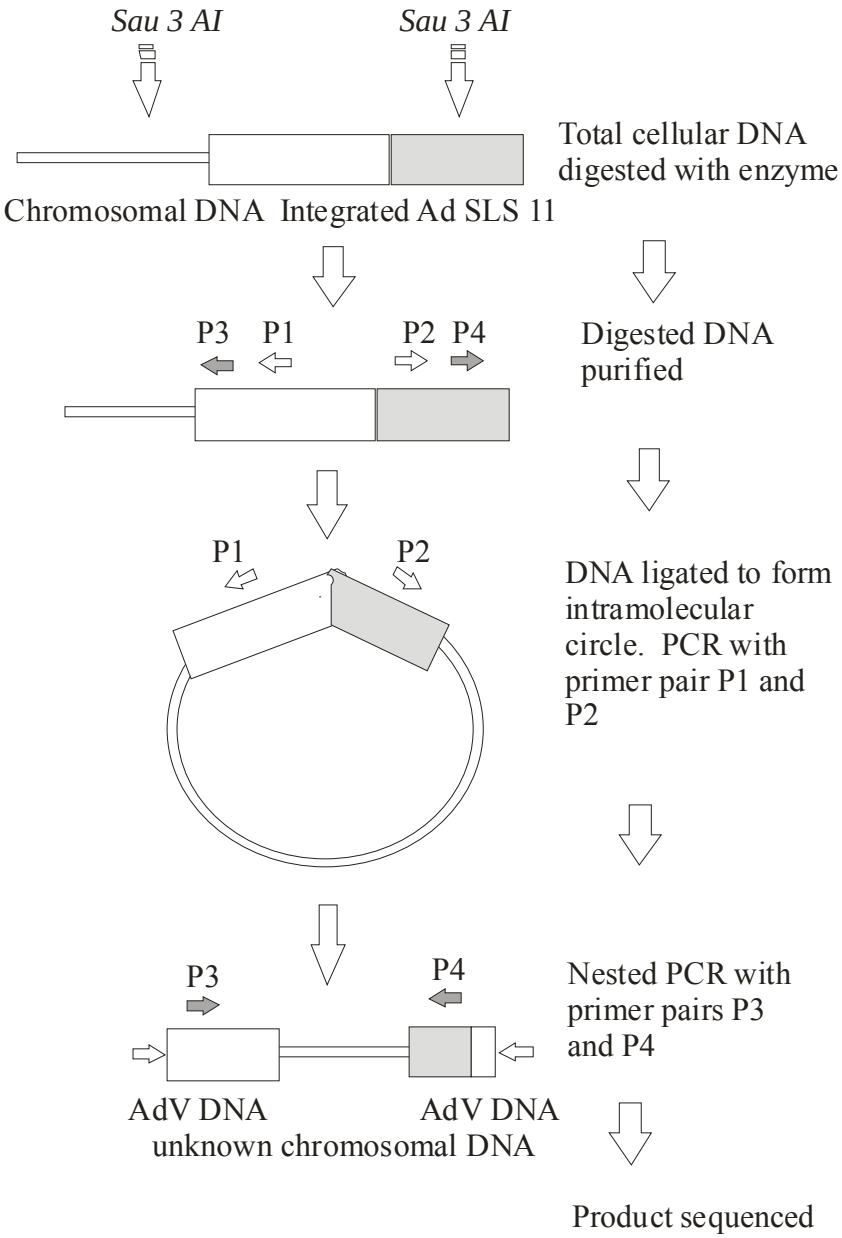

Fig. 32: Scheme of the Inverse PCR carried out on the clones derived from C 32 and HT 1080 cells to determine the sequence of the junction sites of integration of the HC-AdV and the cellular DNA.

In the sequence from the two clones given below, underlined text denotes the primers, **bold text** denotes the ITR sequence, plain text denotes the genomic sequence, and the text in ***bold and italic*** characters denotes the restriction endonuclease recognition site.

Analysis of clone 17e

Clone 17e is a C32 derived Hyg resistant cell line. The Southern blot data (summarized in pg 92) revealed the presence of one single copy of the vector, with a size between 10 and 12 kb. On analysis of the clone following Inverse PCR, a single *Kpn I* site was found at 1397 bps downstream of the integration site. This would give rise to a 11.3 kb band on the above mentioned Southern blot, validating the result. Hybridisation with the terminus probe revealed the presence of one strong band less than 600 bps, and a very weak band less than 300 bps in size. This correlates with the data obtained following the inverse PCR and sequencing of the DNA obtained from 17e, where a *Sau 3A1* site was observed at 85 bps upstream of the integration site of the left terminus, giving any band obtained from that integration a size of 549 bps. A *Sau 3AI* site was also observed 91 bps downstream of the integration site of the right terminus of the vector, giving any band resulting from that integration a size of 281 bps. This tallies with the Southern blot data. The sequence obtained from the Inverse PCR product using the primers for the left terminus is given below.

GCAACATCACACTTCCGCCAC**ACTACTACGTCACCCGCCCCGTTCCCAC**
GCCCCGCGCCACGTCACAAACTCCACCCCCTCATTATCATATTGGCTT
CAATCCAAAATAAGGTATATTATTGATAAAACAAAGGGGCCGGGCGCG
GTGGCTCACGCCTGCAATCCCAGCACTTTGGGAGGCTGAGGCGGGCAGAC
CACGAGGTCAGGA***GATC*AAATGATATCAAAACGCCAACTTTGACCCGG**
AACGCGGAAAACACCTGAGAAAAACACCTGGGCG

NCBI BLAST search was used to align the sequence with the human genome and the integration was observed to have happened in the chromosome 20q13+3, in the 1st intron of the BTPD4 gene. The last 4 bps of the Ad terminus were deleted. The sequence was analysed in the ENSEMBL database to verify the location. The location of the integration in the genome was mapped in the 61876780 bp (numbering based on the ENSEMBL database) of the chr 20.

A

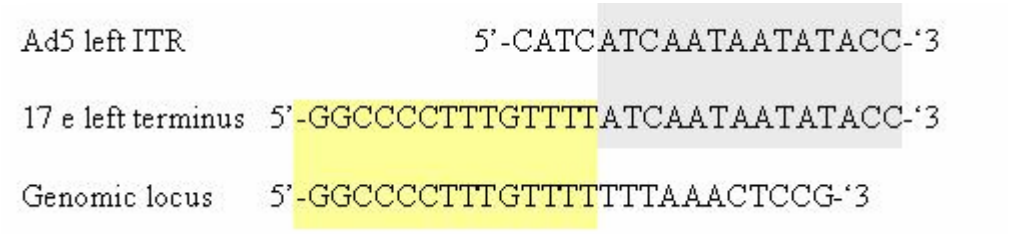

B

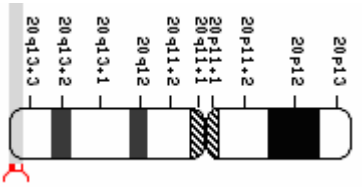

C

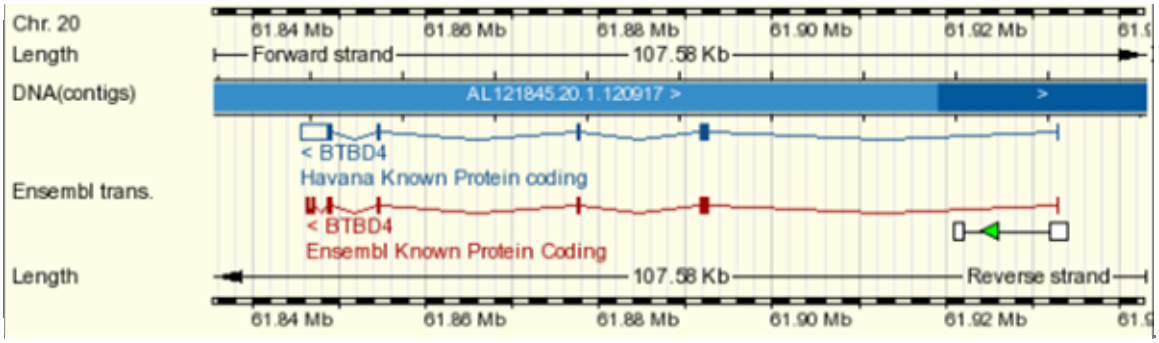

D

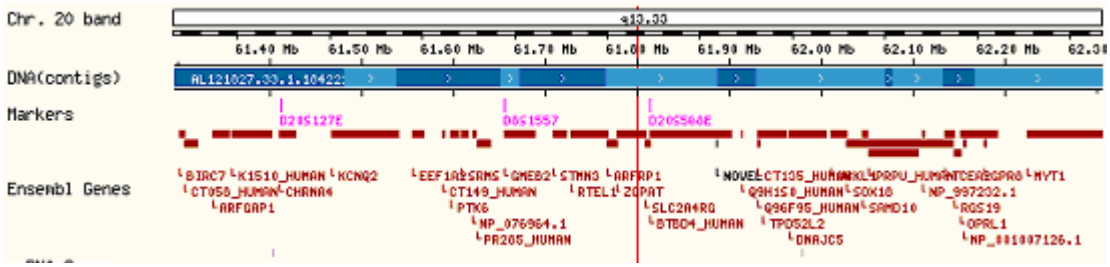

Fig. 33: Analysis of the junction between HC-AdV DNA and chromosomal DNA: clone 17e.
A. Sequence of the junction site. B. Map of chr 20, showing the integration that took place in 20q13.3. C. Closer view of 20q13.3, showing the region where the vector had integrated. D. Map of the BTBD4 gene, showing the integration of the vector in the intron 1-2. The sequence data from the right terminus too was used to obtain the picture.

The sequences obtained from the Inverse PCR product using the primers for the right terminus is given below.

CATCACTCCGCCCTAAAACCTA**CGTCACCCGCCCCGTTCCCACGCCCCG**
CGCCACGTCACAAACTCCACCCCCTCATTATCATATTGGCTTCAATCC
TGCCTCAGCCTCCTGAGTAGCTGGGACTACAGGGCGCCTGCCACCACACC
TGGCTAATTTTTTGTATTTTTAGTAGAGACGGGGTTTCACCGTGTTAGCCA
AGATGGTCTC***GATC*GCGCCCCTAGGGGCCGGCCTTAATTAAATCAA**GC
TTATCGATACCGTCGAGACC

NCBI BLAST search was used to align the sequence with the human genome and the integration was observed to have happened in the chromosome 20q13+3. The last 25 bps of the right terminus of the Ad DNA were deleted. The sequence was analysed in the ENSMBL database to certify the location, and the integration was mapped to bp 61881299 in chr 20 q13.3, in the 1st intron of the BTBD4 gene, 4.5 kb downstream of the left terminus integration.

Ad5 right ITR	5'-GGCTTCAATCCA←21bps→ATG-'3
17e right terminus	5'-GGCTTCAATCCTGCCTCAGCCTCCTG-'3
Genomic locus	5'-GCCATTCTCCTGCCTCAGCCTCCTG-'3

Since all the bands observed in the Southern blotting (summarized in pg 92) can be accounted for, it can be assumed that there was only one event of vector integration in the cellular genome, and during the event, 4519 bps of the cellular DNA were deleted.

IV.5.5.A HT1080 derived cell lines

Clone 3a

A deletion of 9 base pairs was observed in the terminus at the junction site. The integration had taken place in the chromosomal location 7p21, at the 17859816 bp. However, a fusion of sequences from 4q22 was observed 75 bps downstream of the integration site.

Ad5 left ITR	5'-CATCATCAATAATATACCTTATT-'3
3a left terminus	5'-TGTCTGGGATACATGCAATATACCTTATT-'3
Genomic locus	5'-TGTCTGGGATACATGCCTGGTAATAGAGC-'3

Clone 3c

A substitution of a G to C was observed in the terminus at the –3 bp location, where the last bp was missing. The integration was mapped to chromosome 4p21 at the 136793983 bp, but sequences different from those expected from the database were observed for the first 31 bps down stream of the junction site in the genomic region.

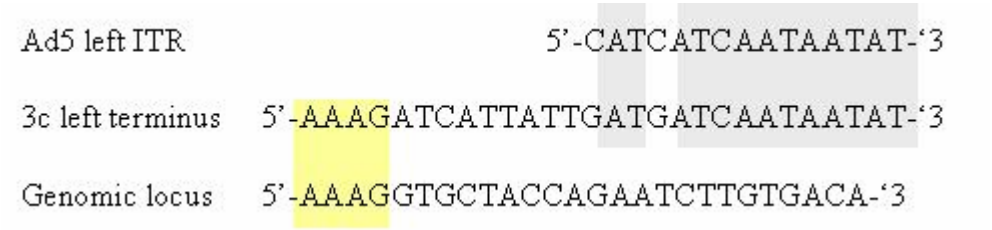

When the sequences are analysed, it looked as if the DNA at the junction site had formed a hairpin structure.

3c left terminus

G
T-A
A-T
G-C
T-A
T-A
A-T
T-A
T-A
5'-ATCA-TAT-'3

Clone 4a

The inverse PCR yielded three sequences, two from the left terminus and one from the right terminus of the integrated vector.

Left terminus sequence 1:

15 base pairs were observed to have been deleted from the terminus. The chromosomal location of the integration was 3p22, in the base pair 32977598.

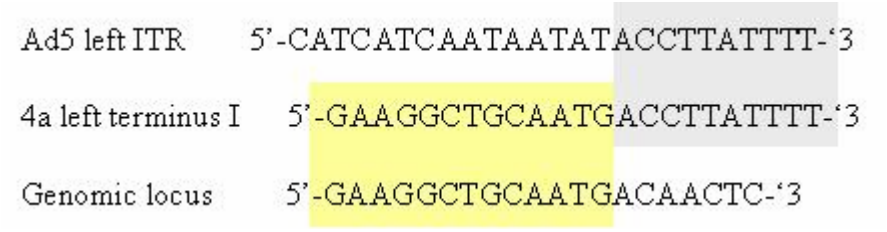

The possibility of the DNA at the junction site forming a stem loop was also noticed in this junction site.

4a left terminus I

5'- CAAAGAGGCAAAGAAGGCTGCAATGACCTTATTTTGGATTGAA-'3

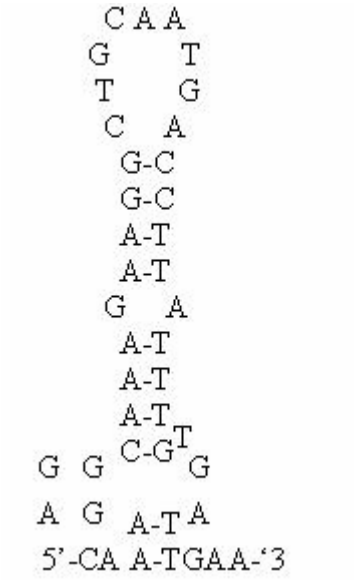

Left terminus sequence 2

A deletion of the last 7 bps of the terminus was observed and the integration was mapped to 13923835 bp in chromosome 5p15.2, in the DNAH5 (dynein, axonemal, heavy polypeptide 5) gene, in the 23rd intron.

Ad5 left ITR	5'-CATCATCAATAATATACC-'3
4a left terminus	5'-ATCCTGCACAAAGAATAATATACC-'3
Genomic locus	5'-ATCCTGCACAAAGAAATGTCTC-'3

Right terminus sequence:

The last 6 bps of the terminus was absent in the sequence and the vector had integrated into the 14466138 bp of the 5p15.1-p14, in the TRIO (triple functional domain, PTPRF interacting) gene, in the 33rd intron. The integration is at a site 542303 bps downstream from that of the above-mentioned left terminus.

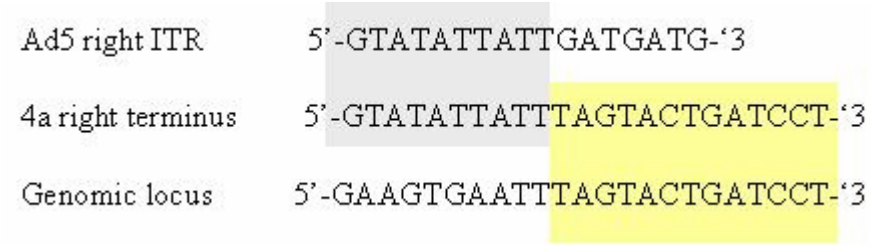

Clone 4b

In the left terminus sequence, a deletion of the last 4 base pairs, and a possible duplication (underlined) of the last 10 base pairs of the terminus present in the junction, and a deletion of a C at the 4th bp from the genomic sequence, was observed. The integration site was mapped as the 125388250 bp of the chromosome 11q 24.2 into the CDON (cell adhesion molecule-related/down-regulated by oncogenes) gene, in the 7th intron.

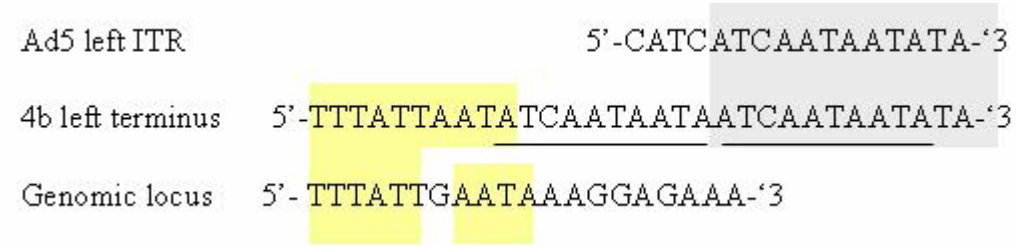

In the right terminus sequence, a deletion of the last 3 bps of the terminus, a duplication (underlined) of the last 8 bps of the terminus present in the junction, and the introduction of two novel base pairs in the junction site, was observed. The integration had taken place in chromosome 11q24 in the124920889 bp, 467361 bps upstream of the left terminus.

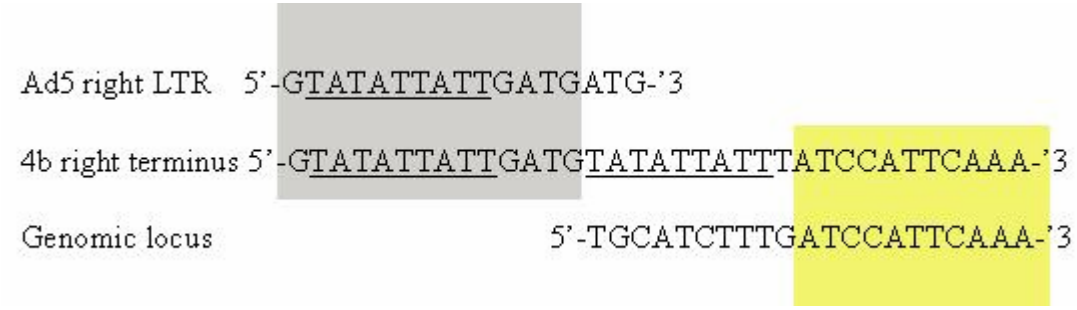

Clone 4c

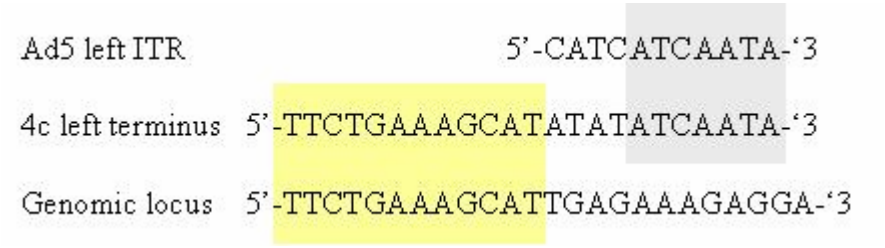

In the left terminus sequence, the 4th bp from the end of the terminus was deleted and 4 novel bps were inserted in that site. The integration site was mapped as the 149348992 of the Xq28, into the intron 4-5 of the CXorf6 gene. In the vector Ad SLS11, this corresponded to bp 29081, located in the c346 cosmid derived stuffer DNA.

In the right terminus sequence, the last 14 base pairs of the terminus were deleted. Of the 64 genomic DNA bps obtained during sequencing, the first 40 bps matched 100% with cDNAs from 11 different genes, with 2 of the genes located in 14 q 23-24 region, the remaining 24 bps did not find matches during BLAST searches. Sequence analysis in Ensembl suggests that the integration took place in chromosome 14 q23, in 66874487 bp in the ATP6V1D gene, and the "unmapped" 24 bps are from the 136554664 bp from 6q23 in PDE7B gene.

The first part matches also in part (17/29) with 130035841 bp in chromosome 6q22.3.

Ad5 right ITR	5'-CCAAAATAAGGTAT← 10bps→ATG-'3
4c right terminus	5'-CCAAAATAAGGTACATGTCTGCAGAG-'3

Clone 4d

The left terminus sequence had a deletion of the last 17 base pairs. The site of integration was mapped into chr 2p24, into non coding area in the 14295915 bp.

Ad5 left ITR	5'-CAT← 13 bps→CCTTATTTT-'3
4d left terminus	5'-TGAAGATTACAGTCTACTTATTTT-'3
Genomic locus	5'-TGAAGATTACAGTCTACTGA-'3

The right terminus sequence had a deletion of the last 68 base pairs. The site of integration was mapped into chr 2p24, into non coding area in the 14311184 bp, 20 bps upstream of the left terminus integration.

Ad5 right ITR	5'-GCCCCGCGCCACGTC←61 bps→ATG-'3
4d right terminus	5'-GCCCCGCGCCAGTGTCGAATGGTA-'3
Genomic locus	5'-TAACCAGTGTCGAATGGTA-'3

Comparison of the junction site

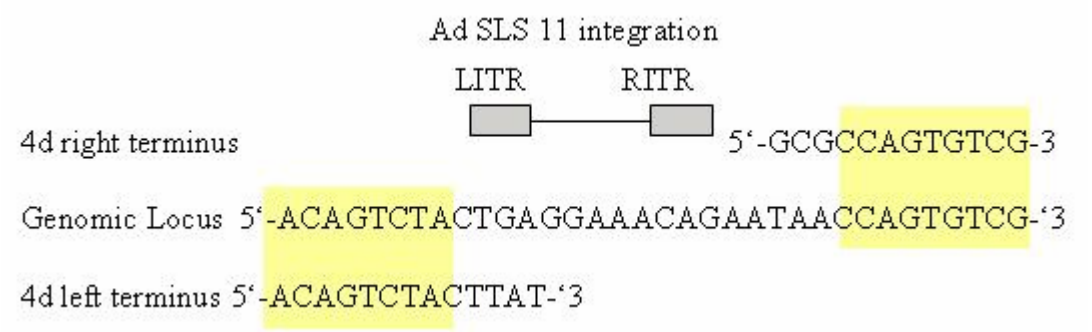

Clone 6a

The last 6 base pairs of the left terminus were found to be deleted and the integration was observed to have happened in the chromosome 17q24, bp 68279602, in the SLC39A11 solute carrier family 39 (metal ion transporter), member 11 in the 8th intron.

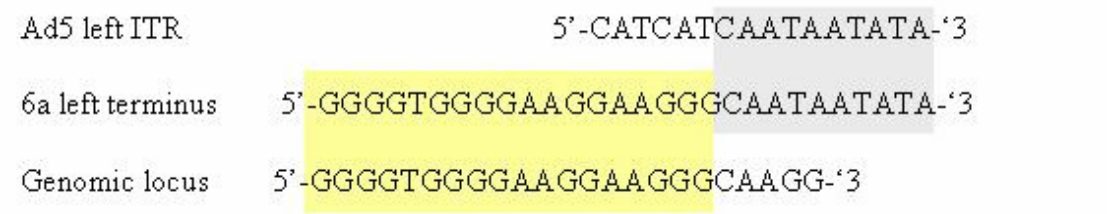

The last 6 base pairs of the right terminus were missing and the integration was observed to have happened in the chromosome 17q24, in the bp 68326313 bp, in the SLC39A11 solute carrier family 39 (metal ion transporter), member 11 in the 8th intron, 46711 bps upstream of the left terminus.

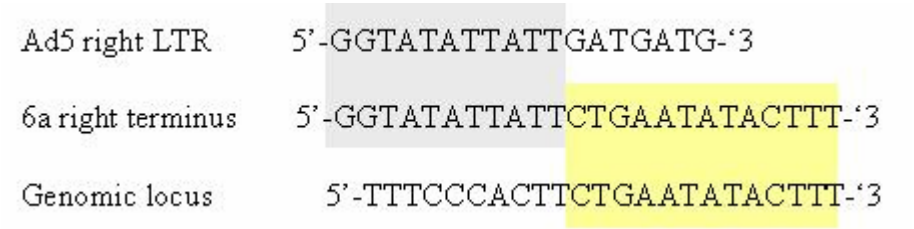

When the sequences are analysed, it looked as if the DNA at the junction site had formed a hairpin structure, possibly in the manner depicted below.

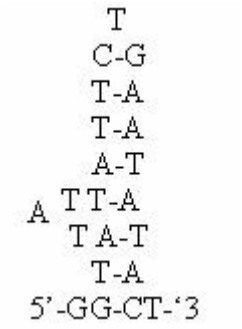

Clone 6b

The last 3 bps of the left terminus was missing. A substitution was noticed at the position +3 of the integrations. The integration was mapped to chromosome 18q24 in bp 74665084, located in non coding area.

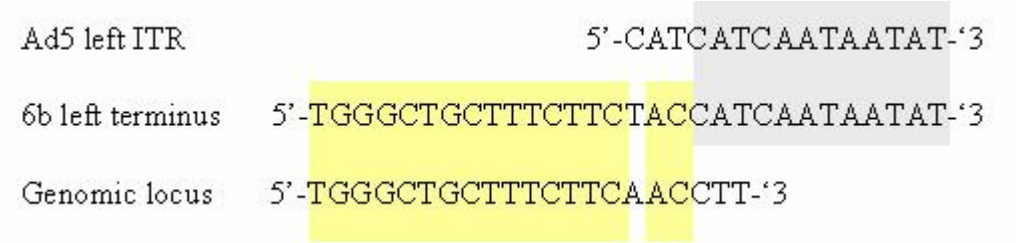

The last 2 bps of the right terminus was absent and the G at –2 position was substituted by a C. Novel 9 bps were introduced at the junction. The integration was mapped to non coding region of chromosome 18q11, in the bp 20386721.

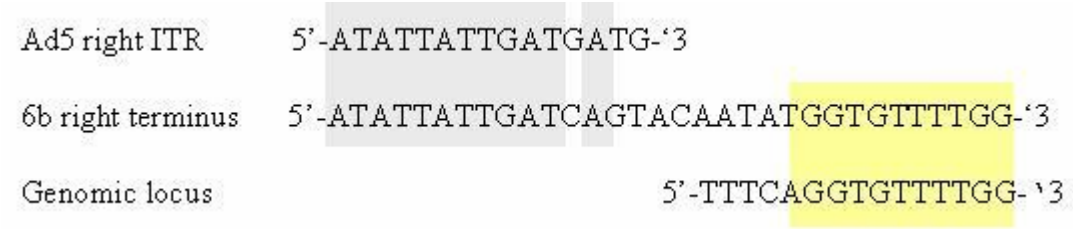

When the sequences are analysed, it looked as if the DNA at the junction site had formed a hairpin structure, possibly in the manner depicted below.

A
C-G
T-T
A-A
G-C
T-A
T-A
A-T
5'- ATT-ATG-'3

Clone 6c

In the left terminus, the last bp was missing. The novel 4 (or possibly 7 bps) bps at the junction of the viral and genomic sequences might be a duplication (underlined) of bps from –12 position relative to the junction. The integration took place the 4325726 bp of chromosome 3p26.1 in the SET domain and mariner transposase fusion gene, in the 1st intron.

Ad5 left ITR	5'-CATCATCAATAAT-'3
6c left terminus	5'-TTGAAAGCCAATAATATCATCAATAAT-'3
Genomic locus	5'-TTGAAAGCCAAGTAGAA -'3

Clone 6e

The entire left terminus was present. The integration was mapped to chromosome 11q22.1, in the 100761198 bp.

Ad5 left ITR	5'-CATCATCAATAAT-'3
6e left terminus	5'- TTAGCTCAATAAATACATCATCAATAAT -'3
Genomic locus	5'- TTAGCTCAATAAATACTAGCCACTT -'3

The last 10 bps of the right terminus were absent in the integration that took place in chromosome 21q in the 39152777 bp, located in non coding region.

Ad5 right ITR	5'-AAAATAAGGTATATTATTGATGATG-'3
6e right terminus	5'-AAAATAAGGTATATTCTCTCTTTCTTC-'3
Genomic locus	5'-TTCTCTCTCTTTCTTC-'3

Clone 6f

The last 7 bps of the left terminus was deleted and the integration was mapped into alpha satellite DNA. A substitution was observed at +3 bp in the genomic DNA in the junction.

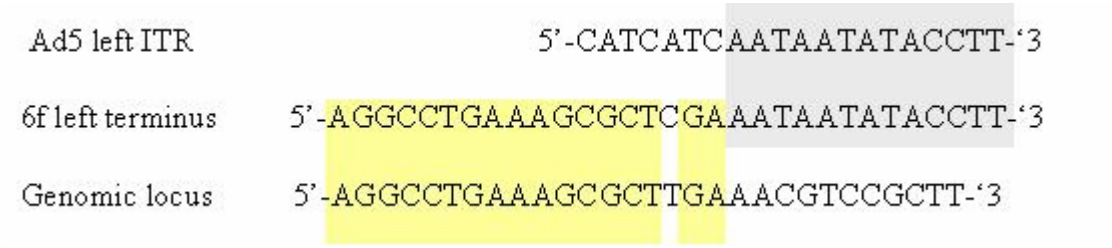

A deletion of the last 29 bps of the right terminus, and in the junction site sequences derived from the genomic DNA, and two substitutions at bp +5 and +10 were observed. The integration was mapped into the 65543774 bp in chromosome 9q12.

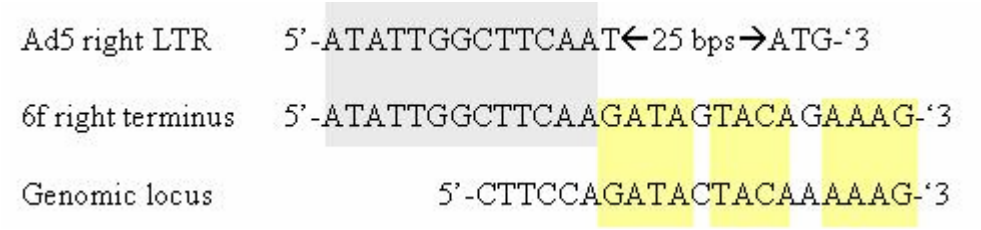

Clone 7a

The last 6 bps of the left terminus were deleted. The vector was found to have been integrated into the 67405840 bp of the chromosome 18q22.3.

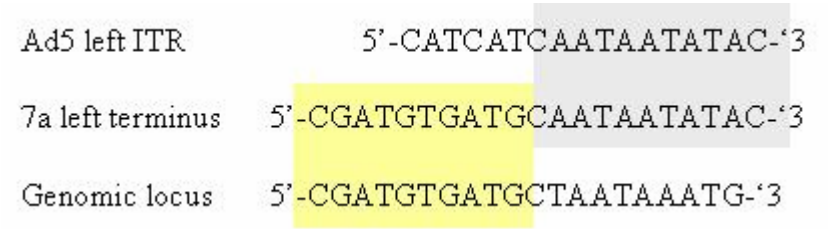

The last 22 bps of the right terminus were missing. The sequence showed similarity to three separate loci, all in chromosome 16p11 region, one in non-coding region (29461478 bp), and two in the same gene (30201478 bp and 29359713 bp).

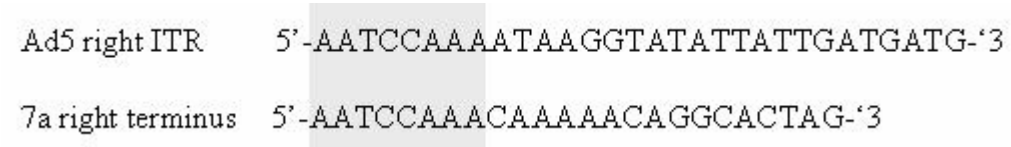

Clone 7b

Left terimus sequence I.

The last 80 bps of the left terminus was missing and the integration had taken place in the 121699946bp of Chr 10q25.

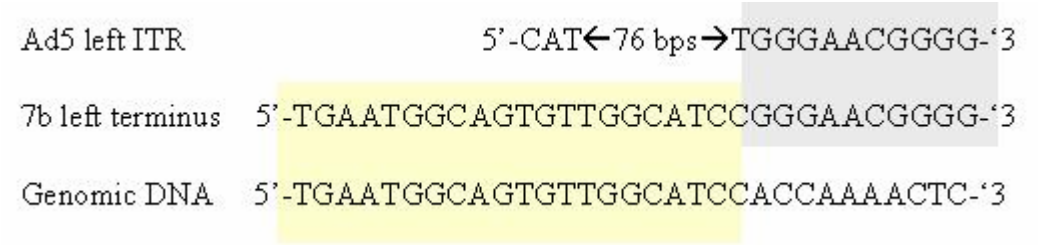

In the second sequence obtained from the left terminus, the last 21 bps of the terminus were missing. The location of the integration in the genome was mapped in the 58075708 bp of the chromosome 15q22.2

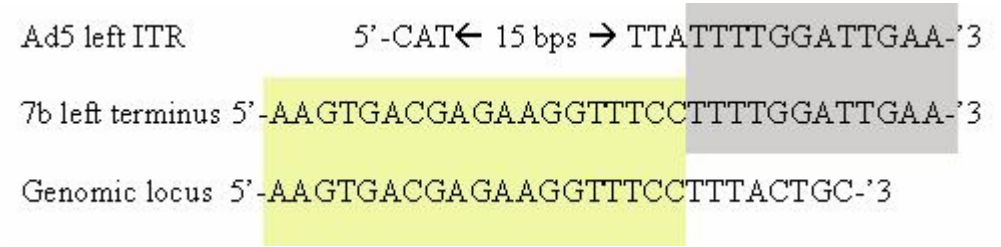

The entire right terminus was observed to be present. The integration had taken place in the chromosome 15q24, in an Alu repeat region in between coding genes at 53144052 bp of the chromosome, 4931656 bps downstream of the observed left terminus.

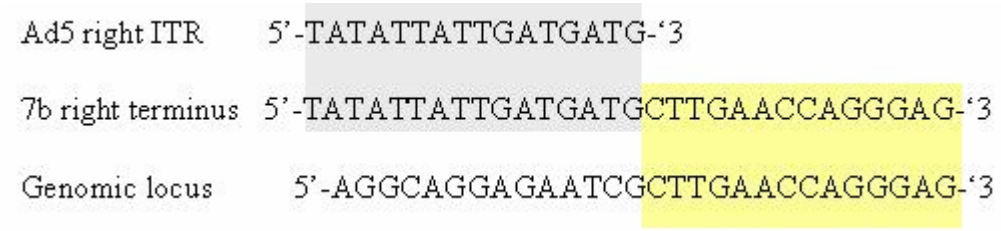

Clone 7c

A deletion of 81 bps of the left terminus was observed the integration, which was mapped into chromosome 3p11 at 68177382 bp, in the FAM 19A1 gene, in the 1st intron.

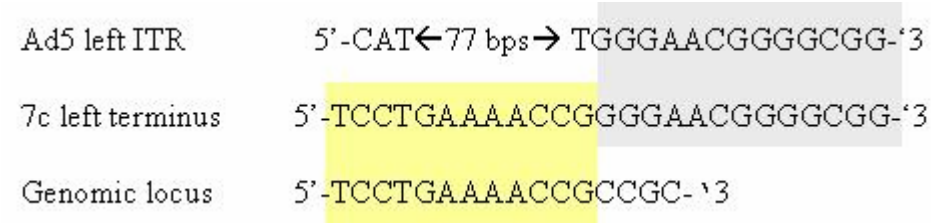

The right terminus integration was mapped in the same locus as the left terminus, 598 bps upstream of the left terminus integration. The last bp of the terminus was missing

Ad5 right ITR 5'-ATATTATTGATGATG-'3

7c right terminus 5'-ATATTATTGATGATCTCATCATTCTA-'3

Genomic locus 5'-AGAATCTCATCATTCTA-'3

Clone 7e

In the left terminus, the last 3 bases were found missing. The integration was mapped into 13q14.11 in the NP_001009814.1 gene into 24th intron in the 41194735 bp.

Ad5 left ITR 5'-CATCATCAATAATATA-'3

7e left terminus 5'-ACATAAAAAGACCATCAATAATATA-'3

Genomic Locus 5'-ACATAAAAAGACATTG-'3

A deletion of the last 20 bps of the right terminus were observed. The integration occurred at the 109261928 bp in chromosome 12q24.11.

Ad5 right ITR 5'-TTCAATCCAAAATAAGGTATATTATTGATGATG-'3

7e right terminus 5'-TTCAATCCAAAATGTTCCCCACCCTGCCTG-'3

Genomic locus 5'-AAATTATGAAATTGTTCCCCACCCTGCCTG-'3

Clone 7g

The last 26 bps of the left terminus were observed to be deleted in junction site, and the integration was localised possibly to chromosome 14q24 into the ATP6V1D gene in the 66874695 bp in exon 9.

Ad5 left ITR 5'-CATC←21 bps→GGATTGAAGCC-'3

7g left terminus 5'-CAGCGCCAAGGTTTGCAAGATTGAAGCC-'3

Genomic locus 5'-CAGCGCCAAGGTTTGCAAGTGGG-'3

In the right terminus sequence, a deletion of the last 14 bps was observed. The integration was in 14q24 into the ATP6V1D gene in the 66874458 bp.

Ad5 right LTR 5'-AAAATAAGGTATATTATTGATGATG-'3

7g right terminus 5'-AAAATAAGGTACATGTCTGCAGAGAAA-'3

Genomic locus 5'-CTACATGTCTGCAGAGAAA-'3

IV.5.5.B C32 derived cell lines

Clone 8a

The last 26 bps of the left terminus were missing and the integration was mapped to chromosome 8q24 into 144983689 bp

Ad5 left ITR	5'-CAT ←18 bps→TTTTGGATTGAAGCC-'3
8a left terminus	5'-GACTCGAGTCCCGATTGAAGCC-'3
Genomic locus	5'-GACTCGAGTCCCGCGGCGCACGCCCC-'3

The last 49 bps of the right terminus were missing and the integration had taken place in the 136554715 bp of 6q22.3 into exon 13 of the PDETB gene.

Ad5 right ITR	5'-CTCCACCCCCTCATTAT←39 bps→ATG-'3
8a right terminus	5'-CTCCACCCCCCAGAGGGCAGAAGCA-'3
Genomic locus	5'-GGCAGGGCCCCCAGAGGGCAGAAGCA-'3

Clone 17a

The last 3 bps of the first left terminus were missing and the integration was mapped to chr Xq26.2 into the 133321215 bp, in the 1st intron of HPRT gene, which also corresponds to the bp 1723 of the Ad SLS 11 vector used in the study.

Ad5 left ITR	5'-CATCATCAATAATATA-'3
17 a left terminus I	5'-ACTATGTAAGTAAACATCAATAATATA-'3
Genomic locus	5'-ACTATGTAAGTAAACATGATGATGGC-'3

In the second left terminus band the presence of the full terminus, with a substitution of a T to C at bp -6 from the junction, was observed. At +18 bps into the genomic sequence from the junction, an A was substituted by a G. The integration had occurred in 24908960 bp of chr 6p22.2.

Ad5 left ITR	5'-CATCATCAATA-'3
17 a left terminus II	5'-TTCAAATGGGGATATCCATCACCAATA-'3
Genomic locus	5'-TTCAAATGGGGATATCAAGCTTGTGA-'3

The last 49 bps were found deleted in the right terminus, and the integration was mapped to Chr 10, in repetitive DNA.

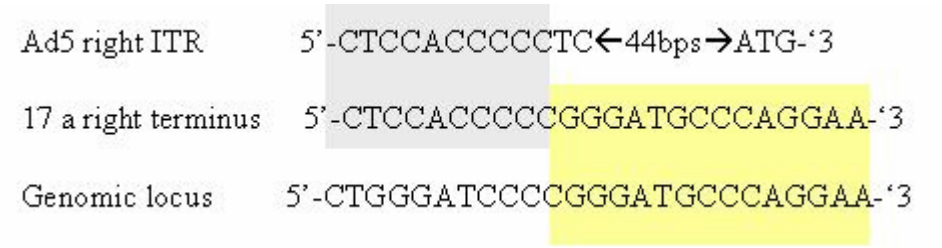

Clone 17c

The last 7 bps of the left terminus were missing and the integration was mapped to the 44962757 bp in chr 16q11.2, a novel A was inserted at the junction site

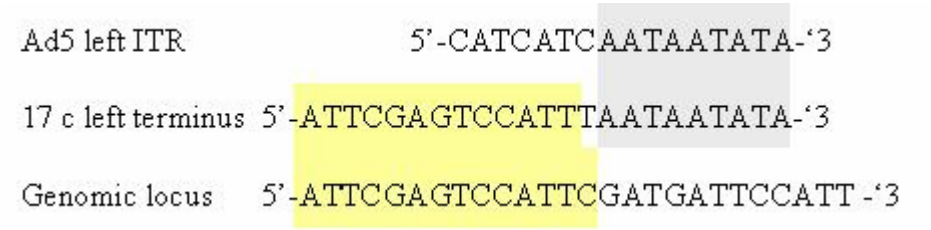

Clone 17d

Two bands were sequenced from the left terminus.

Left terminus sequence, band I:

The last 17 bps of the terminus were deleted and the integration was mapped to 133320237 bp chr Xq26.2, in the 1st intron of the HPRT gene, which also corresponds to the bp 709 of the Ad SLS 11 vector used in the study.

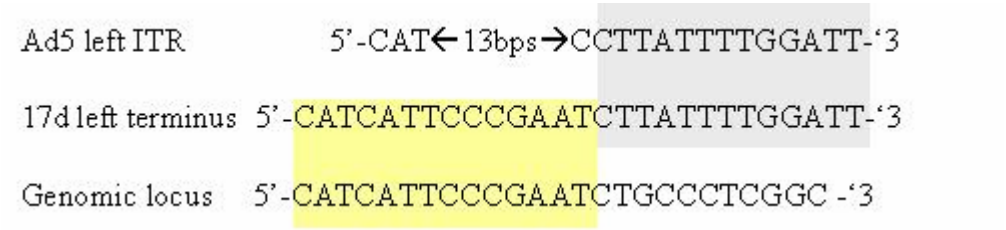

Left terminus sequence, band II

The last 49 bps of the terminus were found missing and the integration had taken place in 170477721 bp of chr 1q25.1in the KLHL20 gene, in the 10th intron.

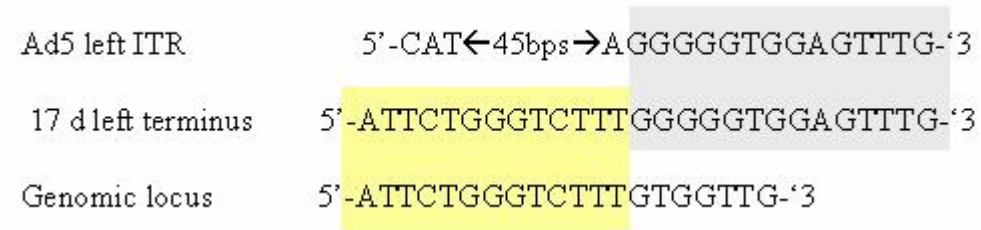

Clone 22a

The last 24 bps of the right terminus were deleted and the integration was localized to sequences similar to satellite 3 mRNA.

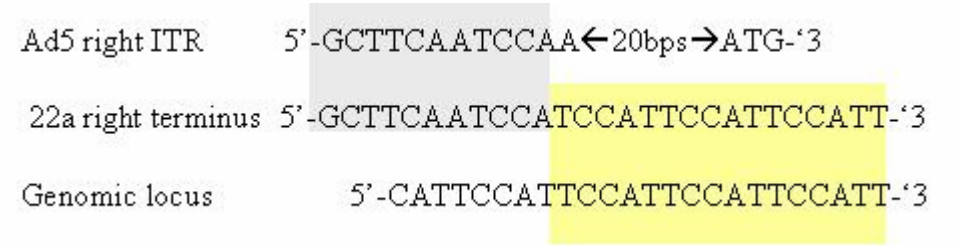

Clone 22b

The entire left terminus was present in the integration, which had taken place in 175256298 bp in Chr 3q26+3, in the NLGN1 gene, in the 5th intron.

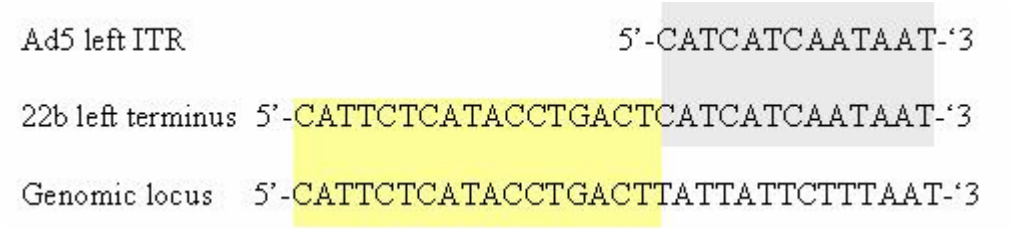

103 bps of the right terminus was deleted and the integration was mapped to Chr 3q26.3 in the bp179409396.

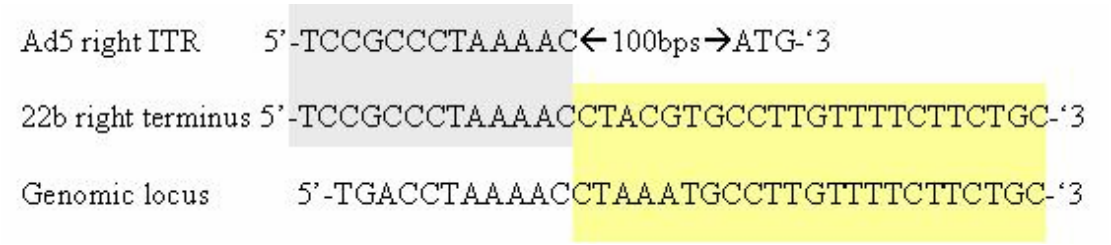

Clone 22c

The last 2 bps of the left terminus were deleted and a novel T was inserted in the junction, which was mapped to the 89017534 bp in Chr 11q15.

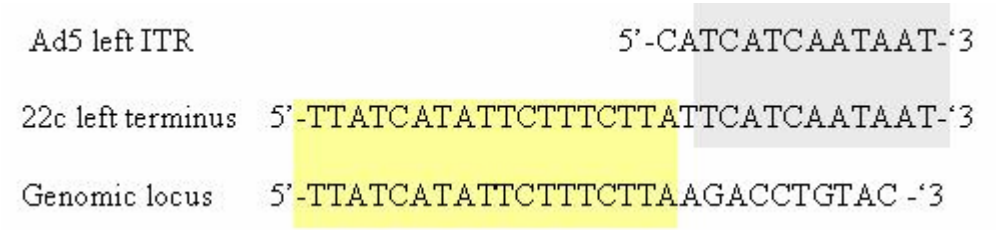

Clone 22d

The last 23 bps of the left terminus were deleted and the integration was mapped to the 70744517 bp of Chr 7q11, in the 3rd intron of the CALN1 gene.

Ad5 left ITR 5'-CAT←19bps→TTTGGATTGAAGCC-'3

22d left terminus 5'-GAGTAAGACGCTGTCTTGGATTGAAGCC-'3

Genomic locus 5'-GAGTAAGACGCTGTCTCAAAGAAATG-'3

Two sequences were obtained from the right terminus.

The last 3 bps of the Ist right terminus were deleted and the integration was localized to an Alu Y repeat element at the 194954088 bp of Chr 3q29.

Ad5 right ITR 5'-GGTATATTATTGATGATG-'3

22d right terminus 5'-GGTATATTATTGATCTGCCTGCCTCAGCCTCCC-'3

Genomic locus 5'-TGACCTTGTGATCTGCCTGCCTCAGCCTCCC-'3

The last 28 bps of the IInd right terminus were deleted and the integration was localized to an alphoid repetitive DNA region.

Ad5 right ITR 5'-ATATTGGCTTCAAT ←24→ATG-'3

22d right terminus 5'-ATATTGGCTTCAACGCAGATTCTACAAAAAGATTGT-'3

Genomic locus 5'-CCAAATCTCCAATCGCAGATTCTACAAAAAGATTGT-'3

Clone 22e

A deletion of the last 17 bps of the left terminus and the substitution of an A to G in the genomic DNA, at the +10 bp from the junction, were observed and the integration was mapped to Chr 3q13 to the 117218961 bp, in the 3rd intron of the LSAMP gene.

Ad5 left ITR 5'- CAT←13bps→CCTTATTTTGG-'3

22e left terminus 5'-ATTTACATAGGCATTTAAGTCTTATTTTGG-'3

Genomic locus 5'-ATTTACATAGACATTTAAGTTAATTAGAAAAGG-'3

Clone 22f

The full left terminus was observed to be present and the integration occurred in chr 7q31 in the bp 111008662 in the 34th intron in the DOCK4 gene.

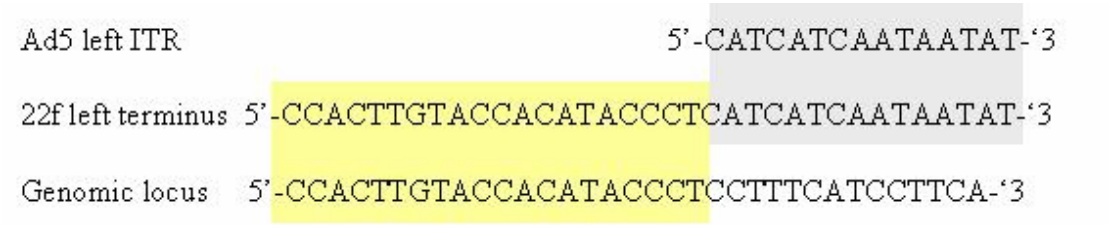

The last 57 bps of the right terminus were missing and the integration was in bp 110989851 of chr 7q31, in intron 39-40 of the DOCK4 gene, 18811 bps upstream of the left terminus, in the event that both of the integrations taken place in the same chromosome.

Clone 22 g

Two sequences were obtained from the left terminus.

In the first left terminus sequence, the last 27 bps were found deleted and the integration had occurred in Chr Xp11.1-11.4 in 45359319 bp. An A to T substitution at bp +1 in the genomic DNA at the junction site was also noted.

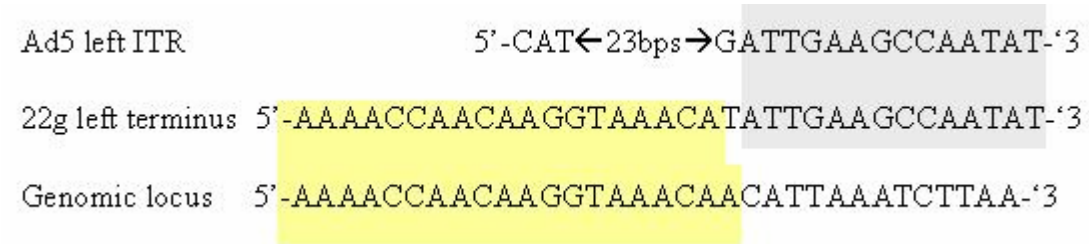

The last 16 bps of the IInd left terminus were deleted and the integration was mapped to the 144984259 bp of Chr 8 q24+3.

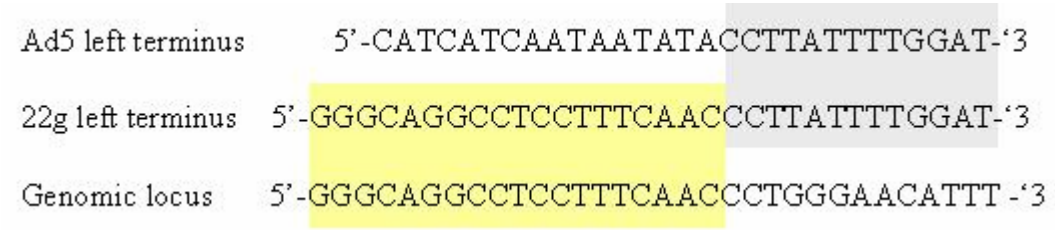

The last 5 bps of the right terminus were missing and the integration was mapped to Chr. 8q23, integration in 108870353 bp. 105 bps downstream of the junction site, the sequences were from Chr 9q12. Owing to the strange nature of the junction, this was reconfirmed by inverse PCR using two different enzymes.

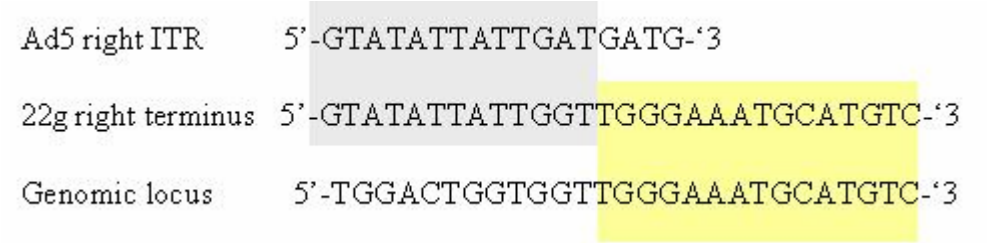

Clone 22h

The presence of the entire left terminus and the introduction/substitution of 1 bp at the junction site were observed and the integration was mapped to Chr 9p12 in the 43592419 bp.

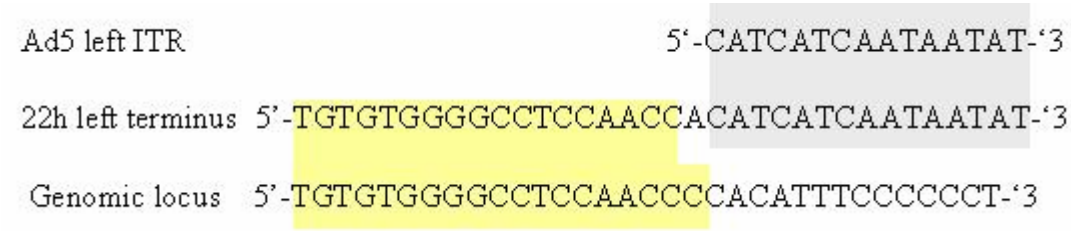

The full right terminus was present and 2 substitutions, G to T at +1 bp and a C to G at +25 bp from the junction site in the genomic sequence, were observed. The integration has taken place in chr 9p12 at position 42373494, in a novel predicted gene.

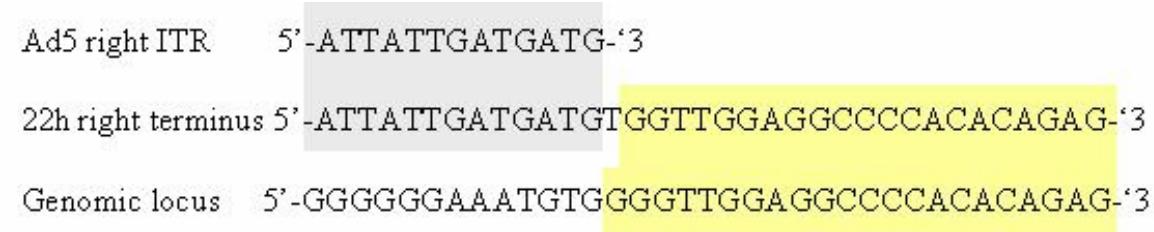

Clone 22i

Two sequences were obtained from the left terminus.

The last 15 bps of the Ist left terminus were missing and the integration was mapped to 44947706 bp of Chr 22q 13, in the 6th intron of the PPARA gene.

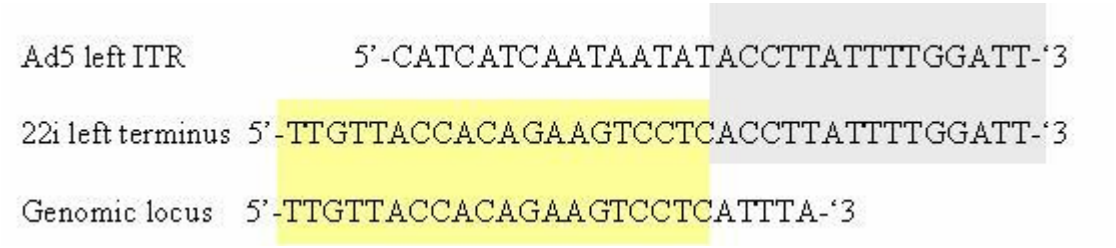

A deletion of 43 bps was observed in the IInd left terminus and the integration had taken place in Chr Xq26.2 in the bp 133321664, corresponding to Hprt 1st intron, and the 2136 bp of the vector used.

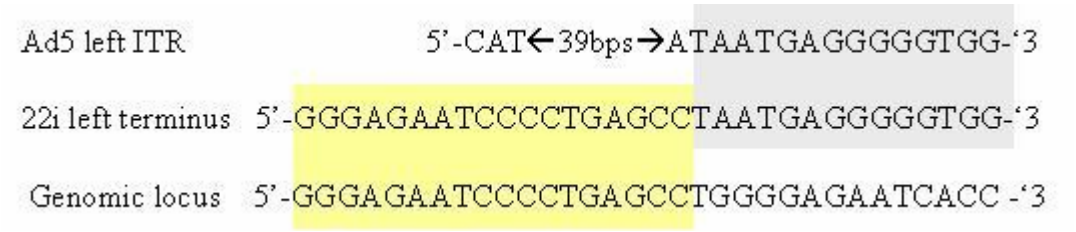

The last 59 bps of the right terminus were deleted and the integration was mapped into the 141523423 bp in Chr 7q35 in a novel gene.

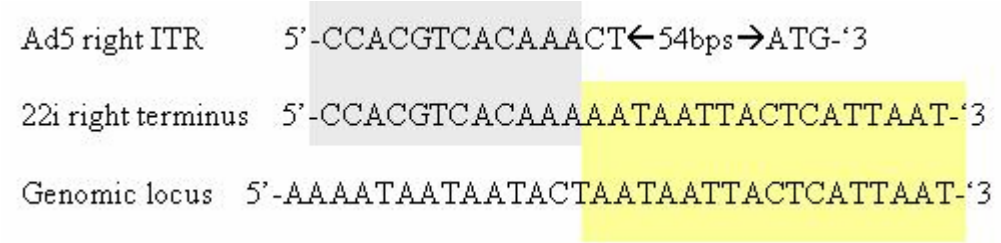

Clone 22k

The last 17 bps of the left terminus were deleted and the integration had taken place in Chr 20p12.1 in the 14643087 bp. A T to C substitution was observed -28 bps upstream of the junction site in the viral terminus.

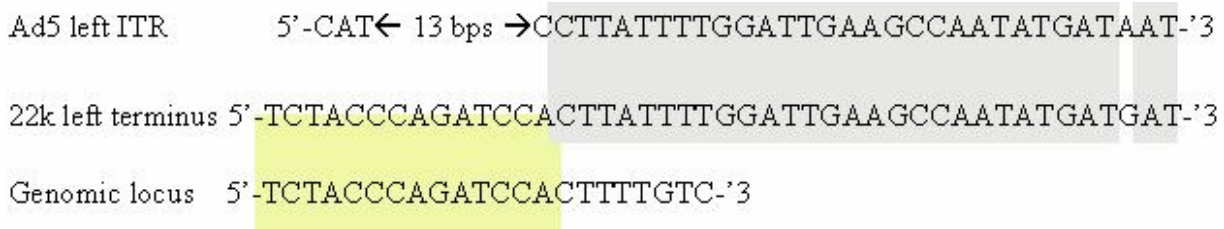

The full right terminus was present and the integration had taken place in the integration had taken place in Chr 20p12.1 in the 14643056 bp, 81 bps downstream of the left terminus, had both of the integrations taken place in the same arm.

Ad5 right ITR	5'-ATATTATTGATGATG-'3
22k right terminus	5'-ATATTATTGATGATGATTTCAACGTGACCCAT-'3
Genomic locus	5'-CCTCCTGCAAAAGATTTCAACGTGACCCAT-'3

The locations of the HC-AdV termini integrated into the cellular genome are mapped here in Fig. 34.

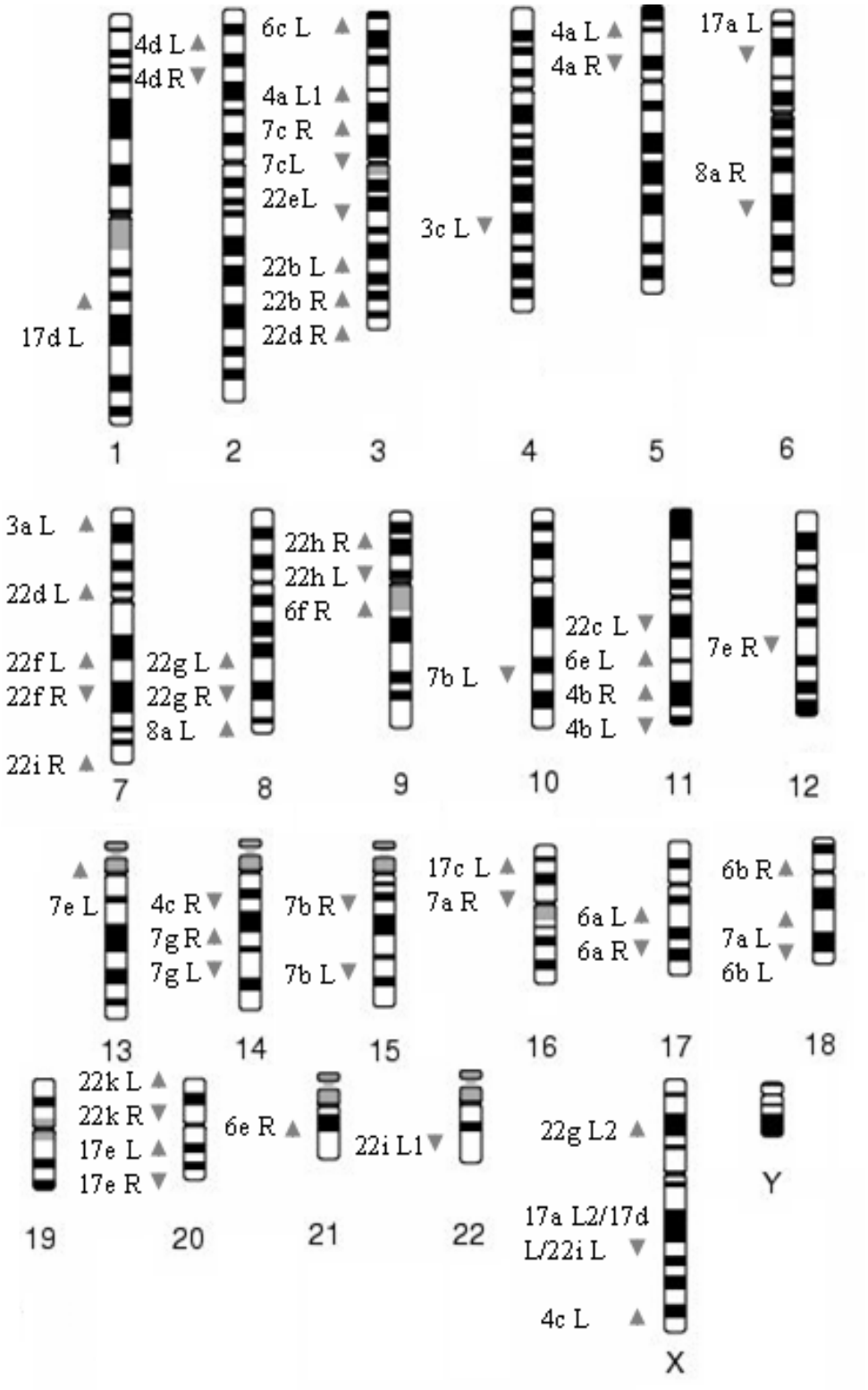

Fig. 34: locations of the HC-AdV termini integrations in the cellular genome. The approximate location of each integration as obtained from the sequence data was mapped on to a map of the genome.

The results obtained in the above section were summarised in Table 8.

Clone	Terminus	Integration in chromosome	Dir. of the vector	Deletion from the termini	Integ. Active gene	Comments on the integration
3a	L	7p 21 17859816 bp	←	11	N	Integrated in a junction of 4q22 and 7p 21
3c	L	4 q 28 136793983 bp	→	1	N	A G to C substitution at –3 of the terminus, rearrangements in the first 31 bps downstream of the integration.
4a	L	3p22 32977598 bp	←	15	N	
4a	L	5p15.2 13923835 bp	←	7	Y	DNAH5 gene, 3’
4a	R	5p15 14466138 bp	→	7	Y	TRIO gene, 3’
4b	L	11q24.2 125388250 bp	→	4	Y	CDON gene, MID. Deletion in +3 from the terminus in the genomic sequence.
4b	R	11q24 124920889 bp	→	3	N	Last 8 bps duplicated, 2 additional bps introduced.
4c	L	Xq28 149348992 bp	←	0	Y	4 bp insertion at the junction. CXorf6 gene
4c	R	14 q23 66874487 bp	→	14	Y	14q23-6q23 junction from +40 bps onwards.ATP6V1D gene
4d	L	2p24 14295915 bp	→	17	N	
4d	R	2p24 14311184 bp	←	68	N	
6a	L	17q24 68279602 bp, 44670 bps away	←	6	Y	SLC39A11 solute carrier family 39 gene
6a	R	17q24 68326313 bp	→	6	Y	SLC39A11 solute carrier family 39 gene

6b	L	18q24 74665084 bp	→	3	N	-2 to -6 of terminus duplicated
6b	R	18q11 20386721 bp	←	2	N	-3 from terminus is substituted, 9 unknown bps at junction
6c	L	3p26.1 4325726 bp	←	1	Y	4 unknown bps in the junction. SETMARgene
6e	L	11q21 100761198 bp	←	0	N	
6e	R	21q22 39152777 bp	←	10	N	
6F	L	Alpha satellite repeated DNA	NA	7	N	3 novel bps introduced in the junction.
6F	R	9q12 65543774 bp	→	29	N	2 substitutions in the genomic region
7a	L	18q22.3 67405840 bp	←	6	N	
7a	R	16p11	→	22	?	In –3 position, an A to G substitution. Integration in 3 different loci possible (2 active genes).
7b	L	10q25 121699946 bp	→	80	N	
7b	L	15q26 58075708 bp	→	21	N	
7b	R	15q24 53144052 bp	→	0	N	
7c	L	3p11 68177382 bp	→	81	Y	FAM19A1
7c	R	3p11 68176784 bp	←	1	Y	FAM19A1
7e	L	13q 14.11 41194735 bp	←	3	Y	NP_001009814.1 gene
7e	R	12 q24.11 109261928 bp	→	20	N	
7g	L	14q24 66874695 bp	→	26	Y	ATP6V1D gene
7g	R	14q24 66874458 bp	←	14	Y	ATP6V1D gene
8a	L	8q24 144983689 bp	←	26	N	
8a	R	6q22.3 136554715 bp	→	49	Y	PDE7B

17a	L	X q26.2 133321215 bp	→	3	Y	HPRT
17a	L	6p22.2 24908960 bp	→	0	N	A T to C and A to G substitutions in –5 and + 18 positions, respectively.
17a	R	10 ?	NA	49	?	Repetitive DNA
17c	L	16q11.2 44962757 bp	←	7	N	A novel A introduced at the junction site.
17d	L	X q26.2 133320237 bp	→	17	Y	HPRT
17d	L	1q24 170477721 bp	←	49	Y	KLHL20
17e	L	20q13+3 61876780 bp	←	4	Y	BTBD4 gene
17e	R	20q13+3 61881299 bp	→	25	Y	“, 4519 bps downstream of the L
22a	R	?	NA	24	Y	Satellite mRNA
22b	L	3q26+3 175256298 bp	←	0	Y	A novel G introduced at the junction site. NLGN1 gene
22b	R	3q26+3 179409396 bp	←	105	N	
22c	L	11q15 89017534 bp	→	2	N	A novel A introduced in the junction.
22d	L	7q11 70744517 bp	←	23	Y	CALN1
22d	R	3q29 194954088 bp	←	3	N	Part of integration into an Alu Y region
22d	R	?	NA	28	N	Alphoid repetitive DNA
22e	L	3q13 117218961 bp	→	17	Y	A T-C substitution in + 10 bps. LSAMP gene.
22f	L	7q31 111008662 bp	→	0	Y	DOCK4
22f	R	7q31 110989851 bp	←	57	Y	“18811 bps upstream of the left terminus
22g	L	Xp11.1-11.4 in 45359319 bp	←	27	N	A T-A substituion at Bp +1.
22g	L	8 q24+3 in 144984259 bp	→	16	N	
22g	R	8q23 108870353 bp	←	5	N*	Chromosomal joining into chr 19 (into a LOC388526 gene, 105 bps downstream of the junction site)
22h	L	9 p 12 in	→	0	N	Deletion of 2 bps at +2 bp from junction.

		43592419 bp				
22h	R	9 p12 42373494 bp	←	0	Y	A C to A substitution at +2 bp from the junction. Novel gene. ENST00000355214
22i	L	22q13 44947706 bp	→	15	Y	PPARA
22i	L	X q26.2 133321664 bp	→	43	Y	HPRT
22i	R	7q35 141523423 bp	←	59	Y	Novel gene ENSG00000197962
22k	L	20p12.1 14643087 bp	←	17	N	A T to C substitution at -28 bps
22k	R	20p12 14643056 bp	→	0	N	

Table 8: Table listing the integration of the vector, the direction of the integration with respect to the chromosome, and the consequences thereof to the cellular and viral DNA. The BLAST searches on NCBI and ENSMBL databases were performed on the sequence obtained from the Inverse PCR.

The HC-AdV Ad SLS 11 appeared to integrate in a random manner in the chromosomal DNA. In all chromosomes, except Chr 19, integrations of the vector were observed.

IV.5.5.C Sequence from both termini of the vector molecule

As mentioned in pg 90, the bands observed in the Southern blots conducted on clone 17e can be correlated with the sequence data obtained from the same clone via Inverse PCR. The sequence data on some other clones suggest that both of the termini of the same molecule have been sequenced. These "probable both termini", observed when the left and the right termini of the vector were found in the same chromosome, are given in the table below, Table 9.

Clone	**Left Terminus integrated in bp**	**Right terminus integrated in bp**	**Probable deletion in the genomic DNA in bp**
4a	5p15.2, 13923835	5p15, 14466138	542,303
4b	11q24.2, 125388250	11q24, 124920889	467,361
4d	2p24, 14295915	2p24, 14311184	15,269
6a	17q24, 68279602	17q24, 68326313	46,711
6b	18q24, 74665084	18q11, 20386721	54,278,363

7b	15q26, 58075708	15q24, 53144052	4,931,656
7c	3p11, 68177382	3p11, 68176784	598
7g	14q24, 66874695	14q24, 66874458	237
17e	20q13+3, 61876780	20q13+3, 61881299	4519
22b	3q26+3, 175256298	3q26+3, 179409396	4,153,088, possible concatomer
22f	7q31, 111008662	7q31, 110989851	18,811
22g	8q24+3, 144984259	8q23, 108870353	36,113,906
22h	9p12, 43592419	9p12, 42373494	1,218,925
22k	20p12.1, 14643087	20p12, 14643056	31

Table 9: Data showing the probable integration of both the left and right termini of the vector into the same chromosome.

However, it is not possible to state dogmatically that the sequence obtained did come from both of the termini of the same vector molecule instead of two individual termini from two different vectors, due to the fact that the bands cannot be corroborated totally by the Southern blot data and in the absence of FISH data. So it must be interpreted with caution.

IV.5.5.D Integration of the vector DNA into genes

Of a total of 61 clones from which the data is presented, 29 integrations were in genes (chromosomal regions identified as genes in the ENSEMBL database), 30 integrations were in non-coding region and the sites of 2 integrations could not be determined. The data was plotted on the following Pie diagram, Fig. 35.

This suggests that HC-AdV integrated in both coding as well as non coding genetic regions, and there seemed not to be any specific preference to either of them.

IV.5.5.E Integration of the vector DNA into common insertional sites

The genes in which the integrations had taken place were compared against the known Common Insertional Sites (CIS) for Retroviral Vectors in the mouse genome to analyse whether HC-AdV preferred integration into certain genes that were commonly targeted by retroviral vectors, given that the genes had the same names in both human and mice genomes. Individual genes were searched for matches the CIS in the Copeland Database http://rtcgd.ncifcrf.gov/ . No matches were found to the CIS in the mouse genome to the genes in which integrations of HC-AdV had taken place.

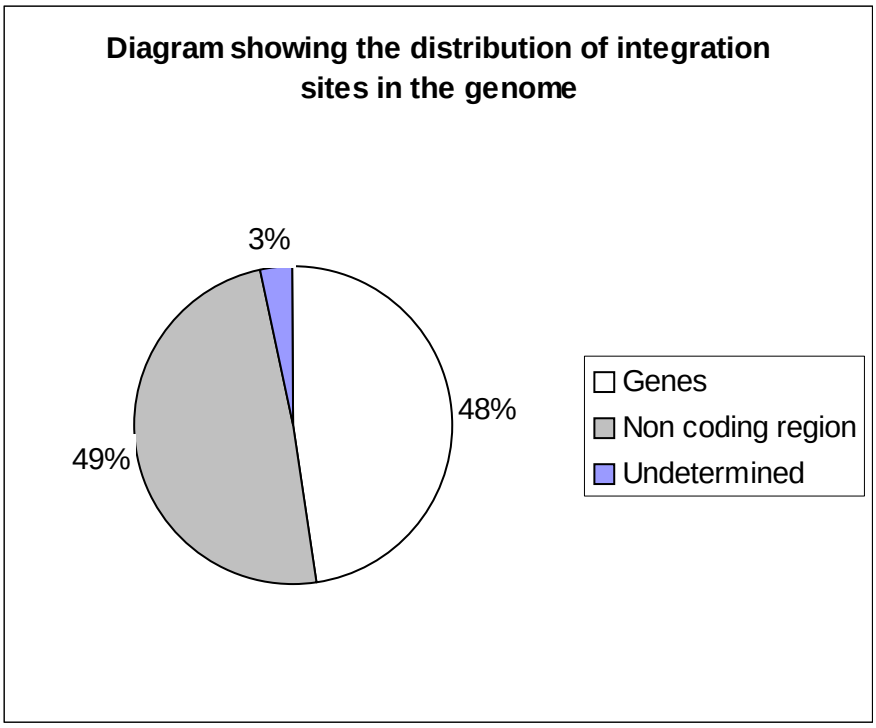

Fig. 35: Pie diagram showing the distribution of integration sites of HC-AdV in the cellular genome. The ENSMBL database was used to verify whether the integration had taken place in a gene or a non coding region

IV.5.5.F Integration of the vector DNA into genes of any particular ontology

To check if the HC-AdV DNA favoured integrations into genes of any particular function, the molecular ontology of the genes involved were analysed using the Swiss prot tool found at http://ca.expasy.org/sprot/ or the ENSEMBL database. The gene ontology of any gene is subdivided into molecular function, biological process and cellular function and the individual results were rechecked using the GO tool at http://www.geneontology.org/GO.doc.shtml. The two insertions into genes from the *in vivo* data given in pg 145 are also included in table 10.

Gene	Molecular functions	Biological processes
DNAH5	i. Microtubule motor activity.	i. Microtubule-based movement.
TRIO	i. Guanyl-nucleotide exchange factor activity. ii. Protein serine/threonine kinase activity	i. Transmembrane receptor protein tyrosine phosphatase signaling pathway ii. protein amino acid phosphorylation

CDON	i. Protein binding	i. Cell adhesion ii. Positive regulation of myoblast differentiatio
Cxorf6	?	?
ATP6V1D	i. Hydrogen-transporting ATPase activity ii. Rotational mechanism	i. Vacuolar acidification ii. ATP biosynthesis
SLC39A11	i. Metal ion transporter activity	i. Metal ion transport
SETMAR	i. DNA binding ii. Histone-lysine N-methyltransferase activity iii. Zinc ion binding	i. Chromatin modification ii. Regulation of transcription
FAM19A1	?	?
NP_001009814.1	i. ATP binding ii. Hydrolase activity, acting on acid anhydrides.	
PDE7B	i. 3',5'-cyclic-AMP phosphodiesterase activity	i. Signal transduction ii. Synaptic transmission
HPRT	i. Hypoxanthine phosphoribosyltransferase activity	i. Purine ribonucleoside salvage ii. Behavior
KLHL20	i. Actin binding ii. Protein binding	i. Cytoskeleton organization and biogenesis
BTBD4	i. Nucleic acid binding ii. Protein binding iii. Zinc ion binding	i. Transcription ii. Regulation of transcription
NLGN1	i. Carboxylic ester hydrolase activity ii. Neurexin binding	i. Calcium-dependent cell-cell adhesion ii. Neuronal ion channel clustering iii. Protein targeting iv. Regulation of neuron differentiation v. Synaptic vesicle targeting vi. Synaptogenesis
CALN1	i. Calcium ion binding	
LSAMP	i. Protein binding	i. Nervous system development ii. Cell adhesion
DOCK4	i. Guanyl-nucleotide exchange factor activity. ii. GTP binding	

	iii. GTPase binding	
ENST00000355214	?	?
PPARA	i. Protein binding ii. Transcription factor activity	i. Fatty acid metabolism ii. Lipid metabolism iii. Transcription from RNA polymerase II promoter
ENSG00000197962	?	?
Bfsp2	i. Structural molecule activity ii. Structural constituent of eye lens	i. Cytoskeleton organization and biogenesis
Gmeb2	i. DNA binding ii. Transcription regulatory function	i. Transcription

Table 10: List of the molecular ontology of the genes where the HC-AdV integrations had taken place.

The aim of conducting this part of the study was to determine whether the HC-AdV favoured integration into genes of any particular molecular function or biological process. There was a special interest to determine whether AdV preferentially integrates into genes that are protooncogenic or those genes that might have oncogenic potential, like the ones involved in cell cycle. In the molecular ontology of the genes analysed, no integration was observed in such genes (two integrations were observed in genes involved in transcription), and HC-AdVs did not seem to exhibit any obvious affinity to integrate into genes of any given ontology.

IV.5.5.G Influence of genes on the integration of the vector DNA into non-coding region

To determine if the integrations of the HC-AdV DNA into the non coding region of the genome was influenced by the presence of neighbouring genes, the site of integration was analysed for the distance between it and the closest gene. Two parameters were selected. The integrations were mapped for 10 kb upstream and down stream and then for 25 kb upstream and downstream of the integration site. 10 (32.3 %) of the integrations that had taken place into the non-coding region, had taken place within 25 kb of genes, 5 integrations (16.2 %) had taken place within the 10 kb window. In three cases (*viz* 8a L, 22g L, and 17a L), integrations had taken place in regions of gene clusters where there were four, four and two genes within the 25 kb window. The data was formulated into table 11.

Clone	Neighbouring gene	Distance (in Kb)
3a L	PRPS1L1	20.13
4a L	CCR4	6.2
4b R	E124	23
6f R	Novel ENSESTG00000033857	11
7b L	SEP32IP	8.3
7b L	FOXB1	8.7
7e R	ANAPC7	2.9
8a L	ENST00000327830	11.2
	NRBP32	12.5
	NP_510965.1	12.7
	SCRIB	14.3
17a L	Q5VV38	5.7
	GMNN	14.7
22g L	ENST00000327830	11.1
	NRBP32	12.4
	NP_510965.1	12.8
	SCRIB	14.4

Table 11: List of the genes located within a 30 kb window of the integration of the HC-AdV into the non coding region of the genome.

This study was carried out to check if in the case of integrations in the noncoding region of the genome, whether the integration would have any possible effects on the transcription of any genes. 33% of the integrations in the "harmless" regions of the genome had occurred within 25 kb of coding regions.

IV.5.5.H Deletions in the adenoviral terminus

The deletions in the terminus were studied, and of the 61 junction sites observed, 14.76 % (n = 9) had no deletions in the termini. In 68.9 % (n = 42) the termini had deletions in the region between 1 and 30 bps, and in 9.8 % (n = 6), the termini had deletions between 31 to 60 bps. In 4.9 % (n = 3), the termini had deletions between 61 and 90 bps. Only one single terminus with a deletion of 105 bps was observed. The deletions from the termini sequences were plotted as Fig. 36.

From the data analysed, it was observed that in the majority of HC-AdV integrations, the vector integrated through the viral termini. The viral terminus seemed to have had

undergone random integration into the chromosomal DNA in the region of the first 30 nucleotides.

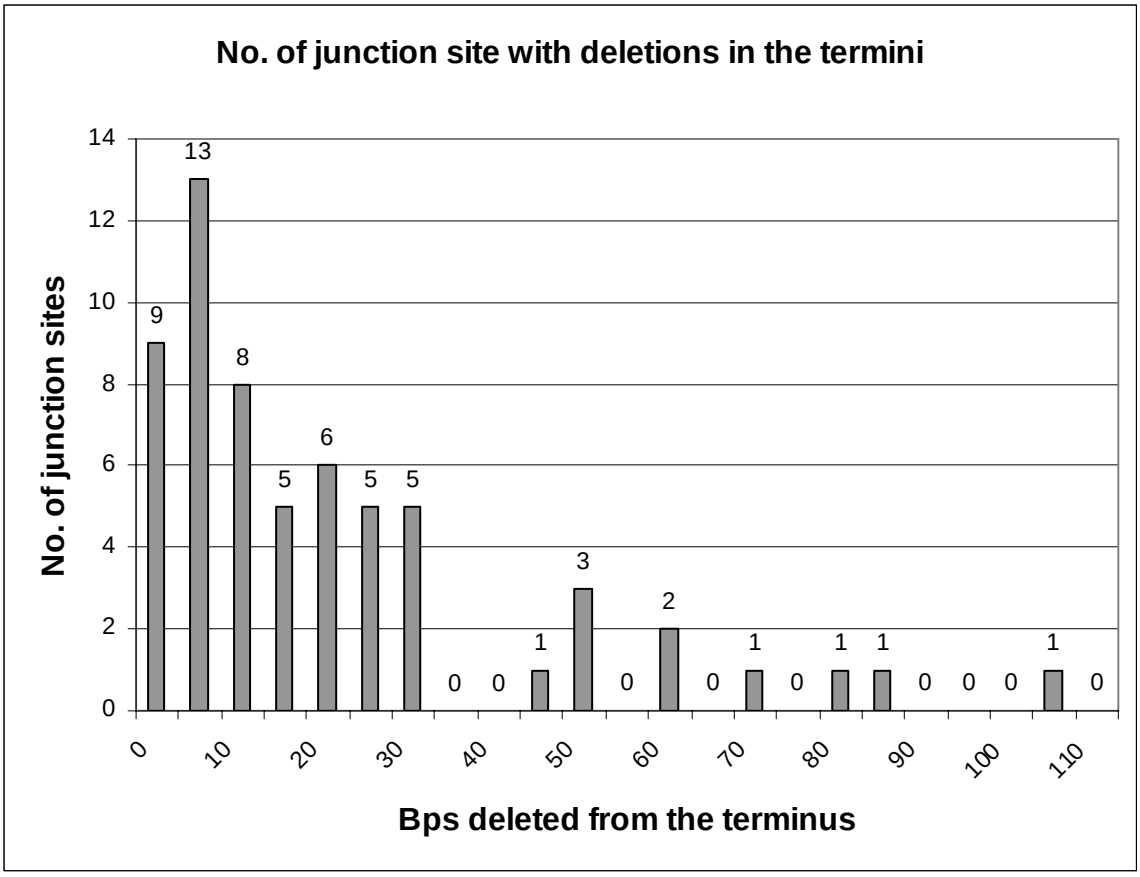

Fig. 36: Graph comparing the number of junction sites to the deletions in the Ad terminus in those junctions.

IV.5.5.I Role of homologous sequences in the random integration of the vector DNA into chromosomal DNA

The role of "patchy homologies/ micro homologies" [eg. (Wronka et al., 2002)] in the integration of the vector DNA into chromosomal DNA was analysed. Four integrations were observed to occur in a homology mediated manner, three in the HPRT gene, and one in the c346 cosmid region. In 36/61 junctions (59 %), patchy homologies between the termini and the genomic DNA of 3 bps or above were observed. The homologies were calculated only from the sense strand. In many cases, overlaps between individual "patchy homologies" were observed. Only homologies to 3 or more bps within the first 30 bps in the junction have been presented as "patchy homologies" (Table 12).

The sequence obtained from the left terminus of the HT1080 derived cell line 6c is given as an example (Fig. 37).

Fig. 37: Patchy homologies between AdV terminus DNA and chromosomal DNA in the junction site in the HT1080 based cell line 6c.

Junction site Id	**Homologous patches in number of bp**	**Distance of the beginning of the patch from the junction**
3a L	3, 4, 4	3, 6, 15
4a L	4	3
4a R	3, 4	0, 11
4a L	3, 4, 3, 4, 3, 3	1, 7, 9, 12, 15, 24
4b L	7, 4, 4	1, 3, 8
4b R	4, 3,	7,5
4c L	3, 3, 3, 3	1, 10, 15, 20
4d R	3, 3, 3, 4, 3	0, 2, 12, 18, 22
6a L	3, 4	0, 2
6b L	3, 5	4, 7
6b R	3,3	7, 10
6c L	3, 4, 5, 6	25, 20, 7, 1
6e L	4, 7, 3, 4	18, 9, 4, 1
6f R	3, 5	2, 9
7a L	4, 4	4, 9
7b L	4, 4, 4	1, 5, 15
7b L (II)	3, 3	0, 5
7c L	5	13
7c R	4	13
7e L	4, 3, 2	0, 8, 14
8a L	3	8
8a R	4	0

17a L	3, 5	0, 14
17a L (II)	3	13
17a R	5	16
17d L	5	2
17e L	3	2
17e R	4, 4	0, 4
22b L	3, 3	1, 7
22 b R	4	5
22d R	5	1
22f L	5	3
22g L	3, 3, 3	2, 5, 11
22g L (II)	4, 3, 4	6, 1, 8
22 h R	3	1
22i L	3	2

Table 12: List of microhomologies between the Ad5 terminus and the site in the cellular genome where the integration had taken place.

From the data analysed, it was observed that the HC-AdV DNA, like wt Ad DNA, can use limited homologies of up to 7 bps between the terminus and the genomic DNA sequence during integration. The homologous patches could be right at the junction site or up to 24 bps away from it.

Three integrations were observed in the Hprt gene, two (22gL and 8aL) in different loci in chr 8q24, three (4cR, 7gL and 7g R) were found integrated in different loci in the ATP6V1D gene in Chr 14q24. In the last case, it is possible that the integrations in 7gL and 7gR are from both the arms of one single vector molecule, though in the absence of FISH analysis, this can only be postulated and not proved. Apart from that, no particular site in the genome was targeted more than once during integration by the vector.

IV.5.5.K Mutations observed at the junction sites of the vector DNA into the chromosomal DNA

To determine whether mutations were associated with the integration of the HC-AdV vector into the genome, the sequences of the terminus and the genomic DNA were studied. By convention, the sequences found in the databases were taken as that for the genomic DNA of HT 1080 and C 32 cells. The deletions in the terminus exactly at the junction site, which occurred during the integration of the vector into the

genome were not considered as mutations in this study. In the sixty one junction sites analysed, there were twenty two junctions with mutations associated either in the part of the viral terminus DNA that had integrated or in the cellular DNA. Eight of these mutations were observed in the genomic region (including those three clones where chromosomal joining was observed), nine had taken place in the junction of the integration and five were observed in the termini. Three junctions had mutations in both the terminus derived sequences and the genomic sequences, and two had mutations in the terminus derived sequences and the junction derived sequences. The data was plotted on to the following Pie diagram (Fig. 39).

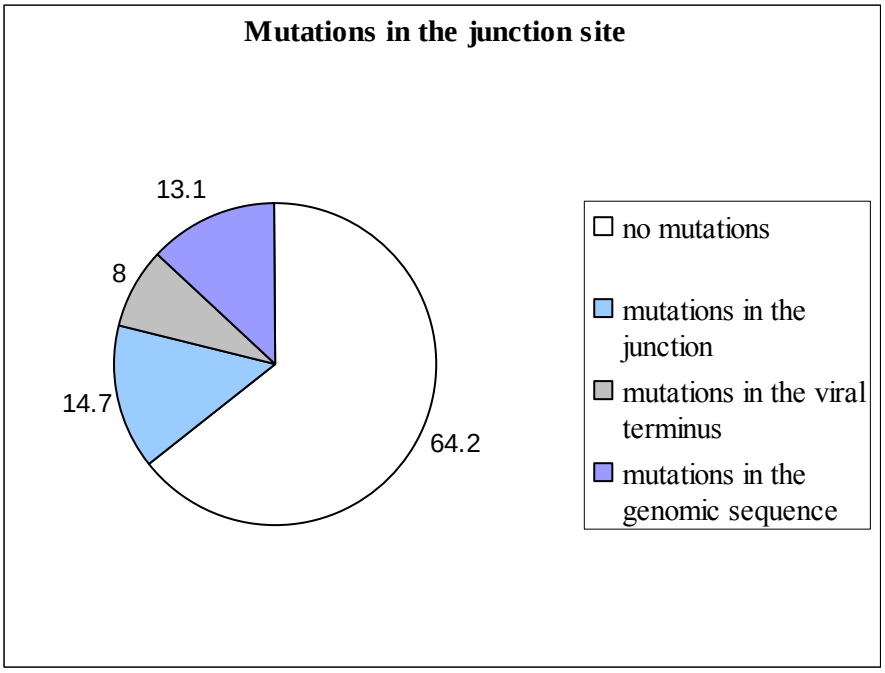

Fig. 39: Pie diagram showing the mutations in the junction site of the region where the HC-AdV had integrated into the genome.

From the data, it was clear that vector DNA integrated in 64% of the cases without causing any mutations. Though no experiments were carried out to eliminate the possibility that some or many of the mutations observed may have been a result of the chromosome instability of the cell lines and may have nothing whatsoever to do with the vector, and should the case be that the mutations were all induced by the integration of the vector, no evidence was seen in the present study to suggest that the mutations observed during vector integration was any different than those described during the non homologous end joining of DNA.

IV.5.5.L Conclusions reached from the study of the junction sites isolated after the random integration of HC-AdV DNA into the chromosomal DNA

The aim of these set of experiments was to determine the nature of the integration of the HC-AdV *in vitro*. Following the molecular analysis of the clones, the following conclusions were reached.

i. Despite the 1 moi used, more than one vector copy had integrated in some (up to 38 %) of the clones studied.
ii. The vector had integrated mainly as a full intact vector molecule (93.3 %), in the studied clones.
iii. The integration of the vector seemed to have taken place through the termini.
iv. The vector did not show any preferential integration into genes of any particular molecular function or biological process.
v. The vector utilized "patchy homologies" during the integration (in 60.7 % of the integrations).
vi. In 6.6 % of the integrations, the event was "homology mediated".
vii. In the ATP6VID gene in Chr 14q24, and Chr 8q24, more than one independent integration of the vector DNA into the gene was observed.
viii. The termini were present either in total, or had deletions up to 105 bps. When deletions had taken place in the termini during integration, 80.7 % of them had occurred within the first 30 bps of the terminus. No specific relationship was observed between the deletions in the terminus and the integrations into active genes.
ix. In 37.7 % of the studied junction sites, mutations in the host genomic sequences or in the termini or right at the junction site were observed.
x. Integrations had taken place in both active as well as non active genes, with no apparent preference.

IV.5.6.A Vitality curve of the 6TG resistant cell lines in medium supplemented with HAT

This series of experiments were carried out to analyze if there was a reversion in the homologous recombination that had taken place and to reconfirm that the recombination was genuine.

$1x10^5$ cells of each of the 6TG resistant cell lines based on both HT1080 and C 32, were plated in 6 well plates and were maintained in α MEM medium supplemented with 1 X HAT supplement. HAT supplement is comprised of hypoxanthine, aminopterin and thymidine. Aminopterin ($C_{19}H_{20}N_8O_5$) is a folic acid antagonistic that blocks the *de novo* synthesis of purine, and hypoxanthine and tymidine are purine analogs. 6TG resistant cells were expected to die in medium containing HAT supplement while revertants were expected to survive. Cell count using Trypan Blue staining was taken once in three days and the numbers of the viable cells, counted using a Haemocytometer were plotted in a graph (Fig. 39).

Based on these results it was concluded that no revertants were present in the number of cells used in the selection experiments and that in these cells, the homologous recombination between the vector and the genomic DNA was likely to be a genuine one.

IV.5.6.B Reconfirmation of the homologous recombination using PCR

These experiments were carried out to reconfirm the events of homologous recombination that had taken place between the vector and the genomic DNA. The DNA isolated from the 6TG resistant clones was used as the template for PCR reactions with primers SSHPRT1 and SSHPRT2 and the product size was expected to be 558 bps. The PCR products were digested with the restriction endonuclease *Eco RV* (fragments of 82 and 476 bps expected) and were run on a 2% 1X TAE gel. The enzyme was expected to cut in the novel *Eco RV* site that had been generated due to homologous recombination between the vector and the genomic DNA. In the case of homology mediated insertional recombination, then the digested and the undigested forms of the product was expected. Plasmid p STK129 that had the original unmutated exon 2 of Hprt was used as the negative control (p2) (Fig. 40).

In these experiments, the earlier results obtained about the 6TG resistant cell lines were reconfirmed. It was evident that the recombinations were all of the classic

replacement type, formed by two recombination events, one upstream and one downstream of exon 2.

IV.5.6.C Nucleotide sequence of the corrected region

The PCR products obtained in the above-mentioned experiments were cloned on a TOPO plasmid and were sent for sequencing and were checked against the controls. In the sequences analysed, the replacement of the wild type exon 2 with the mutated form was observed. The sequence of one of the 6TG mutuants is compared below with the parental control.

2a sequence

CGCCCTTGTATCCTGTAATGCTCTCATTGAAACAGCTATATTTCTTTTTCAG
ATTAGTGATGATGAACCAGGTTATGACCTT**TGATATC**TTTTGCATACCTAA
TCATTATGCTGAGGATTTGGAAAGGGTGTTTATTCCTCATGGACTAATTAT
GGACAGGTAAGTAA

HT1080 sequence

CGCCCTTGTATCCTGTAATGCTCTCATTGAAACAGCTATATTTCTTTTTCAG
ATTAGTGATGATGAACCAGGTTATGACCTT**GATTTA**TTTTGCATACCTAAT
CATTATGCTGAGGATTTGGAAAGGGTGTTTATTCCTCATGGACTAATTATG
GACAGGTAAGTAA

Sequence legend:

Standard font: hprt sequence

Bold font: T insertion and novel *Eco RV* site/ corresponding bps in parental cell

Underlined font : Topo TA vector

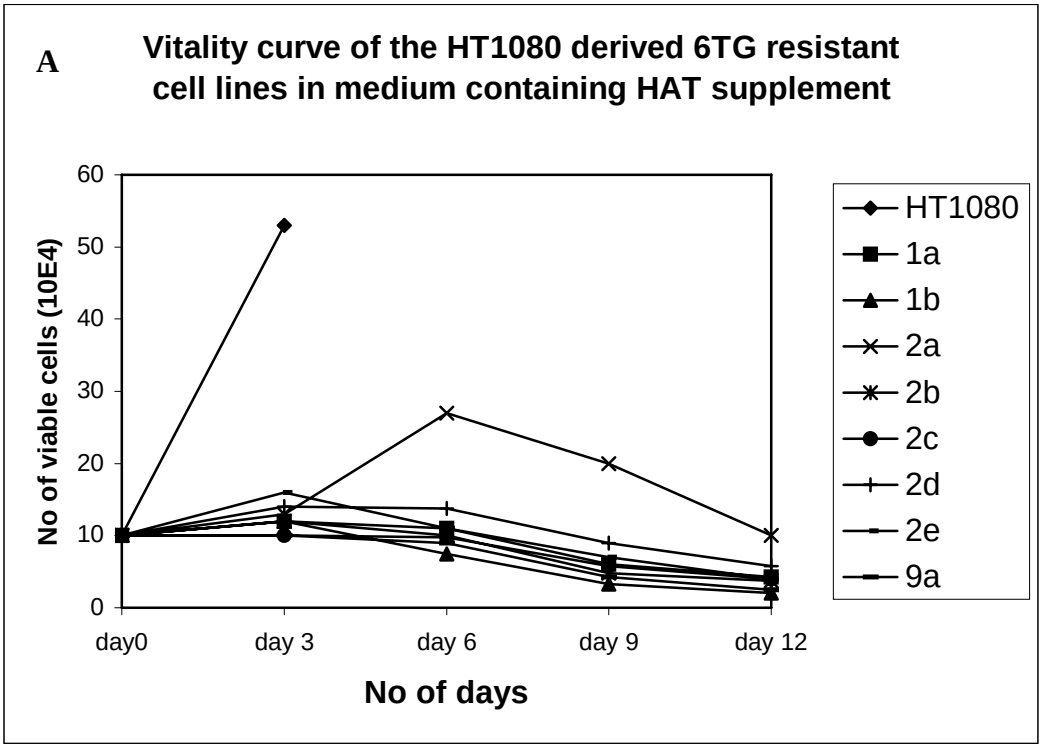

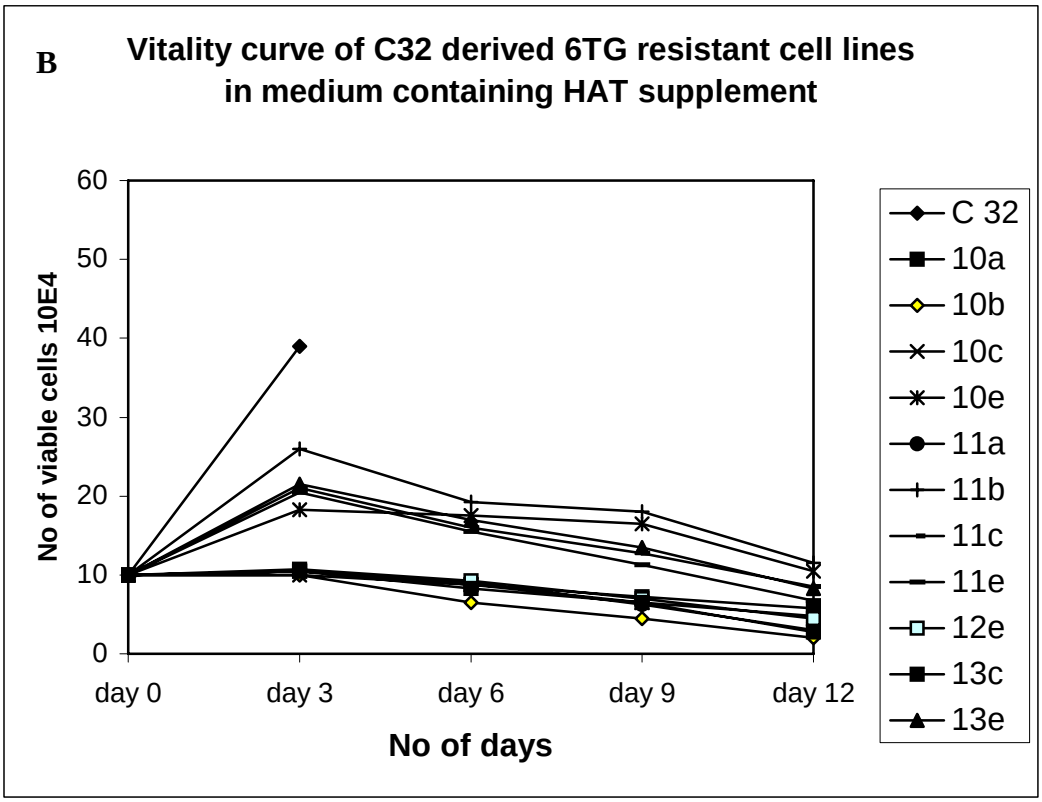

Fig. 39: Vitality curve of 6TG resistant HT 1080 (A) and C32 (B) based clones in HAT medium. Cells were grown in 6 well plates in medium supplemented with HAT, and cell count was taken and plotted on to the graph above.

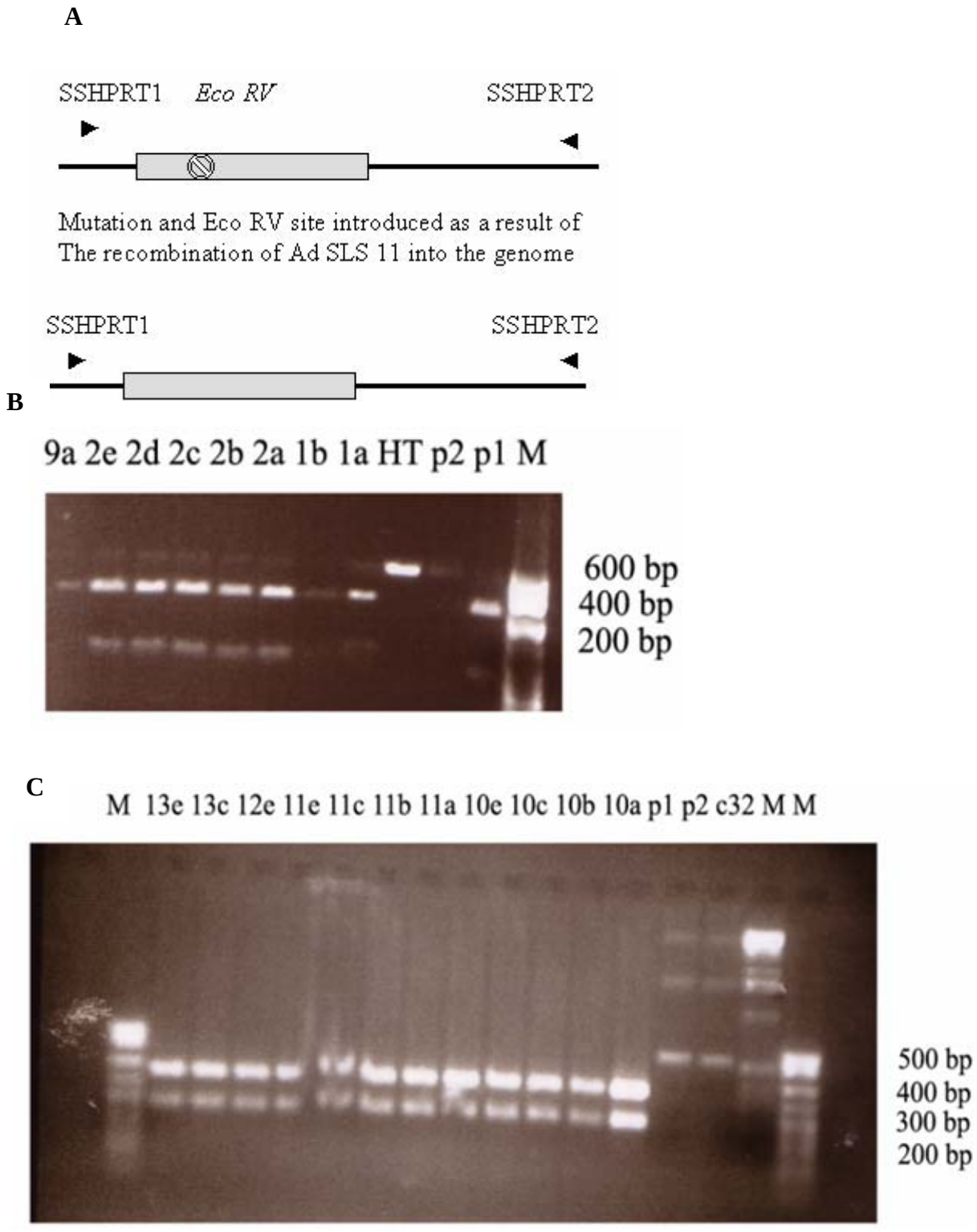

Fig.40. Scheme (A) and the gel electrophoresis photo of the PCR to confirm the event of homologous recombination of the HC-AdV DNA with the cellular genomic DNA. DNA from HT 1080 derived 6TG resistant cells (B) or C 32 derived 6TG resistant cells (C) were amplified with the primers SSHPRT1 and SSHPRT2 and the products were purified, digested with *Eco RV* and run on a 2% gel. M- marker, p1- p SLS 11 DNA (positive control), p2- p STK 129 DNA (negative control), HT- HT1080 DNA, c32- C32 DNA, 1a to 9a- DNA from HT1080 derived 6TG resistant clones, 10a to 13e- DNA from c32 derived 6TG resistant clones

This experiment was carried out to confirm the recombination at the sequence level and from the obtained sequences, it was evident that the cases of recombination of the vector DNA with the Hprt locus were genuine events.

IV.5.6.D Conclusions reached from the molecular analysis of clones obtained through the homologous recombination events of HC-AdV DNA with the Hprt locus

The aim of these experiments was to analyse homologous recombination of the vector DNA with the chromosomal DNA a molecular level. From the results, it was concluded that

i. The cases of homologous recombination observed were all genuine and of the classical double cross over replacement type instead of the single event insertion type.
ii. No terminus of the vector DNA was present in the genome (pg 92).
iii. The sequences downstream of the hprt stuffer, in particular, the HygEGFP expression cassette, were not present in the integrated molecule. (pg 92).
iv. No revertants back to the hprt +ve state were observed.

IV.6 Analysis of the homologous and heterologous rcombination of vector DNA into chromosomal DNA following HC-AdV mediated gene transfer *in vivo*

IV.6.1 Determination of the amount of viral vector particles reaching the mouse liver after a given dose

As a requirement to determine recombination frequencies of HC-AdV DNA in hepatocytes, an accurate determination of the amount of vector DNA present in the hepatocytes following a given dose into the tail vein was essential and this experiment was carried out to determine the amount of viral particles that reach the hepatocytes following the injection of a given dose into the tail vein

As reviewed in (Kuzmin et al., 1997, Overturf et al., 1997, Stein et al., 1998, Wolff et al., 1997, Worgall et al., 1997), the vast majority of the vector injected fails to reach the liver since they are phagocytocised by Kupffer cells and macrophages. So the rationale was that, after injecting a HC-AdV into mice, harvesting the liver 10 days p.i. should allow only the vector molecules present in the hepatocytes to be detected.

The HC-AdV Ad SLS 16, carrying the murine FAH cDNA in a RSV promoter BGH poly A cassette was used for the study. Vector was injected via the tail vein into $Fah^{\Delta exon5}$ mice in doses ranging from $1x10^{10}$ to $5x10^{8}$ inf. units per mouse, and the subjects were sacrificed 10 days post injection. A total of 13 mice were used for the study (including the control). The livers were harvested, the DNA was extracted and the vector DNA load was titered per 3µg and 6µg of DNA using the slot blot method (Fig. 41).

The results are summarised in Table 13. A diploid mouse cell has 6 pg of DNA and so the number of cells used was calculated from the amount of DNA used.

Dose	**Slot blot value**	**No: cells**	**No: of copies reaching each nucleus**
$1x10^{10}$	$10.4 x10^{6}$	$1x10^{6}$	10
$2x10^{9}$	$3.2 x 10^{6}$	$1x10^{6}$	3.2
$1x10^{9}$	$1.1 x 10^{6}$	$1x10^{6}$	1.1
$5x10^{8}$	$0.45 x10^{6}$	$1x10^{6}$	0.45
$1x10^{8}$	N.D.	$1x10^{6}$	N.D.

Table 13: Data showing the number of copies of HC-AdV per hepatocyte as per Slot blot method

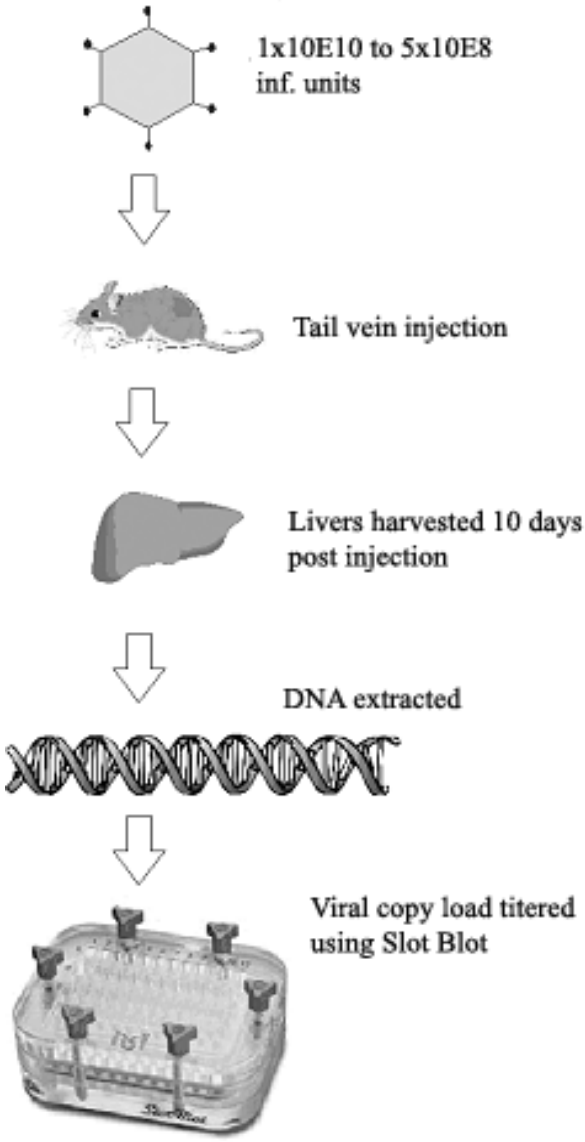

Fig.41. Schematic representation of the experiments carried out to determine the number of HC-AdV molecules reaching the liver following tail vein injection. Mice were injected with different amounts of the vector, sacrificed, the livers harvested and the DNA isolated. Viral load was measured using the Slot blot procedure.

The aim of this experiment was to determine the exact number of HC-AdV vector molecules reaching each hepatocyte following the injection of a given dose, so as to facilitate the calculation of the frequencies of integration and homologous recombination of the HC-AdV *in vivo*. From the experiment, it was evident that the amount of vector reaching the liver is dose dependent and ranges from 10 copies per

hepatocyte following and injection of $1x10^{10}$ inf. Units (in contrast to the expected 300 copies) to 1 copy in 2 hepatocytes following an injection of $5x10^{8}$ inf. units.

IV.6.2 Determination of the rate of random recombination of HC-AdV *in vivo* and molecular analysis of the junction sites of integration

VI.VII.1. Determination of the rate of integration of the vector

This experiment was carried out to determine the rate with which the HC-AdV integrates into the genome *in vivo*.

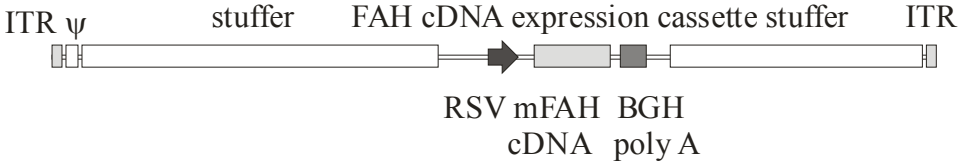

Fig. 42: Diagram of Ad SLS 16

The vector used in this study was Ad SLS16, which expresses the murine FAH cDNA from the RSV promoter (Fig. 42). The $Fah^{\Delta exon\ 5}$ knockout mouse was used as the model in which the vector was tested. The full details of the cloning of the vector are given in the Materials and Methods section.

As explained in the Materials and Methods section, the production of the fumaryl acetoacetate hydroalse transgene was expected to confer resistance to the hepatocytes where the vector would be present. The vector, which remained as an episome, was expected to be gradually lost during the turn over of the hepatocytes. However, on the event of the integration of the vector into the genome, the FAH +ve cell would have a growth advantage in the liver, and given the regenerative capacity of the liver, would give rise to a nodule of Fah +ve cells, which could be visualized following immunohistochemical analysis of the mouse liver with a Fah specific antibody. When such a mouse liver containing a mixture of Fah +ve and negative cells was perfused and the isolated hepatocytes transplanted onto a second recipient, the above-mentioned Fah +ve cells from the donor, were expected to have the growth advantage and repopulate a part of the recipient liver, provided the vector integrated into the genomic DNA.

Fah $^{\Delta\ exon\ 5}$ strain mice (n = 10, including control) were injected with Ad SLS 16 via tail vein injection. Pilot studies with varying doses of the vector had shown that the

optimal amount of vector required to count the Fah +ve nodules was $5x10^8$ inf. units and so that dose was favoured.

The mice were allowed to recover after the injection and were kept for 2 weeks off NTBC. NTBC was then added to the drinking water at a concentration of 7.6 mg/litre, and the mice were kept on the diet for a further two weeks and were sacrificed at predefined time-points, unless specifically mentioned. For the mice predestined for the immunohistochemical analysis of the liver alone, the animals were sacrificed by cervical dislocation and the livers were harvested and fixed in 10% phosphate buffered formalin (Fig. 43). The tissues were dehydrated in 100% ethanol and embedded in paraffin wax and sliced using a microtone. Four-micron sections were selected and rehydrated. The sections were stained with haemotoxylin and eosin and with a polyclonal rabbit antibody to rat FAH, and viewed through a Zeiss Axiovert 135 microscope (Fig. 44 & 45).

A collection of cells in an ellipsoidal block was taken as a Fah +ve nodule (Fig. 46), and number of nodules and the number of cells per nodule was noted. The slides containing the sections were scanned on a flat bed Canon scanner along with a size standard at 300 dpi resolution, the images were opened with NIH image J programme and the surface area of the sections was calculated and in accordance to the methods, the total number of hepatocytes per slide was calculated as in (Wang et al., 2002). The number of viral vector genome per hepatocyte after the mouse was given a particular dose was calculated as mentioned in section VI.VI. The rate of integration of the vector DNA into the chromosomal DNA was calculated as on pg 57. The rate of integration of the viral vector was calculated on the basis of vector molecules as $4.0275x10^{-5}$ (S.E.M = $1.76\ x10^{-5}$) in n = 9 mice (Table 14).

No: of mice injected	**Dose of Ad SLS 16, inf. units**	**Rate of integration (mean, corrected to the number of vector molecules reaching the hepatocytes)**
6	$5\ x10^8$	$6.2075 +/- 2.49, x10^{-5}$
2	$2\ x10^8$	$3.335 +/- 1.185, x10^{-5}$
1	$1\ x10^9$	$2.54\ x\ 10^{-5}$

Table 14: The data obtained from the experiment for calculating the rate of random integration of the HC-AdV into the cellular genome *in vivo*.

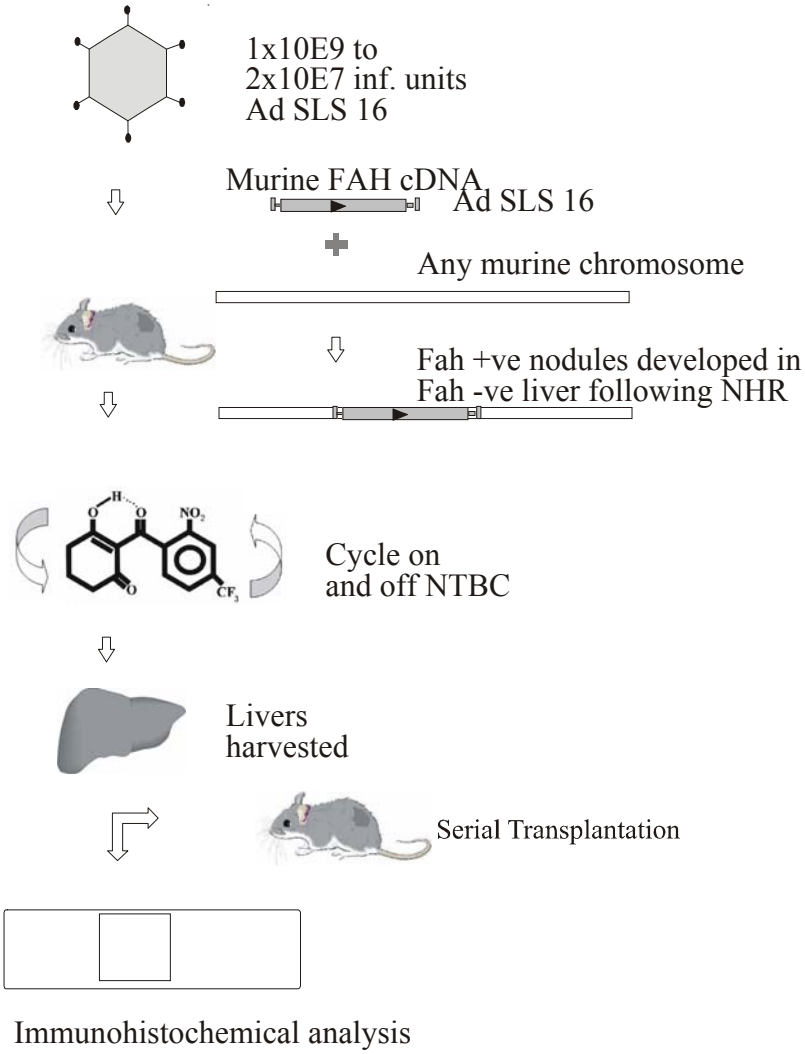

Fig. 44: Schematic representation of the experiments carried out to determine the rate of random integration of HC-AdV *in vivo*. Mice were injected with different amounts of the vector, cycled on and off the NTBC diet to allow them to recover and were sacrificed. The livers were harvested and the immunohistochemistry carried out with an anti-Fah antibody.

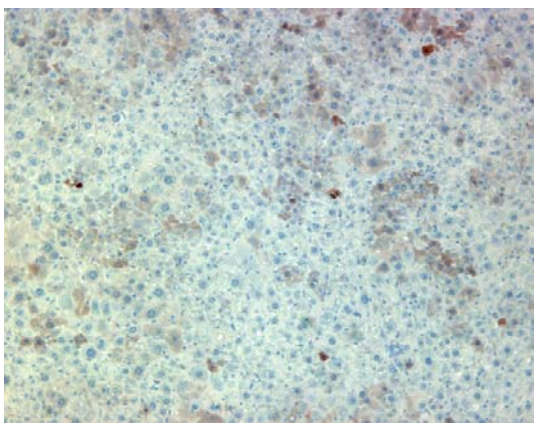

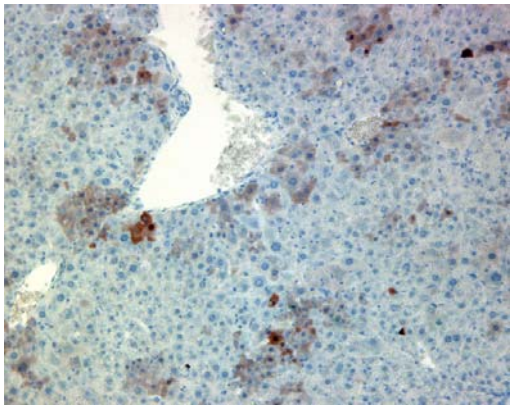

Fig. 44: Liver sections from mice that had been injected with a dose of $1x10^9$ inf. units of Ad SLS 16

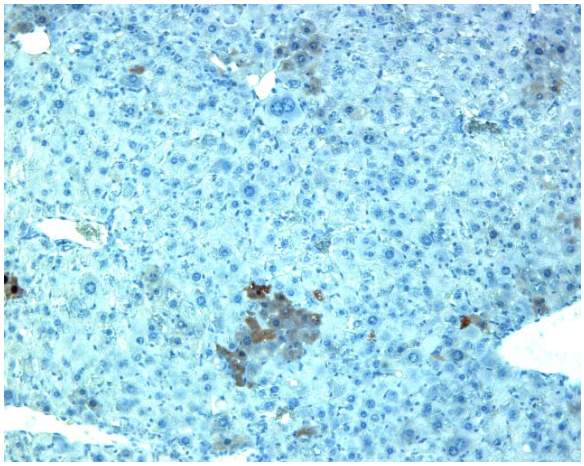

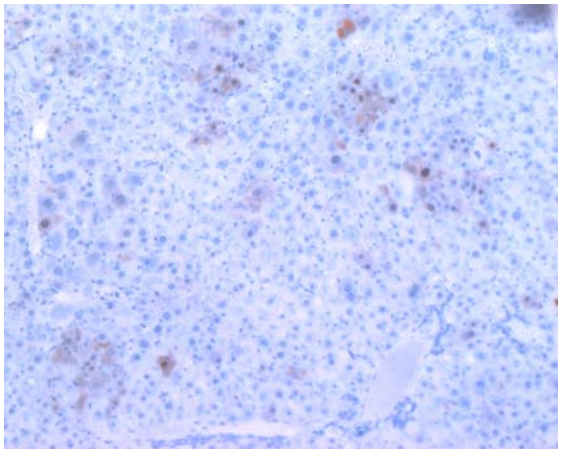

Fig. 45: Liver sections from mice that had received a dose of $5\ x10^8$ inf. units of Ad SLS 16.

The FAH +ve nodules can be visualized more clearly in these liver sections.

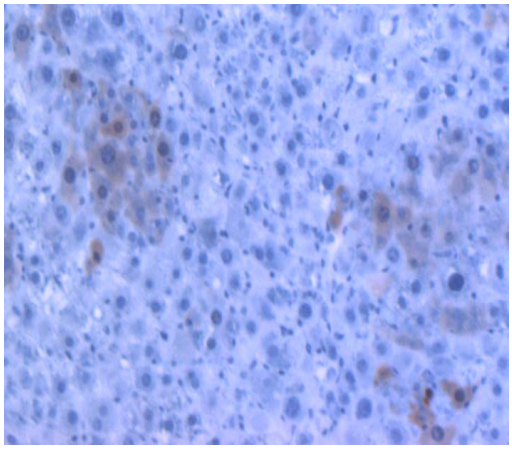

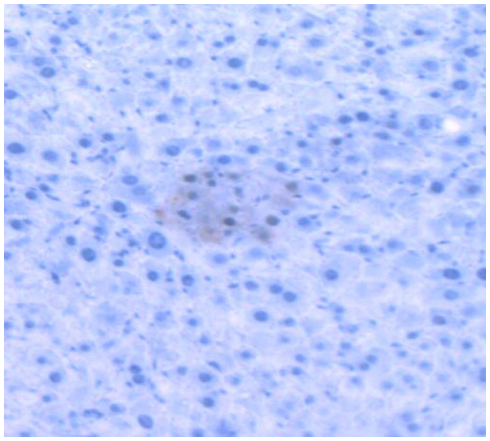

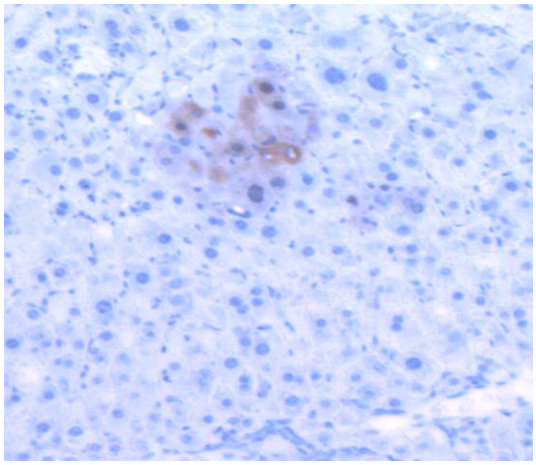

Fig. 46: Liver sections from mice that had received a dose of 5 x10^8 inf. units of Ad SLS 16.

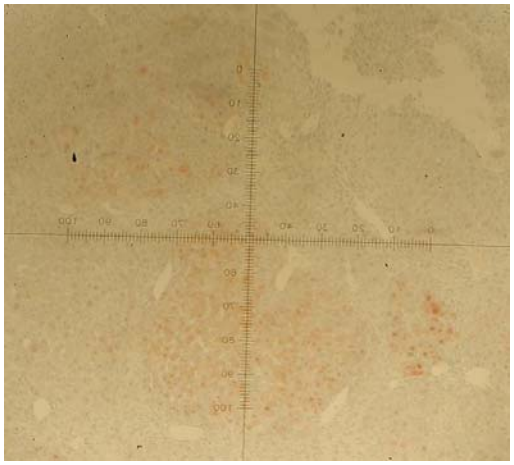

Fig. 47: Liver sections from mice that had received the serial transplantation injections of hepatocytes from the mice injected with Ad SLS 16.

In the serial transplantation experiments (Fig. 47), the mice were anaesthetised, and two lobes of the liver were tied off from the rest, cut out and treated as in the ones mentioned above. The remaining part of the liver was perfused using collagenase, and the prefused liver was filter sterilized and 1x10^6 viable hepatocytes were isolated. Recipient mice were anaesthetized, and the isolated hepatocytes were injected into the spleen, the flesh and the skin were stitched back, and the mice were allowed to recover with NTBC containing drinking water. The mice were sacrificed at set times, the livers were harvested and the DNA was isolated. Standard PCR was carried out to confirm the presence of the vector derived DNA in the recipient liver DNA. Inverse PCR was carried out and the PCR fragments were cloned into TOPO cloning vector and were sequenced.

This series of experiments were carried out to calculate the rate by which the HC-AdV integrates randomly into the genome *in vivo*. This was found out to be 4.0275 x 10^{-5} (S.E.M = 1.76 x10^{-5}) in n = 9 mice, based on the number of infectious units of HC-AdV per cell.

IV.6.2.A PCR to test for the presence of the transgene in the liver of the experimental animals

The DNA obtained from the adenovirus injected and serially transplanted mice were analysed using PCR. A primer pair was used whereby P1 was designed from the RSV

promoter sequence and the P2 from the mFah CDNA. A band of 481 bps was expected to be amplified only in the presence of the entire cassette (Fig. 48 & 49).

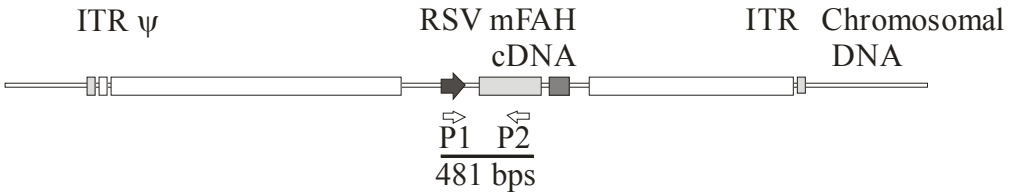

Fig. 48: Scheme of the PCR to test for the presence of the RSV-FahcDNA cassette in the serially transplanted liver.

The DNA bands were cut out and cloned into a TOPO TA cloning vector and the DNA sequences were detemined. The sequences were as expected, showing the RSV promoter sequence and the murine FAH cDNA sequence.

A

Gel i.d.	**Mouse i.d**	**comments**	**Gel i.d.**	**Mouse i.d**	**comments**
1	16.2	Serial transplant	11	Serial 23	Serial transplant
2	16.3	Serial transplant	12	Serial 24	Serial transplant
3	410	injection	13	Serial 511	Serial transplant
4	410 (hep)	injection	14	Serial 524	Serial transplant
5	411	injection	15	16#2	Serial transplant
6	412	injection	16	$Fah^{-/-}$	control
7	412 (hep)	injection	17	Wt	control
8	415	injection	18	p SLS 16	10000 copies
9	416	injection	19	p SLS 16	1 copy
10	Serial 21	Serial transplant	20	H_2O	water

Legend: Serial transplant: subjects that received the serial transplantation

10000 copies: 10000 copies of the vector molecule/mouse genome, spiked in mouse DNA

1 copy: 1 copy of the vector molecule/mouse genome, spiked in mouse DNA.

B

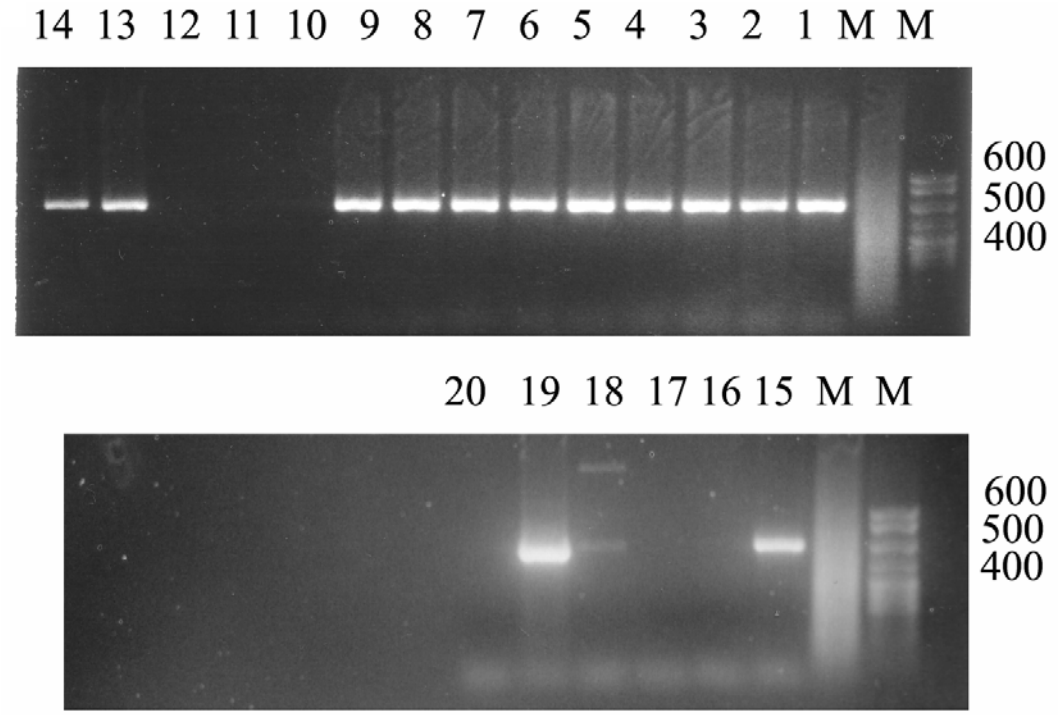

Fig. 49: A. Table with details about the samples used in the PCR. B. PCR experiment carried out on the liver extracted from the liver of mice injected with Ad SLS16 or serially transplanted with viable hepatocytes that had been transduced by that vector. The DNA was amplified with the primers and run on a 2 % 1XTAE agarose gel. See 49.A for details about the samples in each lane.

AATTCGCCCTT**GACAGGTCTGACATGGATTGGACGAACCACTGAATTC**
CGCATTGCAGAGATATTGTATTTAAGTGCCTAGCTCGATACAATAAAC
GCCATTTGACCATTCACCACATTGGTGTGCACCTCCAAGCTAATTCCG
TAGGGGGCTCTGCTGCCCGGTGCTCGTCAGCATGTCCTTTATTCCAGTGGC
CGAGGACTCCGACTTTCCCATCCAAAACCTGCCCTATGGTGTTTTCTCCAC
TCAAAGCAACCCAAAGCCACGGATTGGTGTAGCCATCGGTGACCAGATCT
TGGACCTGAGTGTCATTAAACACCTCTTTACCGGACCTGCCCTTTCCAAAC
ATCAACATGTCTTCGATGAGACAACTCTCAATAACTTCATGGGTCTGGGTC
AAGCTGCATGGAAGGAGAAGGGCGAATT

Sequence code:
Standard font: TOPO TA vector, **Bold font**: RSV promoter,
Underlined font : FAH cDNA

This PCR reaction and the related sequencing reaction were carried out to check for the presence of the transgene in the DNA of the liver of the injected and the serially

transplanted test animals, and the results confirm its presence. However, the vector was lost in some of the serially transplated mice. This was also expected, since the NTBC diet was restored to the experimental animals once they started appearing unhealthy, and so, though under the experimental conditions the mice with FAH positive cells had a selective advantage, mice with FAH negative livers could also survive.

IV.6.2.B Sequence analysis of the junction sites between the Ad SLS 16 DNA and the chromosomal DNA

In the serial transplantation experiments, the mice were anaesthetized, and a part of the liver was harvested and fixed for immunohistochemical staining. The remaining part of the liver was perfused using collagenase, the perfused liver was filter sterilized, $1x10^6$ viable heptocytes were isolated and injected into the spleen of Fah $^{-/-}$ recipient mice, which were then allowed to recover with NTBC containing drinking water. The mice were sacrificed at set times, the livers were harvested and the DNA was isolated. Inverse PCR was carried out using the restriction endonuclease *Tsp 509L* and the PCR fragments were cloned into TOPO cloning vector followed by sequencing.

Sequence of the junction site from mouse 16#2

Mouse 16#2 had received a splenic injection of $1x10^6$ viable hepatocytes from mouse 41, which had been injected with $5x10^8$ inf. units of Ad SLS 16, and had been allowed to recover from the injection with one cycle on and off NTBC. Mouse 41 was sacrificed 4 weeks after the injection. Mouse 16 too was kept on one round on and off NTBC and was sacrificed 4 weeks after it was injected.

A deletion of 31 bps in the right terminus and a T to C substitution was observed at the -9 bp of the terminus. Though the location of the sequence was found to originate

from a clone that contained the preribosomal RNA gene, the exact location is not yet available in the database

Sequence of the junction site from mouse 511

Mouse 511 had been injected with $5x10^8$ inf. units of Ad SLS 16, had been allowed to recover from the injection with one cycle on and off NTBC and was sacrificed 8 months after it was injected.

Ad5 left ITR	5'-CATCATCAATAATATACCTTATTTTGG-'3
511 left terminus	5'-CACAAATACAGATACACAAACCTTATTTTGG-'3
Genomic locus	5'-CACAAATACAGATACACAAACTATACATATGG-'3

The last 15 bps were found deleted from the left terminus and the integration was mapped to the 63673236 bp of Chr 5 C.3 in a non coding region.

Sequence of the junction site from mouse 327

Mouse 3 had received a splenic injection of $1x10^6$ viable hepatocytes from mouse 41, which had been injected with $5 x10^8$ inf. units of Ad SLS 16, and had been allowed to recover from the injection with one cycle one and off NTBC (4 weeks post injection). Mouse 3 was kept on one round on and off NTBC and was sacrificed 4 weeks after it had received the hepatocytes. $1x10^6$ viable hepatocytes from the perfused liver were injected into mouse 327 via the spleen. After a cycle on and off NTBC, mouse 327 was sacrificed, the liver harvested and the DNA prepared.

Ad5 left ITR	5'-CATCATCAATAATAT-'3
327 left terminus	5'-CTTTGAATAGAGTTATATCATCAATAATAT-'3
Genomic locus	5'-CTTTGAATAGAGTTATGAGTGAGGGG-'3

The last bp of the left terminus was missing in the integration event that was mapped to the 37088008 bp in chromosome 10B1.

The entire right terminus was present in junction site that was located in the 103407545 bp of Chr 9, corresponding to the 5th intron of the beaded filament structural protein 2, phakinin (Bfsp2).

Ad5 right ITR 5'-TATATTATTGATGATG-'3

327 right terminus 5'-TATATTATTGATGATGGCCCGGTACCCAGCTTTTG-'3

Genomic locus 5'-TCGAGGGGGGGCCCGGTACCCAGCTTTTG-'3

Sequence of the junction site from mouse S21

Mouse S21 had received a splenic injection of $1x10^6$ viable hepatocytes from mouse 410, which had been injected with $5x10^8$ inf. units of Ad SLS 16, and had been allowed to recover from the injection with one cycle one and off NTBC. Mouse 410 was sacrificed 4 weeks after the injection. Mouse S21 was kept on one round on and off NTBC and was sacrificed 4 weeks after it was injected.

Ad5 right ITR 5'-CAAAATAAGGTATATTATTGATGATG-'3

S21 right terminus 5'-CAAAATAAGGTATATTTAGTCTCTTTTCAAAGG-'3

Genomic locus 5'-CTTTAACTAATTATTTAGTCTCTTTTCAAAGG-'3

The last 10 bps of the right terminus were missing and the integration was mapped to bp 89372401 in chr 2E1.

Sequence of the junction site from mouse S23

Mouse S23 had received a splenic injection of $1x10^6$ viable hepatocytes from mouse 410, which had been injected with $5x10^8$ inf. units of Ad SLS 16, and had been allowed to recover from the injection with one cycle one and off NTBC. Mouse 410 was sacrificed 4 weeks after the injection. Mouse S23 was kept on one round on and off NTBC and was sacrificed 4 weeks after it was injected.

Ad5 left ITR 5'-CAT←60 bps→TGACGTGGCGCGGGG-'3

S23 left terminus 5'-AGAGTATTCTGGCAAGAGAGACGTGGCGCGGGG-'3

Genomic locus 5'-AGAGTATTCTGGCAAGAGAGAAAAGAACAG-'3

The last 64 bps were found deleted from the left terminus in the integration which had taken place in the 2nd intron of the glucocorticoid modulatory element binding protein 2 (Gmeb2), in the 180986861 bp of chromosome 2H1.

Ad5 right ITR 5'-TCCAAAATAAGGTATATTATTGATGATG-'3

S23 right terminus 5'-TCCAAAATAAGGCACACAAACACACAAAC-'3

Genomic locus 5'-AGGTTTTTAATGGCACACAAACACACAAAC-'3

In the integration that took place in the 107788894 bp of Chr 12 in a predicted gene, the last 16 bps of the right terminus was found deleted.

Sequence of the junction site from mouse S24

Mouse S24 had received a splenic injection of $1x10^6$ viable hepatocytes from mouse 410, which had been injected with $5x10^8$ inf. units of Ad SLS 16, and had been allowed to recover from the injection with one cycle one and off NTBC. Mouse 410 was sacrificed 4 weeks after the injection. Mouse S24 was kept on one round on and off NTBC and was sacrificed 4 weeks after it was injected.

Ad5 right ITR 5'-CCGTTCCCACGC←74 bps→ATG-'3

S24 right terminus 5'-CCGTTCCCACGAGGGTGTATACAGAGGG-'3

Genomic locus 5'-GTTAGATGGGCAGAGGGTGTATACAGAGGG -'3

The last 78 bps of the right terminus were deleted in the integration that took place in a non coding region of Chr 18 d4 in the bp 60650359 bp.

The results have been summarized in Table 15.

Mouse ID	**Terminus**	**Integration in chr**	**Direction of the vector in relation to the chr**	**Deletion from the termini**	**Integration in gene**	**Comments**
16.2	R	?	?	31	?	Deletion at –9 bp
511	L	5c 636732361 bp	→	15	N	.

327	L	10B1 37088008 bp	←	1	N	
327	R	9 103407545	→	0	Y Bfsp2	
S21	R	2E1 89372401 bp	→	10	N	
S23	L	2H1 18098686 bp1	→	64	Y Gmeb2	
S23	R	12 107788894 bp	←	16	Y predicted	
S24	R	18D4 60650359 bp	←	78	N	

Table 15 Table listing the integration of the vector, the direction of the integration with respect to the chromosome.

This series of experiments was carried out to directly demonstrate integration events in the mouse liver by determining the sequences of the junctions of integration between vector and cellular DNA.

IV.6.3 Determination of the rate of homologous recombination of HC-AdV *in vivo*

This experiment was carried out to determine the rate with which the HC-AdV recombines with genome *in vivo* via homologous recombination.

The vector used in this study was Ad SLS 14 (Fig. 50), which carries a 12.3 kb fragment of the murine Fah gene spanning the region between the 1st intron and the 10th intron. The Fah $^{\Delta exon5}$ knockout mouse was used as the model in which the vector was tested. The full details of the cloning of the vector are given in the Materials and Methods section.

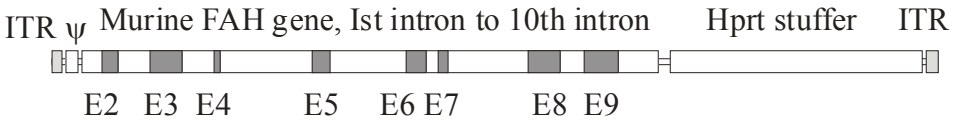

Fig. 50. Diagram of the HC-AdV SLS 16

As explained in the introduction, the Fah enzyme was not produced in the liver of the knockout mice. Since the vector lacks the promoter and exons 1, 10, 11, 12, 13 and 14, it would not confer any selective advantage on the cells where it remained as an episome. However, in the event of the homologous recombination of the vector with the Fah locus, and the subsequent correction of the mutated exon 5 (Fig. 51), the Fah +ve cell would have a growth advantage in the liver, would give rise to a nodule of Fah +ve cells, which could be visualized following immunohistochemical analysis of the mouse liver with the Fah specific antibody. As in the work with Ad SLS 16, when such a mouse liver containing a mixture of Fah +ve and negative cells was perfused and the isolated hepatocytes transplanted onto a second recipient, the above-mentioned Fah +ve cells from the donor were expected to have a growth advantage and repopulate a part of the recipient liver, provided the vector integrated into the genomic DNA.

The $Fah^{\Delta \text{ exon } 5}$ strain mice (n = 10, including control) were injected with Ad SLS 14, via the tail vein. Pilot studies with varying doses of the vector had shown that the optimal amount of vector required to count the Fah +ve nodules was $2x10^9$ inf. units and so that dose was favoured. The mice were allowed to recover after the injection and were kept for 2 weeks off NTBC and the rest of the experiment [treatment of animals and immunohistochemistry (Fig. 53)] was exactly as in the earlier experiment with Ad SLS 16 (Fig. 52). The same method was used to determine the rate of homologous recombination which was calculated on the basis of vector molecules as $5.651x10^{-7}$ (S.E.M = $1.7x10^{-7}$) in n = 11 mice (Table 16).

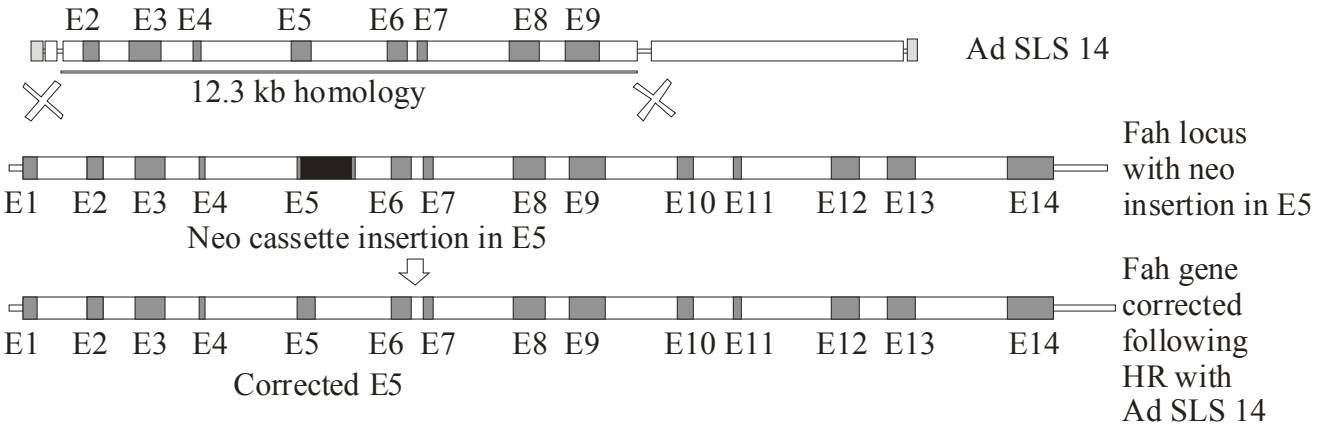

Fig. 51: Schematic representation of the homologous recombination of HC-AdV DNA with the Fah locus in thechromosomal DNA of the $Fah^{\Delta exon\ 5}$ mouse to generate a Fah +ve cell.

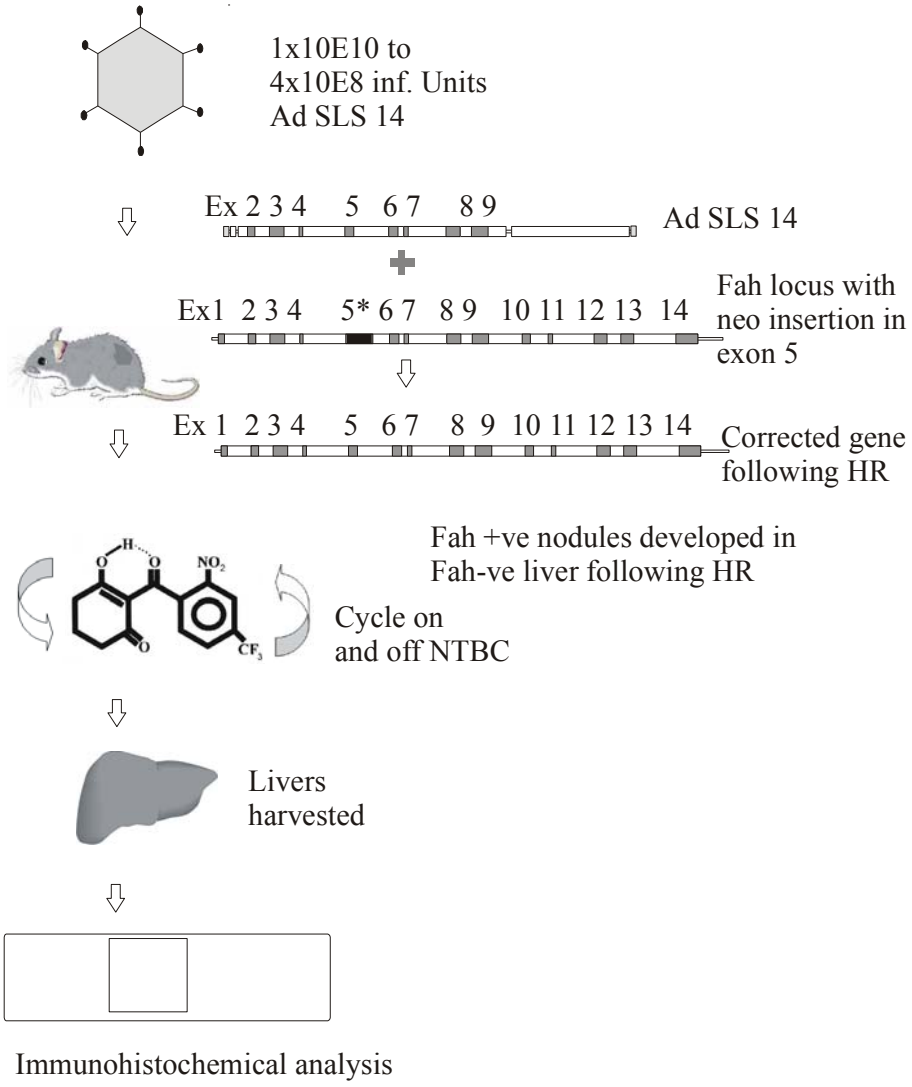

Fig.52. Experimental animals were injected with different doses of vector and maintained on a diet with and without NTBC supplement to allow them to recover. They were sacrificed, the livers harvested and immunohistochemical analysis was carried out with Fah antibody.

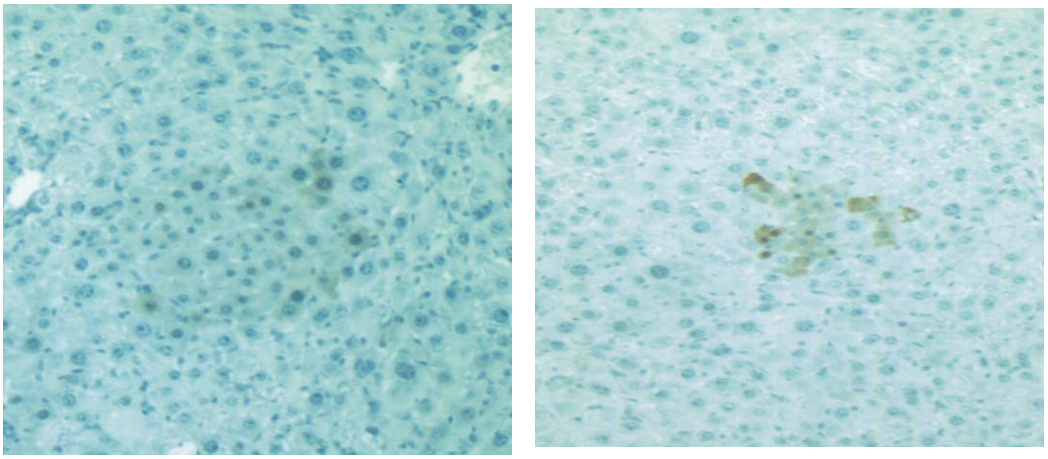

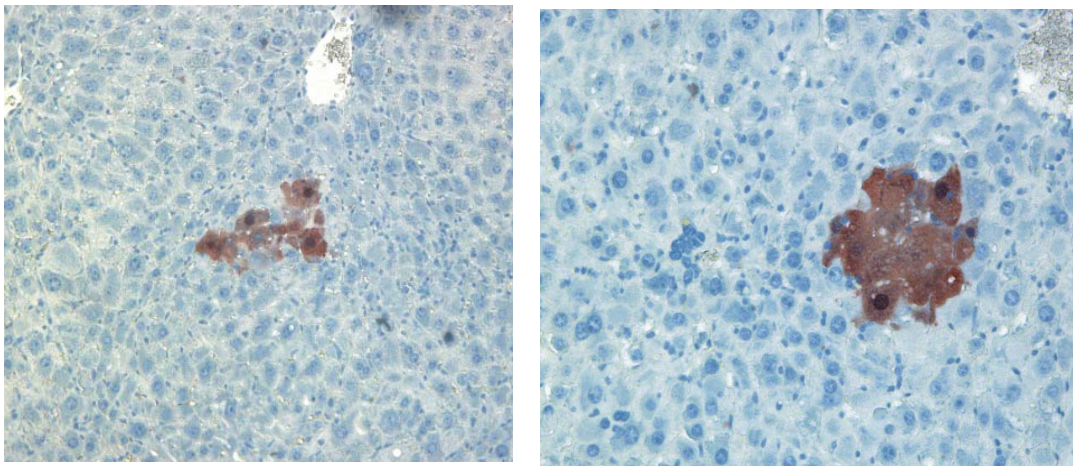

Fig. 53: Liver sections from mice that had received the dose of $1x10^{10}$ inf. units of Ad SLS 14

No: of mice injected	**Dose of Ad SLS 14, inf. units**	**Rate of integration (mean, corrected to the number of vector molecules reaching the hepatocytes)**
2	$1 x10^{10}$	7.34 +/- 1.95, $x10^{-7}$
7	$2 x10^{9}$	4.99 +/- 2.9, $x10^{-7}$
2	$1 x10^{9}$	6.24 +/- 0.23, $x 10^{-7}$

Table 16: The data obtained from the experiment for calculating the rate of homologous recombination of the HC-AdV with the Fah locus *in vivo*.

Taken together, the *in vivo* rate of homologous recombination was found to be $5.7x10^{-7}$.

IV.6.3.A PCR to confirm the correction of exon 5 in the mice

The serial transplantation of the hepatocytes was carried out as described in the earlier experiment with Ad SLS 16. The immunohistochemical analysis revealed the presence of Fah +ve cells and to confirm the correction of exon 5 in the Fah locus of the mice following homologous recombination between the vector DNA and chromosomal DNA, DNA extracted from Ad SLS 14 injected and serially transplanted mice were analysed using PCR. The primers used in the reaction were as follows: Fah A was designed from the 4^{th} intron sequence, Fah B from the neomycin cassette, and Fah C from the Fah exon 5 sequence downstream of the site of the neo insertion. A band of 243 bps was expected to be amplified between Fah A and Fah B primer pairs, and a band of 187 between Fah A and Fah C primer pairs in the presence

of the corrected band or the episome. No product was expected between primer pairs Fah A and Fah C in the non corrected liver under the conditions used (Fig. 54)

A

Gel i.d.	Mouse i.d	Comments
1	401	injection
2	403	injection
3	406	injection
4	14 serial1	Serial transplantation
5	14 serial 2	Serial transplantation
6	14 serial 3	Serial transplantation
7	14 serial 4	Serial transplantation
8	14 serial 5	Serial transplantation
9	16#2	Serial transplantation
10	25.505	Injection, Ist generation AdV Ad SLS25
Fah -	Mouse -	Control, Fah -/- Knockout mouse
p	P SLS 14	Control, Vector plasmid
fah +	Mouse +	Control, Wt mouse, 129 strain
fah+*	Mouse +	Control, Wt mouse, C57/Bl6 strain.
-ve	H_20	
-ve	H_20	

B

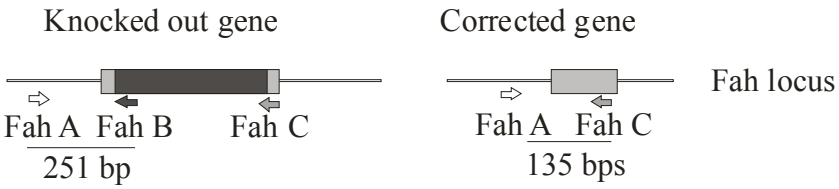

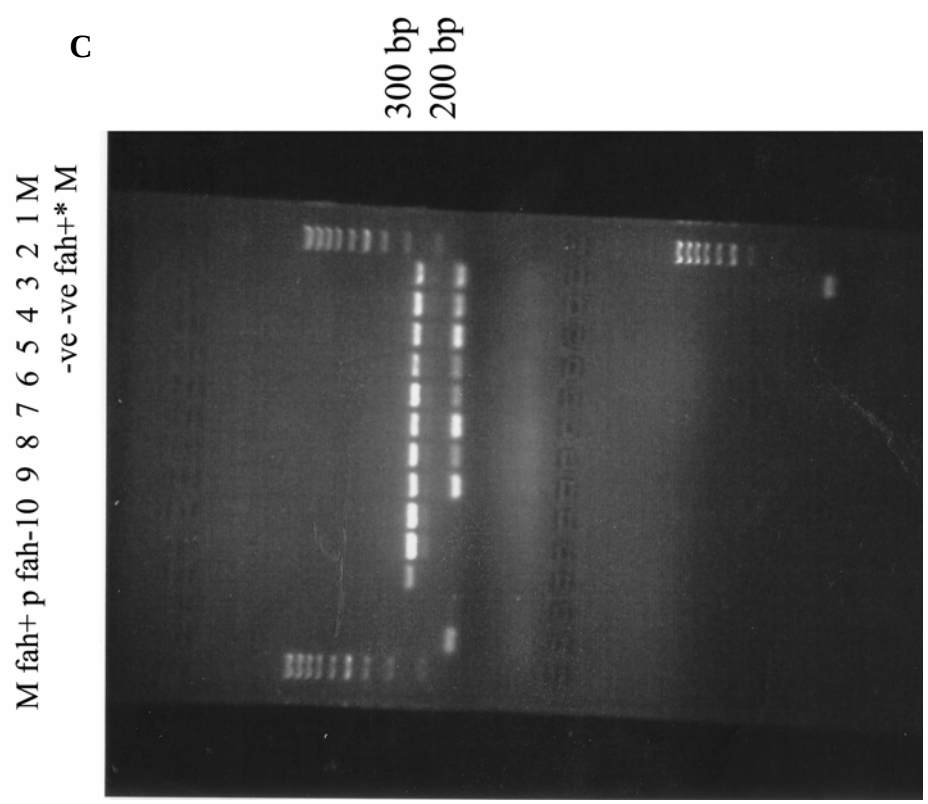

Fig. 54: A. Table detailing the samples used in the PCR. B. The scheme of the PCR. C. The PCR experiment carried out on the DNA extracted from the liver of mice injected with the Ad SLS 14. DNA was amplified with the three primers and run on a 2 % TAE agarose gel.

Sequence from the 135 bp band (corrected band)

AATTCGCCCTT**CTAGGTCAATGGCTGTTTGGGGTGTTCCCTCTGCAGG AGACTACACGGACTTCTACTCTTCTCGGCAGCATGCCACCAATGTTGG CATTATGTTCAGAGGCAAGGAGAATGCGCTGTTGCCAAATTGGTATG TCC**AAGGGCGAATT

Sequence from the 251 bp band (non corrected)

AATTCGCCCTTTAAAATGAGGAAATTGCATCGCATTGTCTGAGTAGGTGTC ATTCTATTCTGGGGGGTGGGGTGGGGCAGGACAGCAAGGGGGAGGATTG GGAAGACAATAGCAGGCATGCTGGGGATGCGGTGGGCTCTATGGCTTCTG AGGCGGAAAGAACCAGCTGGGGCTCGAGATCCACTAGTTCTAGCCTCGA**C**

CACCAATGTTGGCATTATGTTCAGAGGCAAGGAGAATGCGCTGTTGC
CAAATTGGTATGTCCAAGGGCGAATT

Sequence code:
Standard font: CMV
Bold font: Fah gene
Underlined font : TOPO TA vector

This PCR was carried out to confirm that the Fah exon 5 had been corrected in the serially transplanted mice. Though the chances of the 135 bp band arising from the episomal Ad SLS 14 could not be totally ruled out, it was unlikely after the multiple cell divisions arising from the serial transplantation process and therefore, taken together with the immunohistochemical data, it can be safely concluded that the vector had corrected exon 5.

IV.6.4 Conclusions reached from the *in vivo* experiments

At the time of the preparation of the manuscript, the mouse genome has been sequenced, but the data that is available in the database is not as much as compared to the human genome. The following conclusions have been reached from this study.

i. In this experiment, HC-AdV genome underwent integration *in vivo* with the chromosomal DNA at a rate of 4.0275×10^{-5}.
ii. From the available data, it can be stated that HC-AdV display no specific predisposition (37.5 %) to integrate into genes *in vivo*, similar to the results obtained in vitro.
iii. As in the *in vitro* data, deletions were observed in the termini of the AdV. 50 % of the deletions took place within the first 30 bps of the ITR.
iv. In this experiment, HC-AdV genome underwent homologous recombination *in vivo* with the chromosomal DNA at a rate of 5.651×10^{-7}.

V Discussion

At the time the project has started, no study had been performed on the fate of high capacity adenoviral vectors. The risk posed of insertional mutagenesis of the vectors became visibly apparent only after the ill-fated trial in France (Li et al., 2002). By the time of the completion of the lab work, no work had been published on the site of integration of HC-AdV in the genome and as of date, no work has been published about the rate of integration of HC-AdV *in vivo*.

V.1 Selection of the models

In the experiments involving the fate of the HC-AdV genome following gene thransfer *in vitro*, it was of paramount interest to select a system that was very well characterized. The Hprt model has been successfully used since the mid 1980s to study site directed mutagenesis events [for example, see (Lin et al., 1985)], and the positive and negative selections using 6TG and HAT mediums have been very well studied [for example, see (Sharp et al., 1973)], and so that model was chosen. At the time of the experiments, the $FAH^{-/-}$ mouse model was a more characterized knockout model than the $urokinase^{-/-}$ mouse model [reviewed in (Michalopoulos & DeFrances, 1997)] and so it was selected. The drawback of the model was that surgical extraction of single FAH+ve nodules from a FAH-ve liver, without any contamination whatsoever, was not technically feasible; to circumvent this, the system of serial transplantation of the hepatocytes into $Fah^{\Delta exon5}$ mice, was utilized to select for a subset of the Fah+ve cells in the donor mouse's liver, and was carried out with the intention of elucidating some of the sequences of the sites of integration between the vector genome and the mouse genome. Also, when the rate of random integration of the vector was tested, the proof for a case of integration was taken as a clear ellipsoidal Fah +ve nodule.

V.2 Recombination rates of HC-AdV DNA with chromosomal DNA *in vitro*

Cell types may vary with respect to their permissivity for adenoviral infection and that was the rationale behind the testing of the permissivity of the cell types to adenovirus vector transduction. Two of the cell lines used in the study described here, viz., HeLa and HT1080 were used in a similar study in which the rates of integration of HC-AdV

and Ist Gen AdV were compared (Harui et al., 1999). The rate of integration of HC-AdV in HeLa was between 2.6 and 0.5x10^{-4}, and that of HT1080 was between 1.8 and 0.29x10^{-3}, at 10 moi per cell. Ist Gen AdV integrated at slightly higher rates. The rates of HC-AdV integration, observed for the same cell lines in this present study were 3.01x10^{-4} and 4.6x10^{-4} respectively. In the above mentioned work involving KB, CHO, CV-1, cells, the authors had observed HC-AdV DNA integration at rates between 1 to 0.01x10^{-2}, at a moi of 10. (Hillgenberg et al., 2001) had published that the rate of integration of HC-AdV DNA into the genomic DNA of U87-MG cells was 1.6x10^{-4} at a moi of 0.1, as opposed to the rates observed in current study between 5 to 0.1x10^{-3} at a moi of 1 in different cell lines. In the study by (Hillgenberg et al., 2001), the permissivtiy of the cells to AdV was not tested. The authours had also not observed any instances of homologous recombination of the vector into the genome. However, as observed in the experiments described here, the rate of HR is three logs lower than the rate of NHEJ, and so they might have not noticed it. (Ohbayashi et al., 2005) report that in experiments with male ES cells transduced by HC-AdV at a moi of 10, the rate of homologous recombination of the vector DNA into the chromosomal DNA was between 2 to 0.67x10^{-3}, and the rate of random integration of the vector DNA into the chromosomal DNA was between 1.5 to 0.5x10^{-3}. In the experiments described in this study, the rate of homologous recombination of the vector into the genome ranged from 2 to 0.1 x10^{-5} at a moi of 1. The differences between the cell types might be the reason behind the higher rate of homologous recombination reported by that group. Human cells are reported to be 30-100 times less tolerant of integrations of exogenous DNA into their genome as compared with rodent cells (Colbere-Garapin et al., 1986, Hoeijmakers et al., 1987, Lohrer et al., 1988, Mayne et al., 1988), though in the case of established cell lines, there was no significant difference between the rates of integration of the vector in human and non human cells (Harui et al., 1999). The integration patterns of DNA in normal cells are simpler than in transformed cells (Hoglund et al., 1992), though it remains to be seen whether this would result in a significant difference in the rates of homologous recombination. In work involving targeting of the Hprt locus using AAV vectors, Russel et.al. (Russell & Hirata, 1998) report that the rate of integration of the vector in HT1080 was 2x10^{-4} at a moi of 50,000 and the rate of spontaneous mutation of the Hprt gene was 2x10^{-5}. The rate of homologous recombination of HC-AdV in HT1080 cells observed in this present study was 1.1x10^{-6}, and in the experiments involving early

passage cells that were either infected with Ad SLS 21 or PBS treated, no spontaneous mutation was observed under the conditions used. This contrast may be due to the difference of protocols between the labs. Since due to genomic instability (Hanson & Caisander, 2005) the expression level of the proteins involved in cellular DNA repair mechanism can vary between cell lines (Wang et al., 2005), the range in the difference of random integration of the vector into the genome can also be expected. HC-AdV do not code for any proteins involved in DNA repair and recombination and so are dependent on the cellular machinery to carry out the process. Recombination via homologous or non homologous end joining (NHEJ) can be linked to the levels of Rad family proteins and Ku70/Ku80, which compete for the broken ends of the DNA to channel them into the respective pathways (Haber, 1999). The inverse correlation between the rates of random integration and homologous recombination of the HC-AdV DNA observed in this present study in HT1080, C32 and FF-95 cells seem to suggest this. The progression into cell cycle also determines where DNA repair takes place by HR or NHEJ; genes coding for HR machinery are more expressed during the G2 and S phase of the cell cycle, whereas those supporting NHEJ are present throughout the cycle [reviewed in (Takata et al., 1998, Wurtele et al., 2003)]. The HT1080 cell line grows much faster than the C32 and FF-95 cells and have to be passaged more often (see Materials and Methods), and so the difference in the rates of recombination in these cell lines may be linked to the cell cycle. The plans in this study to test for the expression of these proteins were hindered by time constraints.

Earlier work done on the Hprt model using plasmid transfection had suggested that the rate of random integration of plasmid DNA into the genome is 10^{-4} to 10^{-5} and the rate of HR is 10^{-6} to 10^{-8}, and the greater the amount of homology, the higher the rate of HR (Doetschman et al., 1987, Lin et al., 1985, Thomas & Capecchi, 1987, Thomas et al., 1986). The rates at which DNA molecules reach the nuclei are low, being less than 10% in the $CaPO_3$ method (Orrantia & Chang, 1990) and only 1 % and 0.1 % in the case of the DNA complexed with polyethylenimine and cationic lipids respectively (Pollard et al., 1998), and even after that, a large proportion of the DNA gets degraded (Liang & Jasin, 1996). So the amount of DNA used for transfection cannot be directly correlated with the rate of integration as was done in (Harui et al., 1999), but nevertheless, the recombination rates of AdV seem to be higher than that of plasmid DNA. The precursor terminal protein coupled to the ends

of the Ad termini is a DNA binding protein. Two pTP molecules can bind co-operatively to short DNA duplexes in a sequence independent manner. pTP also binds to ssDNA without sequence dependence, and simultaneous interaction of two DNA binding regions within a pTP molecule too has been demonstrated (de Jong et al., 2003) but it remains to be seen if the smaller TP may have similar properties and serve not only in protecting the ends of the DNA, but also in tethering it to specific regions in the genome. TP-linked Adenviral genomes have been used in other studies (Hartigan-O'Connor et al., 2002) and it would be very interesting to determine the rates of recombination of TP-linked Ad genomes, after calculations have been done to determine the number of DNA molecules reaching the nuclei, by Slot Blot Analysis of the transfected nucleii isolated using Hirt's method, and compare them with the rates obtained in this study.

V.3 Southern blot analysis of the clones

The Southern blot data obtained in this study demonstrated that in up to 38% of the clones, more than 1 copy of the vector was present and that in 21% of the clones, there were more Ad termini than expected from the number of transgenes integrated. This agrees with the data presented in (Hillgenberg et al., 2001), where, though in 50 % of the clones both the Ad termini were observed, in 19 % of the clones descrepancies between the number of termini and integrated transgene were observed. However, the Southern data that is presented in this study is handicapped by the fact that the adenoviral left terminus was used the probe. The larger part of the probe hybridised with the packaging signal, but the probe had also cross-hybridised to a lesser extent with the adenovirus right terminus too. In the paper mentioned above, the vector had a RSV-LacZ-SV40Poly A cassette at the right terminus and so in that case, unlike the study described here where a DNA fragment of the cosmid c346 bordered the right terminus, it was possible for the researchers to perform a Southern blot exclusively for the right terminus of their vector using the SV40 PolyA probe. Discrepancies between the number of transgenes and the vector terminus were also reported in (Harui et al., 1999), where possible DNA rearrangements, including internal ones in the vector genome, were observed, also in agreement with the data presented in this present study. The above mentioned study also reported that the integrated vector underwent rearrangements over time. Chromosome instability has been reported in cell lines once past the Hayflick limit [reviewed in (Effros, 2004,

Hanson & Caisander, 2005)] and this might explain some of the data observed. Though 6TG resistant/ Hyg resistant clones were isolated from the primary cell lines FF-95 and HRPE, they failed to survive long enough to generate enough DNA needed for Southern blot and Inverse PCR protocols used in this study. However, the developments of mini southern blot (Lan et al., 2002) and LAM PCR (Schmidt et al., 2003), both of which need far less amount of DNA than that needed in conventional methods, can be used in any future work using primary cells to obtain the result. The Southern blot data obtained in this study has demonstrated that in the clones where the HC-AdV DNA had undergone HR into the genome, viral termini or non homologous sequences such as the transgene were absent. This, along with the data obtained from the PCR analysis of the clones, demonstrates that the HR resulted in a proper exchange of the exon 2 of the Hprt gene and not in an insertion of the homologous sequences. Nevertheless, FISH data on the clones could have pinpointed the data obtained from the Southern blot.

V.4 Sequence analysis of the clones

V.4.1 Mutations in the cellular genome

In the experiments described here, the protocol of Inverse PCR was developed for use in the adenoviral integration system, where the entire Ad terminus may or may not be present. Currently other PCR methods of determining the sequence of the junction of recombination, such as LAM PCR, PCR with various types of linkers, Alu PCR etc do exist, but the best results were obtained using Inverse PCR in the study. However, under normal conditions, PCR tends to amplify the smaller fragments in a pool of DNA fragments of different sizes, and so not all of the junction sites could have been sequenced. In work on HC-AdV DNA recombination into chromosomal DNA published by other labs using Adapter ligated PCR (Ohbayashi et al., 2005), sequences were obtained from both ends in two (possibly 3) out of the twenty clones analysed, and three out of forty three clones when Inverse PCR and Lam PCR were used (Wang et al., 2005). In the work presented here, only in one clone, 17e, it can be stated that the sequences from all of the Ad termini detected in it using Southern blot, have been accounted for. Even in this case, it would not be possible to rule out integrations of the adenoviral termini where extensive deletions had taken place, thereby nullifying the chances of detecting it in the Southern Blot. Wt. AdV have

been reported as forming concatamers and repeats during integration into the genome; deletions of up to 175 bps have been reported in the termini of integrated wt AdV [reviewed by (Doerfler et al., 1984)]. The cell lines themselves were known to have gross chromosomal irregularities and rearrangements in the karyotype, including deletions, additions and translocations in the chromosomes (Chen, 1978, Chen, 1983, Chen & Shaw, 1973, Rasheed et al., 1974). Therefore it is plausible that two independent vector DNA integration events are being coupled as one, when the sequence data from both the left and right termini of the integrated vector in one individual clone comes from the same region of the same chromosome. In the absence of FISH data and of individual karyotyping of the cell lines both at the start and the close of the experiment, a dogmatic assertion cannot be made. The integration events in these clones cannot be pinpointed by the Southern data due to unresolved bands. Nevertheless, the chances of two separate vector DNA integrations taking place in very close regions are at least $1/6x10^{-9}$ (based on the size of diploid human and mouse genome). However, it has also been demonstrated that it was 75 to 470 fold more likely for one integration event to take place in a preintegrated locus (Merrihew et al., 1996), and the Southern blot data from this study has shown that in spite of using a low moi, multiple integrations can take place in the same clone. So it must be treated with caution when the results from 7 clones (4d, 6a, 7c, 7g, 17 e, 22f and 22k) suggest that during the course of integration of the vector, deletions ranging from 31 bps to 46 kb (15 kb, 47 kb, 598 bp, 237 bp, 4.5 kb, 18 kb and 31 bp, respectively), were observed in the chromosomal DNA. Should that be the case, it would not be a novel discovery. Deletions of up to 1.6 kb in the genomic DNA have been reported during integration of Wt AdV (Schulz & Doerfler, 1984). Deletions of 14, 24 and 567 bps (Wang et al., 2005), 21 bp and at least 20 kb (Ohbayashi et al., 2005) in the genomic DNA have been reported during integration of HC-AdV. In the first paper cited above, possible larger deletions were observed in another three clones, though for reasons not published, the authors had determined that the individual 5' and 3' termini interspaced by larger deletions to those mentioned above, found integrated in same chromosome in these three clones did not come from the same vector DNA molecule.

V.4.2 Mutations in the vector genome

Work done on wt AdV revealed that during the process of integration, mutations (deletions, insertions and substitutions) did frequently occur in the viral genome, especially in the termini. In this present study, the vast majority (68 %) of the deletions took place within the first 30 bps of the termini, and 15 % had no deletions in the termini. In the study by Mitani et. al, (Ohbayashi et al., 2005) 86 % (18/21) of the vector termini had deletions up to 30 bps and 9.5 % (2/21) had no deletions in the termini, whereas in the work by Lieber et. al. (Wang et al., 2005), the data from their first series of experiments suggest that 82 % (19/23) had up to the first 30 bps and 14 % (3/21) had no deletions in the termini. The evidence for the use of patchy homology (micro homology) between the recombination partners was evident. This has been reported for wt AdV (Doerfler et al., 1984, Doerfler et al., 1989) and for HC-AdVs (Ohbayashi et al., 2005, Wang et al., 2005). The crucial role played by Mre 11 and the microhomology between the recombination partners during NHEJ has been well established (Paull & Gellert, 2000, Roth & Wilson, 1986), and so it is plausible that AdV DNA too may use cellular NHEJ pathways during integration into the genome.

V.4.3 Is HC-AdV DNA mutagenic?

In this present study, it was observed that in 64 % of the cases, HC-AdV DNA integrated without causing any mutations (deletions in the termini sequences are not included). However in 14.7 % of the junction sites studied, mutations were present at the junction site in the form of insertions or substitutions. In 13 % of the junction sequences, mutations were introduced in the genomic DNA. Deletions, insertions, duplications and chromosomal translocations too were observed and are consistent with the data from wt AdV DNA integration sites where mutations in and around the site of integration have been reported in genomic and viral DNA (Doerfler et al., 1984, Schulz & Doerfler, 1984). Translocations of genomic DNA were also noticed in integration sites of HC-AdV (Ohbayashi et al., 2005). Transposition of genomic DNA in 3 extra integration sites has been observed in integration of HC-AdV-AAV hybrid vector DNA into chromosomal DNA, at the AAV ITR, suggesting that those 68 bps might be involved in the amplification and transposition of the vector copies during DNA replication (Wang et al., 2005).

Such aberrations in the DNA following integration are not unique to AdV. Deletions of genomic DNA, chromosomal translocation, insertion of novel DNA at the junction site, deletions in the vector and the association of the integration site with chromosomal breaks have all been reported for AAV DNA integration (McCarty et al., 2004, Miller et al., 2004, Miller et al., 2002, Miller et al., 2005, Nakai et al., 1999), and HBV DNA integration (Koike et al., 1983, Mizusawa et al., 1985, Tokino et al., 1987, Wang et al., 2001). During integration by HPV DNA into the chromosomal DNA, deletions were observed in the HPV DNA (Kalantari et al., 2001, Luft et al., 2001, Yoshinouchi et al., 1999), translocation of the chromosomal DNA observed during EBV DNA integration (Debiec-Rychter et al., 2003) and integration of SV40 DNA into the genome can be accompanied by deletions in both viral and cellular DNA (Strayer et al., 2002, Strayer, 1999, Wallenburg et al., 1987).

In fact, the modifications of the recipient chromosomal locus and of the integrating DNA are all hallmarks of NHEJ. Point mutations, deletions, concatamer formation and rearrangements have been observed in the integrating DNA (Calos et al., 1983, Wake et al., 1984, Wilson et al., 1982). Although the integration may not change the locus at which the event took place (McFarlane & Wilson, 1996), rearrangements including deletions, duplication, insertions and translocations have been reported (Covarrubias et al., 1986, Covarrubias et al., 1987, Hamada et al., 1993, Kato et al., 1986, Mahon et al., 1988, Mark et al., 1992, Robins et al., 1981, Wilkie & Palmiter, 1987). Stem-loop and hairpin configurations of DNA at junction sites observed in this present study is in agreement with the data that had been observed during studies on wt Ad DNA integration into chromosomal DNA (Doerfler et al., 1984, Knoblauch et al., 1996), other viral DNA integration into chromosomal DNA (Bullock et al., 1984, Romani et al., 1990) and other non homologous recombination events (Krawinkel et al., 1986, Nalbantoglu et al., 1988, Nicholls et al., 1987). So, it can be stated that, as is expected, AdV DNA behaves like any other part of free DNA and the NHEJ mechanism treats it like any other part of the DNA to integrate it into the genome.

V.4.4 A small level of selectiveness during random integration by the vector DNA into the chromosomal DNA?

The study carried out revealed that the integration of HC-AdV DNA in the chromosomal DNA took place in a random manner. However four individual

integrations had occurred in a homology mediated manner, three in the Hprt fragment DNA region, and one in the c346 stuffer DNA region of the X Chr of the vector AdSLS 11. However, this is in agreement with existing data. In the experiments involving a HC-AdV with stuffer DNA from human Chr X (Wang et al., 2005) 2/23 integrations were in Chr X. Interestingly in the above paper, the clone 18/2 integrated in the CXorf6 gene in Chr X, 49 kb upstream of the integration site observed in clone 4c. However, the CXorf6 gene may not point out to any hotspot for HC-AdV integration, since the sequences correspond to the c346 cosmid sequences present in Ad SLS 11 and so it might just be coincidence that both vectors integrated independently in the same gene.

V.4.5 Integration of HC-AdV DNA into genes

An important question is whether HC-AdV integration takes place into genes. According to the latest ENSEMBL release (Aug 2006) there are 22,205 known genes in 3,253,037,807 bps in a human haploid genome and 21,839 known genes in 3,377,887,556 bps in a mouse haploid genome (for more details, visit http://www.ensembl.org/index.html). The average gene length is conserved in eukaryotes (Kiang et al., 2006) and it can be calculated that genes may account for 333,075,000 bps (1/9) of the human genome, based on the calculation that the average size of a human gene is 10-15 kb (for more details, visit http://www.ncbi.nlm.nih.gov/books/bv.fcgi?rid=hmg.table.686). The DNA of the active genes is present in the unbound form and so may be more accessible to foreign DNA. As reviewed in the introduction, retroviral, lentiviral and AAV gene transfer vectors tend to integrate in active genes. Papillomavirus, and possibly HBV tend to integrate into active genes. 43.5 % (23/46) of the HC-AdV integrations had occurred in active genes in the study conducted by (Wang et al., 2005). In contrast to this, (Ohbayashi et al., 2005) have reported that only 28 % of the 18 junction sites of the HC-AdV integrations look place in active genes. The *in vitro* data from this study agrees with the former paper; 48 % (26/61) of the integrations had taken place in genes. The *in vivo* data suggested that the rate of integration was 37.5 % (n = 8). No gene of any specific ontology was targeted. However, another 16.4 % (10/61) integrations had taken place within 30 kb of active genes. Nevertheless, it is interesting to observe that about half of the integrations took place in noncoding regions of the genome, though the active genes are present in the unbound form and

should be more accessible to the vector. In the paper by (Ohbayashi et al., 2005), 44 % (8/18) of the integrations had taken place within this frame, though only 28% had actually integrated into active genes. In contrast to the data by (Wang et al., 2005), no integrations were observed in oncogenes. The rate of integration of HC-AdV DNA into the chromosomal DNA is low compared to retroviral vectors and AAV vectors, and of those vector molecules that do integrate, only half of them integrate in genes. In other viral vector gene transfer systems in use, the rate of integration of the vector DNA into genes are much higher and the overall rate of integration of the vector DNA into the chromosomal DNA too is much higher than the rate of integration of HC-AdV vector DNA into the genome. Taken together it can be concluded that HC-AdV shows less predisposition to integrate into genes than the other vector systems currently in use. But data from more integration sites such as those published in (Wu et al., 2003) and (Mitchell et al., 2004) would be necessarybefore a dogmatic assertion can be issued about the chances of HC-AdV vector DNA integration in to genes.

Though a read-through from the transgene through the gene where the integration has taken place, as in the case of retro and lentiviral vectors is unlikely due to the presence of the poly A in the HC-AdV construct, it may still be a reason for concern. Perturbations of genome wide methylation patterns have been reported with wt AdV integration (Heller et al., 1995, Remus et al., 1999). Since promoter methylation can result in variations of gene expression (Bestor, 1998), this may have adverse results during the integration in and around active genes. The limited promoter and enhancer activity of the ITR of certain Ad types have been published (Hatfield & Hearing, 1993, Matsumoto et al., 1989, Miralles et al., 1989, Xing & Tikoo, 2005). It would be very interesting to investigate if the insertion of HC-AdV DNA at or near a gene can cause fluctuations in the gene expression.

V.5 HC-AdV DNA recombination into chromosomal DNA *in vivo*

As of date, this study furnishes the first proof of random integration and homologous recombination of HC-AdV DNA into chromosomal DNA *in vivo*. There have been publications that on injecting $5x10^9$ PFU of I^{st} gen AdV via tail vein, 14-28 copies were present per hepatocyte (Vrancken Peeters et al., 1996), and after and injection of $2x10^9$ PFU, 1-100 copies were present in the hepatocyte nuclei, with an average of 20 copies (Schowalter et al., 1997). This is contradictory with the data from this study,

where 10 copies reached the liver following an injection of $1x10^{10}$ infectious units of HC-AdV. In the papers mentioned above FISH using the vector plasmid was carried out to determine the number of vector genomes per hepatocyte, and in the present study, slot blot procedure was used to calculate the amount of vector DNA reaching the hepatocytes and this could be one of the reasons for the differences in the results. The differences in the results could also be due to the differences in the methods in which the experiments were carried out.

Every effort was made to be certain that when measuring the rate of random integration of the vector into the genome, only nodules resulting from an integration (circular, spherical shape) were counted. This may have resulted in some genuine cases of integration that did not have the "correct" shape to be discarded as a clump of Fah+ cells. It is quite possible that in some cases, the microtone had sliced off the nodule just at the top, leaving a few Fah+ve cells, that were not counted as an instance of HC-AdV integration. However, it was better to err on the side of caution and as of date, this mouse model has the best phenotype that can be used in such an investigation. The rate of random integration of HC-AdV DNA into the chromosomal DNA *in vivo* was calculated as $4x10^{-5}$ and the rate of homologous recombination of the vector DNA into the genome as $5.6x10^{-7}$. Though serial transplantion of the corrected hepatocytes resulted in sufficient expansion so as to enable the sequencing of the junction sites, the sensitivity of the experiment had to be sacrificed. More cycles of serial transplantion may finally result in single clonal repopulation of the liver, enabling the use of Southern blot experiments, but until then PCR must suffice to provide the evidence for the homologous recombination. As of date, no proof has been presented about the rate of homologous recombination of I^{st} Gen AdV *in vivo* (Ino et al., 2005), though integration of the vector has been shown (reviewed in the introduction). The limited data obtained from the junction sites suggest that the nature of integration of the HC-AdV DNA into chromosomal DNA *in vitro* is no different from that *in vivo*, with the same indifference to integration into genes, and with the introduction of mutations into the vector and chromosomal DNA. Large mutations (such as chromosomal translocations and large deletions) were not observed in the integration sites in the work done *in vitro*.

V.6 Synopsis

Taking everything in account, it is very tempting to propose that a picture is starting to emerge of HC-AdV integration into the genome. The TP might play a role in protecting the Adenoviral DNA termini and when broken DNA fragments are present, the NHEJ repair apparatus of the cell might treat the HC-AdV as any other fragment of cellular DNA and start the mechanisms ending in the integration of the vector into the genome.

Though Ad 12 has been implicated in the formation of tumours in rodents, Ad5 has not displayed any tumorigenic tendencies so far. The expression levels of of MHC class I (Nielsch et al., 1991), peptide transporter Tap-2, chaperone Tapasin, and the immunoproteosome complexes MECL-1, $PA_{28\text{-}\alpha}$, and $PA_{28\text{-}\beta}$ (Vertegaal et al., 2003) were observed to be highly suppressed in Ad 12 than in Ad 5, and this may be one of the reasons contributing to the oncogenic potential of Ad 12. In any case, the HC-AdV used in the current study is based on Ad 5 and so there is only low concern regarding the oncogenic potential with vectors based on this serotype.

So, from all of the data presented in the study, it has been demonstrated HC-AdV does not remain only as an episome, it rarely integrates *in vitro* and *in vivo* in the genome. Yet, of all the gene therapy viral vector systems that are currently available, it seems to be the safest option, seemingly unaffected by the presence of genes in the target DNA. The mutations observed during the integration are to be expected in any case of NHEJ repair of DNA, and the viral vector, by itself, does not seem to induce any of them. No evidence was observed for any preferred integration into potentially dangerous genes such as oncogenes, tumour supressors or those involved in the cell cycle. To conclude, no signs of great risks due to HC-AdV vector DNA integration into the chromosomal DNA, compared to those posed by the other viral gene transfer vector systems currently in use, were detected during this work and this thesis suggests that HC-AdV may have potential to be a safe gene transfer vector system of low mutagenicity.

VI Outlook

As of date, this work is the first instance where HC-AdV integration *in vivo* has been well characterised and has the largest number of junction sequences of HC-AdV *in vitro*. It would be very interesting to see the characteristics of HC-AdV integration in primary cell lines. The 1 moi /cell used in this study may not be feasible in real clinical gene therapy and so it would be worth examining the rates and nature of HC-AdV integration at much higher mois.

The rate of integration of the vector is not as high as that reported for other gene therapy vectors, but to establish this, it is essential to calculate the exact amounts of targeting molecules reaching the nucleus following transfection and then to compare the rates of recombination and integration following HC-AdV infection and transfection of the plasmid in the same cell line. The role of the TP in the integration could also be examined in this study.

According to the current knowledge, the HC-AdV utilises the cellular repair pathway to undergo homologous recombination or random integration into the genome. This could be further characterised and the effects of the key gene products on the rate and nature of integration can be examined.

Though the current work indicates that HC-AdV integrates without resulting in large deletions in the genomic DNA, to state dogmatically that HC-AdV integrates either with or without deletions in the genomic DNA, FISH of the cellular genome of the clones is a necessity. Maybe the future work in the field could utilize the technique.

Following a single or double rounds of serial transplantation of the transduced hepatocytes into recipient subjects, it was possible to isolate the Ad-mouse junction sites. However, the number obtained in this study was not sufficient for detailed statistical analysis of the results. So it would be interesting, from a point of clinical gene therapy, to obtain more junction sites and also try to serially transplant the FAH+ve hepatocytes for more rounds, untill the repopulation of a liver from a single integration event can be obtained.

To conclude, the advantage of the HC-AdV *viz* that it does not seem to be as predisposed as other viral vector systems to integrate into the genome is also its bane. So it would be worthwhile to develop methods of making the vector more suitable so as to make it conform to the idea of the ideal gene therapy vector: to make the vector

undergo homologous recombination at the exact location in the genome where the researcher wants it to. The knowledge in the pathways of integration and homologous recombination can be utilized for this. If the vector can be made to undergo a much higher rate of homologous recombination *in vivo*, for example, by cloning cassettes expressing those genes outside the region of homology in the vector, then it can be used in the treatment of inherited genetic diseases and indeed can come closer to becoming the ideal vector for gene therapy.

VII.1 Summary

Gene therapy trials using adenoviral vectors for gene delivery are currently underway. A clinical trial based on retrovirus-mediated gene transfer resulted in the development of leukaemia in some of the subjects due to insertional mutagenesis. This experience highlights the importance of an evaluation of the biosafety of gene transfer vectors prior to their use in humans. The overall aim of this research was to quantitatively and qualitatively analyse recombination between vector DNA and chromosomal DNA *in vitro* and *in vivo* following HC-Ad vector-mediated gene transfer.

To study the rates, at which HC-AdV DNA underwent homologous recombination with chromosomal DNA following gene transfer *in vitro*, the Hprt model, a classical system in recombination studies, was utilized. A vector was designed to target exon 2 of the human Hprt gene by introducing a stop codon upon homologous recombination. In these experiments, which were performed in primary cells and in established cell lines, the frequency of homologous recombination of the HC-AdV DNA with the HPRT locus was found to be, depending on the cell type, between $2x10^{-5}$ to $1.2x10^{-6}$. In a different set of experiments and using a selection marker strategy, the rate at which HC-AdV DNA integrated randomly into the chromosomal DNA was determined to be between $5.4x10^{-3}$ to $1.1x10^{-4}$.

To more closely mimic the situation following therapeutic gene transfer, *in vivo* experiments were performed. The use of the $Fah^{\Delta exon\ 5}$ knockout model allowed to study homologous and heterologous recombination events following *in vivo* gene transfer to the liver. Correction of the pathological phenotype was achieved either by targeting exon 5 with an HC-AdV carrying a 12.3 kb targeting sequence (homologous recombination) or by measuring integration frequencies following gene transfer with an HC-AdV expressing the FAH cDNA (heterologous recombination). The targeting frequency of exon 5 was estimated to be $5.6x10^{-7}$, and the rate of random integration was found to be $4x10^{-5}$. This study is the first to document evidence of recombination between HC-AdV DNA and chromosomal DNA *in vivo*.

The analysis of the vector integrates following transduction of primary cells and cell lines indicated that HC-AdV DNA integrated as an intact molecule and via the termini in most cases. About half of the vector DNA integrations took place inside genes and none were observed in protooncogenes. Analysis of the junction sequences suggested that the HC-AdV DNA had integrated in a random manner throughout the genome

without an obvious preference for any particular chromosomal regions. Patchy homologies between the vector termini and the chromosomal DNA were observed at the site of integration. Though the majority of the integrations had occurred without causing any mutations in the chromosomal DNA, cases of substitutions and insertions of nucleotides too were observed. This study has established quantitative data on *in vitro* and *in vivo* recombination frequencies of adenoviral vector DNA with genomic DNA and has provided a molecular characterization of observed integration events. These results may contribute to a risk-benefit assessment of adenovirus-mediated gene transfer.

VII.2 Zusammenfassung

Gentherapieversuche mit adenoviralen Vektoren befinden sich zurzeit in der klinischen Testphase. Nach Retrovirus-vermitteltem Gentransfer kam es bei einigen Probanden durch Insertionsmutagenese zur Entstehung von Leukämien. Diese Erfahrung unterstreicht die Bedeutung präklinischer Untersuchungen zur biologischen Sicherheit von Gentransfervektoren. Zielsetzung der vorliegenden Arbeit war die quantitative und qualitative Analyse von Rekombinationsereignissen zwischen Vektor und chromosomaler DNA *in vitro* und *in vivo* nach HC-Ad Vektor-vermitteltem Gentransfer.

Zur Bestimmung der Häufigkeit homologer Rekombination zwischen HC-Ad Vektor DNA und chromosomaler DNA wurde das häufig in Rekombinationsstudien eingesetzte HPRT-Selektionsmodell verwendet. Ein adenoviraler Vektor wurde konstruiert, der das menschliche HPRT Gen durch Einführung eines Stop Codons in Exon 2 mittels homologer Rekombination inaktivierte. In primären Zellen und in etablierten Zellenlinien wurden zelltypabhängig Häufigkeiten homologer Rekombination zwischen $2x10^{-5}$ bis zu $1,2x10^{-6}$ ermittelt. Die Frequenz zufälliger Integrationsereignisse wurde durch HC-Ad Vektor-vermittelte Zelltransduktion unter Verwendung eines Selektionsmarkers ermittelt und lag innerhalb eines Bereiches von $5,4x10^{-3}$ und $1,1x10^{-4}$.

Zur besseren Nachahmung der klinischen Situation wurden *in vivo* Experimente in der Labormaus durchgeführt. Die Verwendung des $Fah^{\Delta exon\ 5}$ Modells erlaubte die Untersuchung homologer und heterologer Rekombinationsereignisse nach *in vivo* Lebergentransfer. Die Korrektur des pathologischen Phenotyps wurde erreicht entweder durch das Targeting von Exon 5 mit einem HC-Ad Vektor, der eine 12.3 kb Targetingsequenz trug (homologe Rekombination) oder durch Bestimmung der Integrationshäufigkeit nach Gentransfer mit einem die FAH cDNA exprimierenden HC-Ad Vektor (heterologe Rekombination). Die Targetinghäufigkeit des Exon 5 wurde mit $4,6x10^{-7}$ bestimmt, die Häufigkeit der zufälligen Integration mit $4x10^{-5}$. Dies ist die erste Untersuchung, die *in vivo* Rekombination zwischen HC-Ad Vektor DNA und chromosomaler DNA dokumentiert.

Analyse der Vektorintegrate nach Transduktion von primären Zellen und von Zelllinien ergab, dass in den meisten Fällen die HC Ad-Vektor DNA als intaktes Molekül und über die viralen Enden integrierte. Ungefähr die Hälfte der

Integrationsereignisse fand innerhalb von Genen statt. Keine Integration wurde in Protoonkogenen beobachtet. Die Analyse der Junktionssequenzen ergab, dass die HC-Ad Vektor DNA zufällig im Genom integrierte und ohne offensichtliche Präferenz für bestimme chromosomale Regionen. Am Ort der Integration wurden häufig Mikrohomologien zwischen den Vektorenden und der chromosomalen DNA beobachtet. Obwohl die meisten Integrationen nicht zu Mutationen in der chromosomalen DNA führten, wurden einige Fälle von Nukleotidsubstitutionen und Insertionen beobachtet.

In dieser Untersuchung wurden quantitative Daten bezüglich der Häufigkeit von *in vitro* und *in vivo* Rekombination zwischen adenoviraler Vektor DNA und genomischer DNA erhoben und die Integrationsereignisse wurden auf molekularer Ebene charakterisiert. Diese Ergebnisse tragen zu einer Risiko-Nutzen Abwägung nach Adenovirus-vermitteltem Gentransfer bei.

VIII Erklärung

Ich versichere, daß ich die von mir vorgelegte Dissertation selbständig angefertigt, die benutzen Quellen und Hilfsmittel vollständig angegeben und die Stellen der Arbeit- einschließlich Tabellen, Karten und Abbildungen-, die anderen Werken in Wortlaut oder dem Sinn nach entnommen sind, in jeden Einzelfall als Entlehnung kenntlich gemacht habe; daß diese Dissertation noch keiner anderen Fakultät oder Universität zur Prüfung vorgelegen hat; daß sie- abgesehen von unten angegebenen Teilpublikationen- noch nicht veröffentlicht worden ist sowie, daß ich eine solche Veröffentlichung vor Abschluß des Promotionverfahrens nicht vornehmen werde.
Die Bestimmungen dieser Promotionsordnung sind mir bekannt. Die von mir vorgelegte Dissertation wurde von Herrn Prof. Dr. S. Kochanek betreut.

Teil publikationen:

Ich versichere, daß ich alle Angabenm wahrheitsgemäß nach bestem Wissen und Gewissen gemacht habe und verpflichte mich, jedmögliche, die obigen Angaben betreffenden Veränderungen, dem Dekanat unverzüglich mitzuteilen

30.10.06 Sam Laurel Stephen

IX.1 Curriculum Vitae

Sam Laurel Stephen
AG Prof. Dr. S. Kochanek
Center for Molecular Medicine
University of Cologne
50931 Cologne

Nationality: Indian

06.09.1975: Born in Trivandrum, India

1985-1991: Secondary School Leaving Certificate Examination, conducted by the Government of Kerala, taken from Christ Nagar English Secondary School, Trivandrum, India.

1991-1993: Pre Degree Course Examination, conducted by the University of Kerala, taken from Government Arts College, Trivandrum, India.

1993-1996: Bachelor of Science Degree Examination in Zoology, conducted by the University of Kerala, taken from the University College, Trivandrum.

1996-1997: Master of Science Degree Examination in Integrative Biosciences, conducted by the University of Oxford, taken from Pembroke College, Oxford, U.K.

1998-2004: Ph.D. Student under the supervision of Prof. Dr. S. Kochanek, at the Faculty of Mathematics and Natural Sciences, Center for Molecular Medicine, University of Cologne.

IX.2 Lebenslauf

Sam Laurel Stephen
AG Prof. Dr. S. Kochanek
Zentrum für Molekulare Medizin
Universität zu Köln
50931 Köln
Staatsangehörigkeit: Indisch

06.09.1975: Geboren in Trivandrum, Indien

1985-1991: Abschlussprüfung, durch die Regierung von Kerala, an der Christ Nagar Englischen Sekundarschule, Trivandrum, Indien.

1991-1993: Pre Degree Course Prüfung, durch die Universität von Kerala, Govt. Arts. College, Trivandrum, Indien.

1993-1996: Bachelor of Science Prüfung, durch die Universität von Kerala, University College, Trivandrum, Trivandrum, Indien.

1996-1997: Master of Science Degree Prüfung, durch die Universität von Oxford, Pembroke College, Oxford, U. K.

1998-2004: Doktorand unter der Betretung von Prof. Dr. S. Kochanek, Fakultät für Mathematik und Naturwissenschaften, am Zentrum für Molekulare Medizin, Universität zu Köln

X References

Agarwal, R., Shukla, S. K., Dharmani, S. & Gandhi, A. (2004). Biological warfare--an emerging threat. *J Assoc Physicians India* **52**, 733-8.

Agrawal, R., Pelkonen, J., Rytkonen, M. & Mantyjarvi, R. A. (1992). Integration of bovine papillomavirus type 1 DNA and analysis of the amplified virus-cell junctions in transformed primary mouse fibroblasts. *J Gen Virol* **73 (Pt 1)**, 201-6.

Al-Dhalimy, M., Overturf, K., Finegold, M. & Grompe, M. (2002). Long-term therapy with NTBC and tyrosine-restricted diet in a murine model of hereditary tyrosinemia type I. *Mol Genet Metab* **75**, 38-45.

Alba, R., Bosch, A. & Chillon, M. (2005). Gutless adenovirus: last-generation adenovirus for gene therapy. *Gene Ther* **12 Suppl 1**, S18-27.

Amtmann, E., Muller, H. & Sauer, G. (1980). Equine connective tissue tumors contain unintegrated bovine papilloma virus DNA. *J Virol* **35**, 962-4.

Anderson, W. F. (1992). Human gene therapy. *Science* **256**, 808-13.

Anderson, W. F. (2000). Gene therapy. The best of times, the worst of times. *Science* **288**, 627-9.

Armentano, D., Sookdeo, C. C., Hehir, K. M., Gregory, R. J., St George, J. A., Prince, G. A., Wadsworth, S. C. & Smith, A. E. (1995). Characterization of an adenovirus gene transfer vector containing an E4 deletion. *Hum Gene Ther* **6**, 1343-53.

Bakowska, J. C., Di Maria, M. V., Camp, S. M., Wang, Y., Allen, P. D. & Breakefield, X. O. (2003). Targeted transgene integration into transgenic mouse fibroblasts carrying the full-length human AAVS1 locus mediated by HSV/AAV rep(+) hybrid amplicon vector. *Gene Ther* **10**, 1691-702.

Basu, U. & Banerjee, S. (2004). An engineered EBV vector expressing human factor VIII and von Willebrand factor in cultured B-cells. *J Gene Med* **6**, 760-8.

Bergelson, J. M., Cunningham, J. A., Droguett, G., Kurt-Jones, E. A., Krithivas, A., Hong, J. S., Horwitz, M. S., Crowell, R. L. & Finberg, R. W. (1997). Isolation of a common receptor for Coxsackie B viruses and adenoviruses 2 and 5. *Science* **275**, 1320-3.

Bestor, T. H. (1998). The host defence function of genomic methylation patterns. *Novartis Found Symp* **214**, 187-95; discussion 195-9, 228-32.

Bett, A. J., Prevec, L. & Graham, F. L. (1993). Packaging capacity and stability of human adenovirus type 5 vectors. *J Virol* **67**, 5911-21.

Bill, C. A. & Summers, J. (2004). Genomic DNA double-strand breaks are targets for hepadnaviral DNA integration. *Proc Natl Acad Sci U S A* **101**, 11135-40.

Bossin, H., Fournier, P., Royer, C., Barry, P., Cerutti, P., Gimenez, S., Couble, P. & Bergoin, M. (2003). Junonia coenia densovirus-based vectors for stable transgene expression in Sf9 cells: influence of the densovirus sequences on genomic integration. *J Virol* **77**, 11060-71.

Branda, C. S. & Dymecki, S. M. (2004). Talking about a revolution: The impact of site-specific recombinases on genetic analyses in mice. *Dev Cell* **6**, 7-28.

Brown, G. R., Thiele, D. L., Silva, M. & Beutler, B. (1997). Adenoviral vectors given intravenously to immunocompromised mice yield stable transduction of the colonic epithelium. *Gastroenterology* **112**, 1586-94.

Brunetti-Pierri, N., Ng, T., Iannitti, D. A., Palmer, D. J., Beaudet, A. L., Finegold, M. J., Carey, K. D., Cioffi, W. G. & Ng, P. (2006). Improved hepatic transduction, reduced systemic vector dissemination, and long-term transgene

expression by delivering helper-dependent adenoviral vectors into the surgically isolated liver of nonhuman primates. *Hum Gene Ther* **17**, 391-404.
Brunetti-Pierri, N., Nichols, T. C., McCorquodale, S., Merricks, E., Palmer, D. J., Beaudet, A. L. & Ng, P. (2005). Sustained phenotypic correction of canine hemophilia B after systemic administration of helper-dependent adenoviral vector. *Hum Gene Ther* **16**, 811-20.
Brunetti-Pierri, N., Palmer, D. J., Beaudet, A. L., Carey, K. D., Finegold, M. & Ng, P. (2004). Acute toxicity after high-dose systemic injection of helper-dependent adenoviral vectors into nonhuman primates. *Hum Gene Ther* **15**, 35-46.
Bullock, P., Forrester, W. & Botchan, M. (1984). DNA sequence studies of simian virus 40 chromosomal excision and integration in rat cells. *J Mol Biol* **174**, 55-84.
Burnett, R. M. (1985). The structure of the adenovirus capsid. II. The packing symmetry of hexon and its implications for viral architecture. *J Mol Biol* **185**, 125-43.
Bushman, F. D. (2003). Targeting survival: integration site selection by retroviruses and LTR-retrotransposons. *Cell* **115**, 135-8.
Cabanas, M. J., Vazquez, D. & Modolell, J. (1978). Dual interference of hygromycin B with ribosomal translocation and with aminoacyl-tRNA recognition. *Eur J Biochem* **87**, 21-7.
Calos, M. P., Lebkowski, J. S. & Botchan, M. R. (1983). High mutation frequency in DNA transfected into mammalian cells. *Proc Natl Acad Sci U S A* **80**, 3015-9.
Campbell, S. A. & Gromeier, M. (2005). Oncolytic viruses for cancer therapy I. Cell-external factors: virus entry and receptor interaction. *Onkologie* **28**, 144-9.
Capecchi, M. R. (1989). Altering the genome by homologous recombination. *Science* **244**, 1288-92.
Caporale, L. (2002). Darwin In the Genome: Molecular Strategies in Biological Evolution MacGrawHill companies.
Carson, S. D., Hobbs, J. T., Tracy, S. M. & Chapman, N. M. (1999). Expression of the coxsackievirus and adenovirus receptor in cultured human umbilical vein endothelial cells: regulation in response to cell density. *J Virol* **73**, 7077-9.
Caskey, C. T. & Stout, J. T. (1989). Molecular genetics of HPRT deficiency. *Semin Nephrol* **9**, 162-7.
Chambers, G., Ellsmore, V. A., O'Brien, P. M., Reid, S. W., Love, S., Campo, M. S. & Nasir, L. (2003). Association of bovine papillomavirus with the equine sarcoid. *J Gen Virol* **84**, 1055-62.
Chang, Y., Cheng, S. D. & Tsai, C. H. (2002). Chromosomal integration of Epstein-Barr virus genomes in nasopharyngeal carcinoma cells. *Head Neck* **24**, 143-50.
Chen, T. R. (1978). Evolution in vitro of stemlines with minimal karyotypic deviations in a human heteroploid cell line. *J Natl Cancer Inst* **61**, 277-84.
Chen, T. R. (1983). Chromosome changes in 6-TG-resistant mutant strains derived from a karyotypically stable human line, C32. *Cytogenet Cell Genet* **35**, 181-9.
Chen, T. R. & Shaw, M. W. (1973). Stable chromosome changes in human malignant melanoma. *Cancer Res* **33**, 2042-7.
Chiu, C. Y., Mathias, P., Nemerow, G. R. & Stewart, P. L. (1999). Structure of adenovirus complexed with its internalization receptor, alphavbeta5 integrin. *J Virol* **73**, 6759-68.

Christ, M., Lusky, M., Stoeckel, F., Dreyer, D., Dieterle, A., Michou, A. I., Pavirani, A. & Mehtali, M. (1997). Gene therapy with recombinant adenovirus vectors: evaluation of the host immune response. *Immunol Lett* **57**, 19-25.

Clemens, P. R., Kochanek, S., Sunada, Y., Chan, S., Chen, H. H., Campbell, K. P. & Caskey, C. T. (1996). In vivo muscle gene transfer of full-length dystrophin with an adenoviral vector that lacks all viral genes. *Gene Ther* **3**, 965-72.

Colbere-Garapin, F., Ryhiner, M. L., Stephany, I., Kourilsky, P. & Garapin, A. C. (1986). Patterns of integration of exogenous DNA sequences transfected into mammalian cells of primate and rodent origin. *Gene* **50**, 279-88.

Covarrubias, L., Nishida, Y. & Mintz, B. (1986). Early postimplantation embryo lethality due to DNA rearrangements in a transgenic mouse strain. *Proc Natl Acad Sci U S A* **83**, 6020-4.

Covarrubias, L., Nishida, Y., Terao, M., D'Eustachio, P. & Mintz, B. (1987). Cellular DNA rearrangements and early developmental arrest caused by DNA insertion in transgenic mouse embryos. *Mol Cell Biol* **7**, 2243-7.

Davidson, B. L., Tarle, S. A., Palella, T. D. & Kelley, W. N. (1989). Molecular basis of hypoxanthine-guanine phosphoribosyltransferase deficiency in ten subjects determined by direct sequencing of amplified transcripts. *J Clin Invest* **84**, 342-6.

Davison, A. J., Benko, M. & Harrach, B. (2003). Genetic content and evolution of adenoviruses. *J Gen Virol* **84**, 2895-908.

de Jong, R. N., Meijer, L. A. & van der Vliet, P. C. (2003). DNA binding properties of the adenovirus DNA replication priming protein pTP. *Nucleic Acids Res* **31**, 3274-86.

de Jong, R. N. & van der Vliet, P. C. (1999). Mechanism of DNA replication in eukaryotic cells: cellular host factors stimulating adenovirus DNA replication. *Gene* **236**, 1-12.

Debiec-Rychter, M., Croes, R., De Vos, R., Marynen, P., Roskams, T., Hagemeijer, A., Lombaerts, R. & Sciot, R. (2003). Complex genomic rearrangement of ALK loci associated with integrated human Epstein-Barr virus in a post-transplant myogenic liver tumor. *Am J Pathol* **163**, 913-22.

Dechecchi, M. C., Tamanini, A., Bonizzato, A. & Cabrini, G. (2000). Heparan sulfate glycosaminoglycans are involved in adenovirus type 5 and 2-host cell interactions. *Virology* **268**, 382-90.

Deng, C. & Capecchi, M. R. (1992). Reexamination of gene targeting frequency as a function of the extent of homology between the targeting vector and the target locus. *Mol Cell Biol* **12**, 3365-71.

Devon, R. S., Porteous, D. J. & Brookes, A. J. (1995). Splinkerettes--improved vectorettes for greater efficiency in PCR walking. *Nucleic Acids Res* **23**, 1644-5.

Doerfler, W. (1968). The fate of the DNA of adenovirus type 12 in baby hamster kidney cells. *Proc Natl Acad Sci U S A* **60**, 636-43.

Doerfler, W. (1970). Integration of the deoxyribonucleic acid of adenovirus type 12 into the deoxyribonucleic acid of baby hamster kidney cells. *J Virol* **6**, 652-66.

Doerfler, W., Burger, H., Ortin, J., Fanning, E., Brown, D. T., Mestphal, M., Winterhoff, U., Weiser, B. & Schick, J. (1975). Integration of adenovirus DNA into the cellular genome. *Cold Spring Harb Symp Quant Biol* **39 Pt 1**, 505-21.

Doerfler, W., Gahlmann, R., Stabel, S., Deuring, R., Lichtenberg, U., Schulz, M., Eick, D. & Leisten, R. (1984). On the mechanism of recombination between

adenoviral and cellular DNAs: the structure of junction sites. *Curr Top Microbiol Immunol* **109**, 193-228.

Doerfler, W., Jessberger, R. & Lichtenberg, U. (1989). Recombination between adenovirus DNA and the mammalian genome. *Curr Top Microbiol Immunol* **144**, 209-16.

Doetschman, T., Gregg, R. G., Maeda, N., Hooper, M. L., Melton, D. W., Thompson, S. & Smithies, O. (1987). Targetted correction of a mutant HPRT gene in mouse embryonic stem cells. *Nature* **330**, 576-8.

Doronin, K., Toth, K., Kuppuswamy, M., Krajcsi, P., Tollefson, A. E. & Wold, W. S. (2003). Overexpression of the ADP (E3-11.6K) protein increases cell lysis and spread of adenovirus. *Virology* **305**, 378-87.

Edelstein, M. L., Abedi, M. R., Wixon, J. & Edelstein, R. M. (2004). Gene therapy clinical trials worldwide 1989-2004-an overview. *J Gene Med* **6**, 597-602.

Effros, R. B. (2004). Impact of the Hayflick Limit on T cell responses to infection: lessons from aging and HIV disease. *Mech Ageing Dev* **125**, 103-6.

Elbrecht, A., DeMayo, F. J., Tsai, M. J. & O'Malley, B. W. (1987). Episomal maintenance of a bovine papilloma virus vector in transgenic mice. *Mol Cell Biol* **7**, 1276-9.

Endo, F. & Sun, M. S. (2002). Tyrosinaemia type I and apoptosis of hepatocytes and renal tubular cells. *J Inherit Metab Dis* **25**, 227-34.

Engelhardt, J. F., Ye, X., Doranz, B. & Wilson, J. M. (1994). Ablation of E2A in recombinant adenoviruses improves transgene persistence and decreases inflammatory response in mouse liver. *Proc Natl Acad Sci U S A* **91**, 6196-200.

Evans, J. D., Hearing, P (2002). Adenovirus Replication, pp. 39-64. Edited by D. T. Curiel, Douglas, J.T.: Academic.

Fanning, E. & Doerfler, W. (1976). Intracellular forms of adenovirus DNA. V. Viral DNA sequences in hamster cells abortively infected and transformed with human adenovirus type 12. *J Virol* **20**, 373-83.

Fechner, H., Noutsias, M., Tschoepe, C., Hinze, K., Wang, X., Escher, F., Pauschinger, M., Dekkers, D., Vetter, R., Paul, M., Lamers, J., Schultheiss, H. P. & Poller, W. (2003). Induction of coxsackievirus-adenovirus-receptor expression during myocardial tissue formation and remodeling: identification of a cell-to-cell contact-dependent regulatory mechanism. *Circulation* **107**, 876-82.

Fechteler, K., Tatzelt, J., Huppertz, S., Wilgenbus, P. & Doerfler, W. (1995). The mechanism of adenovirus DNA integration: studies in a cell-free system. *Curr Top Microbiol Immunol* **199 (Pt 2)**, 109-37.

Ferber, M. J., Montoya, D. P., Yu, C., Aderca, I., McGee, A., Thorland, E. C., Nagorney, D. M., Gostout, B. S., Burgart, L. J., Boix, L., Bruix, J., McMahon, B. J., Cheung, T. H., Chung, T. K., Wong, Y. F., Smith, D. I. & Roberts, L. R. (2003a). Integrations of the hepatitis B virus (HBV) and human papillomavirus (HPV) into the human telomerase reverse transcriptase (hTERT) gene in liver and cervical cancers. *Oncogene* **22**, 3813-20.

Ferber, M. J., Thorland, E. C., Brink, A. A., Rapp, A. K., Phillips, L. A., McGovern, R., Gostout, B. S., Cheung, T. H., Chung, T. K., Fu, W. Y. & Smith, D. I. (2003b). Preferential integration of human papillomavirus type 18 near the c-myc locus in cervical carcinoma. *Oncogene* **22**, 7233-42.

Fischer, A., Abina, S. H., Thrasher, A., von Kalle, C. & Cavazzana-Calvo, M. (2004). LMO2 and gene therapy for severe combined immunodeficiency. *N Engl J Med* **350**, 2526-7; author reply 2526-7.

Fisher, K. J., Choi, H., Burda, J., Chen, S. J. & Wilson, J. M. (1996). Recombinant adenovirus deleted of all viral genes for gene therapy of cystic fibrosis. *Virology* **217**, 11-22.

Fisher, P. B., Babiss, L. E., Weinstein, I. B. & Ginsberg, H. S. (1982). Analysis of type 5 adenovirus transformation with a cloned rat embryo cell line (CREF). *Proc Natl Acad Sci U S A* **79**, 3527-31.

Fujinaga, K., Sekikawa, K., Yamazaki, H. & Green, M. (1975). Analysis of multiple viral genome fragments in adenovirus 7-transformed hamster cells. *Cold Spring Harb Symp Quant Biol* **39 Pt 1**, 633-6.

Fujita, A., Sakagami, K., Kanegae, Y., Saito, I. & Kobayashi, I. (1995). Gene targeting with a replication-defective adenovirus vector. *J Virol* **69**, 6180-90.

Gahlmann, R. & Doerfler, W. (1983). Integration of viral DNA into the genome of the adenovirus type 2-transformed hamster cell line HE5 without loss or alteration of cellular nucleotides. *Nucleic Acids Res* **11**, 7347-61.

Ganoza, M. C. & Kiel, M. C. (2001). A ribosomal ATPase is a target for hygromycin B inhibition on Escherichia coli ribosomes. *Antimicrob Agents Chemother* **45**, 2813-9.

Gao, G. P., Yang, Y. & Wilson, J. M. (1996). Biology of adenovirus vectors with E1 and E4 deletions for liver-directed gene therapy. *J Virol* **70**, 8934-43.

Garnoff A, W. R. (1999). Encyclopedia of Virology, Second edn: Academic Press.

Gilles, C., Piette, J., Ploton, D., Doco-Fenzy, M. & Foidart, J. M. (1996). Viral integration sites in human papilloma virus-33-immortalized cervical keratinocyte cell lines. *Cancer Genet Cytogenet* **90**, 63-9.

Glorioso, J. C. & Fink, D. J. (2004). Herpes vector-mediated gene transfer in treatment of diseases of the nervous system. *Annu Rev Microbiol* **58**, 253-71.

Glover, D. J., Lipps, H. J. & Jans, D. A. (2005). Towards safe, non-viral therapeutic gene expression in humans. *Nat Rev Genet* **6**, 299-310.

Gluecksohn-Waelsch, S. (1979). Genetic control of morphogenetic and biochemical differentiation: lethal albino deletions in the mouse. *Cell* **16**, 225-37.

Goldman, M. J. & Wilson, J. M. (1995). Expression of alpha v beta 5 integrin is necessary for efficient adenovirus-mediated gene transfer in the human airway. *J Virol* **69**, 5951-8.

Grable, M. & Hearing, P. (1990). Adenovirus type 5 packaging domain is composed of a repeated element that is functionally redundant. *J Virol* **64**, 2047-56.

Grable, M. & Hearing, P. (1992). cis and trans requirements for the selective packaging of adenovirus type 5 DNA. *J Virol* **66**, 723-31.

Graham, F. L., Smiley, J., Russell, W. C. & Nairn, R. (1977). Characteristics of a human cell line transformed by DNA from human adenovirus type 5. *J Gen Virol* **36**, 59-74.

Greber, U. F. (1998). Virus assembly and disassembly: the adenovirus cysteine protease as a trigger factor. *Rev Med Virol* **8**, 213-222.

Greber, U. F., Suomalainen, M., Stidwill, R. P., Boucke, K., Ebersold, M. W. & Helenius, A. (1997). The role of the nuclear pore complex in adenovirus DNA entry. *Embo J* **16**, 5998-6007.

Greber, U. F., Webster, P., Weber, J. & Helenius, A. (1996). The role of the adenovirus protease on virus entry into cells. *Embo J* **15**, 1766-77.

Greber, U. F., Willetts, M., Webster, P. & Helenius, A. (1993). Stepwise dismantling of adenovirus 2 during entry into cells. *Cell* **75**, 477-86.

Griesenbach, U., Geddes, D. M. & Alton, E. W. (2004). Advances in cystic fibrosis gene therapy. *Curr Opin Pulm Med* **10**, 542-6.

Gritz, L. & Davies, J. (1983). Plasmid-encoded hygromycin B resistance: the sequence of hygromycin B phosphotransferase gene and its expression in Escherichia coli and Saccharomyces cerevisiae. *Gene* **25**, 179-88.

Grompe, M., al-Dhalimy, M., Finegold, M., Ou, C. N., Burlingame, T., Kennaway, N. G. & Soriano, P. (1993). Loss of fumarylacetoacetate hydrolase is responsible for the neonatal hepatic dysfunction phenotype of lethal albino mice. *Genes Dev* **7**, 2298-307.

Grompe, M., Lindstedt, S., al-Dhalimy, M., Kennaway, N. G., Papaconstantinou, J., Torres-Ramos, C. A., Ou, C. N. & Finegold, M. (1995). Pharmacological correction of neonatal lethal hepatic dysfunction in a murine model of hereditary tyrosinaemia type I. *Nat Genet* **10**, 453-60.

Grompe, M., Overturf, K., al-Dhalimy, M. & Finegold, M. (1998). Therapeutic trials in the murine model of hereditary tyrosinaemia type I: a progress report. *J Inherit Metab Dis* **21**, 518-31.

Haber, J. E. (1999). DNA repair. Gatekeepers of recombination. *Nature* **398**, 665, 667.

Hacein-Bey-Abina, S., von Kalle, C., Schmidt, M., Le Deist, F., Wulffraat, N., McIntyre, E., Radford, I., Villeval, J. L., Fraser, C. C., Cavazzana-Calvo, M. & Fischer, A. (2003a). A serious adverse event after successful gene therapy for X-linked severe combined immunodeficiency. *N Engl J Med* **348**, 255-6.

Hacein-Bey-Abina, S., Von Kalle, C., Schmidt, M., McCormack, M. P., Wulffraat, N., Leboulch, P., Lim, A., Osborne, C. S., Pawliuk, R., Morillon, E., Sorensen, R., Forster, A., Fraser, P., Cohen, J. I., de Saint Basile, G., Alexander, I., Wintergerst, U., Frebourg, T., Aurias, A., Stoppa-Lyonnet, D., Romana, S., Radford-Weiss, I., Gross, F., Valensi, F., Delabesse, E., Macintyre, E., Sigaux, F., Soulier, J., Leiva, L. E., Wissler, M., Prinz, C., Rabbitts, T. H., Le Deist, F., Fischer, A. & Cavazzana-Calvo, M. (2003b). LMO2-associated clonal T cell proliferation in two patients after gene therapy for SCID-X1. *Science* **302**, 415-9.

Hamada, T., Sasaki, H., Seki, R. & Sakaki, Y. (1993). Mechanism of chromosomal integration of transgenes in microinjected mouse eggs: sequence analysis of genome-transgene and transgene-transgene junctions at two loci. *Gene* **128**, 197-202.

Hanson, C. & Caisander, G. (2005). Human embryonic stem cells and chromosome stability. *Apmis* **113**, 751-5.

Hartigan-O'Connor, D., Barjot, C., Crawford, R. & Chamberlain, J. S. (2002). Efficient rescue of gutted adenovirus genomes allows rapid production of concentrated stocks without negative selection. *Hum Gene Ther* **13**, 519-31.

Harui, A., Suzuki, S., Kochanek, S. & Mitani, K. (1999). Frequency and stability of chromosomal integration of adenovirus vectors. *J Virol* **73**, 6141-6.

Hasty, P., Rivera-Perez, J. & Bradley, A. (1991). The length of homology required for gene targeting in embryonic stem cells. *Mol Cell Biol* **11**, 5586-91.

Hatfield, L. & Hearing, P. (1993). The NFIII/OCT-1 binding site stimulates adenovirus DNA replication in vivo and is functionally redundant with adjacent sequences. *J Virol* **67**, 3931-9.

Hausner, T. P., Geigenmuller, U. & Nierhaus, K. H. (1988). The allosteric three-site model for the ribosomal elongation cycle. New insights into the inhibition mechanisms of aminoglycosides, thiostrepton, and viomycin. *J Biol Chem* **263**, 13103-11.

Hay, R. T., Freeman, A., Leith, I., Monaghan, A. & Webster, A. (1995). Molecular interactions during adenovirus DNA replication. *Curr Top Microbiol Immunol* **199 (Pt 2)**, 31-48.

Hefferin, M. L. & Tomkinson, A. E. (2005). Mechanism of DNA double-strand break repair by non-homologous end joining. *DNA Repair (Amst)* **4**, 639-48.

Heilker, R., Spiess, M. & Crottet, P. (1999). Recognition of sorting signals by clathrin adaptors. *Bioessays* **21**, 558-67.

Hellebrand, E., Mautner, J., Reisbach, G., Nimmerjahn, F., Hallek, M., Mocikat, R. & Hammerschmidt, W. (2006). Epstein-Barr virus vector-mediated gene transfer into human B cells: potential for antitumor vaccination. *Gene Ther* **13**, 150-62.

Helleday, T. (2003). Pathways for mitotic homologous recombination in mammalian cells. *Mutat Res* **532**, 103-15.

Heller, H., Kammer, C., Wilgenbus, P. & Doerfler, W. (1995). Chromosomal insertion of foreign (adenovirus type 12, plasmid, or bacteriophage lambda) DNA is associated with enhanced methylation of cellular DNA segments. *Proc Natl Acad Sci U S A* **92**, 5515-9.

Hematti, P., Hong, B. K., Ferguson, C., Adler, R., Hanawa, H., Sellers, S., Holt, I. E., Eckfeldt, C. E., Sharma, Y., Schmidt, M., von Kalle, C., Persons, D. A., Billings, E. M., Verfaillie, C. M., Nienhuis, A. W., Wolfsberg, T. G., Dunbar, C. E. & Calmels, B. (2004). Distinct genomic integration of MLV and SIV vectors in primate hematopoietic stem and progenitor cells. *PLoS Biol* **2**, e423.

Hendrie, P. C., Hirata, R. K. & Russell, D. W. (2003). Chromosomal integration and homologous gene targeting by replication-incompetent vectors based on the autonomous parvovirus minute virus of mice. *J Virol* **77**, 13136-45.

Henry, L. J., Xia, D., Wilke, M. E., Deisenhofer, J. & Gerard, R. D. (1994). Characterization of the knob domain of the adenovirus type 5 fiber protein expressed in Escherichia coli. *J Virol* **68**, 5239-46.

Hidaka, C., Milano, E., Leopold, P. L., Bergelson, J. M., Hackett, N. R., Finberg, R. W., Wickham, T. J., Kovesdi, I., Roelvink, P. & Crystal, R. G. (1999). CAR-dependent and CAR-independent pathways of adenovirus vector-mediated gene transfer and expression in human fibroblasts. *J Clin Invest* **103**, 579-87.

Hilleman, M. R. & Werner, J. H. (1954). Recovery of new agent from patients with acute respiratory illness. *Proc Soc Exp Biol Med* **85**, 183-8.

Hillgenberg, M., Tonnies, H. & Strauss, M. (2001). Chromosomal integration pattern of a helper-dependent minimal adenovirus vector with a selectable marker inserted into a 27.4-kilobase genomic stuffer. *J Virol* **75**, 9896-908.

Hirata, R., Chamberlain, J., Dong, R. & Russell, D. W. (2002). Targeted transgene insertion into human chromosomes by adeno-associated virus vectors. *Nat Biotechnol* **20**, 735-8.

Hoeijmakers, J. H., Odijk, H. & Westerveld, A. (1987). Differences between rodent and human cell lines in the amount of integrated DNA after transfection. *Exp Cell Res* **169**, 111-9.

Hoglund, M., Siden, T. & Rohme, D. (1992). Different pathways for chromosomal integration of transfected circular pSVneo plasmids in normal and established rodent cells. *Gene* **116**, 215-22.

Hohlweg, U., Dorn, A., Hosel, M., Webb, D., Buettner, R. & Doerfler, W. (2004). Tumorigenesis by adenovirus type 12 in newborn Syrian hamsters. *Curr Top Microbiol Immunol* **273**, 215-44.

Hollanderova, D., Raslova, H., Blangy, D., Forstova, J. & Berebbi, M. (2003). Interference of mouse polyomavirus with the c-myc gene and its product in mouse mammary adenocarcinomas. *Int J Oncol* **23**, 333-41.

Holme, E. & Lindstedt, S. (1998). Tyrosinaemia type I and NTBC (2-(2-nitro-4-trifluoromethylbenzoyl)-1,3-cyclohexanedione). *J Inherit Metab Dis* **21**, 507-17.

Hong, S. S. & Boulanger, P. (1995). Protein ligands of the human adenovirus type 2 outer capsid identified by biopanning of a phage-displayed peptide library on separate domains of wild-type and mutant penton capsomers. *Embo J* **14**, 4714-27.

Hong, S. S., Karayan, L., Tournier, J., Curiel, D. T. & Boulanger, P. A. (1997). Adenovirus type 5 fiber knob binds to MHC class I alpha2 domain at the surface of human epithelial and B lymphoblastoid cells. *Embo J* **16**, 2294-306.

Huebner, R. J., Rowe, W. P., Ward, T. G., Parrott, R. H. & Bell, J. A. (1954). Adenoidal-pharyngeal-conjunctival agents: a newly recognized group of common viruses of the respiratory system. *N Engl J Med* **251**, 1077-86.

Ino, A., Naito, Y., Mizuguchi, H., Handa, N., Hayakawa, T. & Kobayashi, I. (2005). A trial of somatic gene targeting in vivo with an adenovirus vector. *Genet Vaccines Ther* **3**, 8.

Inoue, N., Hirata, R. K. & Russell, D. W. (1999). High-fidelity correction of mutations at multiple chromosomal positions by adeno-associated virus vectors. *J Virol* **73**, 7376-80.

Ishibashi, M., Yosida, T. H. & Yasue, H. (1987). Preferential clustering of viral DNA sequences at or near the site of chromosomal rearrangement in fowl adenovirus type 1 DNA-transformed cell lines. *J Virol* **61**, 151-8.

Jeggo, P. A. (1998). Identification of genes involved in repair of DNA double-strand breaks in mammalian cells. *Radiat Res* **150**, S80-91.

Jorquera, R. & Tanguay, R. M. (1997). The mutagenicity of the tyrosine metabolite, fumarylacetoacetate, is enhanced by glutathione depletion. *Biochem Biophys Res Commun* **232**, 42-8.

Jorquera, R. & Tanguay, R. M. (1999). Cyclin B-dependent kinase and caspase-1 activation precedes mitochondrial dysfunction in fumarylacetoacetate-induced apoptosis. *Faseb J* **13**, 2284-98.

Jorquera, R. & Tanguay, R. M. (2001). Fumarylacetoacetate, the metabolite accumulating in hereditary tyrosinemia, activates the ERK pathway and induces mitotic abnormalities and genomic instability. *Hum Mol Genet* **10**, 1741-52.

Kalantari, M., Blennow, E., Hagmar, B. & Johansson, B. (2001). Physical state of HPV16 and chromosomal mapping of the integrated form in cervical carcinomas. *Diagn Mol Pathol* **10**, 46-54.

Karayan, L., Hong, S. S., Gay, B., Tournier, J., d'Angeac, A. D. & Boulanger, P. (1997). Structural and functional determinants in adenovirus type 2 penton base recombinant protein. *J Virol* **71**, 8678-89.

Kato, S., Anderson, R. A. & Camerini-Otero, R. D. (1986). Foreign DNA introduced by calcium phosphate is integrated into repetitive DNA elements of the mouse L cell genome. *Mol Cell Biol* **6**, 1787-95.

Kavana, M. & Moran, G. R. (2003). Interaction of (4-hydroxyphenyl)pyruvate dioxygenase with the specific inhibitor 2-[2-nitro-4-(trifluoromethyl)benzoyl]-1,3-cyclohexanedione. *Biochemistry* **42**, 10238-45.

Kelsey, G., Ruppert, S., Beermann, F., Grund, C., Tanguay, R. M. & Schutz, G. (1993). Rescue of mice homozygous for lethal albino deletions: implications for an animal model for the human liver disease tyrosinemia type 1. *Genes Dev* **7**, 2285-97.

Kiang, A., Hartman, Z. C., Liao, S., Xu, F., Serra, D., Palmer, D. J., Ng, P. & Amalfitano, A. (2006). Fully deleted adenovirus persistently expressing GAA accomplishes long-term skeletal muscle glycogen correction in tolerant and nontolerant GSD-II mice. *Mol Ther* **13**, 127-34.

Kibbe, M. R., Murdock, A., Wickham, T., Lizonova, A., Kovesdi, I., Nie, S., Shears, L., Billiar, T. R. & Tzeng, E. (2000). Optimizing cardiovascular gene therapy: increased vascular gene transfer with modified adenoviral vectors. *Arch Surg* **135**, 191-7.

Kim, I. H., Jozkowicz, A., Piedra, P. A., Oka, K. & Chan, L. (2001). Lifetime correction of genetic deficiency in mice with a single injection of helper-dependent adenoviral vector. *Proc Natl Acad Sci U S A* **98**, 13282-7.

Kimbi, G. C., Kramvis, A. & Kew, M. C. (2005). Integration of hepatitis B virus DNA into chromosomal DNA during acute hepatitis B. *World J Gastroenterol* **11**, 6416-21.

Kirchhausen, T. (1999). Adaptors for clathrin-mediated traffic. *Annu Rev Cell Dev Biol* **15**, 705-32.

Klebig, M. L., Russell, L. B. & Rinchik, E. M. (1992). Murine fumarylacetoacetate hydrolase (Fah) gene is disrupted by a neonatally lethal albino deletion that defines the hepatocyte-specific developmental regulation 1 (hsdr-1) locus. *Proc Natl Acad Sci U S A* **89**, 1363-7.

Klimov, E., Vinokourova, S., Moisjak, E., Rakhmanaliev, E., Kobseva, V., Laimins, L., Kisseljov, F. & Sulimova, G. (2002). Human papilloma viruses and cervical tumours: mapping of integration sites and analysis of adjacent cellular sequences. *BMC Cancer* **2**, 24.

Knoblauch, M., Schroer, J., Schmitz, B. & Doerfler, W. (1996). The structure of adenovirus type 12 DNA integration sites in the hamster cell genome. *J Virol* **70**, 3788-96.

Kochanek, S. (1999). High-capacity adenoviral vectors for gene transfer and somatic gene therapy. *Hum Gene Ther* **10**, 2451-9.

Kochanek, S., Clemens, P. R., Mitani, K., Chen, H. H., Chan, S. & Caskey, C. T. (1996). A new adenoviral vector: Replacement of all viral coding sequences with 28 kb of DNA independently expressing both full-length dystrophin and beta-galactosidase. *Proc Natl Acad Sci U S A* **93**, 5731-6.

Koike, K., Kobayashi, M., Mizusawa, H., Yoshida, E., Yaginuma, K. & Taira, M. (1983). Rearrangement of the surface antigen gene of hepatitis B virus integrated in the human hepatoma cell lines. *Nucleic Acids Res* **11**, 5391-402.

Kootstra, N. A. & Verma, I. M. (2003). Gene therapy with viral vectors. *Annu Rev Pharmacol Toxicol* **43**, 413-39.

Kovacs, G. M., LaPatra, S. E., D'Halluin, J. C. & Benko, M. (2003). Phylogenetic analysis of the hexon and protease genes of a fish adenovirus isolated from white sturgeon (Acipenser transmontanus) supports the proposal for a new adenovirus genus. *Virus Res* **98**, 27-34.

Krawinkel, U., Zoebelein, G. & Bothwell, A. L. (1986). Palindromic sequences are associated with sites of DNA breakage during gene conversion. *Nucleic Acids Res* **14**, 3871-82.

Kren, B. T., Bandyopadhyay, P., Chowdhury, N. R., Chowdhury, J. R. & Steer, C. J. (2002). Oligonucleotide-mediated site-directed gene repair. *Methods Enzymol* **346**, 14-35.

Kreppel, F., Biermann, V., Kochanek, S. & Schiedner, G. (2002). A DNA-based method to assay total and infectious particle contents and helper virus contamination in high-capacity adenoviral vector preparations. *Hum Gene Ther* **13**, 1151-6.

Kubo, S., Sun, M., Miyahara, M., Umeyama, K., Urakami, K., Yamamoto, T., Jakobs, C., Matsuda, I. & Endo, F. (1998). Hepatocyte injury in tyrosinemia type 1 is induced by fumarylacetoacetate and is inhibited by caspase inhibitors. *Proc Natl Acad Sci U S A* **95**, 9552-7.

Kuzmin, A. I., Finegold, M. J. & Eisensmith, R. C. (1997). Macrophage depletion increases the safety, efficacy and persistence of adenovirus-mediated gene transfer in vivo. *Gene Ther* **4**, 309-16.

Kvittingen, E. A., Rootwelt, H., Brandtzaeg, P., Bergan, A. & Berger, R. (1993). Hereditary tyrosinemia type I. Self-induced correction of the fumarylacetoacetase defect. *J Clin Invest* **91**, 1816-21.

Lamaze, C., Fujimoto, L. M., Yin, H. L. & Schmid, S. L. (1997). The actin cytoskeleton is required for receptor-mediated endocytosis in mammalian cells. *J Biol Chem* **272**, 20332-5.

Lan, Z. J., Chung, A. C., Xu, X., DeMayo, F. J. & Cooney, A. J. (2002). The embryonic function of germ cell nuclear factor is dependent on the DNA binding domain. *J Biol Chem* **277**, 50660-7.

Laufs, S., Gentner, B., Nagy, K. Z., Jauch, A., Benner, A., Naundorf, S., Kuehlcke, K., Schiedlmeier, B., Ho, A. D., Zeller, W. J. & Fruehauf, S. (2003). Retroviral vector integration occurs in preferred genomic targets of human bone marrow-repopulating cells. *Blood* **101**, 2191-8.

Laufs, S., Nagy, K. Z., Giordano, F. A., Hotz-Wagenblatt, A., Zeller, W. J. & Fruehauf, S. (2004). Insertion of retroviral vectors in NOD/SCID repopulating human peripheral blood progenitor cells occurs preferentially in the vicinity of transcription start regions and in introns. *Mol Ther* **10**, 874-81.

Lee, P. J. & Krilov, L. R. (2005). When animal viruses attack: SARS and avian influenza. *Pediatr Ann* **34**, 42-52.

Leon, R. P., Hedlund, T., Meech, S. J., Li, S., Schaack, J., Hunger, S. P., Duke, R. C. & DeGregori, J. (1998). Adenoviral-mediated gene transfer in lymphocytes. *Proc Natl Acad Sci U S A* **95**, 13159-64.

Li, E., Stupack, D., Bokoch, G. M. & Nemerow, G. R. (1998a). Adenovirus endocytosis requires actin cytoskeleton reorganization mediated by Rho family GTPases. *J Virol* **72**, 8806-12.

Li, E., Stupack, D., Klemke, R., Cheresh, D. A. & Nemerow, G. R. (1998b). Adenovirus endocytosis via alpha(v) integrins requires phosphoinositide-3-OH kinase. *J Virol* **72**, 2055-61.

Li, S. & Huang, L. (2000). Nonviral gene therapy: promises and challenges. *Gene Ther* **7**, 31-4.

Li, Z., Dullmann, J., Schiedlmeier, B., Schmidt, M., von Kalle, C., Meyer, J., Forster, M., Stocking, C., Wahlers, A., Frank, O., Ostertag, W., Kuhlcke, K., Eckert,

H. G., Fehse, B. & Baum, C. (2002). Murine leukemia induced by retroviral gene marking. *Science* **296**, 497.

Liang, F. & Jasin, M. (1996). Ku80-deficient cells exhibit excess degradation of extrachromosomal DNA. *J Biol Chem* **271**, 14405-11.

Lichtenberg, U., Zock, C. & Doerfler, W. (1988). Integration of foreign DNA into mammalian genome can be associated with hypomethylation at site of insertion. *Virus Res* **11**, 335-42.

Lin, F. L., Sperle, K. & Sternberg, N. (1985). Recombination in mouse L cells between DNA introduced into cells and homologous chromosomal sequences. *Proc Natl Acad Sci U S A* **82**, 1391-5.

Liu, F., Song, Y. & Liu, D. (1999). Hydrodynamics-based transfection in animals by systemic administration of plasmid DNA. *Gene Ther* **6**, 1258-66.

Liu, Q., Perez, C. F. & Wang, Y. (2006). Efficient site-specific integration of large transgenes by an enhanced herpes simplex virus/adeno-associated virus hybrid amplicon vector. *J Virol* **80**, 1672-9.

Lochmuller, H., Jani, A., Huard, J., Prescott, S., Simoneau, M., Massie, B., Karpati, G. & Acsadi, G. (1994). Emergence of early region 1-containing replication-competent adenovirus in stocks of replication-defective adenovirus recombinants (delta E1 + delta E3) during multiple passages in 293 cells. *Hum Gene Ther* **5**, 1485-91.

Lohrer, H., Blum, M. & Herrlich, P. (1988). Ataxia telangiectasia resists gene cloning: an account of parameters determining gene transfer into human recipient cells. *Mol Gen Genet* **212**, 474-80.

Louis, N., Evelegh, C. & Graham, F. L. (1997). Cloning and sequencing of the cellular-viral junctions from the human adenovirus type 5 transformed 293 cell line. *Virology* **233**, 423-9.

Luft, F., Klaes, R., Nees, M., Durst, M., Heilmann, V., Melsheimer, P. & von Knebel Doeberitz, M. (2001). Detection of integrated papillomavirus sequences by ligation-mediated PCR (DIPS-PCR) and molecular characterization in cervical cancer cells. *Int J Cancer* **92**, 9-17.

Lund, A. H., Duch, M. & Pedersen, F. S. (1996). Increased cloning efficiency by temperature-cycle ligation. *Nucleic Acids Res* **24**, 800-1.

Luo, W. J., Takakuwa, T., Ham, M. F., Wada, N., Liu, A., Fujita, S., Sakane-Ishikawa, E. & Aozasa, K. (2004). Epstein-Barr virus is integrated between REL and BCL-11A in American Burkitt lymphoma cell line (NAB-2). *Lab Invest* **84**, 1193-9.

Mahalingam, S., Damon, I. K. & Lidbury, B. A. (2004). 25 years since the eradication of smallpox: why poxvirus research is still relevant. *Trends Immunol* **25**, 636-9.

Mahon, K. A., Overbeek, P. A. & Westphal, H. (1988). Prenatal lethality in a transgenic mouse line is the result of a chromosomal translocation. *Proc Natl Acad Sci U S A* **85**, 1165-8.

Manivasakam, P., Aubrecht, J., Sidhom, S. & Schiestl, R. H. (2001). Restriction enzymes increase efficiencies of illegitimate DNA integration but decrease homologous integration in mammalian cells. *Nucleic Acids Res* **29**, 4826-33.

Mark, W. H., Signorelli, K., Blum, M., Kwee, L. & Lacy, E. (1992). Genomic structure of the locus associated with an insertional mutation in line 4 transgenic mice. *Genomics* **13**, 159-66.

Mathias, P., Wickham, T., Moore, M. & Nemerow, G. (1994). Multiple adenovirus serotypes use alpha v integrins for infection. *J Virol* **68**, 6811-4.

Matsumoto, K., Nagata, K., Yamanaka, K., Hanaoka, F. & Ui, M. (1989). Nuclear factor I represses the reverse-oriented transcription from the adenovirus type 5 DNA terminus. *Biochem Biophys Res Commun* **164**, 1212-9.

Mayne, L. V., Jones, T., Dean, S. W., Harcourt, S. A., Lowe, J. E., Priestley, A., Steingrimsdottir, H., Sykes, H., Green, M. H. & Lehmann, A. R. (1988). SV 40-transformed normal and DNA-repair-deficient human fibroblasts can be transfected with high frequency but retain only limited amounts of integrated DNA. *Gene* **66**, 65-76.

McCarty, D. M., Young, S. M., Jr. & Samulski, R. J. (2004). Integration of adeno-associated virus (AAV) and recombinant AAV vectors. *Annu Rev Genet* **38**, 819-45.

McConnell, M. J. & Imperiale, M. J. (2004). Biology of adenovirus and its use as a vector for gene therapy. *Hum Gene Ther* **15**, 1022-33.

McDongall, J. K., Dunn, A. R. & Gallimore, P. H. (1975). Recent studies on the characteristics of adenovirus-infected and -transformed cells. *Cold Spring Harb Symp Quant Biol* **39 Pt 1**, 591-600.

McFarlane, M. & Wilson, J. B. (1996). A model for the mechanism of precise integration of a microinjected transgene. *Transgenic Res* **5**, 171-7.

Medina-Kauwe, L. K. (2003). Endocytosis of adenovirus and adenovirus capsid proteins. *Adv Drug Deliv Rev* **55**, 1485-96.

Merrihew, R. V., Marburger, K., Pennington, S. L., Roth, D. B. & Wilson, J. H. (1996). High-frequency illegitimate integration of transfected DNA at preintegrated target sites in a mammalian genome. *Mol Cell Biol* **16**, 10-8.

Mian, A., McCormack, W. M., Jr., Mane, V., Kleppe, S., Ng, P., Finegold, M., O'Brien, W. E., Rodgers, J. R., Beaudet, A. L. & Lee, B. (2004). Long-term correction of ornithine transcarbamylase deficiency by WPRE-mediated overexpression using a helper-dependent adenovirus. *Mol Ther* **10**, 492-9.

Michalopoulos, G. K. & DeFrances, M. C. (1997). Liver regeneration. *Science* **276**, 60-6.

Michalopoulos, G. K. & Khan, Z. (2005). Liver regeneration, growth factors, and amphiregulin. *Gastroenterology* **128**, 503-6.

Mikkers, H., Allen, J., Knipscheer, P., Romeijn, L., Hart, A., Vink, E. & Berns, A. (2002). High-throughput retroviral tagging to identify components of specific signaling pathways in cancer. *Nat Genet* **32**, 153-9.

Miller, D. G., Petek, L. M. & Russell, D. W. (2004). Adeno-associated virus vectors integrate at chromosome breakage sites. *Nat Genet* **36**, 767-73.

Miller, D. G., Rutledge, E. A. & Russell, D. W. (2002). Chromosomal effects of adeno-associated virus vector integration. *Nat Genet* **30**, 147-8.

Miller, D. G., Trobridge, G. D., Petek, L. M., Jacobs, M. A., Kaul, R. & Russell, D. W. (2005). Large-scale analysis of adeno-associated virus vector integration sites in normal human cells. *J Virol* **79**, 11434-42.

Miralles, V. J., Cortes, P., Stone, N. & Reinberg, D. (1989). The adenovirus inverted terminal repeat functions as an enhancer in a cell-free system. *J Biol Chem* **264**, 10763-72.

Mitani, K., Graham, F. L., Caskey, C. T. & Kochanek, S. (1995a). Rescue, propagation, and partial purification of a helper virus-dependent adenovirus vector. *Proc Natl Acad Sci U S A* **92**, 3854-8.

Mitani, K., Wakamiya, M., Hasty, P., Graham, F. L., Bradley, A. & Caskey, C. T. (1995b). Gene targeting in mouse embryonic stem cells with an adenoviral vector. *Somat Cell Mol Genet* **21**, 221-31.

Mitchell, R. S., Beitzel, B. F., Schroder, A. R., Shinn, P., Chen, H., Berry, C. C., Ecker, J. R. & Bushman, F. D. (2004). Retroviral DNA integration: ASLV, HIV, and MLV show distinct target site preferences. *PLoS Biol* **2**, E234.

Mizusawa, H., Taira, M., Yaginuma, K., Kobayashi, M., Yoshida, E. & Koike, K. (1985). Inversely repeating integrated hepatitis B virus DNA and cellular flanking sequences in the human hepatoma-derived cell line huSP. *Proc Natl Acad Sci U S A* **82**, 208-12.

Moazed, D. & Noller, H. F. (1987). Interaction of antibiotics with functional sites in 16S ribosomal RNA. *Nature* **327**, 389-94.

Montini, E., Held, P. K., Noll, M., Morcinek, N., Al-Dhalimy, M., Finegold, M., Yant, S. R., Kay, M. A. & Grompe, M. (2002). In vivo correction of murine tyrosinemia type I by DNA-mediated transposition. *Mol Ther* **6**, 759-69.

Morral, N., O'Neal, W., Rice, K., Leland, M., Kaplan, J., Piedra, P. A., Zhou, H., Parks, R. J., Velji, R., Aguilar-Cordova, E., Wadsworth, S., Graham, F. L., Kochanek, S., Carey, K. D. & Beaudet, A. L. (1999). Administration of helper-dependent adenoviral vectors and sequential delivery of different vector serotype for long-term liver-directed gene transfer in baboons. *Proc Natl Acad Sci U S A* **96**, 12816-21.

Morral, N., Parks, R. J., Zhou, H., Langston, C., Schiedner, G., Quinones, J., Graham, F. L., Kochanek, S. & Beaudet, A. L. (1998). High doses of a helper-dependent adenoviral vector yield supraphysiological levels of alpha1-antitrypsin with negligible toxicity. *Hum Gene Ther* **9**, 2709-16.

Morsy, M. A. & Caskey, C. T. (1999). Expanded-capacity adenoviral vectors--the helper-dependent vectors. *Mol Med Today* **5**, 18-24.

Mul, Y. M., Verrijzer, C. P. & van der Vliet, P. C. (1990). Transcription factors NFI and NFIII/oct-1 function independently, employing different mechanisms to enhance adenovirus DNA replication. *J Virol* **64**, 5510-8.

Muller, K., Heller, H. & Doerfler, W. (2001). Foreign DNA integration. Genome-wide perturbations of methylation and transcription in the recipient genomes. *J Biol Chem* **276**, 14271-8.

Murakami, Y., Saigo, K., Takashima, H., Minami, M., Okanoue, T., Brechot, C. & Paterlini-Brechot, P. (2005). Large scaled analysis of hepatitis B virus (HBV) DNA integration in HBV related hepatocellular carcinomas. *Gut* **54**, 1162-8.

Muruve, D. A., Barnes, M. J., Stillman, I. E. & Libermann, T. A. (1999). Adenoviral gene therapy leads to rapid induction of multiple chemokines and acute neutrophil-dependent hepatic injury in vivo. *Hum Gene Ther* **10**, 965-76.

Muruve, D. A., Cotter, M. J., Zaiss, A. K., White, L. R., Liu, Q., Chan, T., Clark, S. A., Ross, P. J., Meulenbroek, R. A., Maelandsmo, G. M. & Parks, R. J. (2004). Helper-dependent adenovirus vectors elicit intact innate but attenuated adaptive host immune responses in vivo. *J Virol* **78**, 5966-72.

Mysiak, M. E., Holthuizen, P. E. & van der Vliet, P. C. (2004). The adenovirus priming protein pTP contributes to the kinetics of initiation of DNA replication. *Nucleic Acids Res* **32**, 3913-20.

Nakai, H., Iwaki, Y., Kay, M. A. & Couto, L. B. (1999). Isolation of recombinant adeno-associated virus vector-cellular DNA junctions from mouse liver. *J Virol* **73**, 5438-47.

Nakai, H., Montini, E., Fuess, S., Storm, T. A., Grompe, M. & Kay, M. A. (2003). AAV serotype 2 vectors preferentially integrate into active genes in mice. *Nat Genet* **34**, 297-302.

Nakai, H., Wu, X., Fuess, S., Storm, T. A., Munroe, D., Montini, E., Burgess, S. M., Grompe, M. & Kay, M. A. (2005). Large-scale molecular characterization of adeno-associated virus vector integration in mouse liver. *J Virol* **79**, 3606-14.

Nakano, M. Y., Boucke, K., Suomalainen, M., Stidwill, R. P. & Greber, U. F. (2000). The first step of adenovirus type 2 disassembly occurs at the cell surface, independently of endocytosis and escape to the cytosol. *J Virol* **74**, 7085-95.

Nalbantoglu, J., Miles, C. & Meuth, M. (1988). Insertion of unique and repetitive DNA fragments into the aprt locus of hamster cells. *J Mol Biol* **200**, 449-59.

Nemerow, G. R. (2002). Biology of Adenovirus Cell Entry. In *Adenoviral Vectors for Gene Therapy*, pp. 19-32. Edited by D. T. Curiel, Douglas, J.T.: Academic Press.

Nicholls, R. D., Fischel-Ghodsian, N. & Higgs, D. R. (1987). Recombination at the human alpha-globin gene cluster: sequence features and topological constraints. *Cell* **49**, 369-78.

Nicklin, S. A., Wu, E., Nemerow, G. R. & Baker, A. H. (2005). The influence of adenovirus fiber structure and function on vector development for gene therapy. *Mol Ther* **12**, 384-93.

Nielsch, U., Zimmer, S. G. & Babiss, L. E. (1991). Changes in NF-kappa B and ISGF3 DNA binding activities are responsible for differences in MHC and beta-IFN gene expression in Ad5- versus Ad12-transformed cells. *Embo J* **10**, 4169-75.

Noutsias, M., Fechner, H., de Jonge, H., Wang, X., Dekkers, D., Houtsmuller, A. B., Pauschinger, M., Bergelson, J., Warraich, R., Yacoub, M., Hetzer, R., Lamers, J., Schultheiss, H. P. & Poller, W. (2001). Human coxsackie-adenovirus receptor is colocalized with integrins alpha(v)beta(3) and alpha(v)beta(5) on the cardiomyocyte sarcolemma and upregulated in dilated cardiomyopathy: implications for cardiotropic viral infections. *Circulation* **104**, 275-80.

Nyhan, W. L. (2005). Disorders of purine and pyrimidine metabolism. *Mol Genet Metab* **86**, 25-33.

O'Driscoll, M. & Jeggo, P. A. (2006). The role of double-strand break repair - insights from human genetics. *Nat Rev Genet* **7**, 45-54.

O'Neal, W. K., Zhou, H., Morral, N., Langston, C., Parks, R. J., Graham, F. L., Kochanek, S. & Beaudet, A. L. (2000). Toxicity associated with repeated administration of first-generation adenovirus vectors does not occur with a helper-dependent vector. *Mol Med* **6**, 179-95.

Ohbayashi, F., Balamotis, M. A., Kishimoto, A., Aizawa, E., Diaz, A., Hasty, P., Graham, F. L., Caskey, C. T. & Mitani, K. (2005). Correction of chromosomal mutation and random integration in embryonic stem cells with helper-dependent adenoviral vectors. *Proc Natl Acad Sci U S A* **102**, 13628-33.

Orrantia, E. & Chang, P. L. (1990). Intracellular distribution of DNA internalized through calcium phosphate precipitation. *Exp Cell Res* **190**, 170-4.

Overturf, K., Al-Dhalimy, M., Manning, K., Ou, C. N., Finegold, M. & Grompe, M. (1998). Ex vivo hepatic gene therapy of a mouse model of Hereditary Tyrosinemia Type I. *Hum Gene Ther* **9**, 295-304.

Overturf, K., al-Dhalimy, M., Ou, C. N., Finegold, M., Tanguay, R., Lieber, A., Kay, M. & Grompe, M. (1997). Adenovirus-mediated gene therapy in a mouse model of hereditary tyrosinemia type I. *Hum Gene Ther* **8**, 513-21.

Overturf, K., Al-Dhalimy, M., Tanguay, R., Brantly, M., Ou, C. N., Finegold, M. & Grompe, M. (1996). Hepatocytes corrected by gene therapy are selected in

vivo in a murine model of hereditary tyrosinaemia type I. *Nat Genet* **12**, 266-73.

Palmer, D. J. & Ng, P. (2005). Helper-dependent adenoviral vectors for gene therapy. *Hum Gene Ther* **16**, 1-16.

Patterson, S. & Russell, W. C. (1983). Ultrastructural and immunofluorescence studies of early events in adenovirus-HeLa cell interactions. *J Gen Virol* **64**, 1091-9.

Paull, T. T. & Gellert, M. (2000). A mechanistic basis for Mre11-directed DNA joining at microhomologies. *Proc Natl Acad Sci U S A* **97**, 6409-14.

Perez, D. R., Sorrell, E. M. & Donis, R. O. (2005). Avian influenza: an omnipresent pandemic threat. *Pediatr Infect Dis J* **24**, S208-16, discussion S215.

Pollard, H., Remy, J. S., Loussouarn, G., Demolombe, S., Behr, J. P. & Escande, D. (1998). Polyethylenimine but not cationic lipids promotes transgene delivery to the nucleus in mammalian cells. *J Biol Chem* **273**, 7507-11.

Quiller-Couch, A. T. (1919). The Oxford Book of English Verse 1250–1900, pp. 228. Edited by A. T. Quiller-Couch: Clarendon Press.

Raper, S. E., Chirmule, N., Lee, F. S., Wivel, N. A., Bagg, A., Gao, G. P., Wilson, J. M. & Batshaw, M. L. (2003). Fatal systemic inflammatory response syndrome in a ornithine transcarbamylase deficient patient following adenoviral gene transfer. *Mol Genet Metab* **80**, 148-58.

Rasheed, S., Nelson-Rees, W. A., Toth, E. M., Arnstein, P. & Gardner, M. B. (1974). Characterization of a newly derived human sarcoma cell line (HT-1080). *Cancer* **33**, 1027-33.

Reese, E. L. & Haimo, L. T. (2000). Dynein, dynactin, and kinesin II's interaction with microtubules is regulated during bidirectional organelle transport. *J Cell Biol* **151**, 155-66.

Reilein, A. R., Tint, I. S., Peunova, N. I., Enikolopov, G. N. & Gelfand, V. I. (1998). Regulation of organelle movement in melanophores by protein kinase A (PKA), protein kinase C (PKC), and protein phosphatase 2A (PP2A). *J Cell Biol* **142**, 803-13.

Remus, R., Kammer, C., Heller, H., Schmitz, B., Schell, G. & Doerfler, W. (1999). Insertion of foreign DNA into an established mammalian genome can alter the methylation of cellular DNA sequences. *J Virol* **73**, 1010-22.

Ren, C., Zhao, M., Yang, X., Li, D., Jiang, X., Wang, L., Shan, W., Yang, H., Zhou, L., Zhou, W. & Zhang, H. (2006). Establishment and Applications of Epstein-Barr Virus-based Episomal Vectors in Human Embryonic Stem Cells. *Stem Cells*.

Ricciardiello, L., Baglioni, M., Giovannini, C., Pariali, M., Cenacchi, G., Ripalti, A., Landini, M. P., Sawa, H., Nagashima, K., Frisque, R. J., Goel, A., Boland, C. R., Tognon, M., Roda, E. & Bazzoli, F. (2003). Induction of chromosomal instability in colonic cells by the human polyomavirus JC virus. *Cancer Res* **63**, 7256-62.

Robins, D. M., Ripley, S., Henderson, A. S. & Axel, R. (1981). Transforming DNA integrates into the host chromosome. *Cell* **23**, 29-39.

Romani, M., De Ambrosis, A., Alhadeff, B., Purrello, M., Gluzman, Y. & Siniscalco, M. (1990). Preferential integration of the Ad5/SV40 hybrid virus at the highly recombinogenic human chromosomal site 1p36. *Gene* **95**, 231-41.

Rosenberg, S. A., Aebersold, P., Cornetta, K., Kasid, A., Morgan, R. A., Moen, R., Karson, E. M., Lotze, M. T., Yang, J. C., Topalian, S. L. & et al. (1990). Gene transfer into humans--immunotherapy of patients with advanced melanoma,

using tumor-infiltrating lymphocytes modified by retroviral gene transduction. *N Engl J Med* **323**, 570-8.

Rosenfeld, M. A., Siegfried, W., Yoshimura, K., Yoneyama, K., Fukayama, M., Stier, L. E., Paakko, P. K., Gilardi, P., Stratford-Perricaudet, L. D., Perricaudet, M. & et al. (1991). Adenovirus-mediated transfer of a recombinant alpha 1-antitrypsin gene to the lung epithelium in vivo. *Science* **252**, 431-4.

Roth, D. B. & Wilson, J. H. (1986). Nonhomologous recombination in mammalian cells: role for short sequence homologies in the joining reaction. *Mol Cell Biol* **6**, 4295-304.

Rowe, W. P., Huebner, R. J., Gilmore, L. K., Parrott, R. H. & Ward, T. G. (1953). Isolation of a cytopathogenic agent from human adenoids undergoing spontaneous degeneration in tissue culture. *Proc Soc Exp Biol Med* **84**, 570-3.

Russell, D. W. & Hirata, R. K. (1998). Human gene targeting by viral vectors. *Nat Genet* **18**, 325-30.

Rutledge, E. A. & Russell, D. W. (1997). Adeno-associated virus vector integration junctions. *J Virol* **71**, 8429-36.

Rux, J. J. & Burnett, R. M. (2004). Adenovirus structure. *Hum Gene Ther* **15**, 1167-76.

Sambrook, J., Botchan, M., Gallimore, P., Ozanne, B., Pettersson, U., Williams, J. & Sharp, P. A. (1975). Viral DNA sequences in cells transformed by simian virus 40, adenovirus type 2 and adenovirus type 5. *Cold Spring Harb Symp Quant Biol* **39 Pt 1**, 615-32.

Sambrook, J., Botchan, M., Hu, S. L., Mitchison, T. & Stringer, J. (1980a). Integration of viral DNA sequences in cells transformed by adenovirus 2 or SV40. *Proc R Soc Lond B Biol Sci* **210**, 423-35.

Sambrook, J., Greene, R., Stringer, J., Mitchison, T., Hu, S. L. & Botchan, M. (1980b). Analysis of the sites of integration of viral DNA sequences in rat cells transformed by adenovirus 2 or SV40. *Cold Spring Harb Symp Quant Biol* **44 Pt 1**, 569-84.

Sambrook, J., Westphal, H., Srinivasan, P. R. & Dulbecco, R. (1968). The integrated state of viral DNA in SV40-transformed cells. *Proc Natl Acad Sci U S A* **60**, 1288-95.

San Martin, C. B., R. M. (2003). Structural studies on adenoviruses. *Curr Top Microbiol Immunol* **272**, 57–94.

Schepis, C., Greco, D., Siragusa, M. & Romano, C. (1996). What syndrome is this? Lesch-Nyhan syndrome. *Pediatr Dermatol* **13**, 169-70.

Schiedner, G., Morral, N., Parks, R. J., Wu, Y., Koopmans, S. C., Langston, C., Graham, F. L., Beaudet, A. L. & Kochanek, S. (1998). Genomic DNA transfer with a high-capacity adenovirus vector results in improved in vivo gene expression and decreased toxicity. *Nat Genet* **18**, 180-3.

Schmid, S. I. & Hearing, P. (1995). Selective encapsidation of adenovirus DNA. *Curr Top Microbiol Immunol* **199 (Pt 1)**, 67-80.

Schmid, S. I. & Hearing, P. (1997). Bipartite structure and functional independence of adenovirus type 5 packaging elements. *J Virol* **71**, 3375-84.

Schmid, S. I. & Hearing, P. (1998). Cellular components interact with adenovirus type 5 minimal DNA packaging domains. *J Virol* **72**, 6339-47.

Schmidt, M., Carbonaro, D. A., Speckmann, C., Wissler, M., Bohnsack, J., Elder, M., Aronow, B. J., Nolta, J. A., Kohn, D. B. & von Kalle, C. (2003). Clonality analysis after retroviral-mediated gene transfer to CD34+ cells from the cord blood of ADA-deficient SCID neonates. *Nat Med* **9**, 463-8.

Schmidt, M., Glimm, H., Lemke, N., Muessig, A., Speckmann, C., Haas, S., Zickler, P., Hoffmann, G. & Von Kalle, C. (2001). A model for the detection of clonality in marked hematopoietic stem cells. *Ann N Y Acad Sci* **938**, 146-55; discussion 155-6.

Schoehn, G., Fender, P., Chroboczek, J. & Hewat, E. A. (1996). Adenovirus 3 penton dodecahedron exhibits structural changes of the base on fibre binding. *Embo J* **15**, 6841-6.

Schowalter, D. B., Tubb, J. C., Liu, M., Wilson, C. B. & Kay, M. A. (1997). Heterologous expression of adenovirus E3-gp19K in an E1a-deleted adenovirus vector inhibits MHC I expression in vitro, but does not prolong transgene expression in vivo. *Gene Ther* **4**, 351-60.

Schroer, J., Holker, I. & Doerfler, W. (1997). Adenovirus type 12 DNA firmly associates with mammalian chromosomes early after virus infection or after DNA transfer by the addition of DNA to the cell culture medium. *J Virol* **71**, 7923-32.

Schulz, M. & Doerfler, W. (1984). Deletion of cellular DNA at site of viral DNA insertion in the adenovirus type 12-induced mouse tumor CBA-12-1-T. *Nucleic Acids Res* **12**, 4959-76.

Schulz, M., Freisem-Rabien, U., Jessberger, R. & Doerfler, W. (1987). Transcriptional activities of mammalian genomes at sites of recombination with foreign DNA. *J Virol* **61**, 344-53.

Segerman, A., Atkinson, J. P., Marttila, M., Dennerquist, V., Wadell, G. & Arnberg, N. (2003). Adenovirus type 11 uses CD46 as a cellular receptor. *J Virol* **77**, 9183-91.

Selkirk, S. M. (2004). Gene therapy in clinical medicine. *Postgrad Med J* **80**, 560-70.

Seth, P., Willingham, M. C. & Pastan, I. (1985). Binding of adenovirus and its external proteins to Triton X-114. Dependence on pH. *J Biol Chem* **260**, 14431-4.

Sharp, J. D., Capecchi, N. E. & Capecchi, M. R. (1973). Altered enzymes in drug-resistant variants of mammalian tissue culture cells. *Proc Natl Acad Sci U S A* **70**, 3145-9.

Sharp, P. A., Pettersson, U. & Sambrook, J. (1974). Viral DNA in transformed cells. I. A study of the sequences of adenovirus 2 DNA in a line of transformed rat cells using specific fragments of the viral genome. *J Mol Biol* **86**, 709-26.

Shenk, T. (1995). Group C adenoviruses as vectors for gene therapy. In *Viral Vectors: Gene Therapy andNeuroscience Applications*, pp. 43–54. Edited by L. A. Kaplitt MG. San Diego: Academic Press.

Shenk, T. (2000). Adenoviridae and their replication, 4th Edition edn, pp. 2265-2300. Edited by B. Fields, Howley, P. & Knipe, D. New York: Raven Press.

Shivapurkar, N., Harada, K., Reddy, J., Scheuermann, R. H., Xu, Y., McKenna, R. W., Milchgrub, S., Kroft, S. H., Feng, Z. & Gazdar, A. F. (2002). Presence of simian virus 40 DNA sequences in human lymphomas. *Lancet* **359**, 851-2.

Silver, J. & Keerikatte, V. (1989). Novel use of polymerase chain reaction to amplify cellular DNA adjacent to an integrated provirus. *J Virol* **63**, 1924-8.

Simon, R. H., Engelhardt, J. F., Yang, Y., Zepeda, M., Weber-Pendleton, S., Grossman, M. & Wilson, J. M. (1993). Adenovirus-mediated transfer of the CFTR gene to lung of nonhuman primates: toxicity study. *Hum Gene Ther* **4**, 771-80.

Spahn, C. M. & Prescott, C. D. (1996). Throwing a spanner in the works: antibiotics and the translation apparatus. *J Mol Med* **74**, 423-39.

Stabel, S., Doerfler, W. & Friis, R. R. (1980). Integration sites of adenovirus type 12 DNA in transformed hamster cells and hamster tumor cells. *J Virol* **36**, 22-40.

Starzinski-Powitz, A., Schulz, M., Esche, H., Mukai, N. & Doerfler, W. (1982). The adenovirus type 12 - mouse cell system: permissivity and analysis of integration patterns of viral DNA in tumor cells. *Embo J* **1**, 493-7.

Stein, C. S., Pemberton, J. L., van Rooijen, N. & Davidson, B. L. (1998). Effects of macrophage depletion and anti-CD40 ligand on transgene expression and redosing with recombinant adenovirus. *Gene Ther* **5**, 431-9.

Stern, M., Ulrich, K., Geddes, D. M. & Alton, E. W. (2003). Poly (D, L-lactide-co-glycolide)/DNA microspheres to facilitate prolonged transgene expression in airway epithelium in vitro, ex vivo and in vivo. *Gene Ther* **10**, 1282-8.

Stewart, P. L. & Burnett, R. M. (1995). Adenovirus structure by X-ray crystallography and electron microscopy. *Curr Top Microbiol Immunol* **199 (Pt 1)**, 25-38.

Stout, J. T. & Caskey, C. T. (1985). HPRT: gene structure, expression, and mutation. *Annu Rev Genet* **19**, 127-48.

Stratford-Perricaudet, L. D., Levrero, M., Chasse, J. F., Perricaudet, M. & Briand, P. (1990). Evaluation of the transfer and expression in mice of an enzyme-encoding gene using a human adenovirus vector. *Hum Gene Ther* **1**, 241-56.

Strayer, D., Branco, F., Zern, M. A., Yam, P., Calarota, S. A., Nichols, C. N., Zaia, J. A., Rossi, J., Li, H., Parashar, B., Ghosh, S. & Chowdhury, J. R. (2002). Durability of transgene expression and vector integration: recombinant SV40-derived gene therapy vectors. *Mol Ther* **6**, 227-37.

Strayer, D. S. (1999). Gene therapy using SV40-derived vectors: what does the future hold? *J Cell Physiol* **181**, 375-84.

Stryer, L. (1998). Biochemistry, Fourth Edition edn. New York: W.H. Freeman and Company.

Stuiver, M. H. & van der Vliet, P. C. (1990). Adenovirus DNA-binding protein forms a multimeric protein complex with double-stranded DNA and enhances binding of nuclear factor I. *J Virol* **64**, 379-86.

Stutts, P. & Brockman, R. W. (1963). A biochemical basis for resistance of L1210 mouse leukemia to 6-thioguanine. *Biochem Pharmacol* **12**, 97-104.

Szybalski, W. & Szybalska, E. H. (1962). Drug sensitivity as a genetic marker for human cell lines. *Med Bull (Ann Arbor)* **28**, 277-93.

Takakuwa, T., Luo, W. J., Ham, M. F., Wada, N. & Aozasa, K. (2005). Identification of Epstein-Barr virus integrated sites in lymphoblastoid cell line (IB4). *Virus Res* **108**, 133-8.

Takata, M., Sasaki, M. S., Sonoda, E., Morrison, C., Hashimoto, M., Utsumi, H., Yamaguchi-Iwai, Y., Shinohara, A. & Takeda, S. (1998). Homologous recombination and non-homologous end-joining pathways of DNA double-strand break repair have overlapping roles in the maintenance of chromosomal integrity in vertebrate cells. *Embo J* **17**, 5497-508.

Tammur, J., Sibul, H., Ustav, E., Ustav, M. & Metspalu, A. (2002). A bovine papillomavirus-1 based vector restores the function of the low-density lipoprotein receptor in the receptor-deficient CHO-ldlA7 cell line. *BMC Mol Biol* **3**, 5.

Tanguay, R. M., Jorquera, R., Poudrier, J. & St-Louis, M. (1996). Tyrosine and its catabolites: from disease to cancer. *Acta Biochim Pol* **43**, 209-16.

Taylor, E. M. & Lehmann, A. R. (1998). Conservation of eukaryotic DNA repair mechanisms. *Int J Radiat Biol* **74**, 277-86.

Thomas, K. R. & Capecchi, M. R. (1987). Site-directed mutagenesis by gene targeting in mouse embryo-derived stem cells. *Cell* **51**, 503-12.

Thomas, K. R., Folger, K. R. & Capecchi, M. R. (1986). High frequency targeting of genes to specific sites in the mammalian genome. *Cell* **44**, 419-28.

Thorland, E. C., Myers, S. L., Gostout, B. S. & Smith, D. I. (2003). Common fragile sites are preferential targets for HPV16 integrations in cervical tumors. *Oncogene* **22**, 1225-37.

Toietta, G., Mane, V. P., Norona, W. S., Finegold, M. J., Ng, P., McDonagh, A. F., Beaudet, A. L. & Lee, B. (2005). Lifelong elimination of hyperbilirubinemia in the Gunn rat with a single injection of helper-dependent adenoviral vector. *Proc Natl Acad Sci U S A* **102**, 3930-5.

Tokino, T., Fukushige, S., Nakamura, T., Nagaya, T., Murotsu, T., Shiga, K., Aoki, N. & Matsubara, K. (1987). Chromosomal translocation and inverted duplication associated with integrated hepatitis B virus in hepatocellular carcinomas. *J Virol* **61**, 3848-54.

Tollefson, A. E., Ryerse, J. S., Scaria, A., Hermiston, T. W. & Wold, W. S. (1996). The E3-11.6-kDa adenovirus death protein (ADP) is required for efficient cell death: characterization of cells infected with adp mutants. *Virology* **220**, 152-62.

Tomiyasu, K., Satoh, E., Oda, Y., Nishizaki, K., Kondo, M., Imanishi, J. & Mazda, O. (1998). Gene transfer in vitro and in vivo with Epstein-Barr virus-based episomal vector results in markedly high transient expression in rodent cells. *Biochem Biophys Res Commun* **253**, 733-8.

Triglia, T., Peterson, M. G. & Kemp, D. J. (1988). A procedure for in vitro amplification of DNA segments that lie outside the boundaries of known sequences. *Nucleic Acids Res* **16**, 8186.

Trobridge, G. D., Miller, D. G., Jacobs, M. A., Allen, J. M., Kiem, H. P., Kaul, R. & Russell, D. W. (2006). Foamy virus vector integration sites in normal human cells. *Proc Natl Acad Sci U S A* **103**, 1498-503.

Tsukui, T., Kanegae, Y., Saito, I. & Toyoda, Y. (1996). Transgenesis by adenovirus-mediated gene transfer into mouse zona-free eggs. *Nat Biotechnol* **14**, 982-5.

Untergasser, A. & Protzer, U. (2004). Hepatitis B virus-based vectors allow the elimination of viral gene expression and the insertion of foreign promoters. *Hum Gene Ther* **15**, 203-10.

Valerie, K. & Povirk, L. F. (2003). Regulation and mechanisms of mammalian double-strand break repair. *Oncogene* **22**, 5792-812.

Van der Vliet, P. C. (1995). Adenovirus DNA replication. *Curr Top Microbiol Immunol* **199 (Pt 2)**, 1-30.

Van Doren, K., Hanahan, D. & Gluzman, Y. (1984). Infection of eucaryotic cells by helper-independent recombinant adenoviruses: early region 1 is not obligatory for integration of viral DNA. *J Virol* **50**, 606-14.

Van Dyck, E., Stasiak, A. Z., Stasiak, A. & West, S. C. (1999). Binding of double-strand breaks in DNA by human Rad52 protein. *Nature* **398**, 728-31.

van Oostrum, J. & Burnett, R. M. (1985). Molecular composition of the adenovirus type 2 virion. *J Virol* **56**, 439-48.

Vardimon, L. & Doerfler, W. (1981). Patterns of integration of viral DNA in adenovirus type 2-transformed hamster cells. *J Mol Biol* **147**, 227-46.

Vasileva, A. & Jessberger, R. (2005). Precise hit: adeno-associated virus in gene targeting. *Nat Rev Microbiol* **3**, 837-47.

Vera, M. & Fortes, P. (2004). Simian virus-40 as a gene therapy vector. *DNA Cell Biol* **23**, 271-82.

Verma, I. M. & Weitzman, M. D. (2005). GENE THERAPY: Twenty-First Century Medicine. *Annu Rev Biochem* **74**, 711-38.

Vertegaal, A. C., Kuiperij, H. B., Houweling, A., Verlaan, M., van der Eb, A. J. & Zantema, A. (2003). Differential expression of tapasin and immunoproteasome subunits in adenovirus type 5- versus type 12-transformed cells. *J Biol Chem* **278**, 139-46.

Vilchez, R. A., Kozinetz, C. A., Arrington, A. S., Madden, C. R. & Butel, J. S. (2003). Simian virus 40 in human cancers. *Am J Med* **114**, 675-84.

Vincent, K. A., York-Higgins, D., Quiroga, M. & Brown, P. O. (1990). Host sequences flanking the HIV provirus. *Nucleic Acids Res* **18**, 6045-7.

Visser, L., van Maarschalkerweerd, M. W., Rozijn, T. H., Wassenaar, A. D., Reemst, A. M. & Sussenbach, J. S. (1980). Viral DNA sequences in adenovirus-transformed cells. *Cold Spring Harb Symp Quant Biol* **44 Pt 1**, 541-50.

Volodin, A. A., Voloshin, O. N. & Camerini-Otero, R. D. (2005). Homologous recombination and RecA protein: towards a new generation of tools for genome manipulations. *Trends Biotechnol* **23**, 97-102.

Volpers, C. & Kochanek, S. (2004). Adenoviral vectors for gene transfer and therapy. *J Gene Med* **6 Suppl 1**, S164-71.

Vrancken Peeters, M. J., Perkins, A. L. & Kay, M. A. (1996). Method for multiple portal vein infusions in mice: quantitation of adenovirus-mediated hepatic gene transfer. *Biotechniques* **20**, 278-85.

Wade-Martins, R., White, R. E., Kimura, H., Cook, P. R. & James, M. R. (2000). Stable correction of a genetic deficiency in human cells by an episome carrying a 115 kb genomic transgene. *Nat Biotechnol* **18**, 1311-4.

Wagner, W., Laufs, S., Blake, J., Schwager, C., Wu, X., Zeller, J. W., Ho, A. D. & Fruehauf, S. (2005). Retroviral integration sites correlate with expressed genes in hematopoietic stem cells. *Stem Cells* **23**, 1050-8.

Wake, C. T., Gudewicz, T., Porter, T., White, A. & Wilson, J. H. (1984). How damaged is the biologically active subpopulation of transfected DNA? *Mol Cell Biol* **4**, 387-98.

Wallenburg, J. C., Nepveu, A. & Chartrand, P. (1987). Integration of a vector containing rodent repetitive elements in the rat genome. *Nucleic Acids Res* **15**, 7849-63.

Wang, H., Shayakhmetov, D. M., Leege, T., Harkey, M., Li, Q., Papayannopoulou, T., Stamatoyannopolous, G. & Lieber, A. (2005). A capsid-modified helper-dependent adenovirus vector containing the beta-globin locus control region displays a nonrandom integration pattern and allows stable, erythroid-specific gene expression. *J Virol* **79**, 10999-1013.

Wang, P. C., Hui, E. K., Chiu, J. H. & Lo, S. J. (2001). Analysis of integrated hepatitis B virus DNA and flanking cellular sequence by inverse polymerase chain reaction. *J Virol Methods* **92**, 83-90.

Wang, Q., Greenburg, G., Bunch, D., Farson, D. & Finer, M. H. (1997). Persistent transgene expression in mouse liver following in vivo gene transfer with a delta E1/delta E4 adenovirus vector. *Gene Ther* **4**, 393-400.

Wang, Q. & Taylor, M. W. (1993). Correction of a deletion mutant by gene targeting with an adenovirus vector. *Mol Cell Biol* **13**, 918-27.

Wang, Y., Camp, S. M., Niwano, M., Shen, X., Bakowska, J. C., Breakefield, X. O. & Allen, P. D. (2002). Herpes simplex virus type 1/adeno-associated virus rep(+)

hybrid amplicon vector improves the stability of transgene expression in human cells by site-specific integration. *J Virol* **76**, 7150-62.

Weber, J. M. (1995). Adenovirus endopeptidase and its role in virus infection. *Curr Top Microbiol Immunol* **199 (Pt 1)**, 227-35.

West, S. C. (2003). Molecular views of recombination proteins and their control. *Nat Rev Mol Cell Biol* **4**, 435-45.

Wickham, T. J., Mathias, P., Cheresh, D. A. & Nemerow, G. R. (1993). Integrins alpha v beta 3 and alpha v beta 5 promote adenovirus internalization but not virus attachment. *Cell* **73**, 309-19.

Wiethoff, C. M., Wodrich, H., Gerace, L. & Nemerow, G. R. (2005). Adenovirus protein VI mediates membrane disruption following capsid disassembly. *J Virol* **79**, 1992-2000.

Wilkie, T. M. & Palmiter, R. D. (1987). Analysis of the integrant in MyK-103 transgenic mice in which males fail to transmit the integrant. *Mol Cell Biol* **7**, 1646-55.

Wilson, J. H., Berget, P. B. & Pipas, J. M. (1982). Somatic cells efficiently join unrelated DNA segments end-to-end. *Mol Cell Biol* **2**, 1258-69.

Wolff, G., Worgall, S., van Rooijen, N., Song, W. R., Harvey, B. G. & Crystal, R. G. (1997). Enhancement of in vivo adenovirus-mediated gene transfer and expression by prior depletion of tissue macrophages in the target organ. *J Virol* **71**, 624-9.

Woods, N. B., Muessig, A., Schmidt, M., Flygare, J., Olsson, K., Salmon, P., Trono, D., von Kalle, C. & Karlsson, S. (2003). Lentiviral vector transduction of NOD/SCID repopulating cells results in multiple vector integrations per transduced cell: risk of insertional mutagenesis. *Blood* **101**, 1284-9.

Worgall, S., Leopold, P. L., Wolff, G., Ferris, B., Van Roijen, N. & Crystal, R. G. (1997). Role of alveolar macrophages in rapid elimination of adenovirus vectors administered to the epithelial surface of the respiratory tract. *Hum Gene Ther* **8**, 1675-84.

Wronka, G., Bernardi, G. & Doerfler, W. (2004). Localization of integrated adenovirus DNA in the hamster genome. *Cell Mol Life Sci* **61**, 2983-90.

Wronka, G., Fechteler, K., Schmitz, B. & Doerfler, W. (2002). Integrative recombination between adenovirus type 12 DNA and mammalian DNA in a cell-free system: joining by short sequence homologies. *Virus Res* **90**, 225-42.

Wu, X., Li, Y., Crise, B. & Burgess, S. M. (2003). Transcription start regions in the human genome are favored targets for MLV integration. *Science* **300**, 1749-51.

Wurtele, H., Little, K. C. & Chartrand, P. (2003). Illegitimate DNA integration in mammalian cells. *Gene Ther* **10**, 1791-9.

Xing, L. & Tikoo, S. K. (2005). Promoter activity of left inverted terminal repeat and downstream sequences of porcine adenovirus type 3. *Virus Res* **109**, 51-8.

Yabe, Y., Trentin, J. J. & Taylor, G. (1962). Cancer induction in hamsters by human type 12 adenovirus. Effect of age and of virus dose. *Proc Soc Exp Biol Med* **111**, 343-4.

Yamada, T., Iwasaki, Y., Tada, H., Iwabuki, H., Chuah, M. K., VandenDriessche, T., Fukuda, H., Kondo, A., Ueda, M., Seno, M., Tanizawa, K. & Kuroda, S. (2003). Nanoparticles for the delivery of genes and drugs to human hepatocytes. *Nat Biotechnol* **21**, 885-90.

Yang, E. Y., Kim, H. B., Shaaban, A. F., Milner, R., Adzick, N. S. & Flake, A. W. (1999). Persistent postnatal transgene expression in both muscle and liver after

fetal injection of recombinant adenovirus. *J Pediatr Surg* **34**, 766-72; discussion 772-3.

Yang, Y., Li, Q., Ertl, H. C. & Wilson, J. M. (1995). Cellular and humoral immune responses to viral antigens create barriers to lung-directed gene therapy with recombinant adenoviruses. *J Virol* **69**, 2004-15.

Yang, Y., Nunes, F. A., Berencsi, K., Furth, E. E., Gonczol, E. & Wilson, J. M. (1994). Cellular immunity to viral antigens limits E1-deleted adenoviruses for gene therapy. *Proc Natl Acad Sci U S A* **91**, 4407-11.

Yoshinouchi, M., Hongo, A., Nakamura, K., Kodama, J., Itoh, S., Sakai, H. & Kudo, T. (1999). Analysis by multiplex PCR of the physical status of human papillomavirus type 16 DNA in cervical cancers. *J Clin Microbiol* **37**, 3514-7.

Yun, S., Lie, A. C. C. & Porter, A. C. (2004). Discriminatory suppression of homologous recombination by p53. *Nucleic Acids Res* **32**, 6479-89.

Zabner, J., Couture, L. A., Gregory, R. J., Graham, S. M., Smith, A. E. & Welsh, M. J. (1993). Adenovirus-mediated gene transfer transiently corrects the chloride transport defect in nasal epithelia of patients with cystic fibrosis. *Cell* **75**, 207-16.

Zeng, M., Cerniglia, G. J., Eck, S. L. & Stevens, C. W. (1997). High-efficiency stable gene transfer of adenovirus into mammalian cells using ionizing radiation. *Hum Gene Ther* **8**, 1025-32.

Zern, M. A., Ozaki, I., Duan, L., Pomerantz, R., Liu, S. L. & Strayer, D. S. (1999). A novel SV40-based vector successfully transduces and expresses an alpha 1-antitrypsin ribozyme in a human hepatoma-derived cell line. *Gene Ther* **6**, 114-20.

Zhang, Y., Chirmule, N., Gao, G. P., Qian, R., Croyle, M., Joshi, B., Tazelaar, J. & Wilson, J. M. (2001). Acute cytokine response to systemic adenoviral vectors in mice is mediated by dendritic cells and macrophages. *Mol Ther* **3**, 697-707.

Zheng, H., Hasty, P., Brenneman, M. A., Grompe, M., Gibbs, R. A., Wilson, J. H. & Bradley, A. (1991). Fidelity of targeted recombination in human fibroblasts and murine embryonic stem cells. *Proc Natl Acad Sci U S A* **88**, 8067-71.